Technische Universität München
TUM School of Natural Sciences

Addressing Workability Challenges in Clay-bearing OPC and Low Carbon Alkali-activated Slag Systems through Innovative PCE Structural Design

Yue Zhang

Vollständiger Abdruck der von der TUM School of Natural Sciences der Technischen Universität

München zur Erlangung eines

Doktors der Naturwissenschaften (Dr. rer. nat.)

genehmigten Dissertation.

Vorsitz: Prof. Dr. Fritz E. Kühn

Prüfer*innen der Dissertation:

1. Prof. Dr. Johann P. Plank
2. apl. Prof. Dr. Wolfgang Eisenreich

Die Dissertation wurde am 02.05.2023 bei der Technischen Universität München eingereicht und

durch die TUM School of Natural Sciences am 24.05.2023 angenommen.

Acknowledgements

I would like to extend my heartfelt appreciation to all those who have provided unwavering support during my pursuit of Ph.D. degree. Without their help, whether direct or indirect, academic or personal, psychological or physical, the successful completion of my doctoral thesis would have been impossible.

First and foremost, I want to acknowledge my two supervisors, whose guidance and expertise have been invaluable. Their support and encouragement have been critical in helping me navigate the challenges of this journey:

Prof. Dr. Johann Plank and Dr. Lei Lei

They have wholeheartedly and comprehensively cultivated me either in the tirelessly exploring scientific topics or responsibly handling everyday tasks, which will benefit me forever. The unforgettable experience of successfully getting through the long-lasting COVID-19 pandemic was precisely because of their encouragement and guidance, which made me feel courageous to face life challenges and overcome research difficulties. The spirit of rigorous and practical scientific research embodied by **Prof. Plank** has greatly influenced me. He has high expectations for the details of experimental operations and the accuracy and reproducibility of experimental data. He personally reviews and edits every submitted article for publication. He is adept at coordinating and formulating detailed plans, and unfailingly implements them with unwavering determination, even when his schedule is packed. He never misses any routine seminars and provides detailed feedback on everyone's biweekly reports. **Dr. Lei Lei** is widely recognized as an outstanding young talent in our research field. She is always approachable and patiently answers any research issue. She is very intelligent and can easily explain complex academic concepts or mechanisms in a clear and concise manner, by citing references or case studies. She always stands out in international conferences, where her keynotes or

List of publications

The structure of the entire dissertation is based on the following research publications that have already been published or are currently undergoing peer review.

Journal papers:

1. L. Lei, Y. Zhang, R. Li. "Specific molecular design of polycarboxylate polymers exhibiting optimal compatibility with clay contaminants in concrete". Cement and Concrete Research 147 (2021): 106504.

2. Y. Zhang, L. Lei, "Molecular Design of an Allyl-ether PCE with Enhanced Clay Tolerance". American Concrete Institute, ACI Special Publication 354 (2022): 99-112.

3. L. Lei, Y. Zhang, "Preparation of isoprenol ether-based polycarboxylate superplasticizers with exceptional dispersing power in alkali-activated slag: Comparison with ordinary Portland cement". Composites Part B: Engineering 223 (2021): 109077.

4. Y. Zhang, L. Lei, J. Plank, L. Chen, "Boosting the performance of low-carbon alkali activated slag with APEG PCEs: a comparison with Ordinary Portland cement".

   Journal of Sustainable Cement-Based Materials, published online: 5 June 2023, DOI: 10.1080/21650373.2023.2219253.

Conference papers with peer–review process:

5. Y. Zhang, L. Lei, "Exploring the dispersion effectiveness of APEG PCEs in the presence of clay: The impact of calcium interaction (in Chinese)". 8th National Conference on Polycarboxylate Superplasticizer and Its Application Technology, Xiamen, China, November 22-23, 2022, p. 239-245.

6. Y. Zhang, L. Lei, J. Plank, "A Roadmap to Low Carbon Cement Concrete". The 10th International Symposium on Cement and Concrete (ISCC 2022), Guangzhou China, 13-16 November 2022, p. 87.

7. Y. Zhang, Y. Liu, L. Lei, J. Plank, "Optimization of molecular structure of allyl ether based PCEs with enhanced clay tolerance". 16th International Congress on the Chemistry of Cement, ICCC 2023 Bangkok, Thailand. (Accepted)

8. N. Miao, Y. Zhang, L. Lei, J. Plank, "Investigation into A Novel Starch-based Superplasticizer for Alkali-activated Slag". 16th International Congress on the Chemistry of Cement, ICCC 2023 Bangkok, Thailand. (Accepted)

List of abbreviations

Abbreviations	Full name
3-MPA	3-Mercaptopropionic acid
AA	Acrylic acid
AAS	Alkali-activated slag
APEG	α-allyl-ω-methoxy or hydroxy poly (ethylene glycol)
APS	Ammonium persulfate
bwos	By weight of slag
C-S-H	Calcium silicate hydrate
CTA	Chain transfer agent
DI water	Deionized water
dRI	Differential refractive index
EO	Ethylene oxide
GGBFS	Ground granulated blast furnace slag
GPC	Gel permeation chromatography
HPEG	α-methallyl-ω-methoxy or -ω-hydroxy poly (ethylene glycol)
IEP	Isoelectric point

Abbreviations	Full name
IPEG	Isoprenyl oxy poly (ethylene glycol) ether
LS	Light scattering
MA	Maleic anhydride
MAA	Methacrylic acid
M_n	Number average molecular weight
MPEG	ω-methoxy poly(ethylene glycol) methacrylate
M_w	Weight average molecular weight
OPC	Ordinary Portland Cement
PCE	Polycarboxylate ether/ester
PDI	Polydispersity index
PEG	Poly (ethylene glycol)
PEO	Poly (ethylene oxide)
SMAS	2-Methyl-2-propene-1-sulfonic acid sodium salt
TOC	Total organic carbon
w/s	Water to slag ratio
XRD	X-Ray diffraction

Abbreviations	Full name
V	vinyl copolymer
MF	melamine formaldehyde
LS	lignosulfonate
BNS	β-naphthalene sulfonate formaldehyde
SMF	Sulfonated melamine formaldehyde
scps	Synthetic cement pore solution

Content

1. Introduction

Over the past few years, there has been a remarkable increase in global construction demand, fueled by economic and population growth, along with the necessity for enhanced infrastructure to meet the demands of society and industry. Cement is a critical component of modern infrastructure, playing a vital role in building highways, skyscrapers, airports, dams, and other essential structures. Before the covid pandemic, in 2020, Germany produced 35.5 million tons of cement, according to the German Cement Works Association (VDZ), contributing to the worldwide production of approximately 4.1 billion tons. During that period, according to data from the National Bureau of Statistics of China, China emerged as the foremost global consumer of cement. **Figure 1** shows the global annual cement production between 1994 and 2022, with over 1.5 billion tons of cement being produced annually after the turn of the millennium. Since 2014, the yearly production of OPC has consistently surpassed 4.1 billion tons, firmly establishing it as the second most utilized substance worldwide, surpassed in consumption only by water [1].
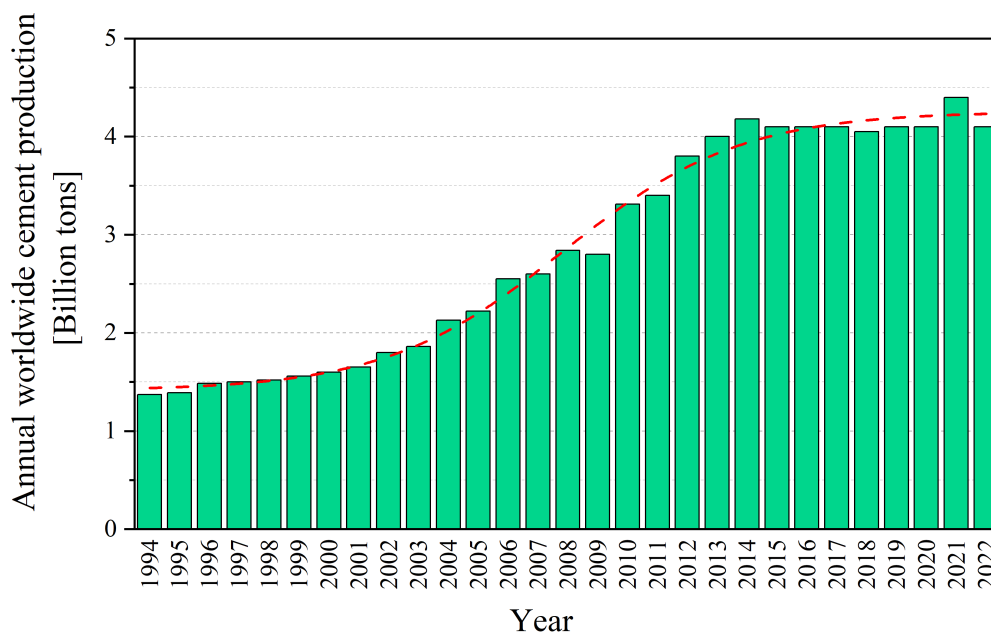
Figure 1: The annual world cement production in billion tons (Source: USGS)

Although the cement industry plays a major role in fostering economic and social development, it unfortunately exacerbates the problem of resource depletion and environmental degradation. This highlights the urgent need for sustainable practices and

technologies in this industry. To achieve this goal, on the one hand, it is necessary to improve the efficiency of using existing natural resources for concrete, and to address issues such as low reserves, low quality, and high impurities in available raw materials. On the other hand, it is important to seek cleaner, greener alternative binders instead of conventional cement. In the following, two major problems of the current concrete industry will be addressed.

- **Rapid depletion of high-quality aggregates and sand**

Currently, the rapid development of the construction industry has resulted in varying degrees of warnings about the reserves of concrete raw materials worldwide. Among them, sand and gravel are the primary types of materials consumed, and according to statistics, their consumption has surpassed that of traditional fossil fuels and biofuels [2]. This large-scale resource extraction will cause ecological damage, such as geological collapses, depletion of underground fresh water, and erosion of beaches [3]. Since the regeneration cycle of sand is very slow and the sand mining rates in many countries around the world have far exceeded the regeneration rate, sand will inevitably become scarce in the foreseeable future, especially high-quality sand that is currently in high demand. Therefore, exploring efficient and sufficient ways to use sand and gravel resources, such as turning to the use of low-quality sand and gravel containing clay, will be a way out that we must face in the future.

When using clay-contaminated aggregates, it can lead to undesirable consequences, such as an increased water demand for the concrete mix or incompatibility with chemical admixtures, particularly polycarboxylate superplasticizers, which are highly effective water-reducing agents for concrete. This can often result in reduced strength and durability of the concrete, as observed by applicators [4]. Initially, washing of aggregates

was a common practice in Europe to eliminate the negative impacts of clay impurities, but it was abandoned due to the need to prioritize water conservation and to avoid the discharge of impure water. Conventional PCEs have been identified very sensitive towards clay contaminants occurring in concrete aggregates [4-7]. Despite extensive research, there is no optimal solution yet. Therefore, there is significant interest in developing novel PCE superplasticizers that possess enhanced clay robustness. The research challenge lies in preventing the undesired intercalation of PEO side chains of PCE polymers into the interlayer space of clay minerals, which can significantly reduce their dispersion power.

- **The need for greener alternative binders with lower CO_2 footprint**

Construction activities are associated with substantial material and energy consumption, resulting in a considerable rise in carbon dioxide emissions. The building industry alone contributes to approximately 40% of primary energy consumption, while the cement production sector is responsible for around 8% of global human-caused CO_2 emissions [8, 9]. Up to 900 kg of carbon dioxide can be emitted per ton of cement produced during the cement manufacturing process [10]. The International Energy Agency (IEA) considers the current level of CO_2 emissions from cement production to be unsustainable. The IEA has emphasized the need to reduce the carbon intensity of primary energy to approximately 60% of its present value by 2050 [11]. The Carbon Neutral Consortium (CNC), formed in 2017, has set an ambitious objective of achieving global "net zero" emissions by 2050 [12].

Researchers and industries have approached the issue of CO_2 emissions from the cement industry through three primary strategies. The first approach involves enhancing energy efficiency, accomplished by incorporating grinding aids during the clinker phase [13-15].

Secondly, advanced carbon sequestration technology has been creatively applied to the cement industry. For example, the Industrial Technology Research Institute (ITRI) has developed a High-efficiency Calcium Looping Technology that can capture CO_2 [15-17]. Thirdly, efforts have been made to develop low-carbon binders as a replacement for cement clinkers [18]. Researchers have explored the potential of supplementary cementitious materials (SCMs), e.g., ground granulated blast furnace slag (GGBFS), pulverized fly ash (PFA), and silica fumes (SF) as alternatives to OPC [19-22].

Ground granulated blast furnace slag (GGBFS) is a by-product derived from the iron and steel industry. It finds widespread use in the construction sector for producing alkali-activated slag (AAS), which is a novel type of binder [23]. This binder, comprising of slag and an activator, has been utilized at industrial scale in several regions, including Eastern Europe (esp. Ukraine) and China [24, 25]. When compared to OPC, the utilization of AAS made from industrial by-products offers significant advantages. It requires less energy during production and leads to a notable reduction in CO_2 emissions, ranging from 55% to 75% [26], based on the type and amount of activator employed. The CO_2 emission necessary to produce 1 ton of GGBFS are remarkably low at $\sim$ 70 kg, as indicated in **Table 1**, in contrast to emissions from OPC [27].

Table 1: Comparison of CO_2 emissions from OPC and GGBFS [27]

Source	from OPC CO_2 emission (kg/t)	from GGBFS CO_2 emission (kg/t)
Calcination of $CaCO_3$	54090	0
Fossil fuel (coal)	340	20
Electricity consumption	90	50
Total	**970**	**70**

In addition to its ability to decrease carbon dioxide emissions, slag has the potential to conserve energy and natural resources while also providing a solution for waste management [28, 29]. As a result, AAS has garnered significant attention in recent years and is considered a promising environmentally friendly binder.

While AAS presents significant potential benefits, its use is often hindered by poor workability and inferior rheological properties compared to OPC. To address these issues, the incorporation of a suitable superplasticizer is crucial for slag-based systems. Previous studies have demonstrated that PCE copolymers are the most effective admixture for use in cement-based materials [30, 31]. Therefore, to practically utilize AAS, it is imperative to identify efficient PCE polymers for dispersing slag pastes, to determine the optimal molecular structure that provides exceptional dispersing power, and to elucidate the underlying dispersing mechanism of PCEs when they are employed. These topics present the research focus of this dissertation.

2. Aims and scope

The aim of this investigation is to confront the scarcity of high-grade sand and aggregate reservoirs and the exigency for novel low-carbon cementitious binders. Specifically, our endeavor is directed towards surmounting the challenges pertaining to poor workability observed in clay-contaminated OPC and AAS systems through molecular modification of PCE architectures. This entails a thorough investigation of the underlying factors contributing to fluidity loss in these systems, including an exploration of the interaction mechanisms between PCEs and various binder systems. Our approach involves the optimization of molecular structural design to identify the optimal molecular parameters that can work effectively in the novel binder systems.

2.1 Molecular design of PCE structures for enhanced clay robustness

The first section primarily focuses on inhibiting the "intercalation" effect that occurs between comb-shaped PCE molecules and clay minerals, such as montmorillonite exhibiting interlayer structures. The research is divided into three parts.

Firstly, it involves the structural design and synthesis of PCE polymers, which includes selecting the appropriate macromonomer, anionic charge density, side-chain length, and molecular weight. To characterize the synthesized PCE products, gel permeation chromatography (GPC), proton nuclear magnetic resonance (^{1}H NMR), and charge titration tests were conducted, with a focus on key parameters such as the macromonomer conversion rate, molecular weight, and polydispersity index (PDI).

The second part of the study involves performance testing to assess the clay tolerance capacity of the synthesized polymers, specifically through mini-slump and mortar tests. The research aims to examine the impact of various molecular architectures on clay

resistance and to identify the optimal structural parameters for the synthesized polymers.

The third part of the study involves a mechanistic analysis, which includes quantitatively assessing the sorption quantity of PCE molecules on the surface and interlayer of bentonite clay through Total Organic Carbon (TOC) analysis. This phase also involves determining the d-spacing values that indicate the intercalation of PCE molecules in interlayer structures using X-Ray Diffraction (XRD) and comparing them with theoretical calculations to assess the molecular size and conformation type. The research aims to establish a direct correlation between the molecular structural parameters of PCE polymers and their clay resistance ability, advancing the understanding of the intercalation mechanism. The study ultimately seeks to propose optimized PCE structures and appropriate approaches for inhibiting the intercalation effect.

2.2 Identification of PCEs suitable for alkali activated slag binder

The objective of the second section is to identify appropriate PCE polymers that can significantly enhance the fresh properties of alkali-activated slag. The initial stage primarily entails the molecular design of PCE architectures. In this process, isoprenyl oxy poly (ethylene glycol) (IPEG) was chosen as the macromonomer, while acrylic acid (AA) was selected as the acid monomer. Subsequently, the specific structural parameters, such as anionic charge density, side-chain length, and molecular weight, were determined. During the experimental implementation, the designated PCE products were synthesized mainly through free radical polymerization. The quality of these products was characterized using gel permeation chromatography (GPC). To validate the dispersing efficacy of the synthesized polymers and their impact on the hydration process of the

alkali-activated slag (AAS) system, a range of tests were conducted, including solubility, rheological properties, fluidity tests, and surface adsorption isotherms. The tests were carried out comparatively between AAS and ordinary Portland cement (OPC) systems to assess the compatibility of PCE polymers in different binder systems.

The study's ultimate objective was to identify specific structural motifs within PCE polymers that exhibit exceptional effectiveness in alkali-activated slag (AAS) system. Moreover, the research aims to determine potential reasons for the selectively dispersing effectiveness of PCE polymers when added to different binder systems. The surface chemistry of these binders and the ionic composition in pore solutions will be given special consideration during this investigation.

3.   Theoretical background

3.1 PCE chemistry and interaction with binders

3.1.1 Chemistry of PCE superplasticizers

In 1981, the invention of a groundbreaking class of superplasticizers called polycarboxylate superplasticizer (PCE) took place in Japan by Nippon Shokubai [32]. The chemical structure of the first synthesized PCE, specifically an MPEG PCE, is presented in **Figure 2**. Typically, PCEs consist of an anionic linear backbone featuring carboxylate groups, accompanied by lateral side chains composed of polyethylene oxide (PEO) that incorporate either ether or ester groups [33, 34]. Prior to the development of PCEs, superplasticizers were mainly synthesized via polycondensation reactions, resulting in the production of two types of admixtures, namely poly(melamine sulfonate) (PMS) and poly(naphthalene sulfonate) (BNS) [35, 36]. **Figure 3** shows that polycondensate-based superplasticizers have high anionic charge density with linear structure, whereas polycarboxylate-based superplasticizers have medium to low charge density and possess side chains. Although PCEs may not exhibit the same level of tolerance to different admixtures or cements as their polycondensate counterparts, they do possess a higher water reducing capability. Even low dosages of PCEs added to concrete effectively enhance its rheological properties, such as fluidity and slump retention. Furthermore, these properties of PCEs have contributed to the development of high-performance concretes, such as ultra-high strength concrete [37-40] and self-compacting concrete [41, 42].
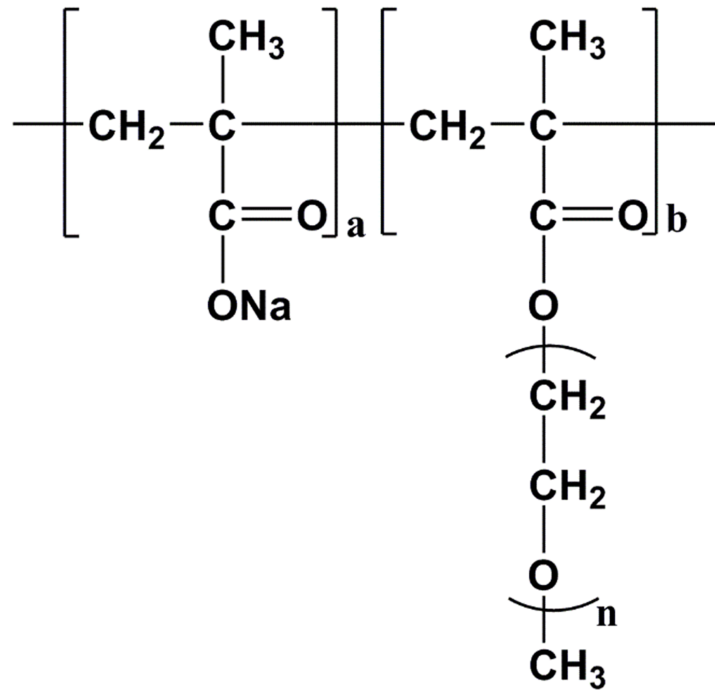
Figure 2: Chemical composition of MPEG PCE superplasticizer, an invention from

Japan in 1981.
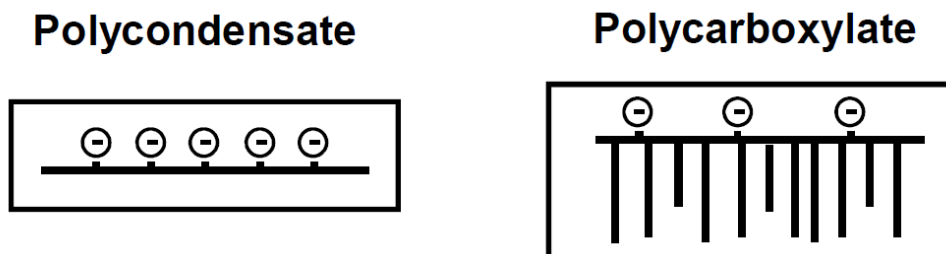
Figure 3: Schematic illustration of the chemical structures of polycondensate and

polycarboxylate admixtures.

During the construction of the Akashi-Kaikyo Bridge, a notable breakthrough in PCEs

occurred in Japan. This bridge connects Kobe City and Awaji Island in Hyogo Prefecture,

spanning a distance of 3.911 km and requiring 149,000 m^3 of PCE-infused concrete to

achieve extraordinary strength (see **Figure 4**). Specifically, PCE was used in the

construction of anchorages, i.e., 1A and 4A, on the Kobe side, which ensured the stability

of the bridge's supporting cables. Additionally, self-compacting concrete was implemented in anchorage 1A.

Figure 4: Pioneering application of PCE in concrete: The construction of the Akashi-Kaikyo Bridge (1988-1998) (Photo by Dr. Tsuyoshi Hirata).

Following the revolutionary advancements made in the construction industry, numerous modifications have been implemented to develop PCEs with superior dispersing capabilities. Consequently, the market now offers a diverse array of PCE products, each exhibiting distinct chemical compositions. Some of these products are presented and briefly described below, while their corresponding chemical structures are exhibited in **Figure 5**.
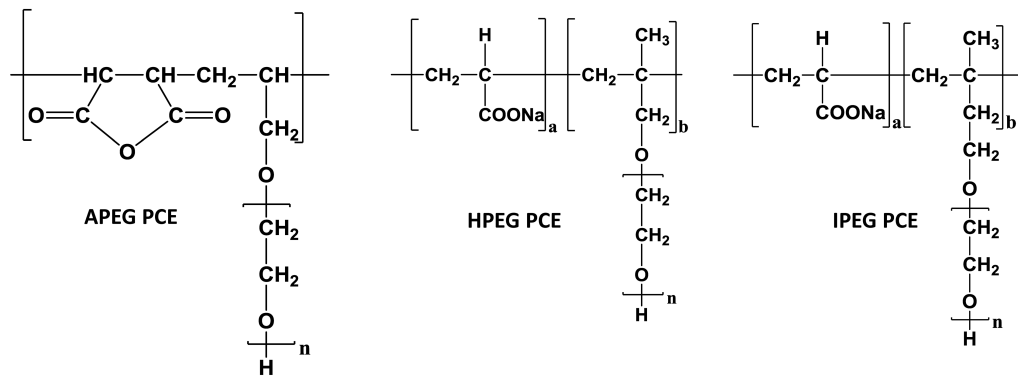
Figure 5: Chemical structures of chemically different polycarboxylate superplasticizers.

- MPEG-type PCEs — The specific classification for this type of PCE falls under first-generation PCE technology, and was synthesized from ω-methoxy poly(ethylene glycol) methacrylate ester (MPEG-MA) using two distinct synthetic methods. These include free radical copolymerization [43, 44] and esterification/transesterification reaction [45].

- APEG-type PCEs — The synthesis of this particular PCE variant involves the free

radical copolymerization of specific monomers, such as α-allyl-ω-methoxy or -ω-hydroxy poly(ethylene glycol) ether, along with maleic anhydride or acrylic acid [46]. This copolymerisation process is commonly conducted either in an aqueous solution or in bulk. When the reaction is performed in an aqueous solution, the resulting copolymers typically have short trunk chains, which are also referred to as "star polymers," and consist of only around 10 repeating units. On the other hand, bulk polymerisation is optimal for side chains that are longer than 34 ethylene oxide (EO) units [36]. Despite the notable benefits of APEG-type PCEs, including their exceptional performance in cement admixtures, the production of these compounds is currently limited on a global scale due to various factors, such as a shortage of APEG macromonomer and the utilization of toxic substances like allyl alcohol [36].

- HPEG-type PCEs — It closely resembles APEG-type PCE, with the primary difference being the utilization of meth allyl ethers in place of allyl ethers. Notably, HPEG-type PCEs exhibit higher reactivity as compared to APEG-type PCEs, as the absence of resonance stabilization allows for greater chemical activity [47]. To synthesize HPEG-type PCEs involves the utilization of α-methallyl-ω-methoxy or ω-hydroxy poly(ethylene glycol) ether as a macromonomer [48].

- IPEG-type PCEs — also referred to as TPEG-type PCEs, are synthesized through copolymerization of isoprenyl oxy poly(ethylene glycol) macromonomers with unsaturated carboxylic acids [49]. This type of polyether polymer has gained significant popularity in China since 2009 due to its exceptional high-range water reducing properties [50]. Notably, IPEG-type PCEs have been found to outperform MPEG- and APEG-type polymers, which, together with their straightforward

synthetic approach via free radical copolymerization, contributes to their wide acceptance [36].

- VPEG-type PCEs — During the 1990s, German researchers synthesized polycarboxylate ethers (PCEs) based on vinyl ethers, specifically 4-hydroxy butyl-poly(ethylene glycol) vinyl ether, using maleic anhydride and acrylic acid co-polymerization at temperatures below 30°C [46]. Vinyl ether technology demonstrates greater reactivity when compared to allyl ether technology, enabling the attainment of a wider range of molecular compositions via low-temperature synthesis.

  More recently, new kinds of vinyl ether polycarboxylates, referred to as EPEG PCE, were introduced. They utilize 2-hydroxy ethyl poly(ethylene glycol) vinyl ether as macromonomer. This macromonomer is co-polymerized with acrylic acid, as depicted in **Figure 5** [51]. Moreover, an alternative form of VPEG PCE, known as GPEG PCE, has been reported recently, which employs a newly developed vinyl ether made from diethylene glycol and ethylene oxide, as presented in **Figure 5** [52]. This polymer was initially introduced in China in 2018, and hence comprehensive information about its unique properties is currently restricted.

- PAAM-type PCEs — In contrast to other PCEs composed solely of PEO/PPO side chains, these zwitterionic PCEs possess a distinctive chemical structure. They incorporate a blend of polyamidoamine (PAAM) and PEO segments as mixed side chains. The PAAM-based PCE has exhibited the capacity to enhance cement flowability even at extremely low water-to-cement ratios, such as 0.12 [53].

However, the primary drawback of this PCE type is its expensive PAAM side chain.

- Polyphosphate Superplasticizers — As early as the late 1990s, superplasticizers for concrete that incorporate phosphonate groups were introduced and made their way into the market [54, 55]. Nevertheless, the utilization of this technology has been somewhat limited due to the elevated cost of the phosphonate group.

Recently, a new class of comb polymers has been developed, wherein the anionic groups are comprised of phosphate functionalities rather than carboxylates. The first variation involves a polyaromatic backbone with polyethylene glycol side chains and phosphate ester groups, synthesized through a polycondensation reaction employing phenol ethoxylate, phenol ethoxy phosphate ester, phenol, and formaldehyde [55]. An alternative synthesis method that does not require CH_2O involves aqueous free radical copolymerization, utilizing hydroxyethyl methacrylate phosphate ester (HEMAP) and the macromonomer used in MPEG-PCE synthesis, i.e., the MPEG ester of methacrylic acid [56], as shown in **Figure 6.**

Studies have demonstrated that the comb polymers containing phosphate groups exhibit exceptional cement dispersing properties, often surpassing those of conventional PCE copolymers [56]. Moreover, these polymers are noteworthy for their ability to maintain effectiveness even in the presence of sulfate and other adsorbing admixtures, which can be attributed to their high calcium binding capacity.
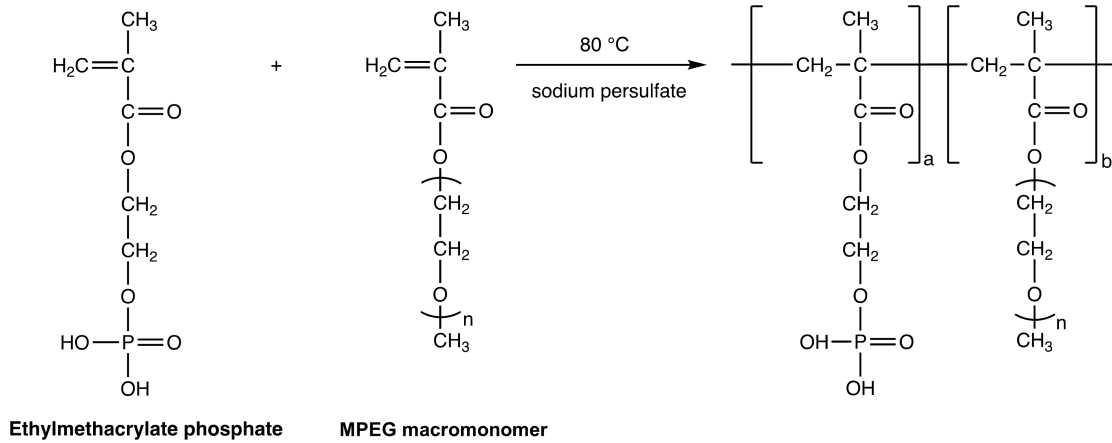
Figure 6: Synthetic route for a phosphate-based MPEG copolymer.

- Organo-silane modified PCEs — In recent studies, two distinct types of silylated PCE polymers have been developed. The first group incorporated a novel comonomer, 3-trimethoxysilyl propyl methacrylate (MAPTMS), into a traditional MPEG-type PCE. On the other hand, the second group utilized an organo-silane modified monomer called N-maleic γ-amidopropyl triethoxy silane (MAPS), as illustrated in **Figure 7** [57-59].

The objective of incorporating a silane group into the PCE molecule was to establish a chemical bond between the C-S-H surfaces and the superplasticizer. This could be achieved by condensation of silanol (-Si-OH) groups present in both compounds, resulting in -Si-O-Si-bridges. If this covalent bond were to occur, it would permanently attach the PCE molecule to the cement hydrate surface, preventing its removal through competitive adsorption, such as from sulfate ions or anionic retarder molecules. As a result, these silylated PCE polymers were found to exhibit high tolerance to sulfates. Moreover, the PCE modified with MAPS exhibited the capability to disperse cement effectively at considerably lower dosages compared to the unmodified PCE [59]. The formation of covalent siloxane bridges between the

silylated PCEs and synthetic C-S-H has been recently confirmed through ^{29}Si NMR

and EXAFS spectroscopy [60].
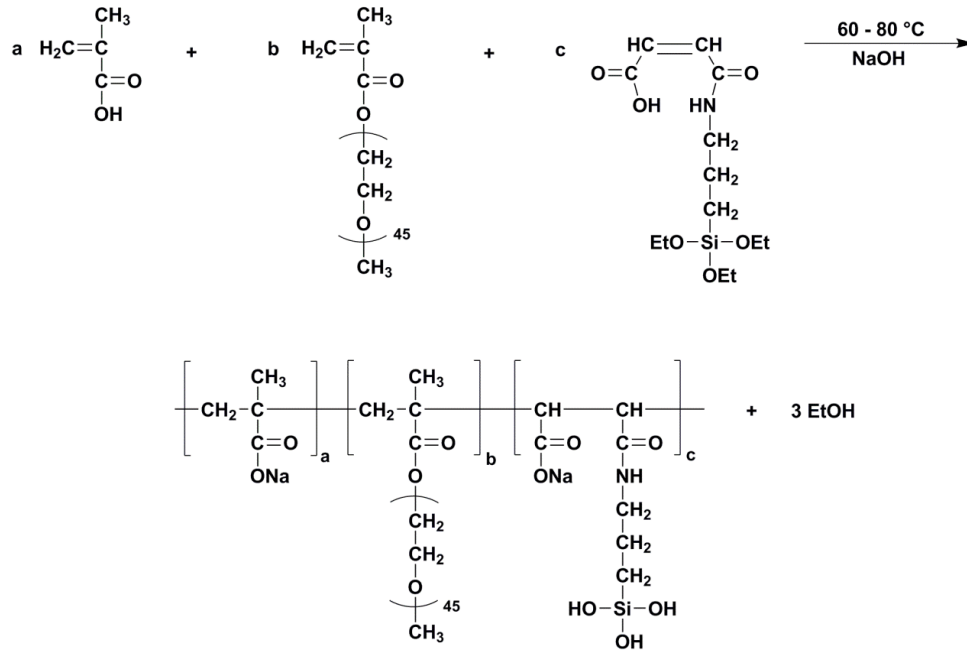
Figure 7: Synthetic pathway of an organo-silane modified PCE polymer.

3.1.2 Working mechanisms of PCE superplasticizers

When water is mixed with cement particles, the attractive forces between positively and

negatively charged sites on the particle surfaces cause them to clump together, a process

known as flocculation. This leads to the entrapment of a portion of the mixing water

within the flocculated cement, forming aggregates. Superplasticizers are added to

facilitate the release of the trapped water and decrease the yield stress of the cement paste.

Figure 8 depicts the processes through which superplasticizers are adsorbed onto the

cement particle surface, leading to a more homogeneous dispersion.

Polycondensate   **Polycarboxylate**

Electrostatic Effect   **Steric Effect**
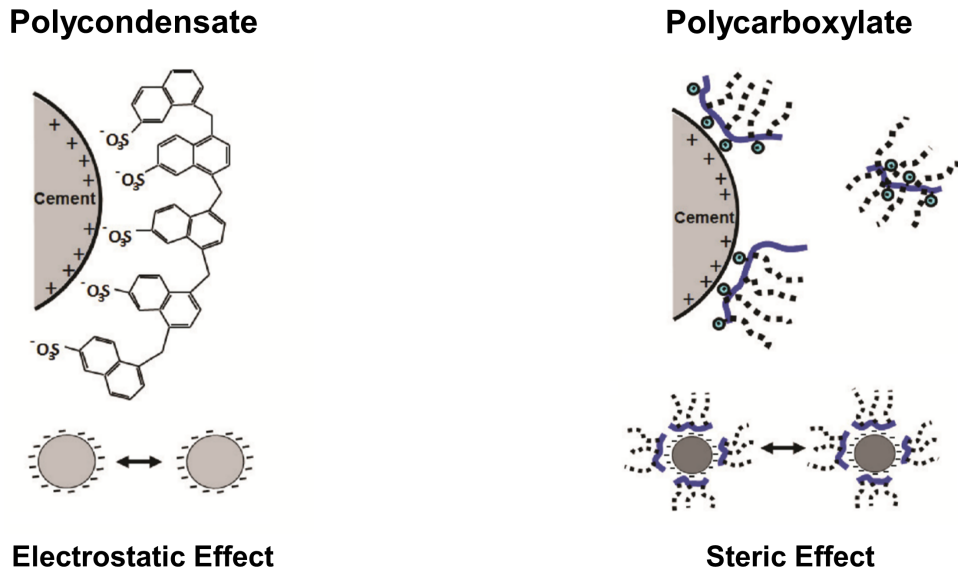
Figure 8: Visualization of the two dispersion mechanisms associated with concrete superplasticizers.

- Electrostatic repulsion

  Superplasticizers are characterized by their negatively charged backbone, resulting from the breaking of double bonds during polymerization to form a linear chain. As the polymer chains adhere to the surface of the cement particles, the particles become negatively charged. This results in the repulsion of the negatively charged cement particles, causing the formation of electrostatic repulsion forces [61-63]. The cement particles eventually align themselves in a matrix structure counterbalance the inter-particle attractive forces.

- Steric hindrance

  When PCE polymers interact with cement particles, steric stabilization occurs, resulting in higher dispersion forces as compared to the linear polycondensate superplasticizers. The presence of hydrophilic pendant chains in the PCE molecule, which extend into the cement pore space, can be attributed to this effect. These

chains create steric hindrance, stabilizing the system.

The Ottewill Walker equation is a theoretical model that describes the steric repulsion between two particles:

$$V_{steric} = \frac{4\pi kT C_V^2}{3v_1^2 p_2^2} \cdot (\Psi_1 - k_1)(\delta - a)^2 (3R + 2\delta + \frac{a}{2}) \qquad \textbf{Equation 1 } [64, 65]$$

where

C_V : concentration of the adsorbents in the adsorbed layer

v_1 : molecular volume of the solvent molecules

p_2 : the density of the adsorbent

Ψ_1 : entropy

k_1 : enthalpy

R : radius of the adsorbed particles

a : distance between two particles

δ : adsorbed layer thickness

Additionally, PCEs can adopt different adsorbed conformations on cement particles, including train, loop, and tail configurations [47], as illustrated in **Figure 9**. Multiple factors affect the adsorbed configuration, encompassing diverse elements like the PCE polymer's molecular traits (such as molar mass, molecular weight distribution, charge density, and pH), the strength of ions in the solution, the existence of multivalent ions, the ratio of surface area to volume, and the interactions between the solvent and polymer, or the quality of the solvent [66-68].
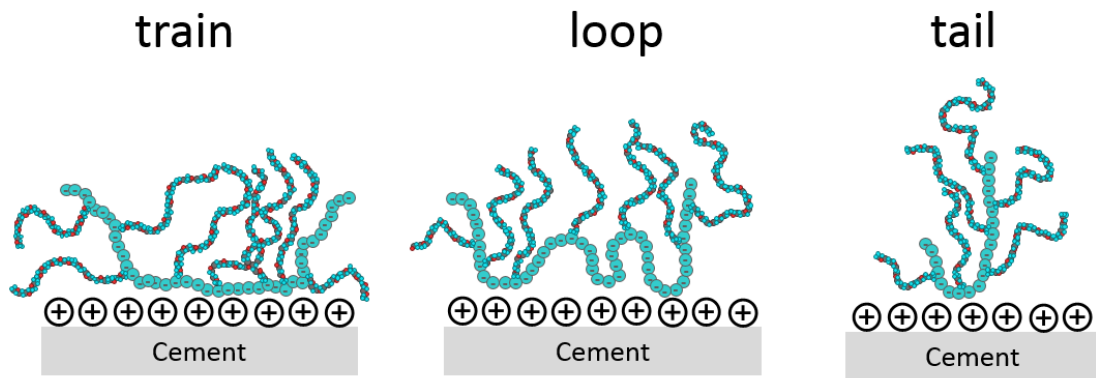
Figure 9: Potential adsorption conformations of PCE polymer

Upon dissolution in water, PCE polymers adopt a specific conformation that is influenced by their unique chemical composition, the pH level, and the ionic species found in the solvent. **Figure 10** illustrates two possible conformations: worm-like or star-like.
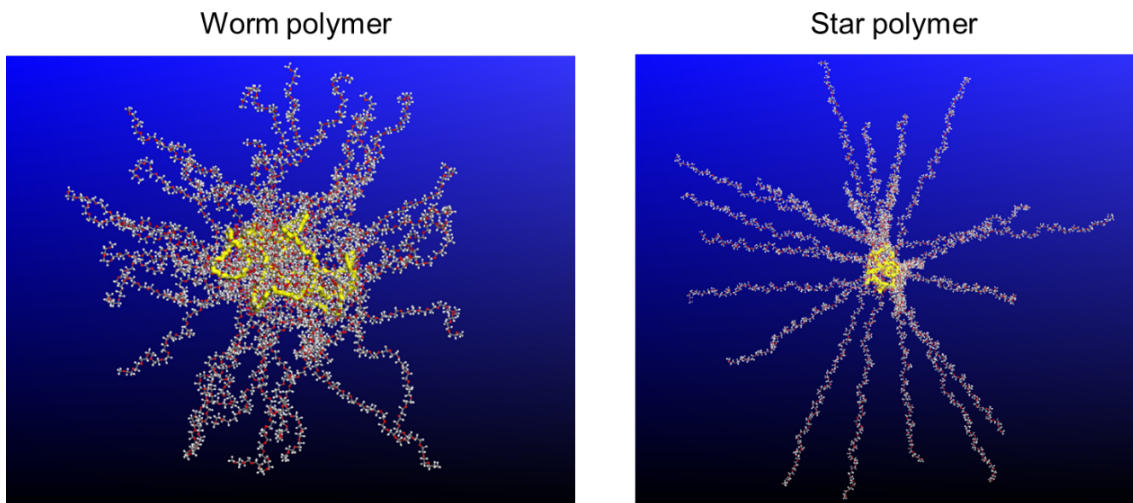
Figure 10: Molecular dynamics (MD) simulations depicting molecular conformations of PCE molecules with varying compositions dissolved in cement pore solution [5].

3.2 Clay chemistry and structure

Clay minerals can be found in diverse sediment types and consist of layered aluminosilicates, featuring tetrahedral silicate sheets and octahedral aluminum sheets. The possible combinations of these sheets are diverse, and clays are categorized based on these combinations, as depicted in **Figure 11**. There are three primary kinds of clays. One prominent group is the 1:1 clay minerals, e.g., kaolinite, which have one silicate and one aluminum sheet. In contrast, 2:1 clay minerals are characterized by the presence of two silicate sheets and one aluminum sheet, such as bentonite. In the case of 2:1:1 clay minerals, an additional octahedral sheet is also present.

Bentonite   **Illite**   **Muscovite/Mica**   **Kaolinite**
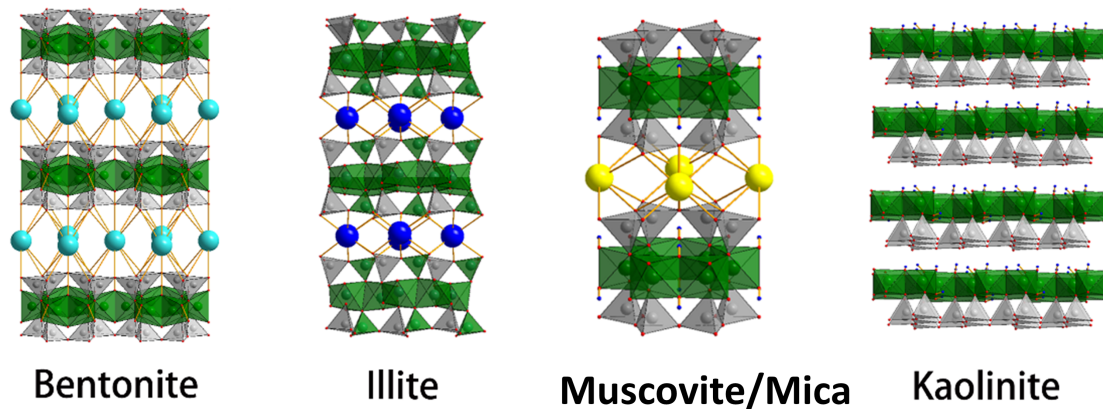
Figure 11: Types and structures of common clay minerals (Redrawn from [69]).

The primary focus of this thesis revolves around Montmorillonite (MMT), the prominent clay mineral found in bentonite. It holds great significance in relation to the dispersing effectiveness of PCE polymers commonly utilized in concrete. This can be attributed to the expansive lattices of MMT, which facilitate processes such as intercalation, swelling, and cation exchange. MMT typically exhibits a high capacity for water sorption and swelling, leading to elevated viscosity in cement pastes or concrete. As a consequence, this results in diminished workability or an increased demand for water to achieve the same level of workability in the absence of clay.

3.2.1 Clay swelling mechanisms

In swelling clays, i.e., montmorillonite, water molecules can infiltrate the interlayer regions of the aluminosilicates and induce expansion by forming multiple mono-molecular layers of water. This phenomenon is referred to as swelling and can manifest through two distinct mechanisms: crystalline and osmotic [70, 71]. Crystalline swelling, which is controlled by surface hydration, involves the organization of multiple layers of water molecules in a structured manner between the unit layers. This results in the development of a quasi-crystalline structure. As a result, the interlayer spacing experiences an increase. In contrast, osmotic swelling predominantly takes place in clay minerals that possess exchangeable cations within their interlayer region.

This phenomenon occurs due to the concentration gradients of cations between the layers, which prompts the osmotic flow of water into the interlayer region. As a result, there is an expansion in the interlayer spacing [72, 73]. Osmotic swelling can result in a much greater overall volume compared to surface hydration, particularly in sodium montmorillonite clay.

3.2.2 Interaction between PCEs and clay minerals

As shown in **Figure 12**, the interaction of PCEs with clay minerals is commonly observed through two separate mechanisms: surface adsorption and chemical intercalation [74].
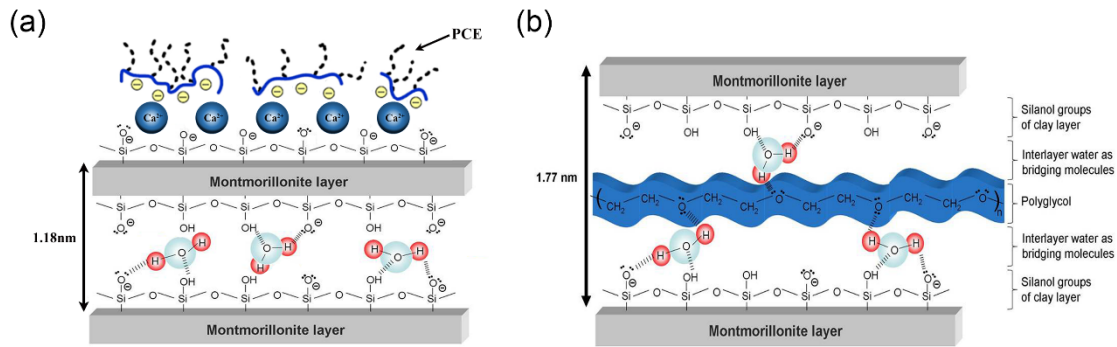
Figure 12: Interactions between PCE molecules and montmorillonite clay: (a) surface physisorption and (b) interlayer chemisorption.

- Physisorption by electrostatic attraction

  In alkaline environment, clay surfaces typically exhibit a negative charge due to the existence of silanol groups. Nevertheless, the introduction of Ca^{2+} ions from the pore solution of cement can lead to a reversal of the surface charge. As a result, negatively charged PCEs can interact with the clay surface via electrostatic interaction, as depicted in **Figure 12 (a).**

- Intercalation

  PCE molecules can become confined within the interlayer spacing of clay minerals, particularly smectites, by means of intercalation. The intercalation process involves the insertion of PCE molecules into the interlayer region of the clay structure, as demonstrated in **Figure 12(b)**. This process is achieved through the interaction of PEG side chains with the silanol groups present on the surfaces of the aluminosilicate layers, aided by water via hydrogen bonding. This phenomenon is primarily observed in clays with a high cation exchange capacity, such as MMT, where cations are situated between the aluminosilicate layers.

3.2.3 Mitigation strategies

Considerable effort has been dedicated to addressing the issue of clay sensitivity for PCEs. **Table 2** provides an overview of the sacrificial agents that have been reported to minimize the interaction between PCEs and clays. These agents have been categorized according to their respective approaches in mitigating the undesirable interaction between PCEs and clays, including inhibitors for clay swelling, blockers for intercalation, and blockers for electrostatic interactions [5].

Table 2: Categorization of additives for clay mitigation [5].

Blockers for intercalation	Reference
PEG	[75-78]
Polyvinylalcohol	[79]
Calcium ions	[80, 81]
Zwitterionic polymer based on Beta-cyclodextrin	[82]
Ferric sulfate polymer	[83]
PCE of high grafting density	[84]
Cationized co-polymer of acrylic acid/acrylamide	[85]
Small cationic agents	[86]
Gemini quaternized reaction product with trialkylamine and dibromo propane	[87, 88]
Cationic organic polymer	[89]
Kraft lignin grafted with PEG	[90]
Inhibitors for clay swelling	
Potassium ion	[78]
High M_w polyacrylamides, polyvinyl pyrrolidones and acrylate copolymers	[91]
Sulfonated lignin	[92]
Imidazolium cation with a long chain	[93]
Electrostatic Blockers	
DMC[1] and DMDAAC[2] copolymer with HEA[3] or butyl acetate	[94]
PMA	[75, 78]
Acetate ion	
Zwitterionic polymer based on Beta-cyclodextrin	[82]
Sodium tripolyphosphate	[95]
Quaternized lignosulfonate[4]	[96]
Quaternized vinylpyridine cationic co-polymer	[97]

Humic acid	[98, 99]
Hybrid Intercalation/Electrostatic Inhibitors	
Quaternary salt/PEG/hydroxycarboxylate blend and Group I cation/quaternary ammonium cation/PMA blend	[100-102]

[1] methacryl oxyethyl trimethylammonium chloride
[2] diallyl dimethylammonium chloride
[3] hydroxyethylene acetate
[4] Quaternizing agent 3-chloro-2-hydroxypropyl trimethylammonium chloride

- Clay Swelling Inhibitors

  Potential clay swelling inhibitors may consist of polyethylene glycol and polypropylene oxides, which operate by intercalating between the clay layers in the PCE, or by encapsulating the clay particles using high M_w polymers like polyacrylamides, polyvinylpyrrolidones, and acrylate copolymers [5, 91].

- Intercalation Blockers

  PEG side chains have demonstrated an increased affinity for the expanded interlayer spacing of clays, suggesting their potential as sacrificial agents for minimizing the intercalation of PCEs into clay [103, 104].

  Additionally, PEG derivatives, such as PEG-grafted lignosulfonates (see **Figure 13)**, have been observed to enhance the flowability of cement pastes that incorporate sodium montmorillonite in the presence of PCE [5, 102]. The effectiveness of PEG-grafted lignosulfonate is attributed to its rapid interaction with MMT clay and subsequent insertion into the interlayer structure of the clay, resulting in the reduction of PCE intercalation. Moreover, the inclusion of polymeric ferric sulfate (PFS) illustrated in **Figure 14**, in a clay-containing cement paste has been noted to lead to the adsorption and encapsulation of Na-MMT particles, consequently impeding the intercalation of polycarboxylate ethers (PCEs) [83].

(a)

Polyethylene glycol (PEG)

(b)

Simplified chemical structure
of lignosulfonate

(c)

PEG-grafted lignosulfonate
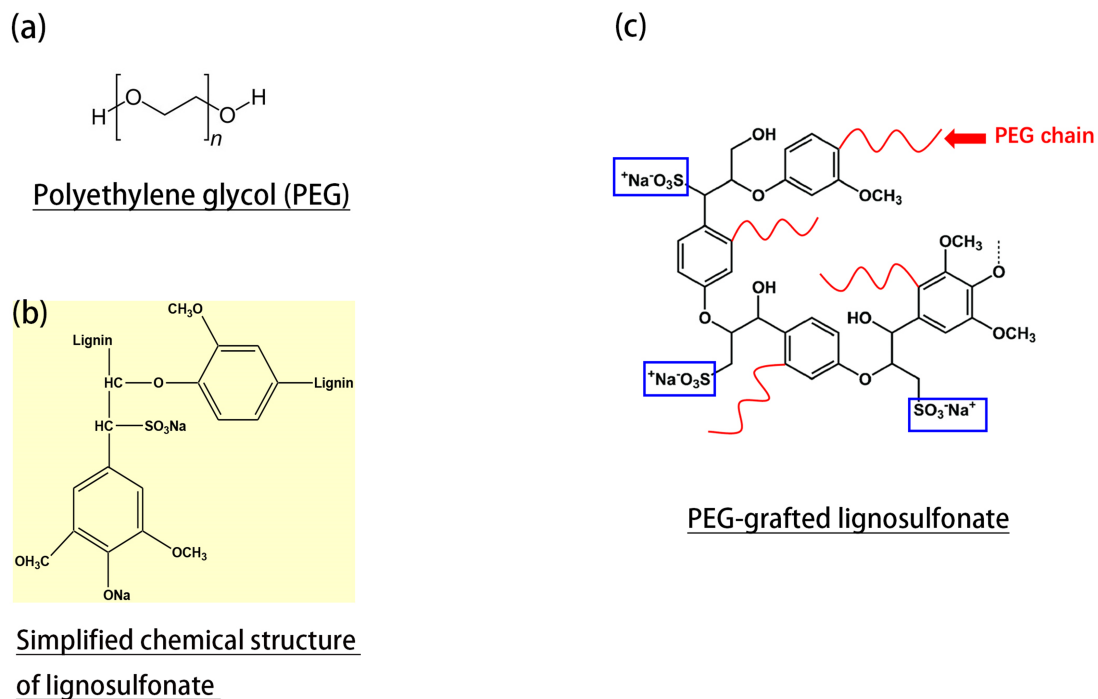
Figure 13: Chemical structure of (a) polyethylene glycol (PEG), (b) lignosulfonate and (c) PEG-grafted lignosulfonate (redrawn from [105]).
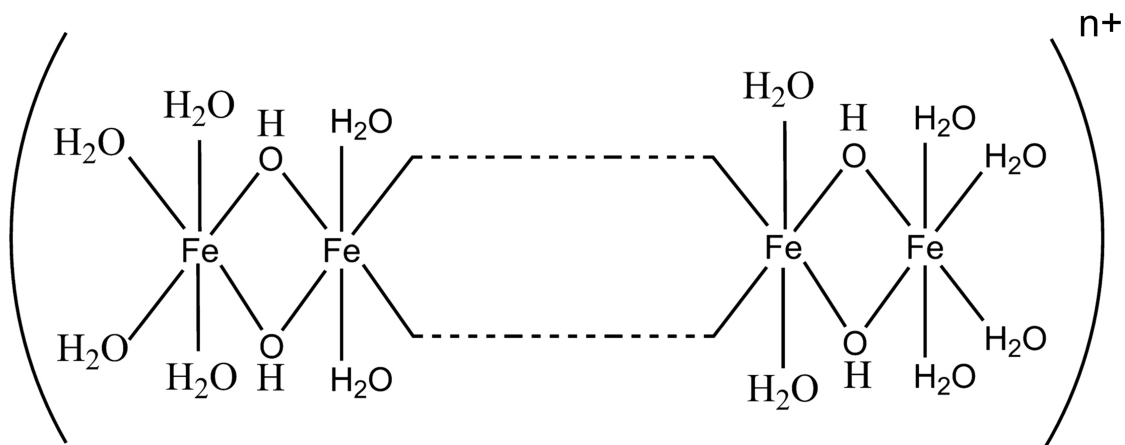
Figure 14: Schematic of the molecular structure of PFS [83].

- Electrostatic Blockers

  Through electrostatic forces, positively charged compounds and polymers, including quaternary ammonium salts, have the capability to interact with the aluminosilicate layers present in clay. Furthermore, quaternary and polyquaternary salts featuring hydrocarbon chains can enhance the hydrophobicity of clay particles, resulting in the formation of a protective layer on the clay surface. This protective layer effectively compacts the interlayer spacing, thereby hindering the intercalation of PEG pendant chains of PCE polymers [5, 74, 85-87].

- Molecular modification of PCE structures

  Despite the clay sensitivity issue, PCEs continue to be the mainstream superplasticizers due to their outstanding price-performance ratio. As the PEG side chains within PCE molecules are known to be easily incorporated into the interlayer region of smectite clays, the replacement of these conventional PEG side chains with alternative groups is considered a promising solution for the problem of clay sensitivity.

  As examples, **Figure 15** shows a novel PCE structure incorporated with a three-dimensional β-cyclodextrin group. **Figure 16** exhibits a new PCE structure with bulky phenyl groups.
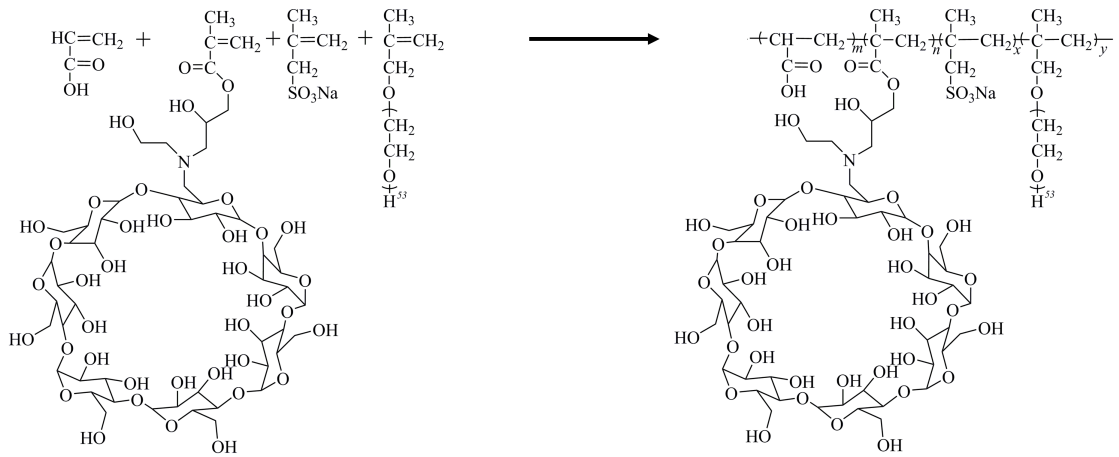
Figure 15: Structural sketch of the modified PCE structure with β-cyclodextrin groups.

Phenyl-modified PCE
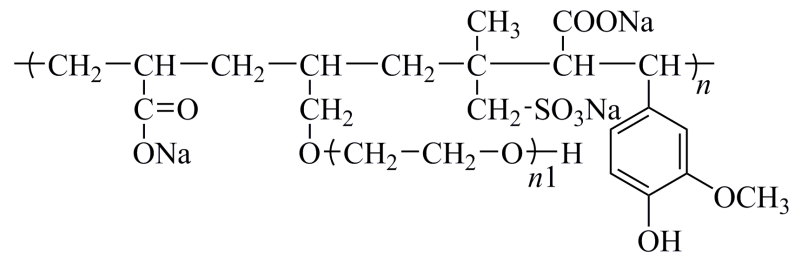
Figure 16: Structural sketch of the modified PCE structure containing bulky phenyl groups.

3.3 Low carbon binder: alkali-activated slag

3.3.1 Fundamental phase compositions

Slag is a type of supplementary cementitious materials (SCMs), which typically exhibit similar primary components, but lower calcium content than Portland cement, except for fine limestone, as depicted in **Figure 17**. This difference in composition leads to variations in the hydrates that develop during hydration, thereby impacting the strength and durability of the final product.
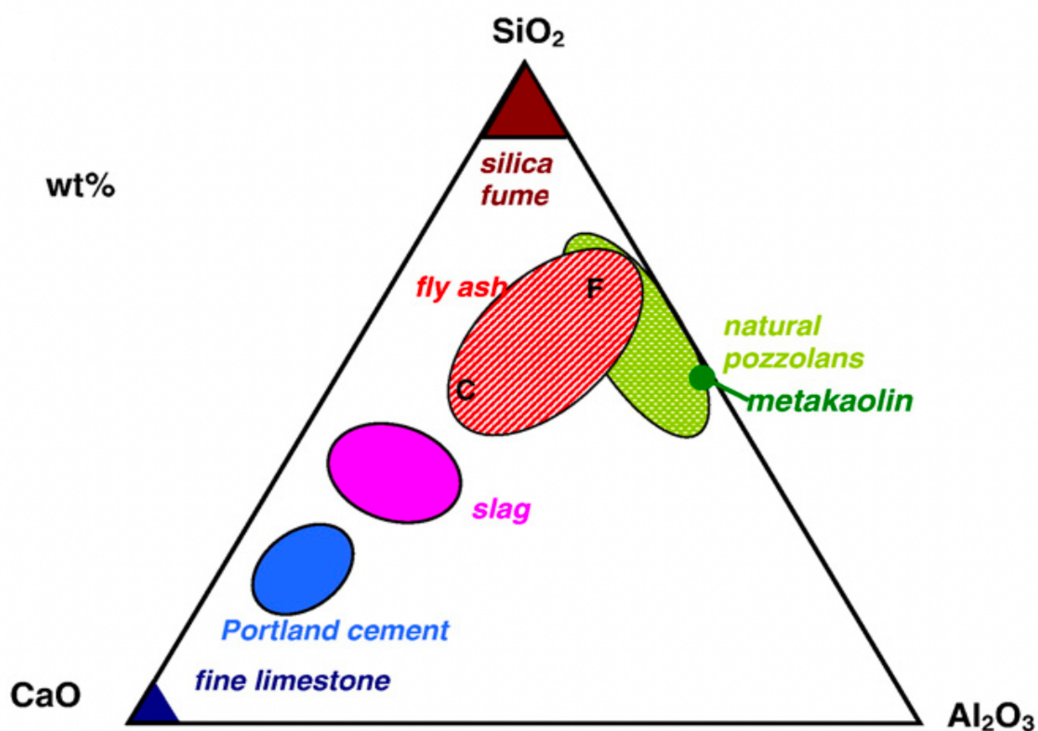
Figure 17: The ternary diagram illustrating the compositions of SCMs based on CaO-Al$_2$O$_3$-SiO$_2$ [106].

3.3.2 Activation and hydration characteristics of AAS

• Activation mechanism of AAS

The latent hydraulic property of slag is widely recognized. Therefore, it is crucial to trigger the hydration of slag to utilize the latent hydraulic properties of slag, and one of the most efficient techniques is through the incorporation of alkali-activators such as

alkali hydroxide, alkali carbonate, and alkali silicate (water glass). Once these alkali

activators are dissolved in the pore solution, the hydration of slag can accelerate

significantly because the high pH level results in the disintegration of the glass network

of slag particles [107].

Although the exact function of alkali cations in AAS hydration is not yet fully

comprehended, Chithiraputhiran [108] has suggested a possible mechanism in which the

alkali cations (M^+) play a crucial role. This mechanism, outlined by Chithiraputhiran,

includes several steps. Firstly, the alkali cations act as a catalyst, triggering the

restructuring process of the outer slag particles, known as the destruction reaction.

Secondly, the alkali cations initiate both dissolution and precipitation. Finally, the alkali

cations promote the diffusion of ionic species into the slag core particles, ultimately

leading to the formation of a C-S-H gel. This proposal is supported by the equations

presented by Glukhovsky et al. and Krivenko [109, 110].

$$\equiv Si\text{-}O\text{-} \;+\; M^+ \quad \rightarrow \quad \equiv Si\text{-}O\text{-}M$$

$$\equiv Si\text{-}O\text{-}M \;+\; OH^- \quad \rightarrow \quad \equiv Si\text{-}O\text{-}M\text{-}OH^-$$

$$\equiv Si\text{-}O\text{-}M\text{-}OH^- \;+\; Ca^{2+} \quad \rightarrow \quad \equiv Si\text{-}O\text{-}Ca\text{-}OH \;+\; M^+$$
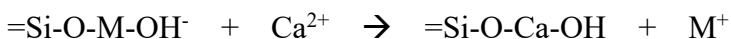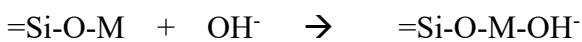
The activator performs two primary functions. Firstly, it expedites the hydration process,

leading to the creation of the C-S-H gel that provides robust mechanical properties,

strength, to slag. Additionally, it aids in the adsorption of Ca^{2+} cations onto the slag

surface, causing the surface to become slightly positive, thereby facilitating the

electrostatic attraction of negatively charged PCE superplasticizer molecules.

- Hydration kinetics of AAS

Isothermal calorimetry is a commonly utilized technique in the investigation of the hydration process in alkali-activated slag. **Figure 18(a)** demonstrates that the heat evolution rate curves typically display up to three peaks: the dissolution peak or first peak, the pre-induction peak or second peak, and the acceleration peak or third peak. These peaks correspond to the stages of maximum precipitation rate for hydration products. The calorimetric curves of various AAS can exhibit significant variations, influenced by the type and concentration of the alkaline activators employed. When a waterglass solution is used as the activator, the pastes demonstrate notably shorter initial and final setting times (2 h and 20 min, see **Figure 18(b)**). Prior to the induction period and well before reaching the peak formation of reaction products, these setting times take place. The presence of a pre-induction peak in the calorimetric curves of this paste demonstrates a correlation with the setting time. Upon utilization of an NaOH solution as the activator in AAS pastes, the heat evolution rate curves exhibit only a singular peak corresponding to the acceleration peak, while the first or second peaks remain undetected due to the exceptionally rapid reaction process. In certain NaOH-activated pastes, the induction period remains indeterminable. Upon comparing the setting times achieved by the paste (3 h and 40 min, as illustrated in **Figure 18(b)**) with the heat evolution rate curves, it becomes apparent that both setting times of AAS cement pastes activated by NaOH coincide with the occurrence of the acceleration peak. The utilization of Na_2CO_3 as the activator in AAS pastes results in the identification of numerous peaks in the heat evolution rate curves, as presented in **Figure 18(a)**. The first indicator, which manifests itself roughly at 8 ± 20 h following the activation, is linked to a pre-induction peak, succeeded by an exceedingly prolonged induction period of approximately 100 h. Following that, there is a subsequent appearance of an acceleration-deceleration peak,

which persists for around 80 h. Significantly, it is worth mentioning that the AAS pastes, when activated with Na_2CO_3, exhibit a prolonged setting time that corresponds to the end of the induction period and the commencement of the acceleration phase as observed in the heat evolution.

(a) Heat evolution rate
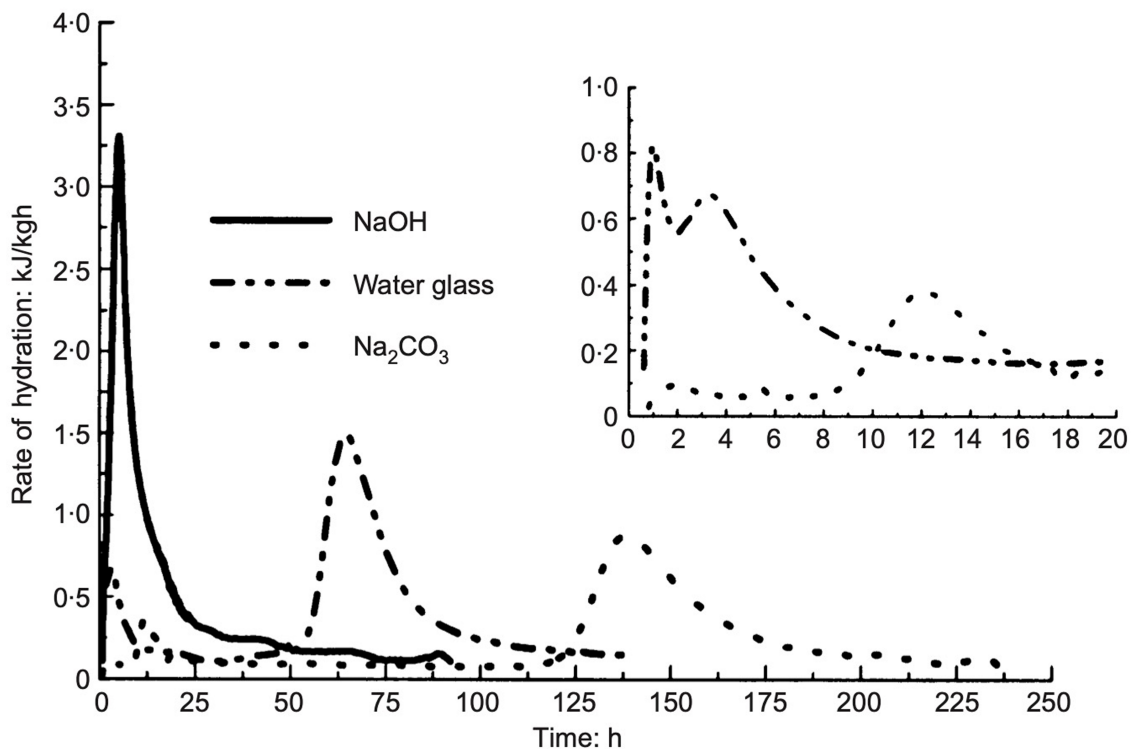
(b) Initial and final setting time

Activators	Initial time (t_1)	Final time (t_f)	$\Delta t = t_i - t_f$
Waterglass	2 h 20 min	4 h 45 min	2 h 25 min
NaOH	3 h 40 min	4 h 40 min	1 h
Na_2CO_3	> 3 días	> días	

Figure 18: Calorimetric curves and setting time for slag pastes with different activators at constant alkali content of 3 % of Na_2O bwos (redrawn from [111]).

Similar to OPC cement pastes, in the heat evolution rate curves, both setting times occur after the completion of the induction period [112]. However, in this particular scenario, the setting time is intricately connected to the acceleration period, which corresponds to the peak precipitation rate of reaction products, particularly C-S-H [113]. According to Fernández-Jiménez [111], by utilizing waterglass as an activator, the setting process accelerates for the formation of an early-stage C-S-H. In contrast, NaOH-activated pastes exhibit longer setting times as a more polymerized C-S-H is formed. When Na_2CO_3 is used as an activator, the initial formation of a sodium calcium carbonate results in longer setting times and retards the reaction processes. Thus, the focus now shifts towards the development of hydration products in AAS.

Figure 19 presents a schematic diagram illustrating the hydration products of AAS. However, the composition (e.g., MgO and Al_2O_3 content), type of alkali activator and curing conditions of slag can result in varied hydration products. Here, the focus is on the influence of activators. When various alkaline solutions are employed as alkali activators, the primary hydration product of slag is C-(A)-S-H. Additionally, the presence of N-A-S-H and C-(N)-A-S-H can also be observed. The other hydration products exhibit variations depending on the specific alkali activator used. The use of NaOH as an activator promotes the production of AFm and leads to a lower crosslinking degree of C–A–S–H. The utilization of Na_2SiO_3 results in an increased availability of SiO_4^{4-} ions, which enhances the bridging units of Si in C-A-S-H and promotes the degree of polymerization of C-A-S-H. Na_2CO_3 leads to the production of more CO_3^{2-} ions via dissociation, which promotes the formation of $CaCO_3$ precipitation. Nonetheless, there is a lack of consensus in research findings regarding the hydration products of slag when exposed to various alkali activators, emphasizing the need for additional investigation to elucidate the underlying mechanisms governing their formation.
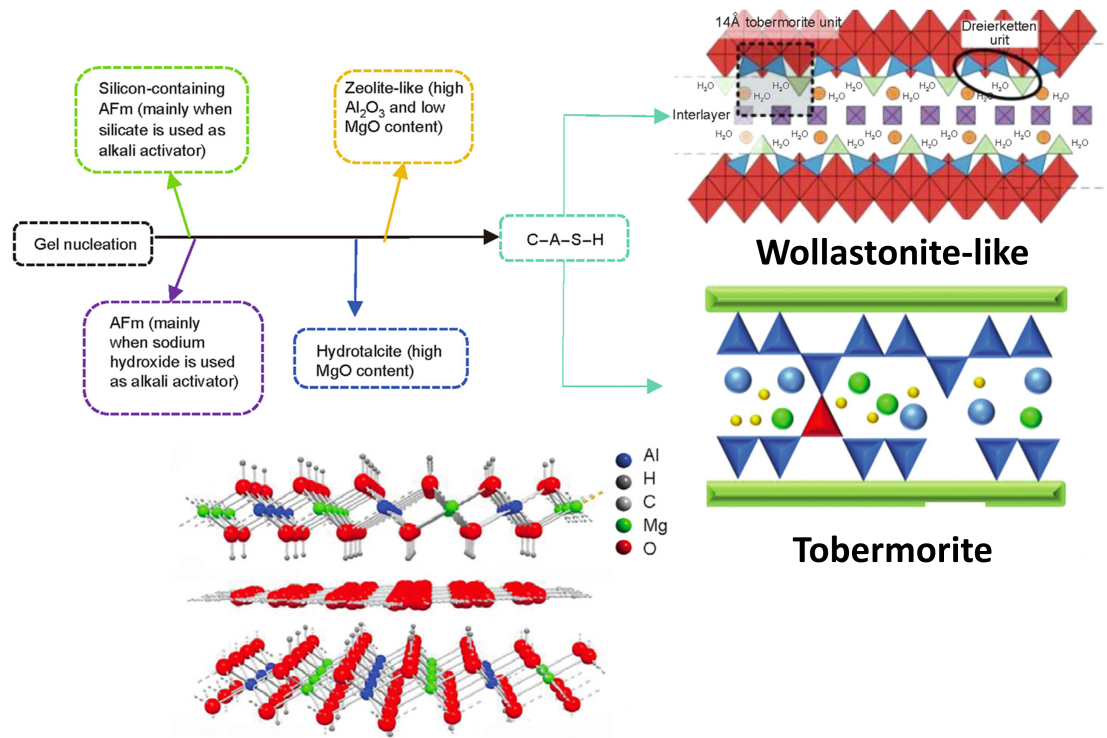
Figure 19: Illustrative representation of hydration products of alkali-activated slag (AAS) under varying curing conditions [114, 115].

3.3.3 Interaction between PCE polymers and AAS

Researchers have been investigating, for decades, the use of high-efficiency superplasticizers for alkali-activated slag (AAS) systems, which have been traditionally used with ordinary Portland cement (OPC). However, the practical application of AAS systems in the construction industry is limited due to the low initial fluidity and rapid setting of AAS paste (esp. NaOH activated) compared to OPC. The higher pH value and ionic strength of the AAS pore solution affect the superplasticizer polymers, leading to insolubility or transformation of molecular structure. Furthermore, the high viscosity of alkaline solutions poses a challenge for the effectiveness of conventional superplasticizers.
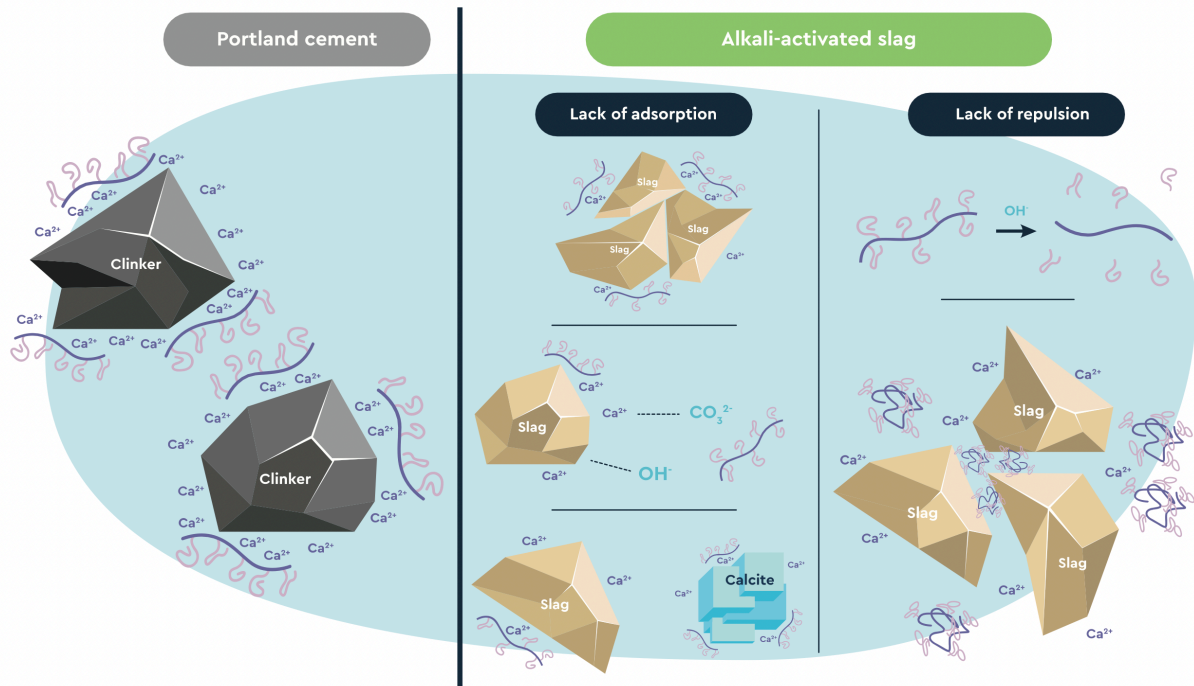
Figure 20: Unraveling the molecular mechanisms behind fluidification and its absence in OPC and AAS induced by PCEs [116] .

Figure 20, as proposed by C. Paillard et. al [116], illustrates various explanations proposed in literatures to account for the observed phenomenon. The alkaline nature of activating solutions potentially leads to the degradation of the polymer structure in MPEG ester PCEs, presenting one plausible explanation [117, 118]. As in **Figure 21**, the proposed reaction scheme outlines the alkaline hydrolysis of polycarboxylate admixtures based on methacrylate esters.

MPEG PCE
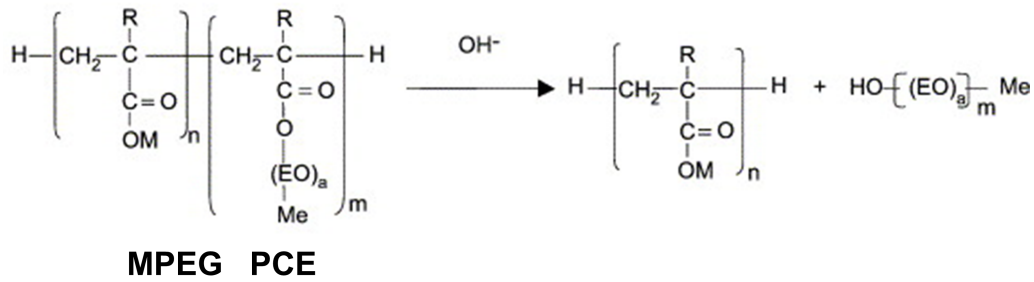
R = H, Me

M = Metal

EO = Oxyethylene

Me = Methyl

Figure 21: The mechanism for MPEG polycarboxylate superplasticizer undergoing alkaline hydrolysis, proposed by M. Palacios et. al [117].

Conte and Plank's study proposes that the limited solubility of superplasticizers could impact steric repulsion, thereby influencing the observed effects [119] (see **Figure 22**). Alternatively, insufficient adsorption of polymers on the slag surface may also explain this phenomenon. Possible contributing factors include lower Ca^{2+} concentrations in the interstitial solution, variations in surface chemistry between slag and clinker particles (as noted in [120, 121]), competitive adsorption between the superplasticizers and other anions (such as carbonate or sulfate) present in the solution (as discussed in [122]), and differing affinities of the polymer towards the slag particles and the hydrates formed during the initial stages (as mentioned in [123]).

C. Paillard [116] attributes the dispersing ineffectiveness of the superplasticizers in Na_2CO_3-AAS to the competive adsorption with CO_3^{2-}, as shown in the center of the schematic representation of **Figure 20**; however, there is still insufficient experimental data to substantiate this claim.
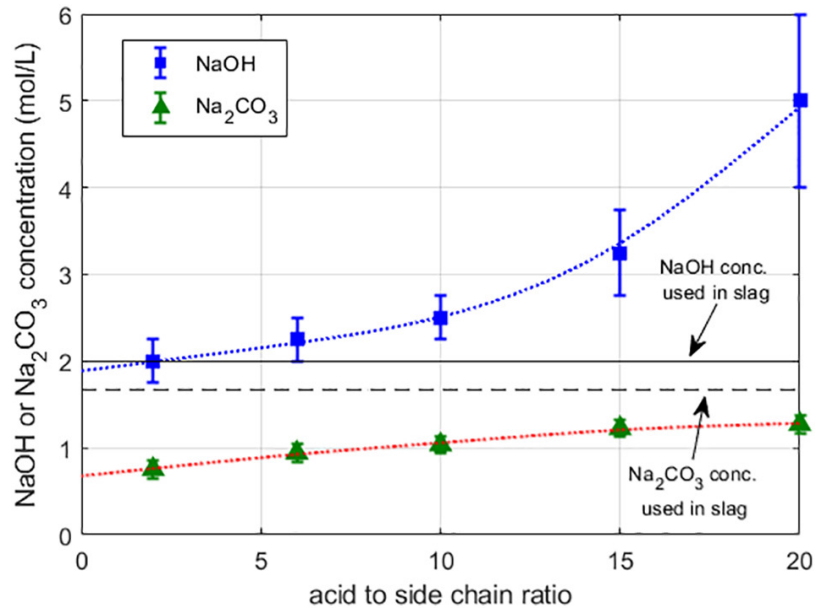
Figure 22: Anionicity-dependent concentration of NaOH and Na_2CO_3 required to achieve the cloud point of differently composed PCE polymers based on methacrylate ester type (reproduced from [119]).

Extensive research has been carried out to tackle the ineffectiveness problem of superplasticizers as mentioned above, and these problems are mainly influenced by the type of activators. [124].

- NaOH-activated slag

The most commonly used activator for AAS is NaOH. However, studies by Puertas et al. [125] showed that superplasticizers based on polyvinyl and polycarboxylic acid did not enhance the workability of NaOH-activated slag binders, but instead reduced their strength. Other researchers have also observed similar results. Palacios et al. [117] examined the effect of different superplasticizers (PCE, MF, BNS, and vinyl copolymer) on the slump retention of NaOH-activated AAS pastes. Only a vinyl copolymer showed a slight increase in fluidity in the first 10 minutes due to its chemical structure changing

in the high pH solution, while melamine formaldehyde dispersant and PCEs behaved similarly. However, BNS enhanced both the initial fluidity and fluidity retention for up to 60 minutes. The poor dispersion performance of PCEs was due to their fast hydrolysis under alkaline conditions. They also found that among MFS, BNS, and vinyl copolymer BNS was the most effective admixture at improving fluidity in NaOH-activated slag slurry paste at pH=13.6, as it remained stable even in highly alkaline solutions [117].

PCEs are unique among superplasticizers because of their diverse molecular structures that can improve the rheological properties of AAS pastes. In a comparative study conducted by Conte et al. [119], various types of PCEs, namely MPEG, APEG, IPEG, and phosphate-type PCEs, were examined. Among them, the APEG-type PCE copolymer with a shorter side chain and a substantial M_w exceeding 30,000 g/mol demonstrated the most effective dispersing capability. This superior performance can be attributed to its high solubility in 2 M NaOH solution and strong affinity towards Ca^{2+} ions, primarily due to the presence of maleic anhydride. Additionally, the researchers found that zwitterionic or cationic superplasticizers were incapable of dispersing the AAS system at any concentration. Other researchers also reported similar results. Habbaba et al. [121] demonstrated that APEG PCEs, with higher M_w > 30,000 Da, were the most effective dispersant. For instance, with only 0.05 wt.% of PCE dosage, APEG2 increased the spread flow of the slag paste from 15.5 cm to 33.7 cm. However, the industrial use of APEG PCEs with very short side chains of 7EO (ethylene oxide) units is limited since they are only produced in laboratories.

A study was performed by Lei et al. to investigate the dispersing capability of HPEG PCEs in NaOH-activated AAS [126]. They synthesized different PCEs with varying

molecular geometries and adequate solubility in a 2M NaOH solution through the utilization of HPEG macromonomer and acrylic acid. Particularly highly anionic PCEs samples were found to disperse well, with 23HPEG7 increasing the spread flow from 14.7 cm to 31cm. The enhanced dispersibility of highly anionic HPEG PCEs was ascribed to the higher adsorption on the surfaces of slag particles in comparison to OPC. Nevertheless, modifying the length of the side chain did not seem to notably enhance the dispersion performance of the PCEs.

The studies mentioned above suggest that modifications to the surface chemistry and ionic strength of the pore solution in AAS pastes can affect the interaction with PCE polymers. This means that it is possible to create PCE molecular structures that are customized to achieve strong surface adsorption in these systems.

- Na_2CO_3 and Na_2SiO_3 activated slag

Earlier studies have emphasized that the rheological properties observed in AAS systems are primarily influenced by the type and concentration of the alkaline activator employed [126]. The consensus is that a slag paste activated with Na_2CO_3 is typically more challenging to disperse compared to a slag paste activated with NaOH. However, current PCE superplasticizers, such as MPEG, APEG, HPEG, and IPEG, do not seem to offer any dispersion in Na_2CO_3 systems. In the study conducted by Conte et al. [119], it was discovered that incorporating 0.5 wt.% MPEG PCE with various molecular architectures had only a slight impact on the fluidity of Na_2CO_3 activated (8 wt.%) slag paste. This limited improvement could be attributed to two factors: first, the insolubility of all PCEs in a 1.67 M Na_2CO_3 solution, and second, the abundant presence of CO_3^{2-} ions, leading to the rapid depletion of Ca^{2+} ions available for PCE polymers. The literature has not

extensively explored the utilization of Na_2SiO_3-activated slag systems. In 1990, Douglas et al. [127] were the first to investigate the effects of sodium lignosulfonate and sulfamate-based superplasticizers on the fluidity of AAS, discovering that neither superplasticizer had an impact on the rheology of Na_2SiO_3-activated slag. Similarly, Puertas et al. [127] found that polyvinyl- and PCE-based superplasticizers did not significantly enhance the workability of Na_2SiO_3-activated slag binders, although they did decrease the strength of the final material.

Currently, there is a significant lack of effective superplasticizers for enhancing the workability of AAS binder systems activated by Na_2CO_3 and Na_2SiO_3, highlighting the need for further investigation in this area. To overcome these challenges, novel polymer structures were explored in this study here.

4.   Experimental materials and methods

Outlined in the diagrams below are the three main stages of the experimental plan for this thesis. The first stage involves characterization of the binder materials, followed by synthesis and quality control of PCEs. The first stage involves the investigation into the interaction occurring between these synthesized PCEs and binder systems.

- **1st stage: determination of the phase composition (Q-XRD analysis) and oxide composition (X-ray fluorescence)**

- **2nd stage: PCE synthesis (via free radical copolymerization) and structural characterization (via GPC & ^{1}H NMR)**
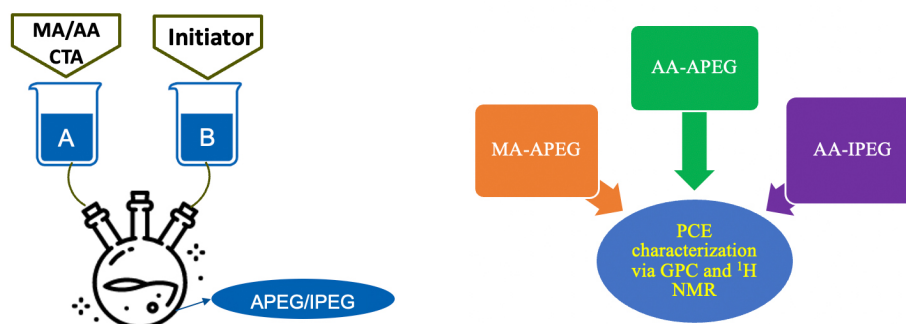
- **3rd stage: investigation of the dispersing effectiveness of the synthesized PCEs and their interaction with different binder systems**

Fludity tests (mini-slump , mortar and rheology)

- To discover the clay robustness of synthesized APEG PCEs in OPC containing bentonite clay
- To identfy the optimal IPEG geometry in the NaOH AAS system via results of mini-slump tests and rheological measurements

Anionic charge amount of polymers

- To determine the anionicity of the synthesized IPEG PCEs
- To detect the calcium binding capacity of structurally differnt APEG polymers copolymerized with either AA or MA

Zeta potentail measurements

- To measure the surface charge variation on OPC and AAS particles upon titration against IPEG PCEs

XRD analysis

- To detect the d-spacing value of bentonite clay occuring in the interlayers after treatment with APEG PCEs

Sorption determination of PCEs via TOC

- To quantitatively examine the amount of PCE intercalated in clay interlayers utlizing NaOH medium instead of SCPS
- To determine the adsorption amount of IPEG PCEs on AAS and OPC

5. Results and discussion

This chapter comprises a series of eight papers, with those in **Sections 5.1** to **5.** 6 already published and those in **Sections 5.7** to **5.8** have reached the final acceptance stage. The primary topic of these papers is the development of customized polycarboxylate ether (PCE) structures for two distinct binder systems: clay-contaminated ordinary Portland cement (OPC) in **Sections 5.1** to **5.3** and **5.7**, and low-carbon alkali-activated slag binders in **Sections 5.4**, **5.6 and 5.8**. These novel binder systems have the potential to replace conventional OPC, which is associated with high energy consumption and significant CO_2 emissions, as discussed in the paper presented in **Section 5.5**. The relevant papers will be discussed in the following.

5.1 Paper # 1

Specific molecular design of polycarboxylate polymers exhibiting optimal compatibility with clay contaminants in concrete

L. Lei, Y. Zhang, R. Li

Cement and Concrete Research, 2021, 147, 106504

This paper focuses on the synthesis and evaluation of a series of allyl ether-based polycarboxylate ether superplasticizers (APEG PCEs) that possess short side chain length of PEG. The main objective of the study was to determine the effectiveness of these PCEs in effectively managing clay impurities in concrete.

The findings showed that APEG PCEs with short side chains exhibited greater resistance to clay contaminants as compared to traditional methoxy polyethylene glycol-based methacrylate polycarboxylate ester superplasticizers (MPEG PCEs) that have long side chains. This was attributed to the lower adsorption, greater solubility, and weaker interaction of APEG PCEs with clay particles, which resulted in reduced loss of dispersing ability and fluidity in concrete.

Furthermore, the impact of various molecular properties, such as molecular weight, anionic charge density, and degree of branching, on the clay tolerance of APEG PCEs was investigated, and it was found that these properties had different effects depending on the type and amount of clay present.

The study suggests that APEG PCEs can be engineered to optimize their compatibility with different types of clay impurities by adjusting their molecular properties.
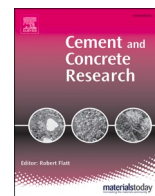
Specific molecular design of polycarboxylate polymers exhibiting optimal compatibility with clay contaminants in concrete

L. Lei [*], Y. Zhang, R. Li

Technische Universität München, Chair for Construction Chemistry, 85747 Garching, Lichtenbergstraße 4, Germany

ABSTRACT

It is widely recognized that the dispersing ability of polycarboxylate superplasticizers (PCEs) could be hindered due to the presence of clay contaminants in concrete. In this study, a series of allyl ether-based polycarboxylate superplasticizers possessing short polyethylene glycol side chains was successfully synthesized and probed for their clay tolerance. The resulting PCE polymers were characterized via Size Exclusion Chromatography (SEC) to obtain their molecular properties. Thereafter, their dispersing ability was probed in the absence and presence of sodium bentonite. Allyl ether-based polycarboxylate (APEG) polymers possessing short side chains were found to exhibit enhanced clay resistance as compared to that of conventional MPEG PCEs holding long pendant chains. The mode of interaction between APEG PCEs and bentonite was investigated via sorption and XRD measurements. The data revealed that APEG PCEs possessing a lower side chain density intercalate less into the interlayer space of bentonite than those exhibiting higher side chain density.

1. Introduction

Polycarboxylate superplasticizers (PCEs) have attracted increasing attention and have been extensively studied in the recent decades [1–3]. Due to the great variability of the polycarboxylate structure, PCEs allow for significant modification of the molecular architecture in order to meet the specific needs of the various applications by the concrete industry [4,5].

From the use of various materials for the manufacture of concrete, PCEs have been found to be very sensitive towards clay contaminants occurring in concrete aggregates [6–10]. This is evidenced by extremely high PCE dosages required to achieve the same fluidity as for the clay-free system. In some cases, even with triple or quadruple dosage of the PCE product, desirable concrete workability cannot be achieved. Obviously, depending on the type of clay which can vary with respect to its composition and physicochemical properties, PCEs can be affected in different ways by such minerals [11]. More specifically, PCE polymers can interact with clay minerals via surface adsorption and/or chemical intercalation. In the case of sodium bentonite, both effects will occur, with intercalation being vastly dominant. The mechanism appears to involve partially polarized polyethylene glycol pendant chains anchoring on the silanol groups present on the surface of the aluminosilicate layers via H-bonding mediated by water molecules [12]. The

specific interaction between superplasticizers and clay minerals is typically evidenced by powder X-ray diffraction analysis [13]. Typically, a change in the *d*-spacing from initial 1.23 nm (sodium montmorillonite without superplasticizer) to 1.72 nm can be detected when polycarboxylate superplasticizers with polyethylene side chains are present, which confirms the intercalation mechanism [13]. In a very recent study, Borralleras et al. tested the fresh clay samples admixed with various dosages of PCE polymer via in situ XRD measurements and proposed a multiple intercalation model of polyethylene glycol (PEG) side chains, which offers a more robust methodology [14,15]. Moreover, it has been reported that the sorbed amounts of PCE superplasticizers on swelling clay are ~100 times higher than on Portland cement [16]. Consequently, PCE performance is severely hindered in the presence of clay, and developing PCE polymers exhibiting high resistance to the negative effect of clay contaminants in aggregates remains as a research priority [17].

Looking into the literature, a handful of studies have attempted to establish mitigation strategies for the clay problem [8,11,13,16,18–23]. For instance, several reports [18] have indicated that addition of polyethylene glycol (PEG) as a sacrificial agent to the clay contaminated cement pastes can hinder the intercalation of PCE completely, and the dispersion capability and workability retention could be maintained. However, the dosage of the sacrificial agent required is extremely high

which renders this approach economically unfeasible. Another approach is to admix a clay tolerant PCE having a modified structure. For example, Lei et al. [13] synthesized novel PCE superplasticizers possessing HAMA (hydroxyl alkyl methacrylate) side chains instead of PEG pendants for enhanced robustness towards clay. This new structure was found to provide good dispersing ability in cement pastes in the presence of clay and was much less affected by montmorillonite as compared to conventional PCEs with polyethylene oxide (PEO) side chains. Unfortunately, due to its extremely short pendant chains, its addition rate required in a clay-free system was relatively high. For another case of modifying the PCE side chains, Xu et al. [24] incorporated a three dimensional β-cyclodextrin into the structure of an HPEG (α-methallyl-ω-hydroxy poly(ethylene glycol)) PCE. Because of this modification, the PCE structure exhibiting bulky side chains could not enter the interlayer structure of montmorillonite. Consequently, the clay robustness of such PCE structure is much enhanced. However, the process of cement hydration was inevitably delayed and a lower hydration heat value was monitored when such bulky groups are incorporated [25].

It is widely accepted that certain clays expand when in contact with water and this accounts for the loss in dispersing efficiency of PCE polymers. A completely new concept to mitigate the clay problem is to prohibit the swelling of clay, in consequence, the intercalation of PCE would be hindered. Jacquet et al. [26] presented that various organic cations, i.e. quaternary amine [27], exhibited a strong affinity for cationic exchange with clay and can be used as clay-activity-modifying agents. In a similar manner, Lawrence et al. [28,29] reported to use cationic copolymers for inerting clays in sand aggregates which are used in concrete. It was found that the cationic polymers would shield the detrimental effects of swelling clays in the concrete and consequently enhance properties, such as workability and fluidity in the cementitious compositions.

Admittedly, a great need exists for suitable PCE polymers with high dispersion ability which are not affected by the presence of clay. In this study, we have synthesized allyl ether-based PCEs with particularly short PEO side chains and further studied their clay tolerance through a series of performance tests. The mode of interaction between allyl ether-based polycarboxylate superplasticizers and montmorillonite was further investigated via sorption and XRD experiments. The sorption behavior of these newly prepared allyl ether-based PCEs was compared with that of β-naphthalene sulfonate (BNS) and a typical MPEG-based PCE superplasticizer with long PEO side chains. The overall goal of this investigation is to identify a specific polycarboxylate molecular design that exhibits tolerance with montmorillonite clay.

2. Experimental

2.1. Materials

2.1.1. Chemicals

Acrylic acid (AA) (>99% purity, Sigma-Aldrich, Germany), α-allyl-ω-hydroxy poly (ethylene glycol) ether (APEG macromonomer, $n_{EO} = 7$) (>98%, NOF Corporation, Japan), ω-methoxy poly (ethylene oxide) methacrylate ester (MPEG macromonomer, $n_{EO} = 45$) (>98%, Clariant, Germany), ammonium persulfate (≥98%, Sigma-Aldrich, Germany), sodium methallyl sulfonate (>98%, Sigma-Aldrich, Germany), 3-mercaptopropionic acid (≥99%, Sigma-Aldrich, Germany), and sodium hydroxide (≥97%, Merck KGaA, Germany) were all used without further purification.

In addition, one MPEG-based PCE and one β-naphthalene sulfonate formaldehyde polycondensate (BNS) were tested and used as reference admixture in this study. The self-synthesized MPEG-PCE, identified as 45PC6 was obtained through aqueous free radical copolymerization of acrylic acid and ω-methoxy poly (ethylene oxide) methacrylate ester with methallyl sulfonic acid added as a chain transfer agent. The molar ratio between acrylic acid and MPEG macromonomer was 6:1, and the side chain consisted of 45 ethylene oxide units. A detailed description of

Table 1
Phase composition of the OPC sample CEM I 42.5 R by Q-XRD using *Rietveld* refinement.

Phase	wt%
C_3S, monoclinic	54.52
C_2S, monoclinic	18.41
C_4AF, orthorhombic	10.85
C_3A, cubic	5.23
C_3A, orthorhombic	0.88
Anhydrite ($CaSO_4$)	0.94
Dihydrate ($CaSO_4 \cdot 2H_2O$)	3.61
Hemihydrate ($CaSO_4 \cdot 0.5H_2O$)	0.33
Calcite ($CaCO_3$)	3.04
Dolomite ($CaMg(CO_3)_2$)	1.13
Quartz (SiO_2)	0.91
Free lime (*Franke*)	0.14
Total	100.00

Table 2
Oxide composition of the bentonite sample as determined by XRF.

Oxide	wt%
SiO_2	55.7
Al_2O_3	16.2
Fe_2O_3	3.5
CaO	3.0
Na_2O	2.0
MgO	1.4
K_2O	0.9
TiO_2	0.3
BaO	0.1
P_2O_5	0.1
MnO	0.1
SrO	0.1
SO_3	0.1
LOI	16.5
Total	100.00

Fig. 1. XRD pattern of the raw clay (M: montmorillonite; C: clinoptilolite-Ca; I: illite; Q: quartz; C′: calcite).

the preparation can be found in reference [30]. In our study, methacrylic acid was substituted by acrylic acid. The BNS polymer is an industrial product commercialized under the trade name FLUBE CA 40 and was obtained from Bozzetto Group, Italy.

2.1.2. Cement

The cement used in this study was an ordinary Portland cement (OPC) sample CEM I 42.5 R. The phase composition as shown in Table 1 was determined by quantitative XRD analysis with *Rietveld* refinement. The average particle size (d_{50} value), obtained by laser granulometry, was 18.83 μm. The density was determined to be 3.13 g/cm³ (by Helium pycnometry).

Table 3

Mineralogical composition of the clay sample via Q-XRD.

Compositions	Montmorillonite	Clinoptilolite-Ca	Illite	Quartz	Calcite
Proportion (%)	80.56	11.21	2.62	4.45	1.15

2.1.3. Clay

An artificial sodium bentonite sample (BYK, Wesel, Germany), which represents a common contaminant in aggregate sources, was selected for this investigation. The oxide composition was determined by X-ray fluorescence and is shown in Table 2. The mineralogical composition was determined by Q-XRD via *Rietveld* refinement as shown in Fig. 1 and Table 3. The particle size distribution of the raw clay is illustrated in Fig. 2, with its d_{50} value of 23.55 μm.

2.2. Synthesis of AA-APEG polycarboxylate polymers

For this study, a series of AA-APEG PCEs possessing the same side chain length but different AA:APEG macromonomer ratios was synthesized according to the molar ratio of AA to APEG. As an example, the detailed synthesis procedure for AA-7APEG4.5 (molar ratio AA: APEG = 4.5:1, $n_{EO} = 7$) is as follows.

At first, 25 g (0.066 mol) of APEG macromonomer ($M_w = 350$ g/mol) and 45 mL of deionized (DI) water were placed in a five-neck flask, which was connected to a reflux condenser, a mechanical stirrer, a nitrogen inlet and two separated feeding inlets. The reaction vessel containing the macromonomer solution was heated to 80 °C and flushed with N_2 for 30 min. Next, two feeding solutions (Solution A and Solution B) were prepared. 21.334 g (0.30 mol) of acrylic acid and 0.225 g (0.002 mol) of 3-mercaptopropionic acid (chain transfer agent) were dissolved in 25 mL of DI water. This solution mixture was named as Solution A. Solution B was prepared by dissolving 5.629 g (0.025 mol) of ammonium persulfate in 30 mL of DI water. Solutions A and B were added dropwise into the reaction vessel using two peristaltic pumps via inlet A over 2.5 h and via inlet B over 3 h respectively. When the addition of solution B had finished, the mixture continued to sit for another hour. Finally, the reaction solution was cooled to ambient temperature and the pH was adjusted to 6.5–7 with 30 wt% sodium hydroxide solution. The

solids content of the final solution was 35 wt%, and was used without further purification.

AA-7APEG2 as well as AA-7APEG15 were synthesized in a similar manner as described above, including the molar ratios of 3-mercaptopropionic acid (chain transfer agent) and ammonium persulfate (initiator). Only the molar ratio of AA:APEG macromonomer varied depending on the designed structure.

2.3. Characterization of AA-APEG polycarboxylate polymers

2.3.1. Size exclusion chromatography (SEC)

Molar mass (M_w and M_n), the polydispersity index (PDI) and macromonomer conversion of the synthesized ether-based PCEs were determined by size exclusion chromatography, also referred to as gel permeation chromatography (GPC). The measurements were performed with a Waters Alliance 2695 instrument (Waters, Eschborn, Germany) equipped with three Ultrahydrogel™ columns (120, 250, 500) and an Ultrahydrogel™ Guard column. The eluent was a 0.1 N $NaNO_3$ (pH = 12) with a flow rate of 1.0 mL/min. For the calculation of M_w and M_n, a dn/dc value of 0.135 mL/g (value for PEO) was utilized [31].

2.3.2. ^1H NMR spectroscopy for structural analysis

^{1}H NMR spectroscopy was used to analyze the structure of the synthesized PCEs. ^{1}H NMR (16 scans, 1 s relaxation delay) were measured on an AVANCE-III 400 MHz NMR spectrometer (Bruker BioSpin GmbH, Karlsruhe, Germany). Prior to measurement, APEG macromonomers and PCE samples were freeze dried overnight at −50 °C at 0.37 mbar. The powdered samples (~0.1 g) were dissolved in 0.4 mL D_2O.

2.3.3. Anionic charge amount measurement

The specific anionic charge amount of the synthesized PCEs was determined using a particle charge detector PCD 03 pH (Mütek Analytic, Herrsching, Germany). Here, 10 mL of the 0.2 g/L PCE solution were titrated with a 0.34 g/L aqueous solution of cationic poly-diallyl dimethyl ammonium chloride (polyDADMAC) until charge neutralization (zero potential) was reached. Then the anionic charge per gram of PCE polymer was derived from the consumption of the cationic polyelectrolyte polyDADMAC [32].
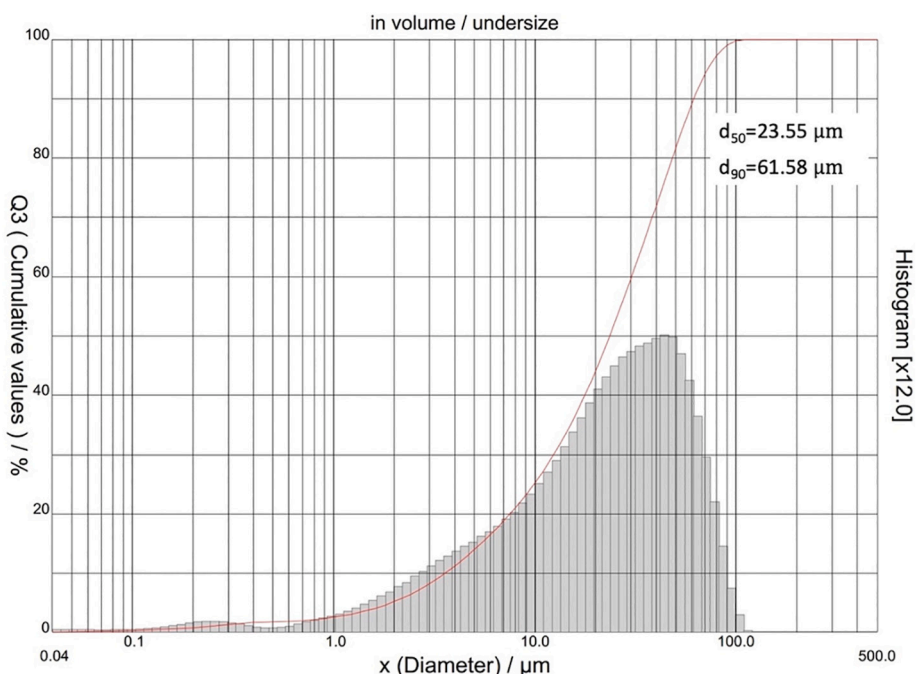
Fig. 2. The particle size distribution of the raw clay determined by laser granulometry.
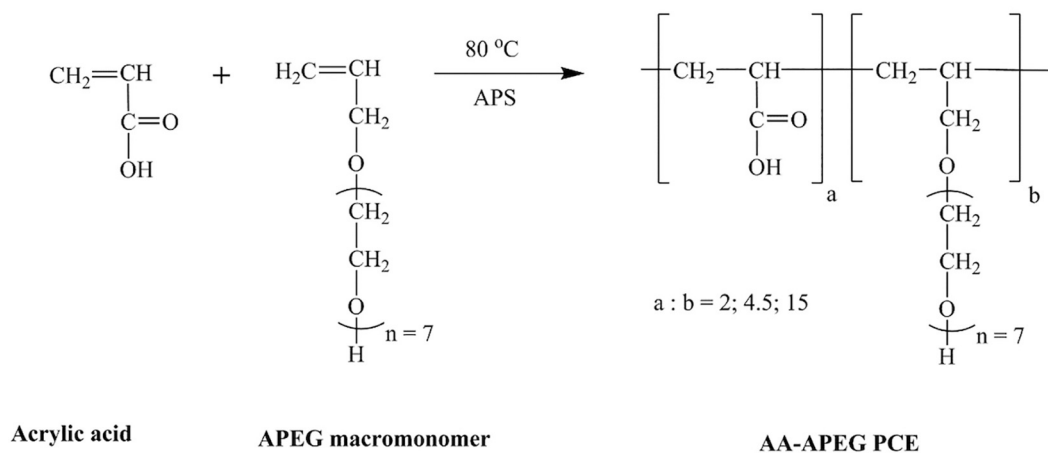
Fig. 3. Synthesis route for the preparation of the AA-APEG PCEs.

2.4. Dispersing performance in cement pastes with/without bentonite clay

For the evaluation of the dispersing effectiveness of the PCEs in cement, a 'mini slump' test was employed, which is described in DIN EN 1015 standard. At first, the water-to-cement (w/c) ratio of the paste without polymer to achieve a spread of 18 ± 0.5 cm was determined. At this w/c ratio, the dosage for each PCE sample to reach a spread flow of 26 ± 0.5 cm was determined.

The test was carried out as follows: The polymer was firstly mixed with DI water in a porcelain cup, whereby the water contained in the polymer solution was subtracted from the amount of mixing water. Then 300 g cement were added to the mixing water within 1 min, the mixture remained at rest for 1 min followed by 2 min of manual stirring. Thereafter, the cement paste was poured into a Vicat cone (height 40 mm, top diameter 70 mm, bottom diameter 80 mm) placed on a glass plate and the cone was quickly lifted vertically. Once the cement paste had stopped flowing, the spread flow was measured twice at two angles perpendicular to each other. Finally, the averaged spread flow of these two values was recorded as the spread flow value.

When the clay tolerance tests were performed, a similar procedure was followed and 1 wt% or 3 wt% of the cement was replaced by sodium bentonite.

2.5. PCE sorption on clay

The sorption of PCEs by sodium bentonite was determined in synthetic cement pore solution (SCPS, pH = 13.06) [13] and 0.1 M NaOH solution by means of total organic carbon (TOC) based on the depletion method. In principle, the amount of non-adsorbed portion of PCEs present in the solution in the equilibrium state was quantified by TOC. The sorbed portion can then be calculated by subtracting the quantity remaining in the supernatant from the amount added.

To further differentiate between physical surface adsorption and chemical intercalation, two fluid systems were chosen, namely a synthetic cement pore solution (SCPS) and 0.1 M sodium hydroxide (NaOH) solution to perform the sorption measurements.

In a typical experiment, 0.25 g of bentonite, 12 g of synthetic cement pore solution or 0.1 M NaOH solution (w/clay ratio = 48) and the different amounts of designated polymers were transferred into a 50 mL centrifuge tube and shaken in a wobbler (VWR International, Darmstadt, Germany) for 2 min at 2400 rpm, then centrifuged for 10 min at 8500 rpm. The resulting supernatant was then removed using a syringe, filtered through a 0.2 μm polyethersulfone syringe filter (Model FPS250020, Graphic Controls, New York, USA) and diluted 20–30 times with DI water. The TOC measurement was conducted on a High TOC II instrument (Elementar Analysensysteme, Hanau, Germany) at the

temperature of 890 °C. The average of the sorbed amount at each concentration was calculated from at least two duplicate measurements.

2.6. XRD analysis

To verify whether the polycarboxylates had chemically incorporated in between the aluminosilicate layers of sodium bentonite, XRD analysis was performed. In a typical test, 0.5 g of clay and 24.25 g of 1.03 wt% PCE solution were added into a 50 mL centrifuge tube, shaken in a wobbler (VWR International, Darmstadt, Germany) for 2 min at 2400 rpm and then centrifuged for 10 min at 8500 rpm. The solid substance at the bottom was dried overnight at 50 °C in an oven, followed by being ground into powder as required for the measurement. The instrument for these XRD measurements was a D8 Advance, Bruker AXS instrument (Bruker, Karlsruhe/Germany) based on Bragg-Brentano geometry. Each sample to be scanned was placed on a mounted round plastic holder. The parameters for the scanning procedure were set as follows: step size of 0.15 s/step, scan spin at a revolution time of 4 s, 0.3° of aperture slit, scan ranging from 0.6° to 20° 2θ, using CuKα, $\lambda = 1.5418$ Å.

2.7. Zeta potential measurement

Measurements of initial zeta potential were performed on a "DT 1200 Electroacoustic Spectrometer" manufactured by Dispersion Technology, Inc., Bedford Hills, NY, USA. The solution-to-clay ratio was set to 48:1, same as in the TOC tests. A clay slurry containing 6 of clay and 288 mL of 0.1 M NaOH (pH = 13) or 288 mL of SCPS (pH = 13) was prepared. The mixture was manually stirred for 4 min and then transferred into the container of the zeta potential instrument with stirring rate of 200 rpm.

2.8. Adsorbed layer thickness of polycarboxylate polymers

To investigate the effect of Ca^{2+} cations on the sorption of polycarboxylate polymers on negatively charged substrates, i.e. clay, the adsorbed layer thickness (ALT) of a PCE polymer was determined in Ca^{2+} and Ca^{2+} free medium. 1% wt. PCE polymer (AA-7APEG 4.5) was dissolved in 0.1 M aqueous NaOH and mixed with their charge equivalent amounts of Ca^{2+} added as $CaCl_2 \cdot 2H_2O$ [33]. In a separate solution, 1 wt% PCE polymer (AA-7APEG 4.5) was dissolved in 0.1 M aqueous NaOH without any Ca^{2+} addition. Both stock solutions were then diluted to prepare a series of PCE concentrations from 0.1–1.5 g/L in a volume of 50 mL. Thereafter, 50 μL of polystyrene nanoparticle were added into the PCE solutions with various concentrations. The polystyrene nanoparticle was prepared according to the literature [33]. The opaque dispersions were subjected to ultrasonication for 15 min and remained at rest for 15 min before the diameter determination with dynamic light
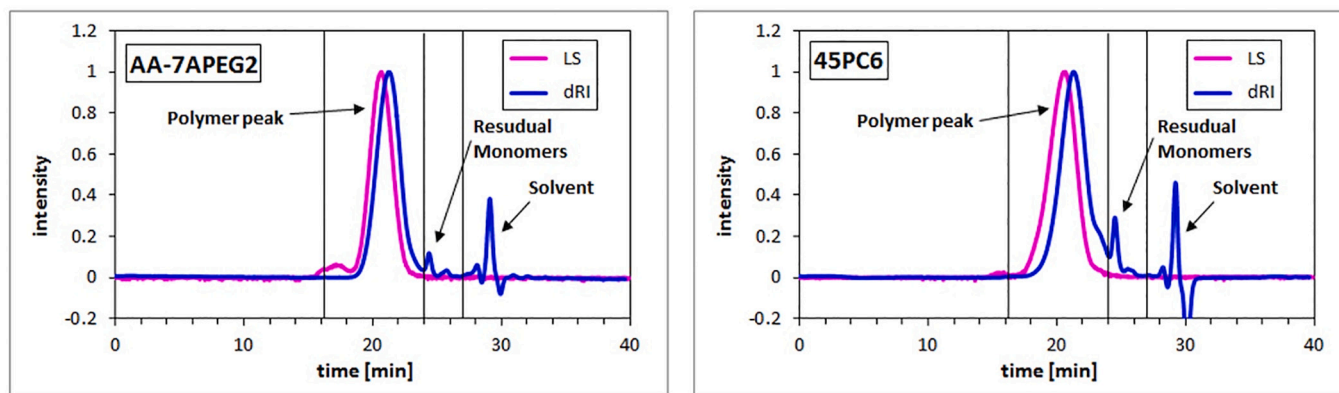
Fig. 4. Size exclusion chromatograms of PCE samples AA-7APEG2 and 45PC6 (MPEG type PCE).

Table 4
Characteristic molecular parameters of the synthesized PCE polymers.

Polymer sample	M_w [Da]	M_n [Da]	PDI	Macromonomer conversion
AA-7APEG2	6700	4000	1.7	91%
AA-7APEG4.5	12,000	6800	1.7	93%
AA-7APEG15	18,000	9900	1.8	97%
45PC6	16,920	8295	2.0	93%

scattering on the ZetaSizer Nano ZS instrument. The corresponding diameters of polymer free polystyrene nanoparticles were measured before each sample measurement. The adsorbed layer thickness of PCE was calculated according to the following equation:

$$ALT = (D_1 - D_0)/2,$$

where D_1 was defined as the particle diameter with adsorbed PCE, and D_0 was noted for the pristine particle diameter.

3. Results and discussion

3.1. Molecular properties of the synthesized AA-APEG PCE polymers and the reference samples

A series of AA-APEG copolymers exhibiting different anionicity was synthesized via aqueous free radical copolymerization of acrylic acid and α-allyl-ω-hydroxy poly (ethylene glycol) ether (APEG, M_w = 350 g/mol). The synthetic route is displayed in Fig. 3.

The molecular characteristics of the resulting APEG PCE polymers were determined via Size Exclusion Chromatography (SEC). In Fig. 4, as examples, the SEC spectra of one APEG PCE polymer (AA-7APEG2) and the comparative PCE sample 45PC6 are displayed.

The molar masses (M_n, M_w), polydispersity index (PDI) and conversion rate of the macromonomer are summarized in Table 4. The three synthesized anionic AA-APEG PCE polymers differ with respect to their AA:APEG ratio, thus possess different anionic charge amounts.

According to the SEC data in Table 4, all synthesized PCE polymers exhibited properties that are characteristic for high-quality PCE polymers, namely relatively low PDIs (≤2), and high macromonomer conversions (>90%). Additionally, the molecular weights (M_w) of all synthesized PCE polymers lie in the range up to 20,000 Da which is comparable to the reference copolymer 45PC6. The molecular weight of PCEs is understood to significantly impact their dispersing effectiveness [34,35].

In order to further characterize the structure of the synthesized APEG polymers, ^{1}H NMR measurements were performed, the spectra are illustrated in Fig. 5 and the calculated parameters are summarized in Table 5.

As shown in the ^{1}H NMR spectrum of APEG macromonomer, the δ (chemical shift) for group C ($-CH_2O-$) and group D [$-(CH_2CH_2O)-$] are at 4.0 ppm and 3.4–3.8 ppm, respectively. Here, we assume the integral intensity of D is 1, the intensity of C is calculated as 0.07. Hence, the number of EO units approximately equals to 7. Next, to determine the conversion rate of APEG macromonomer for the three synthesized APEG PCE polymers, the integral intensity of D is set to 1 since [$-(CH_2CH_2O)_7-$] remains unchanged during the polymerization process. The integral intensity of C varies before and after the copolymerization process. The corresponding conversion ratio of APEG macromonomer for each APEG PCE polymer was calculated according to the formula: $\frac{C(APEG\ MM) - C(PCE\ copolymer)}{C(APEG\ MM)}$.

The calculated values for all three APEG PCE polymers are listed in Table 5.

Furthermore, the conversion rate of AA could also be obtained from ^{1}H NMR spectroscopy. Similarly, the integral intensity of D is set to 1. Group a ($CH_2=$) in AA is selected as the trigger group to calculate the conversion. In the AA-APEG PCE copolymer, the residual AA is detected since a signal at 6.0 ppm appears which can be assigned to $CH_2=$ group (a). And the reacted group a′ (CH_2-) in the PCE copolymer shows a signal at 1.5 ppm. However, group B ($-CH=$) in unreacted APEG macromonomer also appears at 6.0 ppm. The group A′ ($-CH_2-$) from the reacted APEG macromonomer shows a signal at 1.5 ppm. In combination with the conversion rate of APEG macromonomer, the conversion rate of AA for the AA-7APEG PCE polymers can be calculated accordingly (see Table 5).

Based on the conversion rates of AA as well as APEG macromonomer, the actual molar ratios of AA:APEG macromonomer for three AA-APEG PCE copolymers were calculated accordingly. As can be seen in Fig. 5, the actual composition of the synthesized PCE polymers are very close to the designed polymer structure.

3.2. Anionic charge characteristics of synthesized PCE polymers

Anionic charge amount measurements were conducted in 0.01 M NaOH (pH = 12) [32]. The ability of a PCE to adsorb onto the surfaces of cement hydrates has a direct influence on their dispersing effectiveness in concrete. In this study, a correlation between the charge characteristics of the PCE polymer and their sorption behavior on sodium bentonite was evaluated.

As is presented in Fig. 6, the charge amount of the synthesized APEG PCEs increases with increasing AA: APEG molar ratio stemming from the higher number of carboxylic groups in the PCE polymer.

3.3. Dispersing ability of PCEs in neat cement paste (w/o clay)

The dispersing power of the newly synthesized AA-APEG copolymers was evaluated by a 'mini slump' test according to DIN EN 1015. The
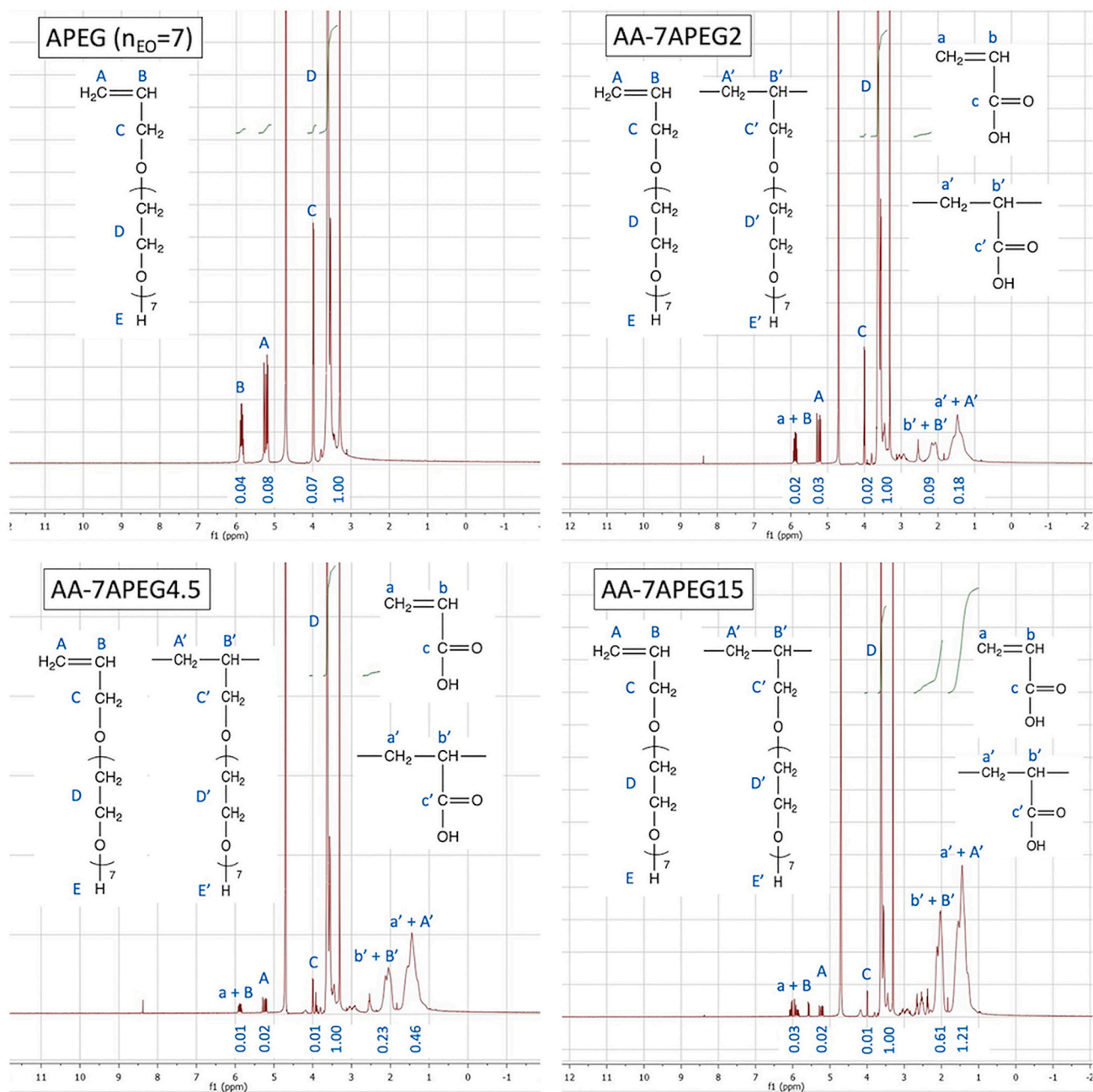
Fig. 5. The ^{1}H NMR spectra of APEG macromonomer and the synthesized AA-APEG PCE copolymers.

Table 5
Structural analysis of the AA-APEG PCE polymers and the monomer conversion rates determined via ^{1}H NMR spectroscopy.

PCE samples	Feeding molar ratio	Actual molar ratio	EO units	APEG conversion [%]	AA conversion [%]
AA-7APEG2	2:1	2.6:1	7	71	93
AA-7APEG4.5	4.5:1	4.6:1	7	86	99
AA-7APEG15	15:1	17:1	7	86	98

reference dispersants 45PC6 and BNS were chosen as the comparative samples for the fact that 45PC6 represents a highly effective PCE polymer which is commonly used in cement and concrete whereas BNS is a widely used polycondensate which is far more tolerant with clay contaminants.

In the following tests, the dosages required for various cement dispersants to achieve a cement paste spread of 26 ± 0.5 cm were determined (Fig. 7). Among them, polymer 45PC6 required the lowest dosage (appr. 0.07% bwoc (by weight of cement)) to obtain the required target, while the dosage increased to 0.26% bwoc in the case of BNS. Compared with these two reference samples, the AA-APEG series required higher dosages than that for 45PC6. The required dosages for AA-7APEG2 and AA-7APEG4.5 were 0.15% bwoc and 0.12% bwoc, respectively. 45PC6 polymer was expected to outperform the short side

Fig. 6. Anionic charge amounts of the synthesized PCE polymers.

Fig. 7. Dosages of the synthesized AA-APEG copolymers, 45PC6 and BNS samples required to achieve a cement paste spread of 26 ± 0.5 cm (w/c = 0.48).

Fig. 8. Spread flow of cement pastes (w/c = 0.48) containing different superplasticizers, measured in the absence and presence of 1% bwoc of clay.

Fig. 9. Spread flow of cement pastes (w/c = 0.48) containing different superplasticizers, measured in the absence and presence of 3% bwoc of clay.

polycarboxylates and BNS were evaluated with dosages determined from the 'mini slump' tests in neat cement pastes. As expected, each cement dispersing polymer exhibits a different degree of tolerance to bentonite which is presented in Figs. 8 and 9.
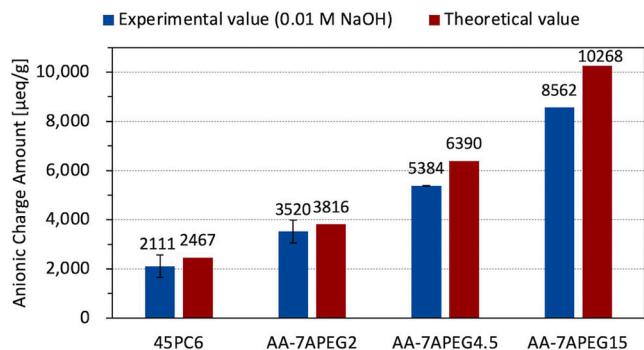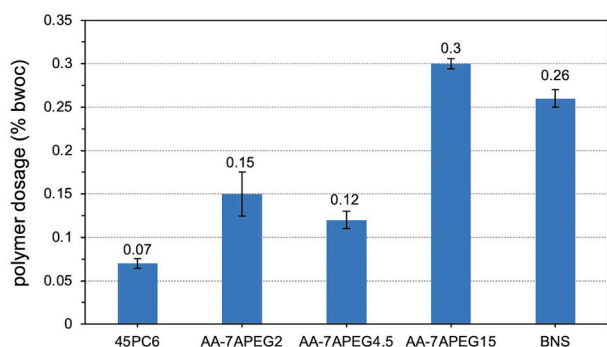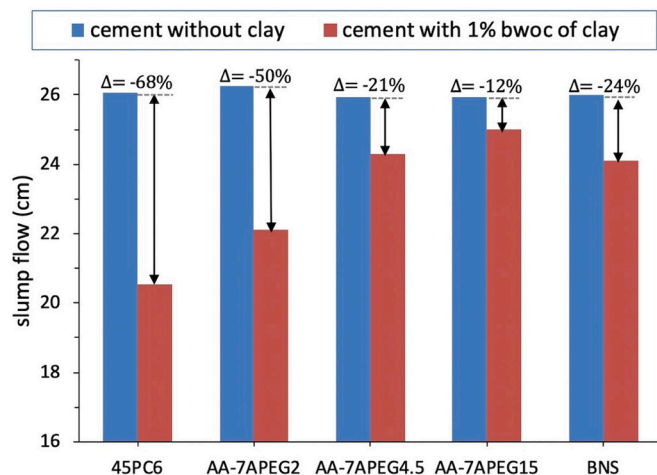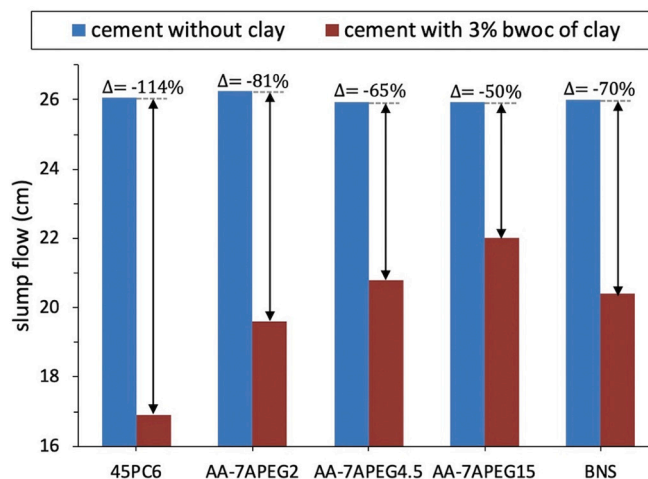
Polymer 45PC6 among all tested samples was affected the strongest by sodium bentonite, in which case the slump flow dropped from 26 cm to 20.6 cm (68% decrease in its dispersing efficiency). Furthermore, in the presence of 3 wt% of bentonite, the spread flow of cement paste prepared with 45PC6 decreased to 16.8 cm, a 114% loss in its effectiveness. As expected, in comparison to 45PC6, BNS was much more resistant to the bentonite, whose spread flow only decreased to 20.6 cm even in the presence of 3 wt% of bentonite.

The aforementioned difference of these two polymers in the dispersing power in the presence of bentonite could be ascribed to their different interaction modes with bentonite. As for the PCE sample 45PC6, its polyethylene glycol side chains can easily incorporate into the interlayer structure of bentonite, hence less PCE polymer is available to provide adequate dispersing force between hydrating cement grains. Whereas, the dispersing power of BNS is hindered only via adsorption onto the surface of bentonite, and is not negatively impacted by intercalation.

All AA-APEG PCE samples exhibited better clay resistance than the MPEG PCE sample 45PC6, although they all contain polyethylene glycol side chains. Especially the more anionic polymers AA-7APEG4.5 and AA-7APEG15 exhibited excellent clay tolerance, even better than that of BNS. In the presence of 1 wt% of sodium bentonite, the efficiency loss ratio for AA-7APEG4.5 and AA-7APEG15 is 21% and 12% respectively, in comparison to that of BNS which had a 24% loss. A similar trend can be observed in the presence of 3 wt% of sodium bentonite. Furthermore, a clear correlation between the anionic character and clay tolerance is observed. Apparently, AA-APEG PCEs possessing higher anionic charge exhibit enhanced clay tolerance.

Furthermore, to detect whether the absolute quantity of PCE itself would exert the influence on the fluidity of cement in the presence of clay, the normalized PCE dosage of 0.15% bwoc was selected to probe its dispersing capacity as well as clay tolerance. As shown in Fig. 10, different superplasticizers exhibited various dispersing capacity in cement pastes in the presence of 1% and 3% bwoc of clay. The cement pastes in the presence of 1% bwoc clay exhibited a spread flow of 16 cm without any polymer. When the same dosage of polymers were applied, 45PC6 reached a spread flow as high as 28 cm. However, it was worth noting that its dispersing power declined the most (−73%) among all the polymers, when another 2% bwoc of clay were added to the system. In

chain AA-APEG PCE polymers because of the relatively long pendant chains ($n_{EO} = 45$ for 45PC6 vs. $n_{EO} = 7$ for AA-APEG series). The highest dosage was recorded for the AA-7APEG15 polymer which required 0.3% bwoc to achieve the required spread flow. This can be ascribed to a very low side chain density producing a relatively weak steric hindrance effect on cement, the primary dispersion mechanism associated with polycarboxylates [4].

3.4. Dispersing effectiveness of superplasticizers in the presence of 1 or 3 wt% bentonite
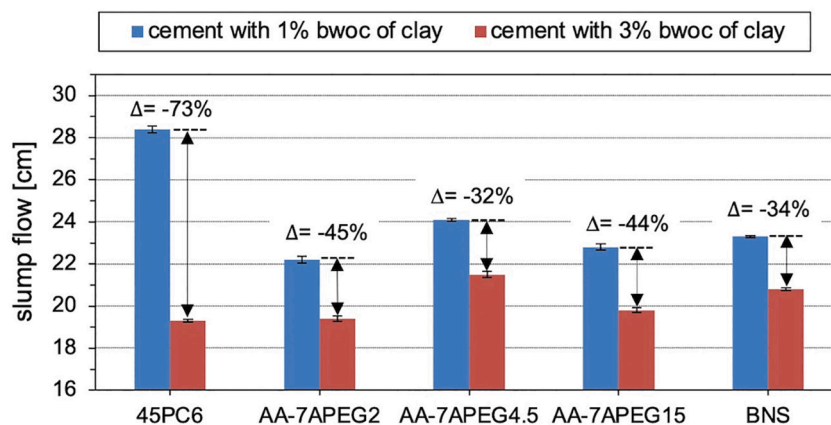
For the cement pastes, the dispersing effectiveness of

Fig. 10. Spread flow of cement pastes (w/c = 0.48) at the same dosage (0.15% bwoc) of various polymer samples, measured in the presence of 1% and 3% bwoc of clay.
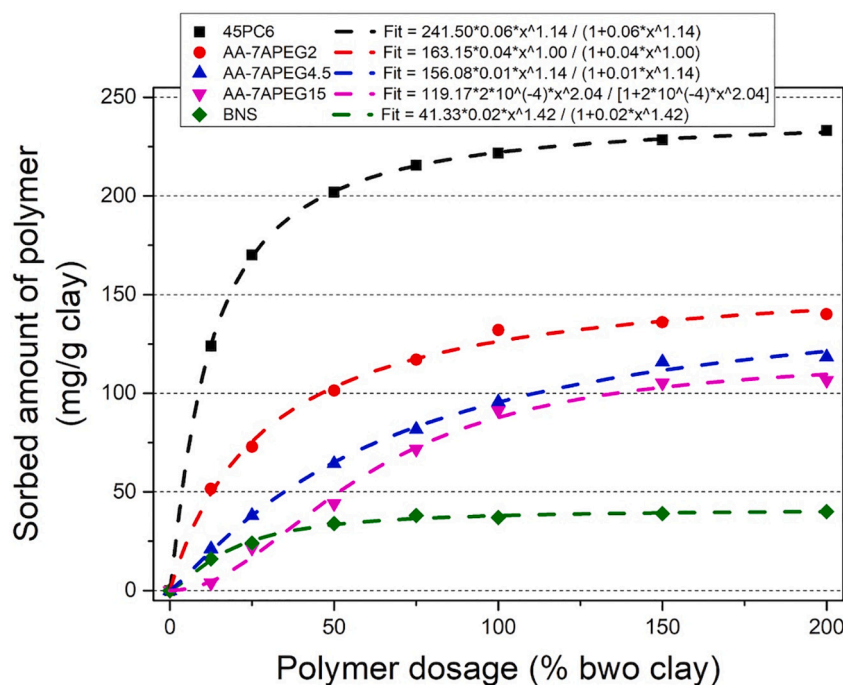
Fig. 11. Sorption isotherms for various polymer samples with sodium bentonite dispersed in synthetic cement pore solution (pH = 13, solution/clay ratio = 48). The Langmuir isotherm here is plotted with the specified solid-liquid ratio on the x-axis for the explicit interpretation of sorption behaviors of polymer on clay. The Langmuir plots normalized with solution concentration on the x-axis and corresponding equations are presented in the supplementary material.

comparison, the three synthesized AA-APEG copolymers showed better resistance against the further addition of clay than that of 45PC6. Furthermore, among all AA-APEG PCE polymers, AA-7APEG4.5 showed the lowest decrease in the dispersing power (−32%) which is even better than that of the BNS sample (−34%). Although AA-7APEG15 possessed lower side chain density than AA-7APEG4.5, but it exhibited higher loss in spread flow (−44%) than the latter polymer at the same dosage. Based on the results here, AA-7APEG4.5 exhibited better clay tolerance than AA-7APEG15 at the same dosed amount.

To summarize, AA-APEG PCEs with shorter side chains exhibit higher tolerance to sodium bentonite as compared to an MPEG PCE with longer side chains. Furthermore, among these AA-APEG PCEs with short PEO side chains, PCEs with lower side chain density generally possessed improved clay resistance. However, when the clay robustness of AA-APEG PCE polymers were compared at the same dosed amount, PCEs with medium side chain density exhibited the best performance.

3.5. Sorption on clay

To investigate the interaction between the individual super-plasticizers and bentonite quantitatively, Langmuir sorption isotherms in synthetic cement pore solution were conducted as shown in Fig. 11.

According to the sorption isotherms, sodium bentonite exhibited an extremely high affinity for the MPEG PCE 45PC6, which was adsorbed at an extremely high amount ~241.5 mg/g at equilibrium. The high affinity for PCE 45PC6 can be attributed to two effects: (1) chemisorption of the relatively long PEO side chain into the layered structure of bentonite, and (2) surface adsorption onto the bentonite. In contrast, BNS exhibits the lowest sorbed amount at equilibrium which lies at ~41 mg/g of clay. As for the AA-APEG PCE series, their saturated sorbed amount varies between 110 and 170 mg/g clay which is nearly half of the sorbed value as compared to PCE sample 45PC6. This result indicates a weak interaction between the AA-APEG PCEs and sodium bentonite.
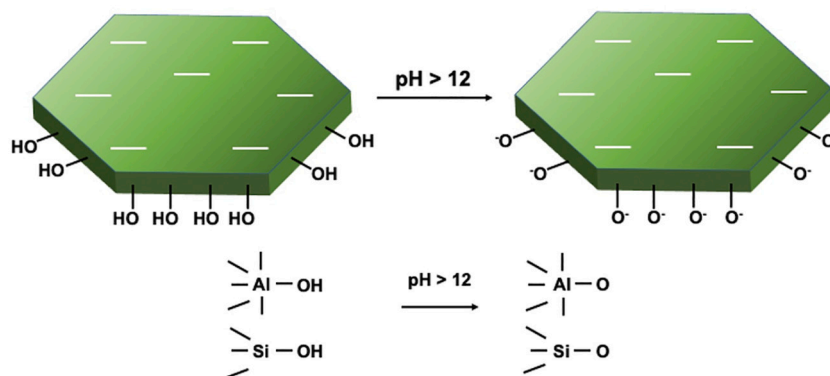
Fig. 12. Schematic illustration of charge distribution of a montmorillonite particle. The basal planes carry permanent negative charge, whereas edge faces exhibit pH-dependent behavior. Reproduced with permission from [16].
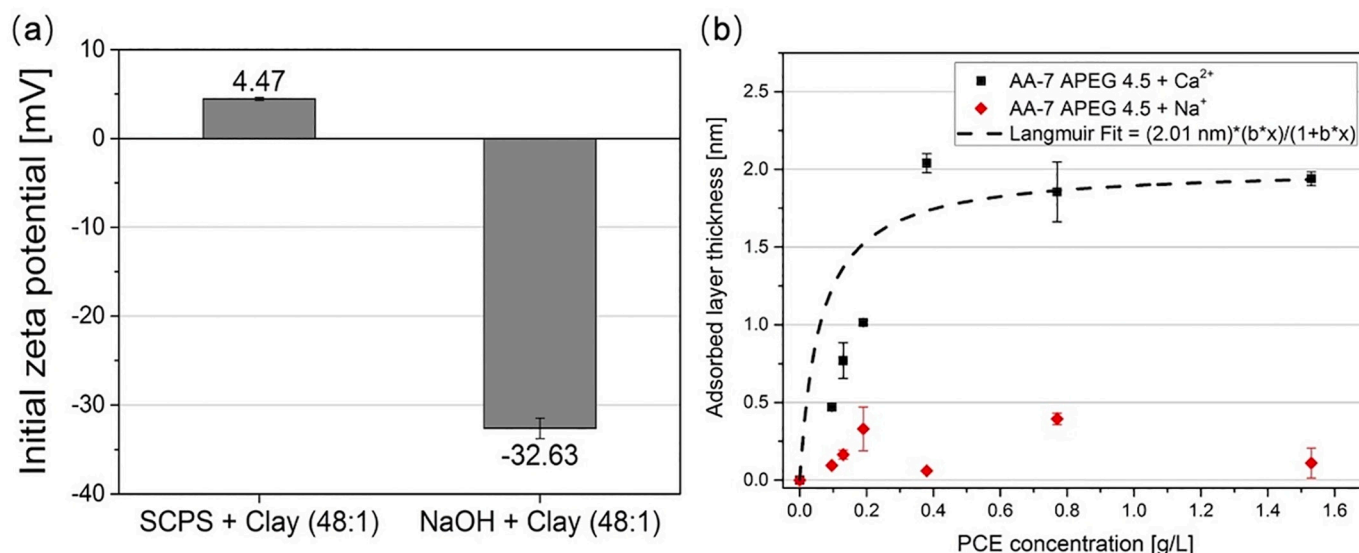
Fig. 13. (a) Initial Zeta potential of bentonite sample dispersed in SCPS and NaOH solution; (b) Adsorbed layer thickness of AA-7APEG4.5 determined in 0.1 M NaOH solution (pH = 13) with or without Ca^{2+} [33].

Furthermore, the lower side chain density of the AA-APEG PCEs leads to a lower amount sorbed on bentonite which is in line with the clay tolerance tests. There, we found that AA-APEG PCEs possessing lower side chain density generally exhibited increased clay tolerance (Figs. 8 and 9).

In above we have intensely discussed the interaction between the various superplasticizer polymers and the bentonite sample, however for the individual mineralogical components including montmorillonite, clinoptilolite-Ca, illite etc. they would exhibit different mode of interaction with the PCE polymers. For example, montmorillonite represents a typical expandable 2:1 clay mineral, and interacts with PCEs in two different manners, namely, surface adsorption and chemisorption. In contrast, illite which belongs to a typical non-swelling 2:1 dioctahedral clay, can only interact with PCE polymers via surface adsorption [11].

3.6. Chemisorption of PCE polymers on bentonite

In order to quantify the portion of PCE being intercalated into the layered structure of bentonite, the amount adsorbed from a 0.1 M NaOH solution instead of in synthetic cement pore solution was measured.

The unique charge heterogeneity of bentonite platelets has been well known for decades [36]. The basal surfaces of the clay minerals (i.e. montmorillonite, kaolinite, mica) often carry permanent negative

charges resulting from the isomorphic substitution within the particles, whereas edge surfaces show pH-dependent colloidal behavior [36]. Under high pH conditions, the deprotonation of the terminal hydroxyl groups at the amphoteric clay edge surfaces leads to a negative charge [37,38]. The charge distribution of montmorillonite platelets (the main component of bentonite) is illustrated in Fig. 12.

The generally accepted viewpoint is that Ca^{2+} plays a critical role for anionic polymers to be adsorbed onto the negatively charged cement or clay particles [16,39]. In 0.1 M NaOH solution, without Ca^{2+} cations, anionic PCE polymers cannot adsorb onto the surfaces of bentonite platelets (basal and edge surfaces) which are negatively charged. Hence, the sorbed amounts of PCEs found in the tests here are solely attributed to chemisorption into the interlayer gallery of sodium bentonite [40].

To prove the validity of this methodology, surface potential of clay sample as well as adsorbed layer thickness of PCE polymers have been determined, and the results are shown in Fig. 13. According to Fig. 13 (a) the surface potential of bentonite turned out to be 4.47 mV in SCPS while −32.63 mV in NaOH solution. Therefore, anionic PCE polymers can only adsorb onto the surface of bentonite which are positively charged in SCPS solution, not in NaOH medium.

The adsorbed layer thickness of AA-7APEG4.5 (for example) on polystyrene nanoparticles – a model substrate – was determined in Ca^{2+} and Ca^{2+} free medium. According to the results in Fig. 13 (b), in the

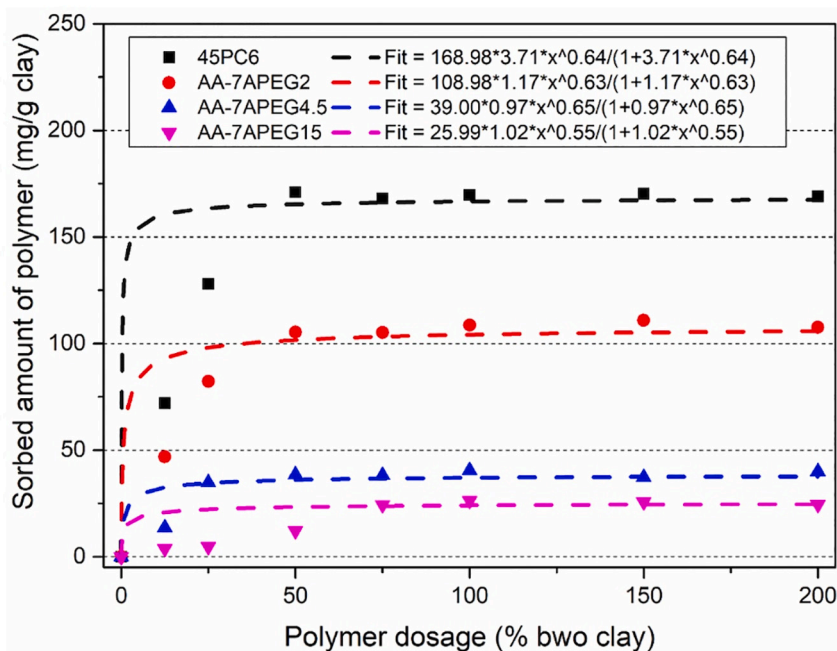**Fig. 14.** Sorption isotherms for various superplasticizer samples on bentonite dispersed in 0.1 M sodium hydroxide solution (pH = 13, w/clay ratio = 48). The proper Langmuir plots of adsorption isotherms with solution concentration on the x-axis are provided in the supplementary material.
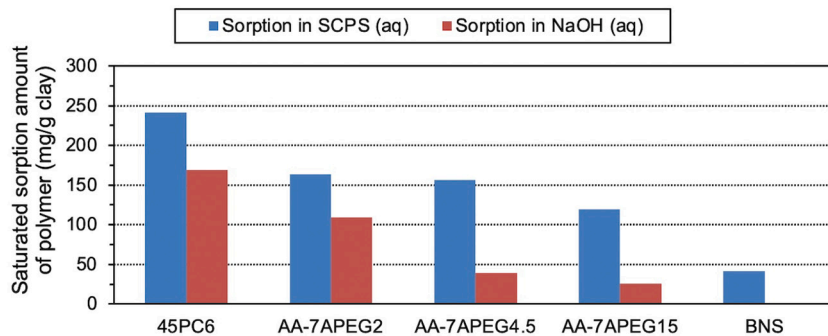

Fig. 15. Saturated sorbed amount of various superplasticizers at equilibrium in SCPS or 0.1 M NaOH as obtained from Figs. 11 and 14.

presence of Ca^{2+}, AA-7APEG4.5 polymer reached the adsorbed layer thickness of ~2 nm indicating the successful adsorption on the surface of the model substrate. Whereas, in the absence of Ca^{2+}, basically no adsorbed layer thickness value can be obtained which confirms that AA-7APEG4.5 polymer cannot adsorb on the surface of model substrate.

To summarize, as proven by zeta potential and adsorbed layer thickness measurements, in 0.1 M NaOH solution, without Ca^{2+} cations, anionic PCE polymers cannot adsorb onto the surfaces of bentonite platelets, therefore, the sorbed amounts of PCEs determined here are solely attributed to chemisorption into the interlayer gallery of sodium bentonite.

As depicted in Fig. 14, in 0.1 M NaOH solution without Ca^{2+}, the sorbed amounts of all PCE polymers are lower as compared to those in synthetic cement pore solution (Fig. 11). Again, PCE sample 45PC6 exhibits the highest sorbed amount (~170 mg/g at equilibrium), followed by AA-APEG2, AA-APEG4.5 and AA-APEG15. All AA-APEG PCE samples exhibit relatively low saturated sorbed amounts (≤110 mg/g), especially for AA-APEG15 only ~25 mg/g. This experiment clearly reveals that intercalation of the PCEs into bentonite is dependent on the side chain density of the polymer. PCE polymers possessing lower side chain density intercalate less than those with higher side chain density.

The difference between PCE polymers becomes even more evident when plotting the saturated sorbed amount in synthetic cement pore

solution, in 0.1 M NaOH solution, and the intercalated portion of polymer, as is shown in Fig. 15. It was found that polymers from the AA-APEG PCE series exhibit lower sorbed amounts in both fluid systems (SCPS and 0.1 M NaOH) in comparison to polymer 45PC6 which indicates weaker interaction between the AA-APEG PCEs and bentonite. This finding corresponds to their better clay robustness as evidenced in the 'mini slump' tests (Figs. 8 and 9).

Next, the intercalated portion of various PCE polymers was calculated and compared. The saturated sorbed amount in SCPS results from the sum of surface adsorbed and intercalated polymer, whereas the saturated sorbed amount in 0.1 M NaOH only accounts for the part of intercalated polymer. The intercalated portion was calculated by dividing the intercalated amount of the polymer by the total sorbed amount. The intercalated portion shown in Fig. 15 demonstrate that AA-7APEG15 possesses the lowest proportion of intercalated polymer which indicates the lowest affinity to the interlayer of bentonite. Thus PCE polymer predominantly sorbs onto the surface of bentonite. PCE sample AA-7APEG4.5 behaves similar to AA-7APEG15, the amount of 7APEG4.5 sorbed by bentonite decreases from 156 mg/g clay (in SCPS) to ~39 mg/g clay (in 0.1 M NaOH), suggesting that only 25% of this PCE polymer is consumed by intercalation while the rest is taken up via electrostatically induced surface adsorption. The intercalated portion for polymer 45PC6 is 70%, which explains the poor dispersing
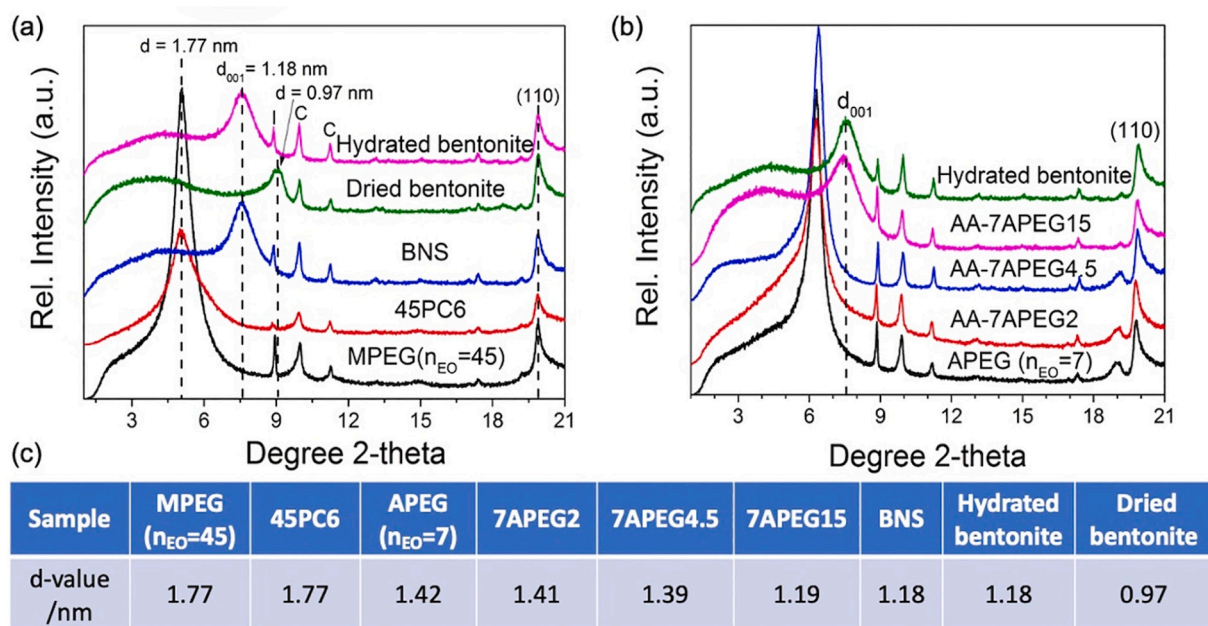
Fig. 16. XRD patterns of bentonite dispersed in synthetic cement pore solution containing 50% by weight of (bwo) clay of AA-APEG copolymers, α-allyl-ω-hydroxy poly (ethylene glycol) ether macromonomer (n_{EO} = 7), ω-methoxy poly (ethylene oxide) methacrylate ester macromonomer (n_{EO} = 45), conventional MEPG PCE (45PC6) as well as BNS, after drying at 50 °C (solution/clay ratio = 48) (C: clinoptilolite-Ca; I: illite).

performance in the presence of bentonite. Surprisingly, also sample AA-7APEG2 exhibits a very high intercalated portion (67%), but still provides better clay robustness than polymer 45PC6 which can be attributed to its overall lower sorbed amount on bentonite, thus more PCE samples remain available to disperse cement particles.

3.7. XRD study of PCE/clay interaction

To further investigate the mode of interaction between AA-APEG PCEs and bentonite, XRD analysis was performed. From the interlayer spacing as evidenced in the XRD results (Fig. 16), the extent of intercalation of the AA-APEG PCEs can be deduced.

In the absence of PCE, the pure sodium bentonite shows a d-spacing of 1.18 nm, while it decreased to the 0.97 nm when dried at 50 °C for 24 h. Based on the PCE intercalation model in bentonite clay proposed by P. Borralleras, the reported thickness of H_2O monolayer is 2.81 Å [14]. The d-spacing was detected decreasing from 1.18 nm to 0.97 nm after drying here, it can be calculated that the hydrated bentonite incorporated H_2O monolayer in the gallery structure. When ω-methoxy polyethylene

glycol methacrylate (MPEG, M_w = 2000 Da) and 45PC6 are present (Fig. 16 (a)), a shift in the d-spacing from 1.18 nm to 1.77 nm is detected. These results are in accord with recent studies indicating that the PEO side chains of PCEs exhibit a similar tendency as polyglycols to intercalate in between the aluminosilicate layers [16,41,42]. For BNS (Fig. 16 (a)), no shift in the d-spacing is found indicating the absence of intercalation. Moreover, XRD patterns of bentonite dispersed in synthetic cement pore solution containing α-allyl-ω-hydroxy poly (ethylene glycol) ether macromonomer (APEG, n_{EO} = 7) and the synthesized AA-APEG PCEs are compared in Fig. 16 (b), and the observed d values are listed in Fig. 16 (c). When α-allyl-ω-hydroxy poly (ethylene glycol) ether macromonomer is added to bentonite, the basal spacing expands from 1.18 nm to 1.42 nm. This interlayer spacing at 1.42 nm differs from that of methoxy polyethylene glycol methacrylate macromonomer (MPEG, n_{EO} = 45) (1.77 nm), and this difference between the two macromonomers can be attributed to their difference in the number of EO units presented, which is consistent with previous reports [18]. Furthermore, the basal spacings of bentonite containing the AA-APEG PCEs exhibit very different values for d-spacing. For example, 7APEG2 with the
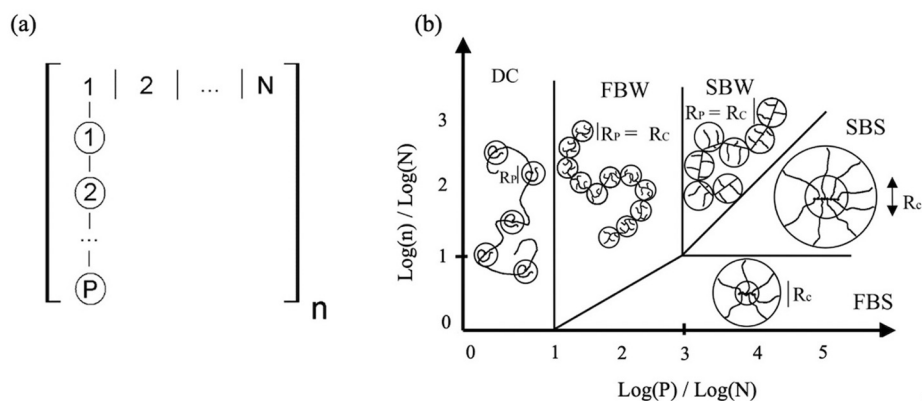
Fig. 17. Schematic conformation diagram for the comb polymers [43]. (a) The polymer backbone is defined as the assemblage of **n** repeating structure units with Mw, each containing **N** backbone monomers and one side chain of **P** units of EO; (b) Different conformation types are then defined in five regimes: decorated chain (DC), flexible backbone worm (FBW), stretched backbone worm (SBW), stretched backbone star (SBS), and flexible backbone star (FBS).

Table 6
Modeling parameters of PCEs and the resulting quantities derived from a classic Flory free energy approach.

PCE samples	Configuration	P	N	n	R/nm	R_P/nm
AA-7APEG2	FBW	7	3	13	3.16	1.26
AA-7APEG4.5	FBW	7	5.5	17	4.19	1.18
AA-7APEG15	DC	7	16	12	5.86	1.16

lowest anionic charge exhibits a similar *d*-spacing value to that of the APEG macromonomer. 7APEG4.5 and 7APEG15 exhibit a lower *d*-spacing value, namely 1.39 nm and 1.19 nm respectively, which again confirms that PCE polymers possessing lower side chain density intercalate less than those with high side chain density.

Here, a parameterized model is introduced to quantitatively determine the molecular conformation, from which a clear correlation between the *d*-value and the molecular size is provided.

As depicted in Fig. 17, the conformation type of APEG PCEs has been defined, AA-7APEG2 and AA-7APEG4.5 belong to the flexible backbone worm while the "best polymer" AA-7APEG15 belongs to the decorated chain conformation. A few parameters for further calculation are defined as follows: R is the radius of gyration of overall conformation of comb molecules, R_{nN} and R_p stand for the radius of gyration of main chain and side chain, respectively [44]. The relevant parameters a_N and a_P indicate the size of monomer anchored in the backbone and side chains. For the polymers used in this study, a_P is 0,36 nm and a_N is 0.25 nm [43]. For DC regime, $R = R_{nN} = a_N(nN)^{3/5}$, $R_p = a_p P^{3/5}$, while in the domain of FBW, $R = R_{nN} = a_N n^{3/5} P^{2/5} N^{1/5}$, $R_p = a_p P^{7/10} N^{-1/10}$ [44].

The calculated values for each PCE are presented in Table 6. It can be seen clearly that with decrease of the side chain density, R increases gradually from AA-7APEG2 (3.16 nm) to AA-7APEG15 (5.86 nm), while R_p decreases accordingly, whereby AA-7APEG15 shows the minimum value of 1.16 nm. We could therefore conclude that AA-7APEG15 with the highest R would encounters the strongest steric effect, thus possesses the least intercalation tendency. Moreover, the lowest R_p from AA-7APEG15 indicates that the polymer possesses the smallest size of side chains, which corresponds to its lowest *d*-value (see Fig. 16).

To further establish a correlation between the intercalated amount of polyethylene glycol within the layers of the sodium bentonite, the clay

was mixed with different dosages of α-allyl-ω-hydroxy poly (ethylene glycol) ether macromonomer (n_{EO} = 7), from 5% to 50% bwo clay. From the dry substances, XRD diagrams were taken.

As is shown in Fig. 18, the peak indicating the layer distance shifts towards lower 2θ degrees with higher amounts of polyethylene glycol used, indicating that increased interlayer *d* values signify a higher intercalation degree. For example, when bentonite is mixed with 50% bwo clay of the APEG macromonomer, a *d*-value of 1.42 nm is observed, whereas when only 5% bwo clay of APEG macromonomer are present, a *d*-spacing of 1.28 nm is recorded. Therefore, we can now demonstrate that there is a clear correlation between the intercalated amount of polyethylene glycol (intercalation degree) and the characteristic adsorption by the sodium bentonite.

4. Conclusion

In this study, a series of allyl ether-based PCEs exhibiting short side PEO chains (n_{EO} = 7) was synthesized via free radical copolymerization. The resulting APEG PCEs possessed comparable M_w and high macromonomer conversion was achieved. Among these AA-APEG PCEs with short PEO side chains, PCEs with lower side chain density generally possessed improved clay resistance. However, when the clay robustness of AA-APEG PCE polymers were compared at the same dosed amount, PCEs with medium side chain density exhibited the best performance. Furthermore, through a series of performance tests it was found that these AA-APEG PCE samples possessing short side chains exhibited superior clay resistance compared to a conventional PCE polymer such as 45PC6 with long PEO pendant chains. Although the optimum PCE for clay resistance (AA-7APEG4.5) requires 1.7× greater dose versus the standard 45PC6 PCE without clay, it actually offers a more economically advantaged means to use PCEs when clay-bearing aggregates are used in concrete production versus more standard PCEs with typical 2000 Mw PEO side chains.

According to total organic carbon analysis of the supernatant, the sodium bentonite exhibited an extremely high affinity for reference polymer 45PC6 which possesses long PEO side chains. Whereas, in the case of the AA-APEG PCE series, their saturated sorbed amounts were almost half as compared to that of 45PC6, indicating much less affinity of the AA-APEG PCE polymers to clay. In all prior literature, the sorbed

Dosage of APEG (n_{EO}=7) (% bwo clay)	50%	25%	15%	10%	5%
d-value (nm)	1.42	1.35	1.34	1.30	1.28
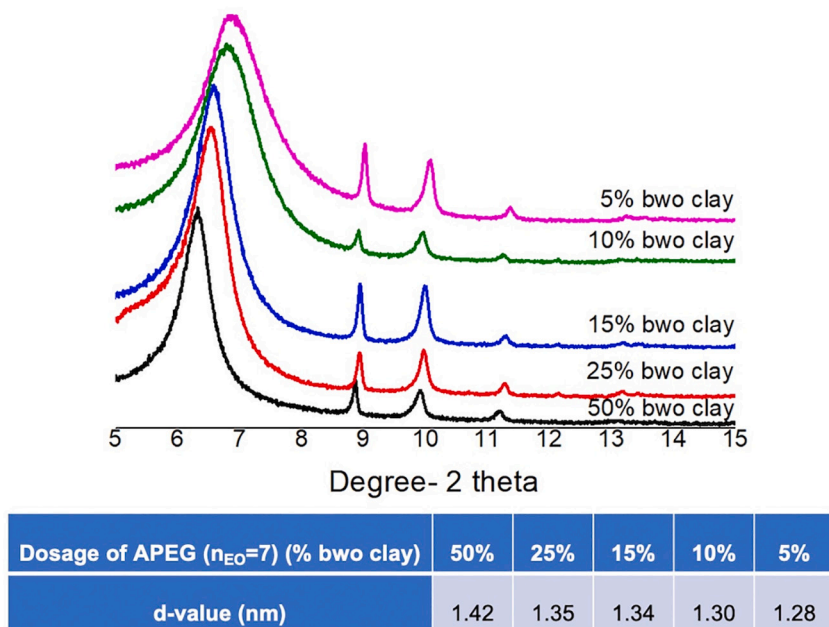
Fig. 18. Bentonite dispersed in synthetic cement pore solution holding different dosages of α-allyl-ω-hydroxy poly (ethylene glycol) ether macromonomer (n_{EO} = 7) varying from 5% to 50% bwo clay.

amounts of PCE polymers comprising of both surface adsorbed and intercalated amount on sodium bentonite were reported. In this study, for the first time, the portion of PCE being intercalated into the layered structure of bentonite was quantified. Sorption measurements of the AA-APEG PCEs in 0.1 M NaOH solution revealed that from the AA-APEG PCEs featuring lower side chain density only a small portion intercalated into the bentonite interlayer space. The validity of this methodology was proven by zeta potential and adsorbed layer thickness measurements, in 0.1 M NaOH solution, without Ca cations. Anionic PCE polymers cannot adsorb onto the surfaces of bentonite platelets, therefore, the sorbed amounts of PCEs determined here are solely attributed to chemisorption into the interlayer gallery of sodium bentonite. Furthermore, an XRD analysis of clay/PCE samples confirmed again that AA-APEG PCEs possessing short side chains intercalated less than the conventional PCE sample with long PEO side chains. Among AA-APEG PCEs, it was also theoretically demonstrated that the PCEs with lower side chain density would exhibit lower side chain size (R_P) and thus lower d-values are recorded in the XRD analysis. Due to the weak interaction between the AA-APEG PCEs and bentonite, more PCE polymers are available to disperse cement and achieve high fluidity.

CRediT authorship contribution statement

Lei Lei: Conceptualization, Resources, Investigation, Supervision, Writing - Review & Editing.

Yue Zhang: Methodology, Data Curation, Software, Writing - Original draft preparation.

Ran Li: Methodology, Formal analysis, Visualization.

Declaration of competing interest

The authors declare that they have no known competing financial interests or personal relationships that could have appeared to influence the work reported in this paper.

Acknowledgment

Appendix A. Supplementary data

Supplementary data to this article can be found online at https://doi.org/10.1016/j.cemconres.2021.106504.

References

[1] K. Yamada, T. Takahashi, S. Hanehara, M. Matsuhisa, Effects of the chemical structure on the properties of polycarboxylate-type superplasticizer, Cem. Concr. Res. 30 (2000) 197–207.

[2] J. Plank, E. Sakai, C. Miao, C. Yu, J. Hong, Chemical admixtures—chemistry, applications and their impact on concrete microstructure and durability, Cem. Concr. Res. 78 (2015) 81–99.

[3] R.J. Flatt, Y.F. Houst, A simplified view on chemical effects perturbing the action of superplasticizers, Cem. Concr. Res. 31 (2001) 1169–1176.

[4] G. Gelardi, S. Mantellato, D. Marchon, M. Palacios, A. Eberhardt, R. Flatt, Chemistry of Chemical Admixtures, Science and Technology of Concrete Admixtures, Elsevier, 2016, pp. 149–218.

[5] Y.F. Houst, P. Bowen, F. Perche, A. Kauppi, P. Borget, L. Galmiche, J.-F. Le Meins, F. Lafuma, R.J. Flatt, I. Schober, Design and function of novel superplasticizers for more durable high performance concrete (superplast project), Cem. Concr. Res. 38 (2008) 1197–1209.

[6] P.-C. Aïtcin, High Performance Concrete, E & FN SPON, London, UK, 2011.

[7] K. Yoshioka, E.-i. Tazawa, K. Kawai, T. Enohata, Adsorption characteristics of superplasticizers on cement component minerals, Cem. Concr. Res. 32 (2002) 1507–1513.

[8] M.L. Nehdi, Clay in cement-based materials: critical overview of state-of-the-art, Constr. Build. Mater. 51 (2014) 372–382.

[9] E. Sakai, D. Atarashi, M. Daimon, Interaction between superplasticizers and clay minerals, in: Proceedings of the 6th International Symposium on Cement & Concrete, 2006, pp. 1560–1566.

[10] A.A. Jeknavorian, L. Jardine, C.C. Ou, H. Koyata, K. Folliard, Interaction of Superplasticizers With Clay-bearing Aggregates, Canmet/aci International Conference on Superplasticizers & Other Chemical Admixtures in Concrete, 2003.

[11] L. Lei, J. Plank, A study on the impact of different clay minerals on the dispersing force of conventional and modified vinyl ether based polycarboxylate superplasticizers, Cem. Concr. Res. 60 (2014) 1–10.

[12] S. Burchill, P. Hall, R. Harrison, M. Hayes, J. Langford, W. Livingston, R. Smedley, D. Ross, J. Tuck, Smectite-polymer interactions in aqueous systems, Clay Miner. 18 (1983) 373–397.

[13] L. Lei, J. Plank, A concept for a polycarboxylate superplasticizer possessing enhanced clay tolerance, Cem. Concr. Res. 42 (2012) 1299–1306.

[14] P. Borralleras, I. Segura, M.A. Aranda, A. Aguado, Influence of experimental procedure on d-spacing measurement by XRD of montmorillonite clay pastes containing PCE-based superplasticizer, Cem. Concr. Res. 116 (2019) 266–272.

[15] P. Borralleras, I. Segura, M.A. Aranda, A. Aguado, Absorption conformations in the intercalation process of polycarboxylate ether based superplasticizers into montmorillonite clay, Constr. Build. Mater. 236 (2020) 116657.

[16] S. Ng, J. Plank, Interaction mechanisms between Na montmorillonite clay and MPEG-based polycarboxylate superplasticizers, Cem. Concr. Res. 42 (2012) 847–854.

[17] J. Cheung, L. Roberts, J. Liu, Admixtures and sustainability, Cem. Concr. Res. 114 (2018) 79–89.

[18] H. Tan, B. Gu, S. Jian, B. Ma, Y. Guo, Z. Zhi, Improvement of polyethylene glycol in compatibility with polycarboxylate superplasticizer and poor-quality aggregates containing montmorillonite, J. Mater. Civ. Eng. 29 (2017), 04017131.

[19] G. Xing, W. Wang, G. Fang, Cement dispersion performance of superplasticisers in the presence of clay and interaction between superplasticisers and clay, Adv. Cem. Res. 29 (2017) 194–205.

[20] Y.-G. Li, Y. Li, Y. Wan, C. Deng, Z. Wang, J.-S. Qian, Effects of clay on the dispersibility of cement paste mixed with polycarboxylate superplasticizer, Chongqing Daxue Xuebao (Ziran Kexue Ban) 35 (2012) 86–92.

[21] S. Ng, J. Plank, Study on the Interaction of Na-montmorillonite Clay With Polycarboxylates 288, ACI Special Publication, 2012.

[22] Y. Ma, C. Shi, L. Lei, S. Sha, B. Zhou, Y. Liu, Y. Xiao, Research progress on polycarboxylate based superplasticizers with tolerance to clays-a review, Constr. Build. Mater. 255 (2020) 119386.

[23] L. Lei, J. Plank, Synthesis and properties of a vinyl ether-based polycarboxylate superplasticizer for concrete possessing clay tolerance, Ind. Eng. Chem. Res. 53 (2014) 1048–1055.

[24] H. Xu, S. Sun, J. Wei, Q. Yu, Q. Shao, C. Lin, β-Cyclodextrin as pendant groups of a polycarboxylate superplasticizer for enhancing clay tolerance, Ind. Eng. Chem. Res. 54 (2015) 9081–9088.

[25] X. Liu, Z. Wang, Y. Zheng, S. Cui, M. Lan, H. Li, J. Zhu, X. Liang, Preparation, characterization and performances of powdered polycarboxylate superplasticizer with bulk polymerization, Materials (Basel) 7 (2014) 6169–6183.

[26] J. Alain, V. Emmanuel, W. Olivier, Method for inerting impurities, US Patent US 0,287,794 A1 (2007).

[27] L.A. Jardine, H. Koyata, K.J. Folliard, C.-C. Ou, F. Jachimowicz, B.-W. Chun, A.A. Jeknavorian, C.L. Hill, Admixture and method for optimizing addition of EO/PO superplasticizer to concrete containing smectite clay-containing aggregates, US Patent US 6, 352, 952 B1, (2002).

[28] L.L. Kuo, Y. Chen, H. Koyata, Cationic polymers for treating construction aggregates, US Patent US 9,034,968 B2 (2015).

[29] L.L. Kuo, Y. Chen, H. Koyata, Hydrophobic, cationic polymers for treating construction aggregates, US Patent US 9,828,500 B2, (2017).

[30] S. Pourchet, S. Liautaud, D. Rinaldi, I. Pochard, Effect of the repartition of the PEG side chains on the adsorption and dispersion behaviors of PCP in presence of sulfate, Cem. Concr. Res. 42 (2012) 431–439.

[31] M.T.R. Laguna, R. Medrano, M.P. Plana, M.P. Tarazona, Polymer characterization by size-exclusion chromatography with multiple detection, J. Chromatogr. A 919 (2001) 13–19.

[32] J. Plank, B. Sachsenhauser, Experimental determination of the effective anionic charge density of polycarboxylate superplasticizers in cement pore solution, Cem. Concr. Res. 39 (2009) 1–5.

[33] J. Stecher, J. Plank, Adsorbed layer thickness of polycarboxylate and polyphosphate superplasticizers on polystyrene nanoparticles measured via dynamic light scattering, J. Colloid Interface Sci. 562 (2020) 204–212.

[34] Q. Ran, J. Liu, Y. Yang, X. Shu, J. Zhang, Y. Mao, Effect of molecular weight of polycarboxylate superplasticizer on its dispersion, adsorption, and hydration of a cementitious system, J. Mater. Civ. Eng. 28 (2016), 04015184.

[35] F. Winnefeld, S. Becker, J. Pakusch, T. Götz, Effects of the molecular architecture of comb-shaped superplasticizers on their performance in cementitious systems, Cem. Concr. Compos. 29 (2007) 251–262.

[36] E. Tombacz, M. Szekeres, Colloidal behavior of aqueous montmorillonite suspensions: the specific role of pH in the presence of indifferent electrolytes, Appl. Clay Sci. 27 (2004) 75–94.

[37] E. Tombácz, M. Szekeres, Surface charge heterogeneity of kaolinite in aqueous suspension in comparison with montmorillonite, Appl. Clay Sci. 34 (2006) 105–124.

[38] T. Preocanin, A. Abdelmonem, G. Montavon, J. Luetzenkirchen, Charging behavior of clays and clay minerals in aqueous electrolyte solutions - experimental methods for measuring the charge and interpreting the results, in: Clays, Clay Minerals and Ceramic Materials Based on Clay Minerals, 2016, pp. 51–88.

[39] E. Sakai, K. Yamada, A. Ohta, Molecular structure and dispersion-adsorption mechanisms of comb-type superplasticizers used in Japan, J. Adv. Concr. Technol. 1 (2003) 16–25.

[40] G.B.S. Ng, Interactions of Polycarboxylate Based Superplasticizers with Montmorillonite Clay in Portland Cement and With Calcium Aluminate Cement, Technische Universität München, 2013.

[41] P.D. Svensson, S. Hansen, Intercalation of smectite with liquid ethylene glycol—resolved in time and space by synchrotron X-ray diffraction, Appl. Clay Sci. 48 (2010) 358–367.

[42] J.L. Suter, P.V. Coveney, Computer simulation study of the materials properties of intercalated and exfoliated poly (ethylene) glycol clay nanocomposites, Soft Matter 5 (2009) 2239–2251.

[43] R.J. Flatt, I. Schober, E. Raphael, C. Plassard, E. Lesniewska, Conformation of adsorbed comb copolymer dispersants, Langmuir 25 (2009) 845–855.

[44] C. Gay, E. Raphaël, Comb-like polymers inside nanoscale pores, Adv. Colloid Interface Sci. 94 (2001) 229–236.

5.2 Paper # 2

Molecular design of an allyl ether PCE with enhanced clay tolerance

Y. Zhang, L. Lei

In this study, two PCE polymers were synthesized utilizing the same α-allyl ω-hydroxy poly(ethylene glycol) (APEG) macromonomer. The side-chain lengths of these PCEs consisted of 7 EO units. However, they differed in terms of the co-monomers employed: one PCE utilized maleic anhydride (MA) as the co-monomer, while the other utilized acrylic acid (AA). Both APEG PCEs possessed comparable molecular weights and had an equivalent amount of anionic charge.

The dispersing performance of the two polymers on cement was evaluated with and without montmorillonite clay. The results revealed that AA-7APEG had superior clay tolerance as compared to MA-7APEG.

In order to explore the interaction between PCEs and montmorillonite in greater detail, the study involved conducting XRD analysis and adsorption measurements. Additionally, charge titration experiments were performed to assess the Ca^{2+} binding capacity of the two PCE polymers.

The findings indicated that MA-7APEG was capable of chelating more calcium cations, resulting in decreased anionic charge density and reduced electrostatic repulsion towards montmorillonite clay.

Molecular Design of an Allylether PCE with Enhanced Clay Tolerance

Yue Zhang, Lei Lei

Synopsis: The sensitivity problem of polycarboxylate superplasticizers (PCEs) towards clay contaminants becomes more and more severe nowadays. The negative impact of clay contaminants, especially montmorillonite (MMT) on PCEs is stemming from the intercalation of polyethylene glycol side chains into the interlayer gallery of montmorillonite. In this study, two PCE polymers were synthesized from the same α-allyl ω-hydroxy poly (ethylene glycol) (APEG) macromonomer with designated side-chain lengths of 7 EO units, but different acids as co-monomers, namely, maleic anhydride (MA) and acrylic acid (AA). These two APEG PCEs were designed such as to possess the same anionic charge amounts and similar molecular weights. The dispersing performance of the two polymers was tested in the absence and presence of montmorillonite clay. It turned out that AA-7APEG exhibited much better clay tolerance as compared to that of MA-7APEG. To further investigate the interaction mode between PCEs and montmorillonite, XRD and adsorption measurements were carried out. Additionally, the Ca^{2+} binding capacity of the two PCE polymers was probed via charge titration experiments. The results show that MA-7APEG could chelate more calcium cations and thus lead to the decreased anionic charge density and also reduced electrostatic repulsion towards MMT.

Keywords: Polycarboxylate superplasticizers; Ca^{2+} binding; Montmorillonite; Adsorption

INTRODUCTION

More recently, polycarboxylate superplasticizers (PCE) have been intensively used in cement and concrete owing to their excellent dispersing performance and hence water-reduction capacity [1-3]. However, conventional PCEs in the industrial practice are very sensitive to clay contaminants in the aggregates, such as bentonite, illite, montmorillonite (MMT) [4-6]. As a consequence, the dispersing capacity of PCEs is much reduced. Generally, PCE polymers interact with cement in two distinct manners: either intercalate into the interlayer of clay or then adsorb on the surface of clay particles with the complexation of Ca^{2+}. Moreover, the intercalation of PCE polymers accounts for the main root cause for the much depressed dispersing performance in the cement slurries [7]. Developing PCE products with enhanced clay tolerance, therefore is of great importance. With respect to PCE structure, PCE comb copolymers typically consist of a trunk chain holding carboxylate groups and polyethylene glycol side chains [8, 9]. Hence, there are various compositional parameters, such as anionicity, side-chain density, molecular weight could be adjusted in order to achieve good clay robustness.

Extensive studies have provided multiple approaches based on the structural modifications of PCEs for the enhancement of clay tolerance [7, 10-12]. To be specific, it has been recognized that PCE without polyethylene oxide (PEO) side chains or with short PEO side chains could effectively hinder intercalation [13, 14]. Lei et. al [15] has proposed a novel vinyl ether-based PCE, a terpolymer of MA-monoalkyl maleate-HBVE with short side chains, which could achieve the same flowability using low dosages and exhibit low sorbed amount (~ 20 mg/g) on montmorillonite than traditional PCEs. Moreover, it has been reported before, by changing the shape of side chain could also suppress the intercalation tendency of PCE polymers. Liu et. al [4] synthesized a star-shaped PCE first by esterification to form a core structure and followed by polymerization. Such stereoscopic structure could produce a large steric hindrance to prevent most PCE molecules from intercalating into the gallery layer of clay and hence remain in the solution to disperse cement particles. It could also be an alternative approach to introduce various functional

groups to the PCE structure. Such structures could lead to the enhancement of dispersibility of modified PCEs and simultaneous limitation of their adsorptions on clays. Grafting terminal tertiary amine into PCE structure, as an example, forms such a special structure that could overcome the interparticle forces and thereby avoid the flocculation of cement particles [16]. This could ensure the good flowability of cement pastes with / without clays. It could be explained that the tertiary amine group forms large quantities of cationic ammonium and work as a clay swelling inhibitor in the aqueous solution [7].

RESEARCH SIGNIFICANCE

Indeed, a handful of literature could be found to provide solutions for clay sensitivity problem. However, none of them could lead to large scale application due to the sophisticated synthesis method or limited improvement in concrete. A solution is still missing in the industry. In this study, the influence of carboxylate group in the α-allyl ω-hydroxy poly(ethylene glycol) (APEG) PCE structure is investigated in terms of the clay sensitivity. It is hoped that the findings in this study could provide a guideline for the future synthesis of PCEs with enhanced clay robustness.

EXPERIMENTAL INVESTIGATION

Chemicals

Maleic anhydride (≥ 99 %, purchased from Sigma Aldrich, Germany), Acrylic acid (> 99 % purity, purchased from Sigma Aldrich, Germany),Acrylic acid (> 99 % purity, purchased from Sigma Aldrich, Germany), α-allyl-ω-hydroxy poly (ethylene glycol) ether (APEG macromonomer, n_{EO} = 7) (> 98 %, obtained from NOF Corporation, Japan), ammonium persulfate (≥ 98 %, purchased from Sigma Aldrich, Germany), sodium methallyl sulfonate (> 98% purchased from Sigma Aldrich, Germany), 3-mercaptopropionic acid (≥ 99 %, purchased from Sigma Aldrich, Germany), sodium hydroxide (≥ 97 % purchased from Merck KGaA, Germany) were all used without further purification.

Cement

As cement, an Ordinary Portland Cement sample CEM I 42.5 R provided by Schwenk company, Allmendingen plant, Germany was used. Its phase compositions were determined by Q-XRD using *Rietveld* refinement and shown in **Table 1**. Its *Blaine* value was 3.105 cm^2/g.

Table 1 – Phase composition of the OPC sample CEM I 42.5 R by Q-XRD using *Rietveld* refinement.

Phase	wt. %
C$_3$S, monoclinic	59.55
C$_2$S, monoclinic	11.08
C$_4$AF, orthorhombic	10.07
C$_3$A, cubic	6.94
Anhydrite (CaSO$_4$)	2.59
Dihydrate (CaSO$_4$• 2H$_2$O)	3.09
Hemihydrate (CaSO$_4$• 0.5H$_2$O)	0.10
Calcite (CaCO$_3$)	2.34
Dolomite (CaMg(CO$_3$)$_2$)	0.97
Quartz (SiO$_2$)	0.42
Free lime (*Franke*)	1.32

periklas	0.53
portlandit	0.78
arcanite	0.22
Total	100.00

Clay

For clay samples, an artificial type of sodium bentonite (BYK, Wesel, Germany) was selected for this study. The oxide composition of clay was determined by X-ray fluorescence as shown in **Table 2**. The mineralogical composition was measured by Q-XRD via *Rietveld* refinement and is illustrated in **Fig. 1** and **Table 3**. From particle size distribution of the bentonite clay (**Fig. 2**), the d_{50} value of 23.55 μm can be obtained.

Table 2 – Oxide composition of the bentonite sample as determined by XRF.

Oxide	wt. %
SiO_2	55.7
Al_2O_3	16.2
Fe_2O_3	3.5
CaO	3.0
Na_2O	2.0
MgO	1.4
K_2O	0.9
TiO_2	0.3
BaO	0.1
P_2O_5	0.1
MnO	0.1
SrO	0.1
SO_3	0.1
LOI	16.5
Total	100.00

Fig.1 – XRD pattern of bentonite clay **(**M: Montmorillonite; C: Clinoptilolite-Ca; I: Illite; Q: Quartz; C': Calcite).

Table 3 – Mineralogical composition of the bentonite clay sample via Q-XRD

Compositions	Montmorillonite	Clinoptilolite-Ca	illite	Quartz	Calcite
Proportion (%)	80.56	11.21	2.62	4.45	1.15
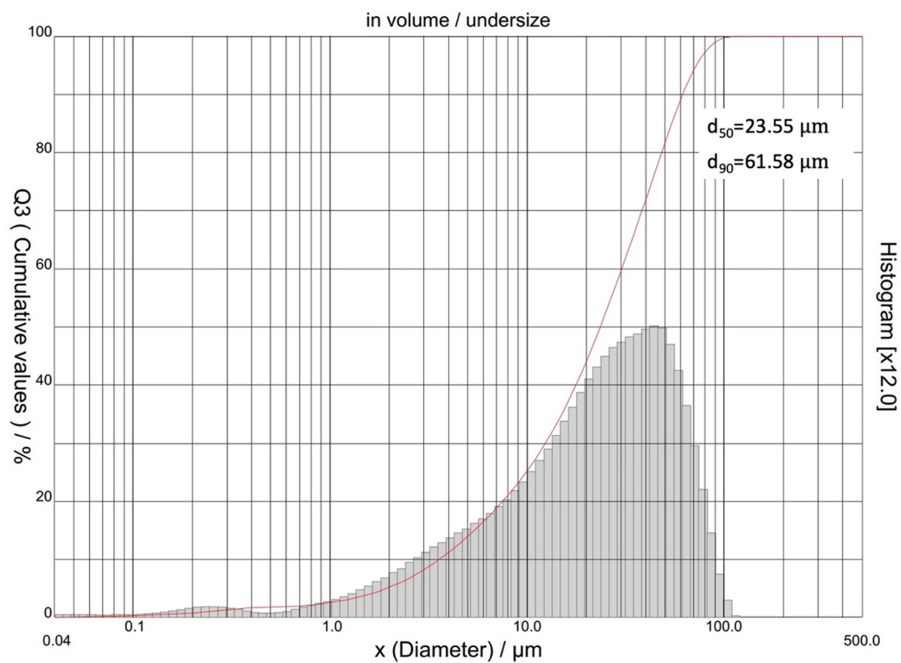
Fig.2 – The particle size distribution of bentonite clay determined by laser granulometry.

Synthesis of MA-7APEG and AA-7APEG2 superplasticizers

A conventional maleic anhydride-based APEG 7 PCE was synthesized by bulk copolymerization. The synthetic route is shown in **Fig. 3(a).** 21.80 g of maleic anhydride (0.222 mol) and 77.7 g of allyl ether (APEG 7 with $n_{EO} = 7$) (0.222 mol) were added into a 250 mL 5-neck reaction flask purged with nitrogen gas feed, reflux condenser and 200 rpm stirring rate at 70 °C, keep for 1 h. Then 0.51 g of benzoyl peroxide powder as an initiator was added in one portion into the reactor, followed by 1.03 g of benzoyl peroxide powder continuously added at an interval of 10 min over a total time of 90 min. Upon finishing addition, the mixture was heated up to 90 °C and stirred for another 90 min. Thereafter, 150.08 g of deionized (DI) water was added while the reaction mixture kept still hot to yield the polycarboxylate solution. The product was cooled down and titrated to neutral pH with 30 % concentration NaOH solution.

Fig. 3 – The synthetic routes of MA-7APEG (a) and AA-7APEG2 (b).

For AA-7APEG 2 (molar ratio AA: APEG = 2, $n_{EO} = 7$), the synthetic route is according to **Fig. 3(b)** and the preparation steps are disclosed in the following: At first, 25 g (0.066 mol) of APEG macromonom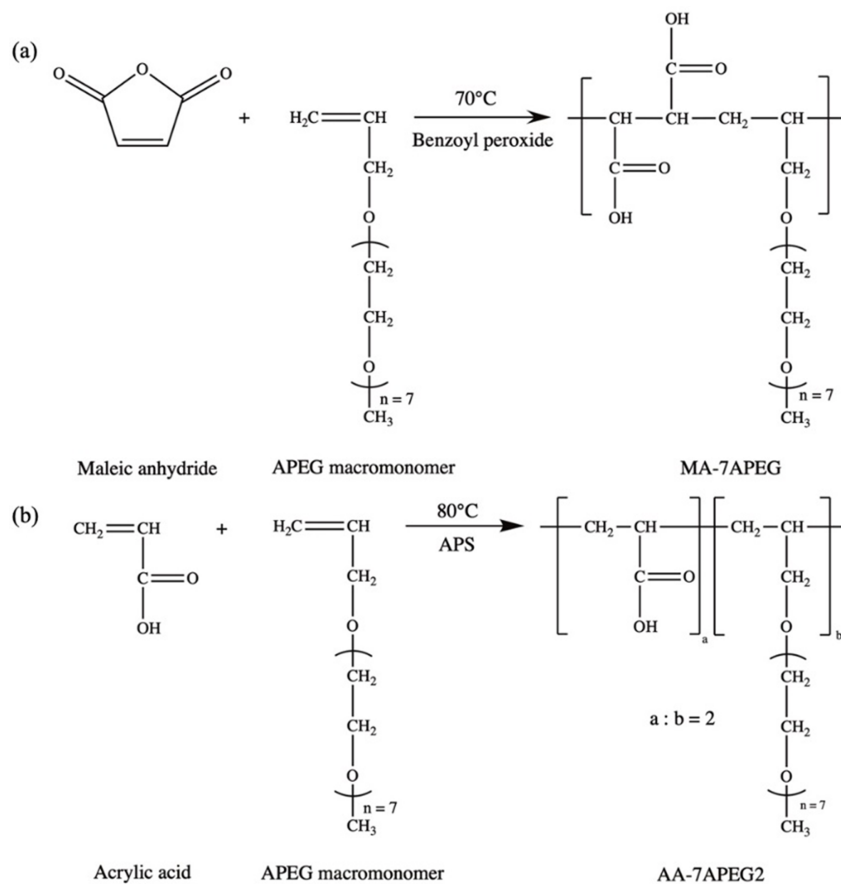er ($M_w = 350$ g/mol) and 45 mL of DI water were placed in a five-neck flask which connected to a reflux condenser, a mechanical stirrer, a nitrogen inlet and two separated feeding inlets. The reaction vessel containing the macromonomer solution was heated to 80 °C and flushed with N_2 for 30 minutes. Next, two feeding solutions (Solution A and Solution B) were prepared. 9.387 g (0.132 mol) of acrylic acid and 0.225 g (0.002 mol) of 3-mercaptopropionic acid (chain transfer agent) were dissolved in 25 mL of DI water. This solution mixture was named as Solution A. On the other hand, 5.629 g (0.025 mol) of ammonium persulfate were dissolved in 30 mL of DI water. This solution was labeled as Solution B. Solutions A and B were added dropwise into the reaction vessel using two peristaltic pumps via inlet A over 2.5 hours and via

inlet B over 3 hours respectively. When the addition of solution B finished, then the mixture was kept under stirring for another hour. Finally, the PCE solution was cooled to ambient temperature and the pH was adjusted to 6.5 - 7 by using 30 wt. % sodium hydroxide solution. The solution exhibited a solids content of 35 wt. % was used without further purification.

Characterization of AA-APEG Polycarboxylate polymers

(1) Size exclusion chromatography (SEC)

Molar mass (Mw and Mn), the polydispersity index (PDI) and macromonomer conversion of the synthesized ether-based PCEs were determined by size exclusion chromatography, also referred to as gel permeation chromatography (GPC). The measurements were performed with a Waters Alliance 2695 instrument (Waters, Eschborn, Germany) equipped with three UltrahydrogelTM columns (120, 250, 500) and an UltrahydrogelTM Guard column. The eluent was a 0.1 N NaNO$_3$ (pH = 12) with a flow rate of 1.0 mL/min. For the calculation of Mw and Mn, a dn/dc (refractive index increment) value of 0.135 mL/g (value for PEO) was utilized [17].

(2) Anionic charge amount measurement

The specific anionic charge amount of the synthesized PCEs was determined using a particle charge detector PCD 03 pH (Mütek Analytic, Herrsching, Germany). Here, 10 mL of the 0.2 g/L PCE solution were titrated with a 0.34 g/L aqueous solution of cationic poly-diallyl dimethyl ammonium chloride (polyDADMAC) until charge neutralization (zero potential) was reached. Then the anionic charge per gram of PCE polymer was derived from the consumption of the cationic polyelectrolyte polyDADMAC [18].

Dispersing performance in cement pastes with/without clay

For the evaluation of the dispersing effectiveness of the PCEs in cement, a 'mini slump' test was employed, which is described in DIN EN 1015 standard [19]. At first, the water-to-cement (w/c) ratio of the paste without polymer to achieve a spread of 18 ± 0.5 cm was determined to be 0.48. At this w/c, the dosage for each PCE sample to reach a spread flow of 26 ± 0.5 cm was determined.

The test was carried out as follows: The polymer was firstly mixed with DI water in a porcelain cup, whereby the water contained in the polymer solution was subtracted from the amount of mixing water. Then 300 g cement were added to the mixing water within 1 minute, the mixture remained at rest for 1 minute followed by 2 minutes of manual stirring. Thereafter, the cement paste was poured into a Vicat cone (height 40 mm, top diameter 70 mm, bottom diameter 80 mm) placed on a glass plate and the cone was quickly lifted vertically. Once the cement paste had stopped flowing, the spread flow was measured twice at two angles perpendicular to each other. Finally, the averaged spread flow of these two values was recorded as the spread flow value.

When the clay tolerance tests were performed, a similar procedure was followed and 1 wt. % or 3 wt. % of the cement was replaced by clay minerals.

PCE sorption on clay

The sorption of PCEs by clay was determined in synthetic cement pore solution (SCPS, pH = 13.06) [6] and 0.1 M NaOH solution by means of total organic content (TOC) based on the depletion method. In principle, the amount of non-adsorbed portion of PCEs present in the solution in the equilibrium state was quantified by TOC. The sorbed portion can then be calculated by subtracting the quantity remaining in the supernatant from the amount added.

In a typical experiment, 0.25 g of clay, 12 g of synthetic cement pore solution (w/clay ratio = 48) and the different amounts of designated polymers were transferred into a 50 mL centrifuge tube and shaken in a wobbler (VWR

International, Darmstadt, Germany) for 2 minutes at 2400 rpm, then centrifuged for 10 minutes at 8500 rpm. The resulting supernatant was then removed using a syringe, filtered through a 0.2 μm polyethersulfone syringe filter (Model FPS250020, Graphic Controls, New York, USA) and diluted 20 - 30 times with DI water. The TOC measurement was conducted on a High TOC II instrument (Elementar Analysensysteme, Hanau, Germany) at the temperature of 890 °C. The average of the sorbed amount at each concentration was calculated from at least two duplicate measurements [13].

XRD analysis

In a typical test, 0.5 g of clay and 24.25 g of 1.03 wt. % PCE solution were added into a 50 mL centrifuge tube, shaken in a wobbler (VWR International, Darmstadt, Germany) for 2 minutes at 2400 rpm and then centrifuged for 10 minutes at 8500 rpm. The solid substance at the bottom was dried overnight at 50 °C in an oven, followed by being ground into a powder as required for the measurement. The instrument for these XRD measurements was a D8 Advance, Bruker AXS instrument (Bruker, Karlsruhe/ Germany) based on Bragg-Brentano geometry. Each sample to be scanned was placed on a mounted round plastic holder. The parameters for the scanning procedure were set as follows: step size of 0.15 s/step, scan spin at a revolution time of 4 s, 0.3° of aperture slit, scan ranging from 0.6° to 20° 2θ, using CuKα, λ=1.5418 Å [13].

EXPERIMENTAL RESULTS AND DISCUSSION

Molecular properties of the synthesized APEG polycarboxylate polymers
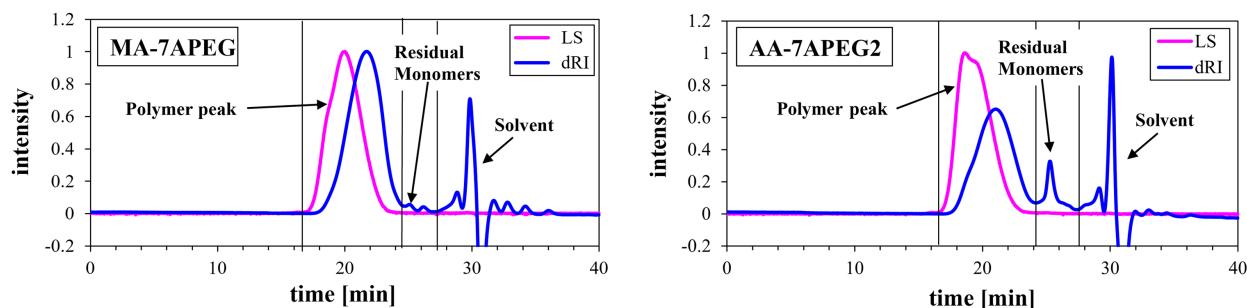
Fig. 4 – GPC spectra of synthesized polymers MA-7APEG and AA-7APEG2, respectively.

To detect the molecular properties of synthesized PCE polymers, SEC measurements were carried out. The chromatograms are displayed in **Fig. 4**. The molecular properties are listed in **Table 4**. Both APEG PCEs are high quality PCE products evidenced by low PDIs and high conversion rates of macromonomer.

Table 4 – Characteristic molecular parameters of the synthesized PCE polymers

Polymer sample	M_w [Da]	M_n [Da]	PDI	Macromonomer Conversion (%)
MA-7APEG	38,100	15,875	2.4	96.6
AA-7APEG2	41,320	17,965	2.3	84.3

Anionic charge measurements of synthesized PCE polymers

According to the anionicity measurements, the two APEGs with structurally different acid monomers (MA-7APEG and AA-7APEG2) exhibited comparable negatively charge from theoretical calculation or measurements in the NaOH solution **(Fig. 5)**. When additional Ca^{2+} was added into the fluid, the anionic charge amounts of both polymers dropped dramatically, which can be explained by the combination of the functionality of COO^- with Ca^{2+} by electrostatic interaction. Moreover, the drop in the anionicity for the MA-7APEG polymer was much higher as compared to AA-7APEG2 polymer, indicating a stronger calcium binding capacity of the former PCE.
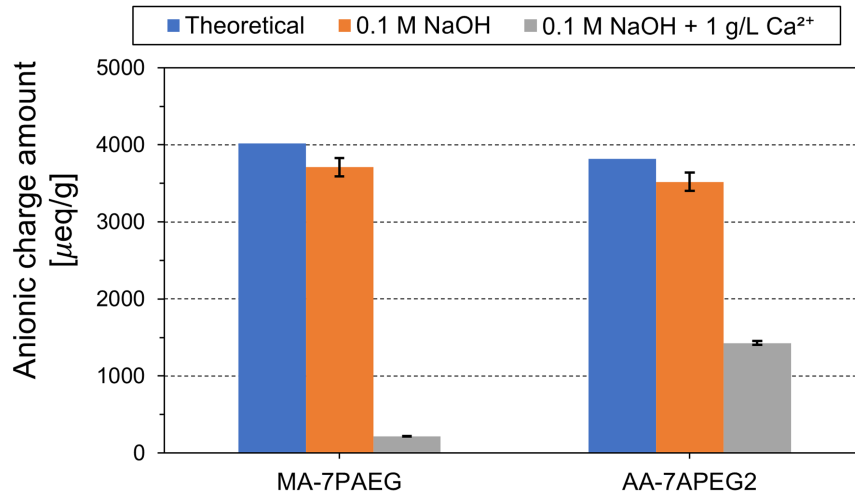
Fig. 5 – Anionicity determination of MA-7APEG and AA-7APEG by theoretical calculation compared with real experiments.

Dispersing performance of APEG PCEs in neat cement pastes

In addition to detect the influence of polymers on cement pastes, we therefore did 'Mini-slump' tests, as illustrated in **Fig. 6.** AA-7APEG could achieve the spread flow of 26 cm with dosage of 0.21 % bwoc, and MA-7APEG to reach the same fluidity even consumed 0.07 % of concentration which was comparable to the dosage (0.06 % bwoc) of 45MPEG6, a widely used conventional PCE polymer.

Fig. 6 – Dispersing performance of polymers in the neat cement paste.

Dispersing capacities of PCEs in the presence of 1 and 3 wt.% clay

To further detect the clay tolerance of the resulting PCE polymers, 1 wt. % and 3 wt. % of bentonite was added into the cement paste. "Mini slump" test results are shown in **Fig. 7**. In the presence of 1 wt.% of bentonite the fluidity of cement paste admixed with 45MPEG6 decreased by 60 % for 1 wt.% and up to 101% in the presence of 3 wt.% bentonite addition. In comparison, the two APEG type PCEs exhibited relatively good clay robustness as compared to the MPEG type. The decrease of dispersing efficiency for both MA-7APEG and AA-7APEG2 was ~ 30 % in the presence of 1 wt.% of bentonite. When the bentonite content rose to 3 wt. %, the drop in the spread flow of two APEGs was still less than the MPEG PCE. Furthermore, AA-7APEG2 prepared from acrylic acid exhibited better clay robustness as compared to the MA-7APEG polymer made from maleic anhydride. The reason behind this could be further clarified by investigating the mode of action between PCE polymers and bentonite via XRD analysis and sorption measurements.

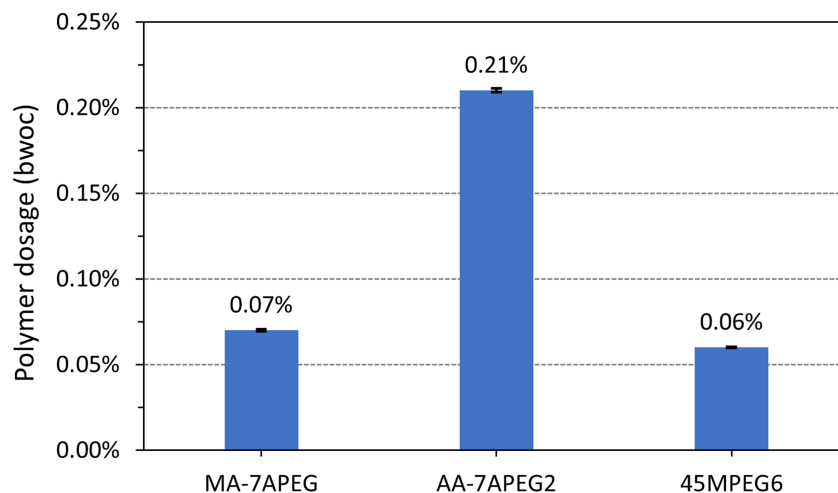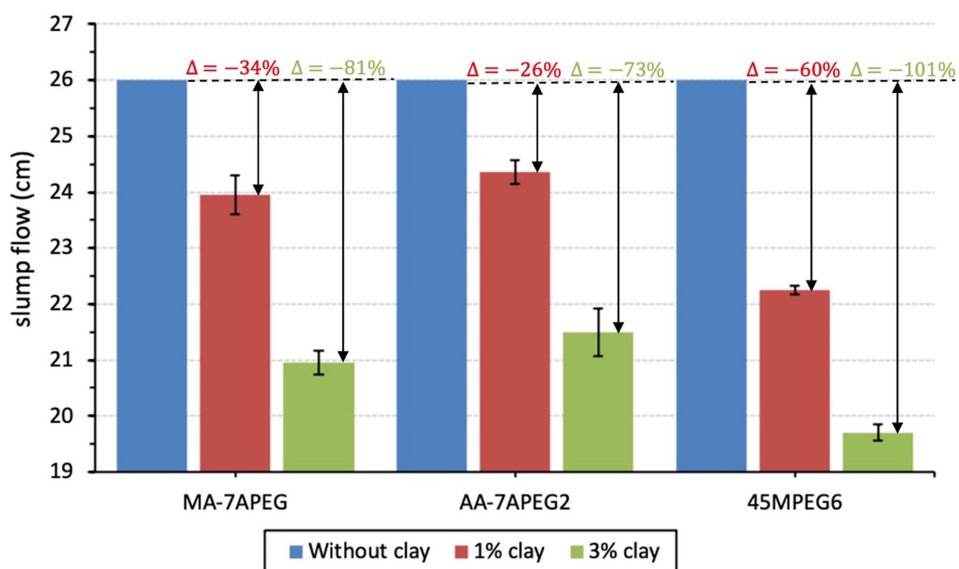**Fig. 7** – Dispersing capacities of PCEs in the presence of 1wt. % and 3 wt. % of bentonite.

XRD study of PCE/clay interaction

To verify whether the polycarboxylates were chemically incorporated in between the aluminosilicate layers of clay particles, XRD analysis of MA-7APEG and AA-7APEG2 as well as conventional 45MPEG6 polymer was performed, as displayed in **Fig. 8**. It turned out that 45MPEG6 exhibited the strongest shift towards lower 2-Theta, indicating the highest d-spacing value (calculated to be 1.77 nm) in the interlayers of clay compared to the hydrated MMT without PCEs (d-value = 1.18 nm). For MA-7APEG and AA-7APEG2 PCEs of same polymer dosage (50 % bwo clay), they presented to possess the enhanced clay resistance with approximately equal d-values of ~ 1.41 nm.
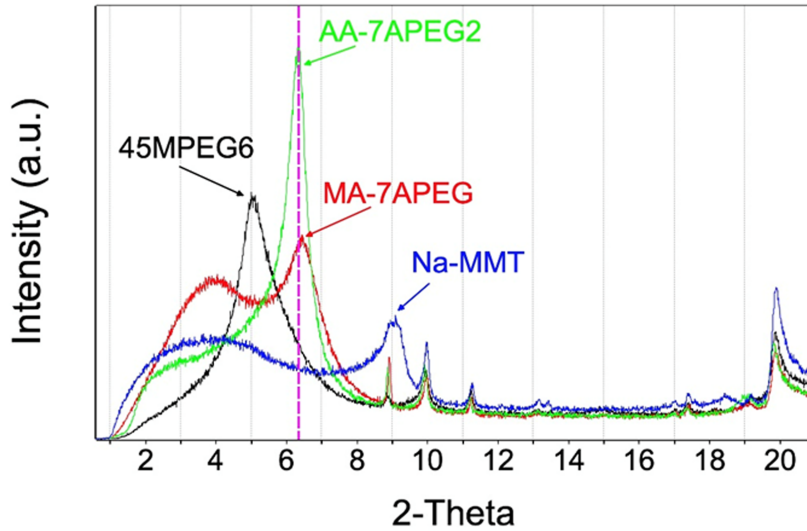
Fig. 8 – XRD patterns of clay dispersed in synthetic cement pore solution containing 50% by weight of (bwo) clay of AA-APEG copolymers, and conventional MEPG PCE (45PC6) after drying at 50 °C (solution/clay ratio = 48).

Sorption of PCEs on clay

To further investigate the intercalation degree between PCEs and clay particle, sorbed amounts of MA-7APEG, AA-7APEG2 and 45MPEG6 were hence determined in a variety of dosages. All PCEs exhibited typical Langmuir adsorption isotherm as presented in **Fig. 9**, i. e, the sorbed amount of PCE increased firstly with the dosage and reached a plateau defined as saturated adsorption amount. To be more specific, the maximum sorbed amount of MA-7APEG was calculated to be ~ 175 mg per gram clay compared to AA-7APEG2 with ~ 125 mg /g clay and 45MPEG6 with ~ 225 mg /g clay. Apparently, conventional 45MPEG6 PCE presented the highest sorbed amount of polymer which corresponds well to its highest d-spacing value in XRD diffraction for the strongest chemical intercalation of PEO side chain. Furthermore, MA-7APEG polymer exhibited a stronger affinity to clay as compared to that of AA-7APEG2 polymer. The results here are in good agreement with the mini slump test results (**Fig. 7**) that MA-7APEG exhibited less clay tolerance due to the less PCE molecules available to disperse cement grains.
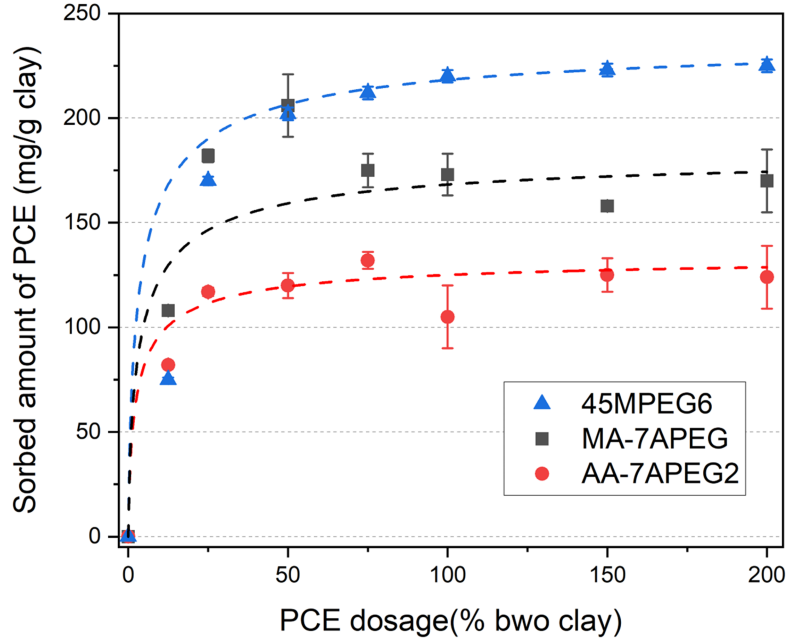
Fig. 9 – Adsorption isotherms of MA-7APEG, AA-7APEG2 and 45MPEG6 PCEs in the clay suspensions dispersed in the synthetic cement pore solutions.

Conformation model within APEG PCEs and clay particles

To further investigate the interaction generated when PCE dispersants approach clay particles, a parameterized model developed by Flatt. et.al [20] is introduced, which is in detail illustrated as shown in **Fig. 10.**

Based on parameters and relevant coefficients proposed in the model, the layer thickness R_{AC} could be obtained through **Eq. (1):**

$$R_{AC} = \left[2\sqrt{2}(1-2\chi)\frac{a_P}{a_N}\right]^{1/5} a_P P^{7/10} N^{-1/10} \qquad (1)$$

Where the Flory parameter χ is about 0.37 at 25 ℃, a_P (0.25 nm) corresponds to the side-chain monomer size and a_N (0.36 nm) refers to the backbone monomer size.

The interaction force F induced when polymers approach and interact with the substrate could be calculated **from Eq (2):**

$$F = \beta \left(\frac{5}{2^{1/3}} R_{AC}^{2/3} - \frac{1}{2} D^{-1/3} \left(3D + 4(2^{\frac{2}{3}}) R_{AC} (\frac{R_{AC}}{D})^{2/3}\right)\right) \qquad (2)$$

in which,

$$\beta = \frac{2\pi k_B T R_{tip}}{\alpha} P^{-29/30} N^{-13/30} \qquad (3)$$

where the interest D is the separation distance; R_{tip} is the tip radius taken as 25 nm and the adjusted parameter α could be obtained from **Eq. (4):**

$$\alpha = \pi 2^{-\frac{3}{10}} a_P^{\frac{5}{3}} a_N ((1-2\chi)\frac{a_P}{a_N})^{2/15} \qquad (4)$$

11
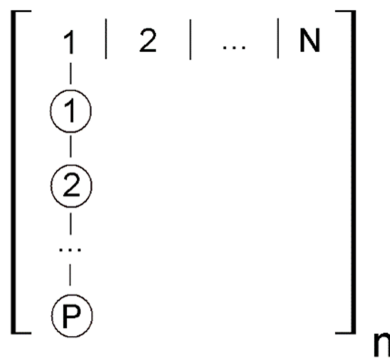
Fig. 10 – Schematic diagram for the comb polymers according to Flatt [20]. In this model, the polymer backbone is defined as the assemblage of n repeating structure units with Mw, each containing N backbone monomers and one side chain of P units of EO.

The structure parameters and the resulting interaction force F, given the separation distance D as the layer thickness R_{AC}, are displayed in **Table 5**. MA-7APEG exhibits higher adhesion force (0.61 nN) than (0.50 nN) of AA-7APEG2, indicating the former polymer is more inclined to get close to the clay particles. Combined with the aspect of calcium binding abilities, MA-7APEG would capture more Ca^{2+} ions cheating with negatively charged carbonate groups, leading to the decrease of anionicity of PCE. Hence, there would be a lower repulsion force between MA-7APEG and clay and make it easier to intercalate into the clay interlayers.

Table 5 – Modeling parameters and the resulting layer thickness and interaction force between polymers and clay particles.

PCE samples	AA-7APEG2	MA-7APEG
P	7	7
N	3	2
n	80	79
R_{AC} / nm	0.76	0.80
F /nN *	-0.50	-0.61

* "-" means the adhesion type of interaction force.

FURTHER RESEARCH

For the outlook of the research focus, it would be of great interest to quantitatively detect the intercalated amount of PCEs into the bentonite. Moreover, to establish a chelation model between calcium and PCEs with structural-different anchor group could help the future targeted synthesis work.

CONCLUSIONS

Two APEG PCEs were synthesized choosing the same macromonomer with designated side-chain lengths of 7 EO units, but with different acids as co-monomers, namely, maleic anhydride (MA) and acrylic acid (AA). These two PCE were determined to possess a similar anionicity and comparable molecular weight. However, MA-7APEG exhibited much lower effective charge in the presence of Ca^{2+} ions as compared to AA-7APEG2 polymer, indicating that the 7APEG PCE with MA group exhibited stronger calcium binding capacity than the counterpart with anchor group of AA. This fundamental structural difference further influenced their distinct adsorption behavior on clay and hence the dispersing capacity in the presence of clay. TOC results suggest that MA-7APEG polymer exhibited a

stronger affinity to clay as compared to that of AA-7APEG2 polymer. Applying a parameterized model, it was found that MA-7APEG exhibits higher adhesion force (0.61 nN) than (0.50 nN) of AA-7APEG2, indicating the former polymer is more inclined to get close to the clay particles. Apparently, the type of carboxylate groups present in the PCE structure exhibited an impact on the dispersing power of PCE polymers as well as their clay robustness. It is hoped our findings here could guide the targeted synthesis in the future.

REFERENCES

[1] Y. Ma, S. Sha, B. Zhou, F. Lei, Y. Liu, Y. Xiao, C. Shi, Adsorption and dispersion capability of polycarboxylate-based superplasticizers: a review, Journal of Sustainable Cement-Based Materials, (2021) 1-38.

[2] H. Feng, Z. Feng, W. Wang, Z. Deng, B. Zheng, Impact of polycarboxylate superplasticizers (PCEs) with novel molecular structures on fluidity, rheological behavior and adsorption properties of cement mortar, Construction and Building Materials, 292 (2021) 123285.

[3] J. Plank, E. Sakai, C. Miao, C. Yu, J. Hong, Chemical admixtures—Chemistry, applications and their impact on concrete microstructure and durability, Cement and concrete research, 78 (2015) 81-99.

[4] X. Liu, J. Guan, G. Lai, Y. Zheng, Z. Wang, S. Cui, M. Lan, H. Li, Novel designs of polycarboxylate superplasticizers for improving resistance in clay-contaminated concrete, Journal of industrial and engineering chemistry, 55 (2017) 80-90.

[5] S.S. Mousavi, C. Bhojaraju, C. Ouellet-Plamondon, Clay as a Sustainable Binder for Concrete—A Review, Construction Materials, 1 (2021) 134-168.

[6] L. Lei, J. Plank, A concept for a polycarboxylate superplasticizer possessing enhanced clay tolerance, Cement and Concrete Research, 42 (2012) 1299-1306.

[7] Y. Ma, C. Shi, L. Lei, S. Sha, B. Zhou, Y. Liu, Y. Xiao, Research progress on polycarboxylate based superplasticizers with tolerance to clays-A review, Construction and Building Materials, 255 (2020) 119386.

[8] M. Werani, L. Lei, Influence of side chain length of MPEG–based polycarboxylate superplasticizers on their resistance towards intercalation into clay structures, Construction and Building Materials, 281 (2021) 122621.

[9] S. Sha, M. Wang, C. Shi, Y. Xiao, Influence of the structures of polycarboxylate superplasticizer on its performance in cement-based materials-A review, Construction and Building Materials, 233 (2020) 117257.

[10] J. Ren, S. Luo, S. Shi, H. Tan, X. Wang, M. Liu, X. Li, Synthesis and optimization of a montmorillonite-tolerant zwitterionic polycarboxylate superplasticizer via Box-Behnken design, Clay Minerals, (2021) 1-9.

[11] P. Borralleras, I. Segura, M.A. Aranda, A. Aguado, Influence of experimental procedure on d-spacing measurement by XRD of montmorillonite clay pastes containing PCE-based superplasticizer, Cement and Concrete Research, 116 (2019) 266-272.

[12] X.-K. Li, D.-F. Zheng, T. Zheng, X.-L. Lin, H.-m. Lou, X.-q. Qiu, Enhancement clay tolerance of PCE by lignin-based polyoxyethylene ether in montmorillonite-contained paste, Journal of Industrial and Engineering Chemistry, 49 (2017) 168-175.

[13] L. Lei, Y. Zhang, R. Li, Specific molecular design of polycarboxylate polymers exhibiting optimal compatibility with clay contaminants in concrete, Cement and Concrete Research, 147 (2021) 106504.

[14] P. Borralleras, I. Segura, M.A. Aranda, A. Aguado, Absorption conformations in the intercalation process of polycarboxylate ether based superplasticizers into montmorillonite clay, Construction and Building Materials, 236 (2020) 116657.

[15] L. Lei, J. Plank, Synthesis and Properties of a Vinyl Ether-Based Polycarboxylate Superplasticizer for Concrete Possessing Clay Tolerance, Industrial & Engineering Chemistry Research, 53 (2014) 1048-1055.

[16] G. Xing, W. Wang, J. Xu, Grafting tertiary amine groups into the molecular structures of polycarboxylate superplasticizers lowers their clay sensitivity, RSC advances, 6 (2016) 106921-106927.

[17] M.T.R. Laguna, R. Medrano, M.P. Plana, M.P. Tarazona, Polymer characterization by size-exclusion chromatography with multiple detection, Journal of Chromatography A, 919 (2001) 13-19.

[18] J. Plank, B. Sachsenhauser, Experimental determination of the effective anionic charge density of polycarboxylate superplasticizers in cement pore solution, Cement and Concrete Research, 39 (2009) 1-5.

[19] DIN EN 1015-3:2007-5, Methods of Test for Mortar for Masonry -Part 3: Determination of Consistence of Fresh Mortar, DIN, Berlin/Germany, 2007.

[20] R.J. Flatt, I. Schober, E. Raphael, C. Plassard, E. Lesniewska, Conformation of adsorbed comb copolymer dispersants, Langmuir, 25 (2009) 845-855.

BIOGRAPHY

Lei Lei is a Habilitand at the Institute of Inorganic Chemistry at Technische Universität München, Germany. Her research focuses on chemical admixtures, supplementary cementitious materials (SCMs) and interaction between admixtures and binders. Dr. Lei has published 40 scientific papers in peer reviewed journals and conferences and served on numerous committees. She is a member of RILEM (Development Activities Committee (DAC)), American Concrete Institute (ACI) and Gesellschaft Deutscher Chemiker (GDCh), construction chemistry section.

Yue Zhang is a Ph.D. candidate at the Institute of Inorganic Chemistry at Technische Universität München, Germany. For his Ph.D. study, he mainly focuses on the synthesis and characterization of novel PCE superplasticizers for conventional OPC binder as well as low carbon binder systems, such as alkali-activated slag. He has authored several scientific journals and conference papers.

American Concrete Institute

Always advancing

Yue Zhang
Country: Germany (DEU)
Address: Lichtenbergstr.4
State: Any... ()
City: Garching
Zip code: 85748
May 30, 2023

Subject: Use of ACI Copyrighted Material

Your request to:

   X   Use information/figures/tables indicated below. Please credit American Concrete Institute, author(s) and publication.

   X   Reprint the information described in the quantity indicated. Please add a note to the reprint similar to: *Authorized reprint from (publication) (issue/volume/year as appropriate.)* Payment of Right-to-Reprint fee of ($000 per Table/Figure/Section, $000 total) is required.

Permission is granted to reference and reprint
The paper, *Molecular Design of an Allylether PCE with Enhanced Clay Tolerance*, found in SP-354, 2022.

Signed: **Ryan Jay**_____ Date: **30 May 2023**

Ryan Jay
Supervisor/Graphic Designer, Publishing Services
Ryan.Jay@Concrete.org

5.3 Paper # 3 (Conference paper)

Exploring the dispersion effectiveness of APEG PCEs in the presence of clay: the impact of calcium interaction

(in Chinese)

Y. Zhang, L. Lei

Multiple studies have provided evidence that the capacity of polycarboxylate superplasticizers (PCE) to withstand the effects of clay is closely associated with the molecular structure of the PCEs. In this paper, we developed and produced two varieties of α-allyl ω-hydroxy polyethylene glycol – based superplasticizers, namely 7APEG-PCE, with a side chain length of 7 ethylene oxide (EO) units and explored other potential factors affecting PCE resistance to clay. Those included structural differences of carboxylic anchoring groups and the resulting variations in PCE's Ca^{2+} chelating capacity.

基于 APEG 型聚羧酸系减水剂的抗粘土性能研究

张岳 [1]，雷蕾

慕尼黑工业大学无机化学系，德国慕尼黑

摘要：如何提高聚羧酸系减水剂的抗粘土性能已成为建筑材料领域一个热议的课题。以蒙脱土（MMT）为例，PCE 会通过支链插层的形式进入粘土的层间，从而使得其分散性能受到抑制。本文通过自由基聚合反应设计合成了两种 α-烯丙基 ω-羟基聚乙二醇（APEG）型聚羧酸，它们具备相同的支链长度（7 个环氧乙烷单元），但分别由马来酸酐（MA）和丙烯酸（AA）两种类型羧酸聚合而成。两种聚合产物具有相近的带电荷量和分子质量。通过性能测试表明，AA-7APEG2 的抗粘土性能比 MA-7APEG 优越。为进一步分析聚合产物的性能差异，引入 Ca^{2+} 测定其对两种聚羧酸阴离子电荷密度的影响，结果发现，相比 AA-7APEG2，MA-7APEG 的电荷量降低更多，推断得出 MA-7APEG 具备更强的 Ca^{2+} 螯合能力，进而在接近 MMT 时，MA-7APEG 受到更少的静电斥力，更容易发生插层，所以抗粘土性能比 AA-7APEG2 弱。

关键词：聚羧酸；APEG；Ca^{2+} 螯合；抗粘土性能

1 引言

广泛研究表明，聚羧酸系减水剂（PCE）的抗粘土性能与 PCE 的分子结构紧密相关。比如，不含聚乙二醇（PEO）侧链或具有短支链长度的 PCE 可以很大程度地避免粘土插层。Lei 等人设计了一种乙烯基醚型的新型 PCE，这是带有短侧链的单烷基马来酸酯的三元共聚物，可以在保证流动性的同时进一步降低聚合物用量，其在粘土上的吸附量仅为 20 mg/g（传统类型 PCE：230 mg/g）。此外，通过改变侧链的形状，也可以增强 PCE 的抗粘土性能。Liu 等人通过酯化反应成核，后接聚合反应制备了星形 PCE。这种立体结构可以产生很大的空间位阻，防止大多数 PCE 与粘土发生插层，保留其分散水泥浆体的能力。一般来说，通过 PCE 的结构修饰或改性及可以增强 PCE 的抗粘土性能。然而，通过我们的研究发现，结构属性相似的 PCE 在含粘土的水泥浆体中的分散能力可能有仍然存在差异。于是，我们设计合成了选取了两种侧链长度为 7 个环氧乙烷(EO)的 α-烯丙基 ω-羟基聚乙二醇，即，7APEG-PCE，揭示了其他可能存在的影响 PCE 抗粘土性能的因素，比如 PCE 对 Ca^{2+} 螯合能力的差异。

2 实验

2.1 实验材料

（1）水泥

选用德国 Schwenk 公司生产的普通硅酸盐水泥样品 CEM I 42.5R。其主要物相组成为：C_3S 59.55 %, C_2S 11.08 %, C_4AF 10.07 %, C_3A 6.94 %, $CaSO_4$ 2.59 %, $CaSO_4 \cdot 2H_2O$ 3.09 %, $CaSO_4 \cdot 0.5H_2O$ 0.10 %, $CaCO_3$ 2.34 %, $CaMg(CO_3)_2$ 0.97 %, SiO_2 0.42 %。水泥样品的 *Blaine* 值为 3105 cm^2/g。

---

[1] 张岳，男，1992 年 11 月，博士研究生

Technical University of Munich, Lichtenbergstr. 4, Garching bei München, 85747, Tel.: +49 (089) 289 13217

（2）粘土

通过 X 射线荧光测定粘土的氧化物组成为：SiO_2 55.7%，Al_2O_3 16.2%，Fe_2O_3 3.5%，CaO 3.0%，Na_2O 2.0%，MgO 1.4%，K_2O 0.9%，TiO_2 0.3%，BaO 0.1%，P_2O_5 0.1%，MnO 0.1%，SrO 0.1%，SO_3 0.1%，烧失量（LOI）16.5%。样品粒径分布的 D_{50} 值为 23.55 μm。

（3）聚羧酸合成原料

丙烯酸（> 99 %，德国 Sigma Aldrich 公司），α-烯丙基-ω-羟基聚乙二醇醚（APEG 大单体，7 个环氧乙烷单元）（> 98 %，日本 NOF 公司），过硫酸铵（APS，≥ 98 %，德国 Sigma Aldric 公司），过氧化苯甲酰 (> 98 %，德国 Sigma Aldrich 公司)，甲代烯丙基磺酸钠（> 98 %，德国 Sigma Aldrich 公司），3-巯基丙酸（≥ 99 %，德国 Sigma Aldrich 公司），氢氧化钠（NaOH，≥ 97 %，德国 Merck KGaA 公司），马来酸酐（> 99 %，德国 Sigma Aldrich 公司）。

2.2 实验方法

2.2.1 APEG 聚羧酸制备

MA-7APEG 聚羧酸是通过本体共聚反应合成的，合成路线如图 1（a）所示。在装有搅拌器和回流冷凝管的 250 mL 反应烧瓶中，加入 21.80 g MA（0.222 mol）和 77.7 g 烯丙基醚（7APEG, 0.222 mol），在 200 rpm 转速 和 70 ℃ 恒温条件下，搅拌 1 h。然后将 0.51 g 过氧化苯甲酰粉末作为引发剂一次性加入反应器中，然后每隔 10 min 加入 1.03 g 过氧化苯甲酰粉末，直至 90 min。加料完成后，提高温度至 90 ℃，持续搅拌 90 min， 反应完成后加入 150.08 g 去离子水，保持恒温，至形成均匀的聚羧酸溶液。最后，将产物静置冷却，用 30 wt.% 浓度的 NaOH 溶液调节 pH 至中性。

对于 AA-7APEG2，其合成路线如图 1（b）所示。制备步骤如下：首先，将 25 g（0.066 mol）APEG 大单体 (Mw = 350 g/mol) 和 45 mL 去离子水混合加入五颈烧瓶中，烧瓶分别与回流冷凝器、机械搅拌器、氮气入口和两个分开的进料入口相连。将上述大单体溶液加热至 80 ℃ 并用 N_2 吹扫 30 min。然后，制备两种进料溶液（溶液 A 和溶液 B）。将 9.387 g（0.132 mol）AA 和 0.225 g（0.002 mol）3-巯基丙酸（链转移剂）溶解在 25 mL 去离子水中，此溶液标记为溶液 A；将 5.629 g (0.025 mol) 过硫酸铵 （APS）溶解在 30 mL 去离子水中，此溶液为溶液 B。使用两个蠕动泵分别经两个不同进料口，将溶液 A 和 B 逐滴加入反应容器中，控制溶液 A 在 2.5 h，溶液 B 在 3 h 内进样完毕。当溶液 B 的添加完成时，持续搅拌 1 小时。最后，将 PCE 溶液冷却至室温，同样使用 30 wt. % NaOH 溶液将 pH 值调节至 6.5-7。
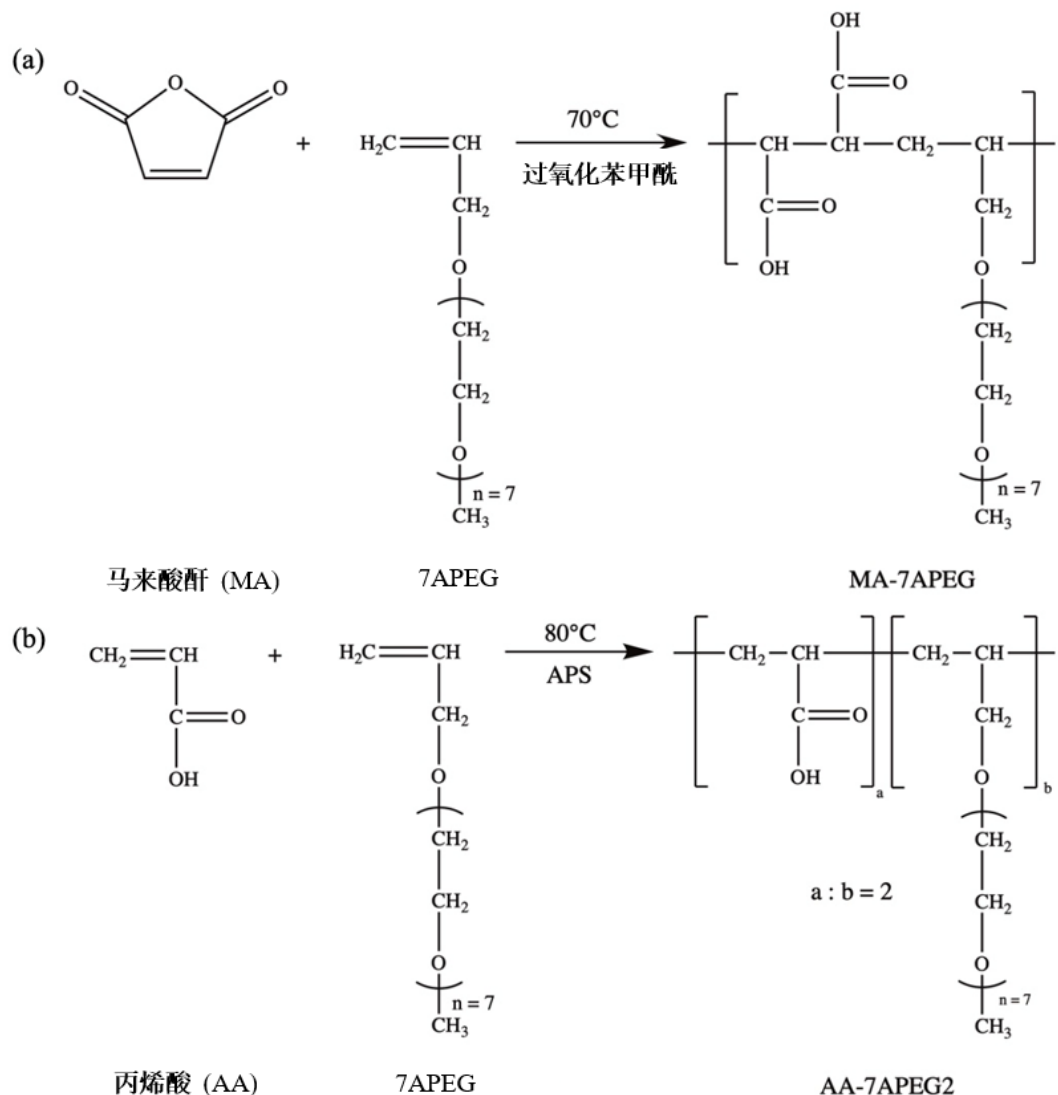
图 1. MA-7APEG 和 AA-7APEG2 聚羧酸合成路线

2.2.2 凝胶色谱法表征

通过凝胶色谱法(GPC) 测定制备的 PCE 的分子质量 (Mw 和 Mn)、分散系数 (PDI) 和大单体转化率等分子特性参数。测试仪器为 Waters Alliance 2695 （Waters，德国），配备有三个 Ultra hydrogel 柱（120、250、500）和一个 Ultra hydrogel TM Guard 柱。洗脱液为 0.1 N NaNO₃ (pH = 12)，流速为 1.0 mL/min。对于 *Mw* 和 *Mn* 的计算，参数 dn/dc 为 0.135 mL/g（聚乙二醇）。

2.2.3 净浆流动度测试

为了评估 PCE 在水泥浆体中的分散效果，采用"微型坍落度"测试。根据 DIN EN 1015 标准规定的实验方法：首先，确定一个未加入 PCE 时净浆的水灰比，能够实现 18 ± 0.5 cm 的摊铺直径。然后，在此水灰比下，确定对每个 PCE 样品净浆达到 26 ± 0.5 cm 扩散直径时的掺量。试验步骤描述如下：首先，在瓷杯中将 PCE 与去离子水混合，计算需水量时需减去 PCE 溶液本身的含水量。然后，在 1 min 内将 300 g 水泥加入混合水中，静置 1 min，接着保持恒定速率搅拌 2 min。最后，将混合均匀的净浆倒入放置在玻璃板上的 Vicat 锥体（高 40 mm，顶部直径

3

70 mm，底部直径 80 mm）中，然后，快速垂直取出锥体，使水泥浆体向四周摊铺。等至浆体停止流动，任取相互垂直的两个方向测量净浆直径两次，取其平均值作为最终摊铺直径。当水泥中掺入 1 wt. % 和 3 wt. % 粘土时，参照以上试验步骤进行测定。

2.2.4 阴离子电荷密度测定

使用粒子电荷检测器 PCD 03 pH (Mütek Analytic, Herrsching, 德国) 测定合成 PCE 的阴离子电荷量。量取 10 mL 0.2 g/L PCE 溶液，用 0.34 g/L 带正电的聚二烯丙基二甲基氯化铵 (polyDADMAC) 水溶液进行滴定，直至达到电荷中和（零电位），则 PCE 聚合物的阴离子电荷密度可以通过阳离子聚电解质 polyDADMAC 的消耗量求得。

3 结果与讨论

3.1 聚羧酸产物的分子属性表征
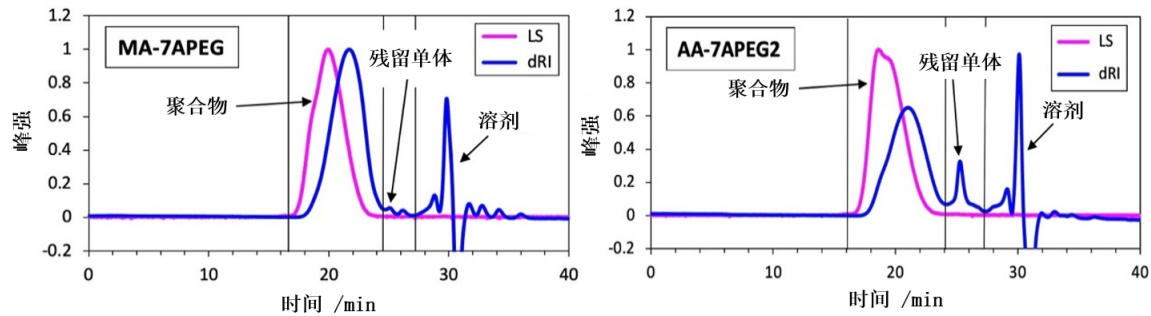
图 2. MA-7APEG 和 AA-7APEG2 的凝胶色谱图

如图 2 所示，通过凝胶色谱法对合成的 MA-7APEG 和 AA-7APEG2 的分子属性进行了表征，根据光散射信号（LS）和示差折光指数（dRI）随流出时间的变化趋势，得出反应产物的分子量分布。聚合产物的分子质量（M_w，M_n），分散系数（PDI）以及大单体转化率等参数值，详见表 1。分析可知，合成的两种 APEG PCE 均具有较好的纯度，即相对较低的分散系数（PDI ≈ 2）和较高的转化率(MA-7APEG：96.6 %，AA-7APEG2：84.3 %)。

表 1. APEG 聚羧酸分子结构参数

聚羧酸	M_w/g·mol^{-1}	M_n/g·mol^{-1}	PDI	大单体转化率 (%)
MA-7APEG	38,100	15,875	2.4	96.6
AA-7APEG2	41,320	17,965	2.3	84.3

3.2 净浆流动度测试

3.2.1 扩散直径 26 ± 0.5 cm 的 PCE 掺量

首先，为了比较 PCE 在水泥体系中的分散性能，我们测定了 MA-7APEG，AA-7APEG2 和常见的聚羧酸 45MPEG6 作为参照样，对应的水泥净浆的流动度。经测试，保持相同的水灰比（0.48），确定不同 PCE 使净浆摊铺直径达到 26 cm 所需的用量。由图 3 可知，与 45MPEG6

的外加剂用量（0.06 % 水泥质量）相比，MA-7APEG 的掺量较低为 0.07 %，AA-7APEG2 的所需剂量较高，达到了 0.21 %，由此说明，MA-7APEG 与相似分子结构的 AA-7APEG2 相比，在水泥浆体中具有更好的分散性能。
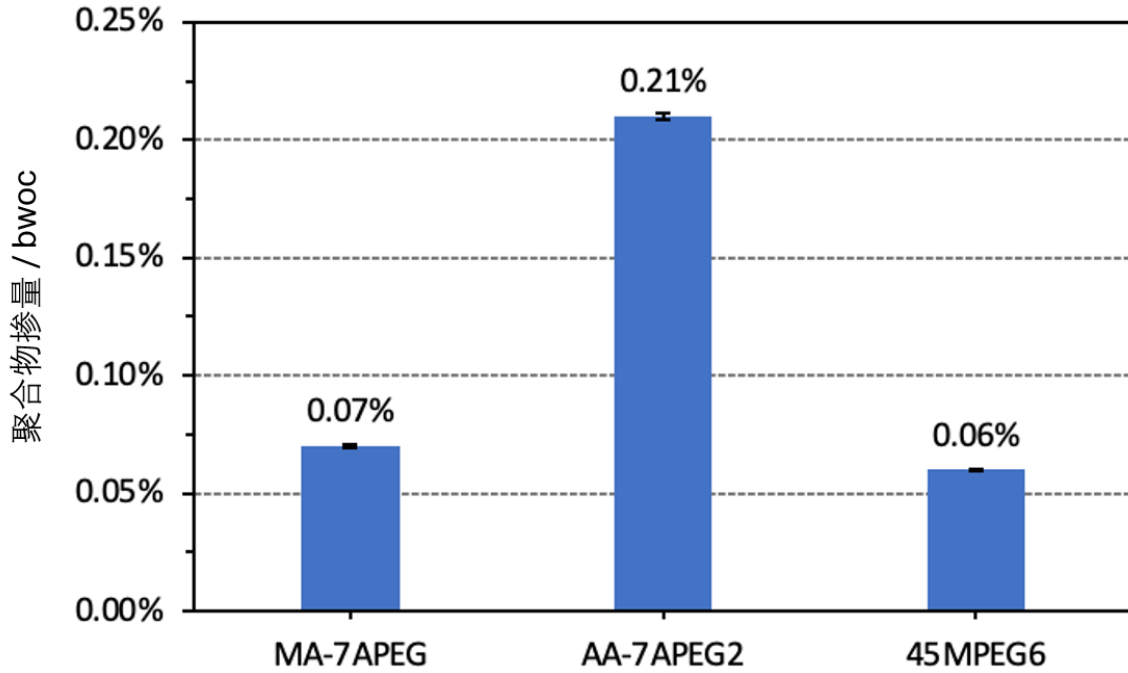
图 3. 净浆扩散直径达到 26 ± 0.5 cm PCE 所需用量（水灰比：0.48）

3.2.2 粘土掺量对净浆流动度的影响

进一步，为了测定上述 PCE 的抗粘土性能，我们向水泥中分别掺入了 1 wt.% 和 3 wt.% 的粘土，以此来 比较不同 PCE 对应的净浆流动度的损失。由图 4 可知，没有加入粘土时，MA-7APEG，AA-7APEG2 以及 45MPEG6 的初始摊铺直径均为 26 cm。向水泥中加入 1 wt.% 粘土后，不同 PCE 对应的水泥净浆的流动度均有损失，即，三种 PCE 的分散性能，由于粘土的加入均受到不同程度的抑制。当粘土掺量达到 3 wt.%，PCE 的分散性能损失更严重了，AA-7APEG2 分散性能损失为 73%，MA-7APEG 为 81%，作为对照样的 45MPEG6 分散性能损失最大，达到了 101%。比较可知， AA-7APEG2 的分散性能在粘土掺杂后损失最小，即表明其具有最好的抗粘土性能。
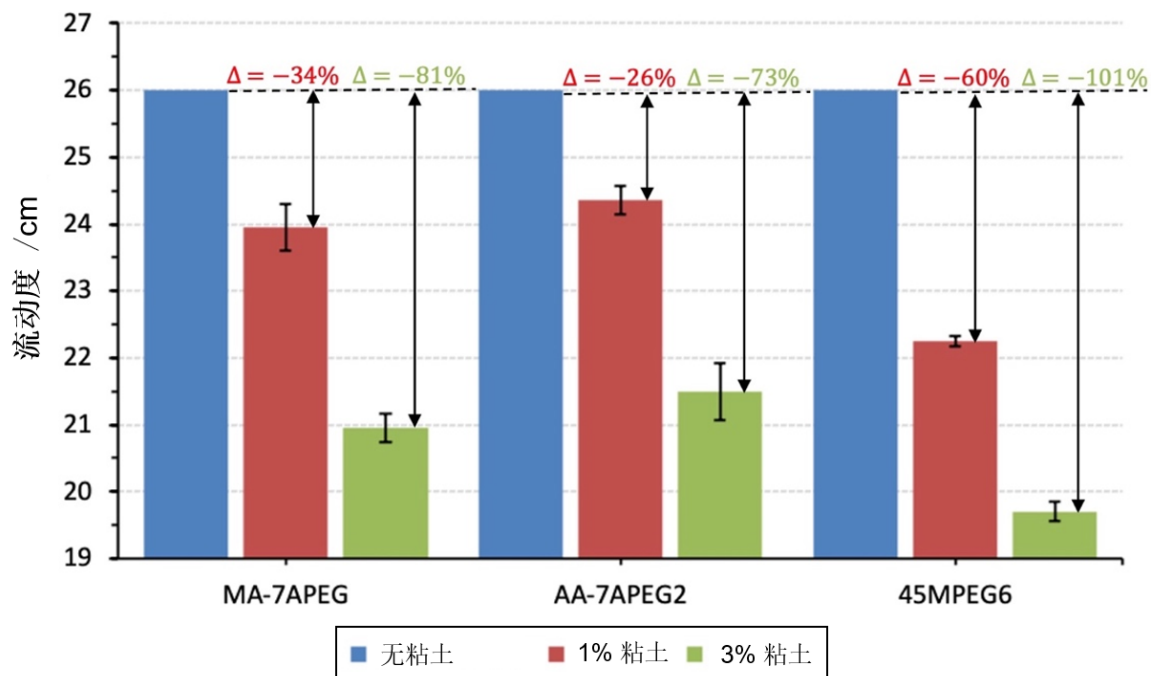
图 4. 不同粘土掺量下净浆的流动度对比(水灰比：0.48)

3.3 Ca^{2+} 对 PCE 阴离子电荷密度的影响

为了探究结构属性相似的 MA-7APEG 和 AA-7APEG2 抗粘土性能存在差异的原因，我们通过测定阴离子电荷密度，比较了两种 PCE 对 Ca^{2+} 的螯合能力，测定结果如图 5 所示。通过理论值计算和未加 Ca^{2+} 条件下的实验测定，我们发现，MA-7APEG 和 AA-7APEG2 的阴离子电荷量相近，均为 3500～4000 μeq/g。但加入 Ca^{2+} 后，上述 PCE 的阴离子电荷密度出现较大的降低，AA-7APEG2 降低至～1500 μeq/g，MA-7APEG 降幅更大，实际电荷量仅为～ 200 μeq/g。这表明 MA-7APEG 对于 Ca^{2+} 的结合能力更强，同时也很好地解释了图 3 中 MA-7APEG 分散性能比 AA-7APEG2 优越，因为在水泥孔隙液中，电离后的 PCE 带负电荷，通过主链的羧酸基团与 Ca^{2+} 发生螯合作用吸附在同样电荷属性的水泥颗粒表面，通过聚乙二醇的支链形成的空间位阻效应使得 PCE 分子能够分散水泥颗粒，增强其流动度。另一方面，MA-7APEG 能够螯合更多的 Ca^{2+} 使得其本身的阴离子电荷密度降低更多，如图 5 所示，在接近同样带负电荷属性的层状粘土时，遇到的静电阻力相比 AA-7APEG2 会削弱更多，使得其支链更容易进入粘土层间发生插层作用，这很好地说明了图 4 中 MA-7APEG 的抗粘土性能不及 AA-7APEG2 的原因。

6
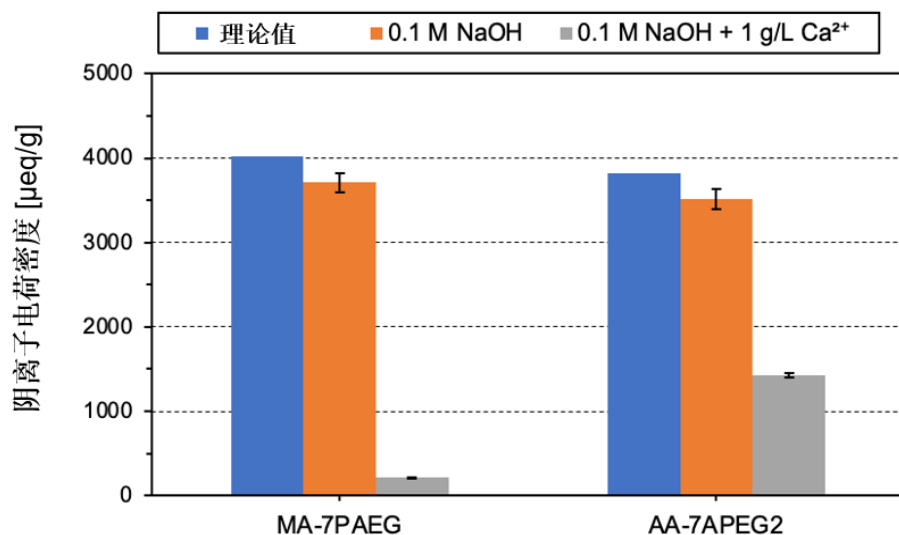
图 5. Ca²⁺对 MA-7APEG 和 AA-7APEG2 阴离子电荷密度的影响

4 结论

选择相同的大单体，指定侧链长度为 7 个环氧乙烷单元，但以不同的羧酸作为共聚单体，即马来酸酐(MA)和丙烯酸(AA)，合成了两种 APEG 聚羧酸系减水剂，这两种 PCE 具有相近的阴离子带电量和分子质量。经测定，MA-7APEG 在水泥基体系中的分散性能更好，但是抗粘土性能不及 AA-7APEG2。实验表明，这是由于 MA-7APEG 具有更强的 Ca²⁺结合能力，能够螯合更多游离的 Ca²⁺，从而降低 PCE 与粘土之间的排斥力，使粘土更容易与 PCE 的聚乙二醇侧链发生插层作用，即抗粘土性能更低。关于 MA-7APEG 和 AA-7APEG 与粘土相互作用机理，在后续会进行更加深入和系统的探究。

参考文献

[1] Li X L, Zheng D F, Zheng T, et al. Enhancement clay tolerance of PCE by lignin-based polyoxyethylene ether in montmorillonite-contained paste [J]. Journal of Industrial and Engineering Chemistry, 2017 (49): 168 – 175.

[2] Tang X, Zhao C, Yang Y, et al. Amphoteric polycarboxylate superplasticizers with enhanced clay tolerance: Preparation, performance and mechanism [J]. Construction and Building Materials, 2020 (252): 119052.

[3] Lei L, Plank J. Synthesis and properties of a vinyl ether-based polycarboxylate superplasticizer for concrete possessing clay tolerance [J]. Industrial & Engineering Chemistry Research, 2014 (53): 1048 – 1055.

[4] Liu X, Guan J, Lai G, et al. Novel designs of polycarboxylate superplasticizers for improving resistance in clay - contaminated concrete [J]. Journal of industrial and engineering chemistry, 2017 (55): 80 – 90.

[5] Li B, Gao R, Wang L. Synthesis and Properties of a Starch-based Clay Tolerance Sacrificial Agent [J]. Starch – Stärke, 2021 (73): 2000223.

[6] Methods of test for mortar for masonry – Part 3: Determination of consistence of fresh mortar (by flow table) [S]. DIN EN 1015 – 3: 2007 – 05.

[7] Plank J, Sachsenhauser B. Experimental determination of the effective anionic charge density of polycarboxylate superplasticizers in cement pore solution [J]. Cement and Concrete Research, 2009 (39): 1 – 5.

5.4 Paper # 4

Preparation of isoprenol ether-based polycarboxylate superplasticizers with exceptional dispersing power in alkali-activated slag: comparison with ordinary Portland cement

L. Lei, Y. Zhang

In this paper, we synthesized and evaluated a range of polycarboxylate ether superplasticizers (PCEs) based on isoprenol ether (IPEG) with varying molecular structures for their ability to disperse alkali-activated slag (AAS) and ordinary Portland cement (OPC) systems.

The study demonstrated that IPEG PCEs with high molecular weight, long side chains, and high anionic charge density exhibited exceptional dispersing power in AAS systems, effectively reducing the yield stress and viscosity of AAS pastes. We attributed this to the strong electrostatic repulsion and steric hindrance effects of these PCEs, which prevented slag particle aggregation and flocculation.

Furthermore, the paper compared the performance of IPEG PCEs in AAS and OPC systems and found that these PCEs had better dispersing efficiency and compatibility in AAS than in OPC systems, due to the differences in the hydration mechanisms, chemical compositions, particle sizes, and surface properties of these binders.

The paper concluded that IPEG PCEs could be used as effective superplasticizers for AAS systems, which can help to reduce the CO_2 emissions associated with cement production.

Preparation of isoprenol ether-based polycarboxylate superplasticizers with exceptional dispersing power in alkali-activated slag: Comparison with ordinary Portland cement

Lei Lei [*], Yue Zhang

Technische Universität München, Chair for Construction Chemistry, 85747, Garching, Lichtenbergstraße 4, Germany

ARTICLE INFO

ABSTRACT

For this study, a series of isoprenol ether (IPEG) based PCE superplasticizers with specially designed molecular architectures (molecular weight, side chain length, anionicity) was successfully synthesized. All synthesized PCEs exhibited high macromonomer conversion rates as well as relatively low PDIs indicating high quality. Dispersing efficiency of the synthesized IPEG PCEs was captured via spread flow and shear-dependent rheology tests in AAS or OPC pastes. It was found that in AAS pastes all polymers perform as highly effective superplasticizers and require extremely low dosages (~0.05%). Whereas, none of the PCE polymers prepared could provide fluidity in OPC, even at high dosages (e.g. 0.3%). For a mechanistic understanding, the interaction between the polycarboxylate superplasticizers and AAS and OPC was investigated via adsorption and zeta potential measurements. It was concluded that all IPEG PCE samples produced typical Langmuir adsorption curves on AAS pastes, but exhibited linear relationships in cement pastes which signifies precipitation of these PCEs from the pore solution. The study highlights the disparity in performance of specific superplasticizers in different binder systems resulting from their different surface chemistry. Specific molecular motifs are required to address these differences in surface compositions at the atomistic level.

1. Introduction

Globally, approximately 8% of the annual anthropogenic CO_2 emission originates from the production of ordinary Portland cement (OPC) [1]. In order to tackle this issue, some researchers have been dedicated to increase the energy efficiency in the calcination process, and others intend to replace the cement clinker with "low-carbon" supplementary cementitious materials (SCMs) [2–5]. One of the promising substitutes is ground granulated blast furnace slag (GGBFS). According to the study performed by Flower and Sanjayan [6], GGBFS can effectively reduce carbon footprint by 22% in typical concrete mixes. Furthermore, Weil et al. [7] estimated that the global warming potential of alkali-activated (AA) concrete is 70% lower compared to that of OPC concrete from a lifecycle analysis. In fact, the nature, concentration, and dosage of the alkali activators as well as the curing conditions for the concrete and the specific mix design of the concrete exert influence on the carbon footprint reduction of alkali-activated (AA) concrete [8]. To attain desired properties, alkali activators are selected. Generally, most of the alkali ions used as activators have relatively high CO_2 emissions. It

is reported that the production of 1 kg of sodium hydroxide emits about 1.1 kg of CO_2, and 1.2 kg of CO_2 is released for every kg of sodium silicate produced [9,10]. In comparison to GGBFS, alkali activators have contributed tremendously to the environmental impact calculations of AAS. Therefore, finding sustainable activators with lower environmental impacts to substitute commercial alkali-activators based on bulk chemicals presents to be a feasible method to achieve a targeted CO_2 reduction in AAS [10]. Other advantages of using slag as a binder include the conservation of natural resources, since slag is a by-product of the iron industry and the enhancement of the mechanical properties and durability [11–14]. However, this substitution brings about technical hurdles that need to be considered. One of them is the latent hydraulic property of slag, as a result, slag needs to be "activated". Common activators are alkalis, therefore the designation alkali-activated slag [15]. Second, slag exhibits some drawbacks including poor workability, quick setting and high shrinkage after hydration. Third, the superplasticizers commonly applied in OPC fail to provide sufficient dispersing power in AAS systems. These problems have discouraged the large-scale application of AAS.

Table 1
Phase composition of the OPC sample CEM I 42.5 R according to Q-XRD analysis using *Rietveld* refinement.

Phase	wt. %
C_3S, monoclinic	54.52
C_2S, monoclinic	18.41
C_4AF, orthorhombic	10.85
C_3A, cubic	5.23
C_3A, orthorhombic	0.88
Anhydrite ($CaSO_4$)	0.94
Dihydrate ($CaSO_4 \cdot 2H_2O$)	3.61
Hemihydrate ($CaSO_4 \bullet 0.5H_2O$)	0.33
Calcite ($CaCO_3$)	3.04
Dolomite ($CaMg(CO_3)_2$)	1.13
Quartz (SiO_2)	0.91
Free lime (*Franke*)	0.14
Total	100.00

Table 2
Oxide composition of the slag used in this study.

Oxide content	[%]
CaO	43.9
SiO_2	37.4
Al_2O_3	10.9
MgO	6.5
FeO	0.7
TiO_2	0.5
SO_3	0.1
Na_2O	0.3
K_2O	0.2
Total	100

High effectiveness for AAS requires specific molecular design. Lei et al. [16] have presented tailor-made α-methallyl-ω-hydroxy poly (ethylene glycol) ether (HPEG) based polycarboxylate superplasticizers possessing high anionic charge density, short side chains and a relatively high molecular weight (M_w) which are highly effective in NaOH activated slag paste. The interaction occurring between superplasticizers and cement has been investigated thoroughly and is described in numerous literatures [13,17–21]. Different dispersing mechanisms have been proposed when superplasticizers possessing various chemical structures adsorb onto the surface of cement particles. Polymers based on melamine or naphthalene polycondensates function by electrostatic repulsion [22,23]. Whereas the main driving force for polycarboxylate superplasticizers to disperse cement particles is steric hindrance. Moreover, the type, dosage as well as the specific molecular architecture of the dispersing agent greatly influences its effectiveness [24]. Among others, the molecular geometry affects the adsorption behavior of PCE polymers. Several trends were identified: PCE polymers possessing higher anionicity adsorb in larger amounts as compared to the ones with lower anionicity; Whereas PCE polymers with high side chain density adsorb in lower amounts and also at a slower adsorption rate.

However, so far very few studies have focused on the fluidizing effect of PCE superplasticizers in alkali activated slag and also the mode of action occurring between them and slag. In a prior study, Palacios et al. [25] compared the fluidizing effect of three different types of superplasticizers (poly (naphthalene sulfonate), poly (melamine sulfonate) and a vinyl copolymer) and found that in OPC pastes all three admixtures exhibited significant fluidizing capacity whereas in NaOH activated AAS (pH = 13.6), poly (naphthalene sulfonate) was the only effective dispersant. These authors also reported a much lower adsorbed amount of the superplastizers in AAS as compared to OPC. A similar observation was made by Sakai et al. [26]. They discovered that an ether-based PCE absorbs far less on slag (1.2–1.9 molecules/100 nm^2) than on cement (2.2–3.2 molecules/100 nm^2). The reason behind the reduced adsorption of PCE superplasticizers on AAS was attributed to competitive adsorption between $COOH^-$ from PCE polymers and OH^- from NaOH, as presented by Marchon et al. [27].

Up to now, no systematic investigation on the interaction between PCEs exhibiting specific molecular architecture and alkali activated slag exists which compares the behavior with in OPC. To fill this gap, a series of five IPEG PCE superplasticizers with specifically designed molecular architectures (molecular weight, side chain length and anionicity) were successfully synthesized. Their dispersing efficiency was captured via spread flow and rheology tests in AAS and OPC pastes, respectively. Finally, the physicochemical interaction occurring between these PCE superplasticizers and the two different binder systems (AAS and OPC) was investigated via adsorption and zeta potential measurements.

2. Experimental

2.1. Materials

2.1.1. Chemicals

Acrylic acid (>99% purity, purchased from Sigma Aldrich, Germany), isoprenyl oxy poly (ethylene glycol) ether (IPEG) (>98%, obtained from Jilin Zhongxin Chemical Group Co., Ltd, China), ammonium persulfate (≥98%, purchased from Sigma Aldrich, Germany), sodium methallyl sulfonate (>98% purchased from Sigma Aldrich, Germany), sodium hydroxide (≥97.0% purchased from Merck KGaA, Germany) were all used without further purification.

2.1.2. OPC

The cement used in this study was an OPC sample CEM I 42.5 R (Schwenk cement company, Ulm, Germany). Table 1 lists its phase composition which was determined by quantitative XRD analysis involving Rietveld refinement. Its average particle size (d_{50} value) was obtained via laser granulometry to be 18.83 μm. Its density was determined at 3.13 g/cm^3 (Helium pycnometry).

2.1.3. Slag

The slag used in this research was provided by Ecocem, Fos sur mer plant. Its fineness was 4450 ± 250 cm^2/g which corresponds to a GGBFS Class A according to the concrete standard NF EN 206–1/CN (Dec. 2012). Its oxide composition as determined by X-ray fluorescence analysis (Axios, PANalytical, Almelo, The Netherlands) is shown in Table 2.

2.2. PCE synthesis and characterization

2.2.1. Synthesis of IPEG PCE superplasticizers

Synthesis of the IPEG PCE polymers was performed via aqueous free radical copolymerization as follows. In total, five PCE samples denominated as 7IPEG3, 7IPEG4.5, 7IPEG15, 23IPEG15 and 50IPEG15 were synthesized. As an example, preparation of 7IPEG7 polymer is described:

37.45 g (0.107 mol) of IPEG macromonomer (M_w = 350 g/mol, n_{EO} = 7) were dissolved in 75 g of deionized (DI) water and charged into a five-neck flask equipped with a stirrer (400 rpm stirring rate), reflux condenser, a nitrogen inlet and two separated feeding inlets. Then the flask was heated to 60 °C and flushed with N_2, 30 min prior to the start of the polymerization.

While flushing the flask with N_2, solutions A and B were prepared separately. Firstly, 5.08 g (0.032 mol) of sodium methallyl sulfonate and 53.97 g (0.75 mol) of acrylic acid (AA) were mixed with 50 g of DI water, and named as Solution A. Secondly, 4.13 g (0.018 mmol) of ammonium persulfate (APS) were dissolved in 25 g of DI water, and labelled as Solution B.

Thereafter, Solutions A and B were charged separately into the reaction vessel over 3 h via two peristaltic pumps, followed by additional
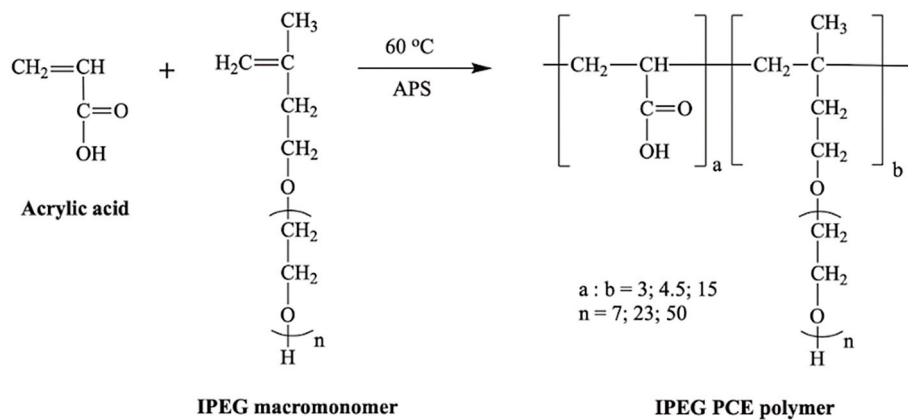
Fig. 1. Synthesis route for the IPEG PCE polymers.

stirring for 2 h at 60 °C. The resulting liquid was cooled to ambient and adjusted to a pH value 6.5–7 by using 30 wt% NaOH solution, yielding a transparent PCE solution exhibiting a solid content of ~40 wt%.

2.2.2. Size exclusion chromatography (SEC)

Molar masses (M_w and M_n), the polydispersity index (PDI) and the macromonomer conversion of the synthesized ether-based PCEs were determined by size exclusion chromatography (SEC), also referred to as gel permeation chromatography (GPC). The measurements were deployed by a Waters Alliance 2695 instrument (waters, Eschborn, Germany) equipped with three Ultrahydrogel™ columns (120, 250, 500) and an Ultrahydrogel™ Guard column. As eluent, 0.1 N NaNO$_3$ (pH = 12) was used with a flow rate of 1.0 mL/min. For the calculation of M_w and M_n, a dn/dc value of 0.135 mL/g (value for PEO) was utilized [28].

2.3. Anionic charge measurement

The specific anionic charge of the IPEG PCEs was determined using a particle charge detector (PCD 03 pH from Mütek Analytic, Herrsching, Germany). Here, 10 mL of the 0.2 g/L PCE solution were titrated against a 0.34 g/L aqueous solution of poly-diallyl dimethyl ammonium chloride (polyDADMAC) until the appearance of charge neutralization (zero potential). From the amount of cationic polyelectrolyte (polyDADMAC) consumed in each test, the amount of negative charge per gram of anionic PCE polymer was calculated.

2.4. Performance testing

2.4.1. Dispersing effectiveness in AAS and OPC

The spread flow of slag pastes containing different IPEG PCEs was determined by performing a "mini-slump" test following a modified version of DIN EN 1015 standard. The water to binder ratio was set to 0.5. In experiment, 300 g of slag were charged into a porcelain cup which contained 150 mL of an 8 wt% NaOH solution (= alkali activator) [16,20,29]. Once the mixture was manually agitated for 90 s, 0.05% of aqueous PCE polymer (by weight of slag, bwos) were added into the mixture. In order to homogenize the slag paste, additional 2.5 min of hand-mixing was applied. Then the slag paste was poured into a Vicat cone (height 40 mm, top diameter 70 mm, bottom 80 diameter) which was placed on a glass plate. After the slag paste was completely filled to the rim, the Vicat was lifted vertically. The resulting spread flow was measured twice, with the second measurement being in a 90° angle from the first one, and the averaged value was noted.

The spread flow tests of cement pastes followed the same procedure as described above, the only difference being that instead of NaOH, DI water was used as mixing water.

2.4.2. Rheology tests

Rheology of AAS and cement pastes was measured as a function of IPEG PCE dosage added as follows: Firstly, the water-to-binder ratio was fixed at 0.48 for both AAS and cement pastes. Then, respective dosages of the IPEG PCE polymers of 0.05%, 0.1%, 0.2% and 0.3% by weight of binder (bwob) were admixed. The AAS and cement suspensions were prepared by mixing 400 g of binder in 8 wt% NaOH solution or deionized (DI) water containing the appropriate amount of PCE polymer. After mixing, the pastes were placed in a Couette - type coaxial viscosimeter Fann$^@$ Model 35SA, and subjected to a 2-cycle measuring procedure whereby the shear rate was increased in 10 s intervals from 3 rpm to 6, 100, 200, 300 and 600 rpm and then decreased back in the same steps as before. The shear stress values obtained from the up-and-down measurements were averaged and reported as shear stress at a given shear rate.

Slurry preparation: the binder (slag and cement) slurries were prepared according to the procedures proposed in API Recommended Practice 10B-2 [30]. The slurries were mixed in a blade-type blender at a water-to-binder (w/b) ratio of 0.48, as this water to binder ratio (rather than 0.5 from Section 2.3.1) would result in a more homogenous slurry. PCE dosages ranged from 0.05 to 0.3% bwob. In a typical preparation, within 15 s the binder was added at 4000 rpm mixing speed to the respective PCE solution placed into the cup of the blender and then mixed for 35 s at 12,000 rpm.

Rheology measurements: a FANN 35SA viscometer (FANN Instrument Company, Houston, TX) equipped with R1 rotor sleeve (rotor radius:18.415 mm), B1 bob (bob radius:17.425 mm, bob height: 3.8 cm) and F1 torsion spring was employed for the rheological tests. The dial readings were converted into Pa by multiplying the values indicated by the instrument with the factor 0.511 and the torsion spring factor F = 1, and the shear rates (3, 6, 100, 200 and 300 rpm) were converted into s^{-1} by multiplying with the factor 1.705. It is worth mentioning that all samples remained homogeneous during the test, no segregation was observed.

2.5. Adsorption of PCE polymers on cement and AAS

Adsorbed amounts of the PCEs on the binders (cement or slag) were determined by analyzing the total organic carbon (TOC) content in the supernatant separated from the solid after contact between binder and mixing water. In a typical experiment, 16 g of binder (cement/slag), 0.64 g of NaOH (only applied in AAS pastes) and 8 g of DI water holding a certain amount of PCE were filled into a 50 mL centrifuge tube and shaken for 2 min at 2400 rpm in a wobbler (VWR International, Darmstadt, Germany). After centrifugation at 8500 rpm for 10 min, the supernatant was retrieved and filtered through a 0.2 μm syringe filter. The filtrate was diluted with DI water (1/30 vol ratio) and its pH value was adjusted to 2 using 0.1 M HCl to remove inorganic carbonates.

Table 3

Molar masses (M_w and M_n), PDI and macromonomer conversion of the synthesized IPEG PCE polymers.

PCE sample	Side chain length [n_{EO}]	AA:IPEG MM molar ratio	M_w [Da]	M_n [Da]	PDI [M_w/M_n]	Macromonomer conversion [%]
7IPEG3	7	3	50,760	20,740	2.4	95.3
7IPEG4.5	7	4.5	99,980	38,620	2.6	97.7
7IPEG15	7	15	96,280	43,220	2.2	98.6
23IPEG15	23	15	86,930	35,240	2.5	95.6
50IPEG15	50	15	87,740	33,070	2.7	91.7
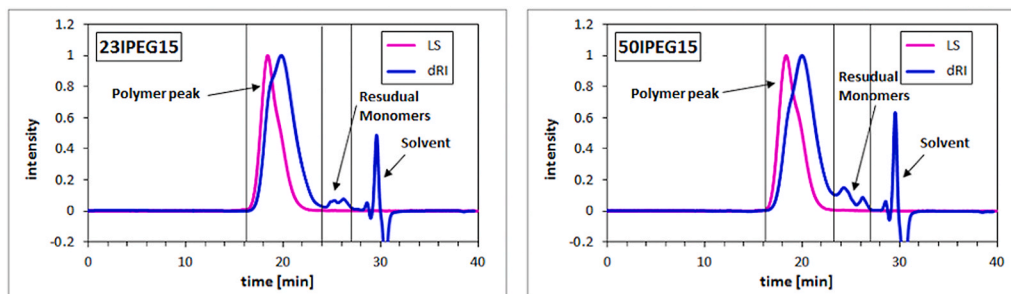
Fig. 2. GPC spectra of the PCE samples 23IPEG15 and 50IPEG15, respectively.

Determination of the TOC content was performed on a High TOC II Instrument (Elementar Analysensysteme, Hanau, Germany).

2.6. Zeta potential measurement

Measurements of zeta potentials were performed on a "DT 1200 Electroacoustic Spectrometer" manufactured by Dispersion Technology, Inc., Bedford Hills, NY, USA. The water-to-binder ratio was set to 0.5, same as in the spread flow tests before (section 2.3.1). A binder slurry containing 350 g of binder (cement/slag), 14 g of NaOH (4% bwos, by weight of slag, only applied in AAS pastes) and 175 mL of DI water was prepared. The binder paste was manually mixed for 4 min and then charged into the container of the zeta potential instrument at a stirring rate of 200 rpm. Then a 30 mL of a 0.117 g/mL PCE solution were titrated step-wise into the binder paste yielding a total of 30 measurement points.

3. Results and discussion

3.1. Molecular properties of the PCE samples

The nomenclature xIPEGy for the synthesized PCE samples was as following: First, the side chain length x of the macromonomer ($n_{EO} = 7$, 23 or 50) is given which is followed by the generic name "IPEG" and finally the feeding molar ratio between acrylic acid (AA) and the IPEG macromonomer y is provided.

Fig. 1 illustrates the synthesis route of the IPEG PCEs prepared in this study. The molecular properties and composition of the resulting polymers are listed in Table 3. All of the synthesized PCEs exhibited not only high macromonomer conversion (>92%) but also relatively low PDIs indicating successful synthesis of high – quality PCEs. As examples, the GPC spectra of 23IPEG15 and 50IPEG15 polymers are displayed in Fig. 2.

3.2. Anionic charge of the IPEG PCE samples

It is generally accepted that the anionic character of PCE polymers represents the most prominent parameter which determines their adsorption behavior. Therefore, quantification of the synthesized anionic charge amount of the PCEs is of great importance.

Here, the anionic charge amount measurements were conducted in 0.01 M NaOH (pH = 12) since at pH $\geq$ 10, carboxylic acid groups are
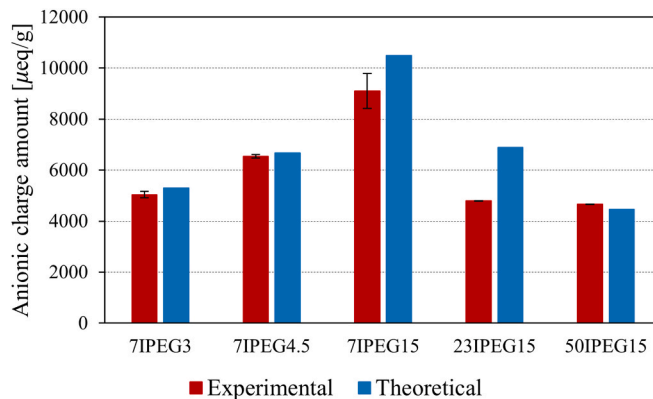
Fig. 3. Anionic charge amounts of the IPEG PCE samples as determined in 0.01 M NaOH solution.
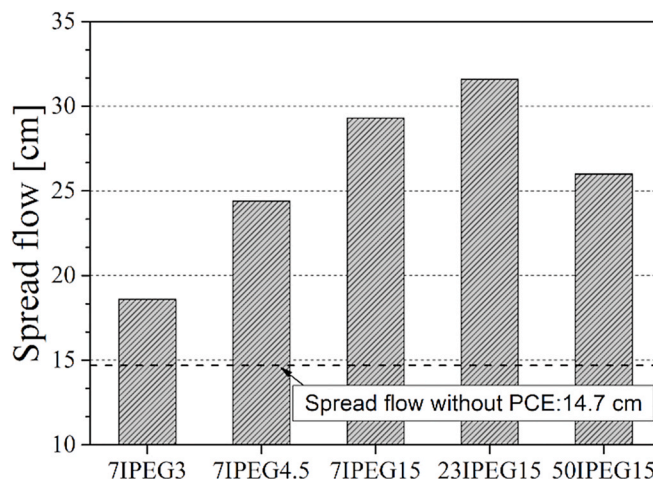
Fig. 4. Spread flow of slag pastes containing 0.05% bwos of the synthesized IPEG PCEs.

AAS paste   Cement paste

(a) 7IEPEG3

(b) 7IPEG4.5

(c) 7IPEG15

(d) 23IPEG15

(e) 50IPEG15
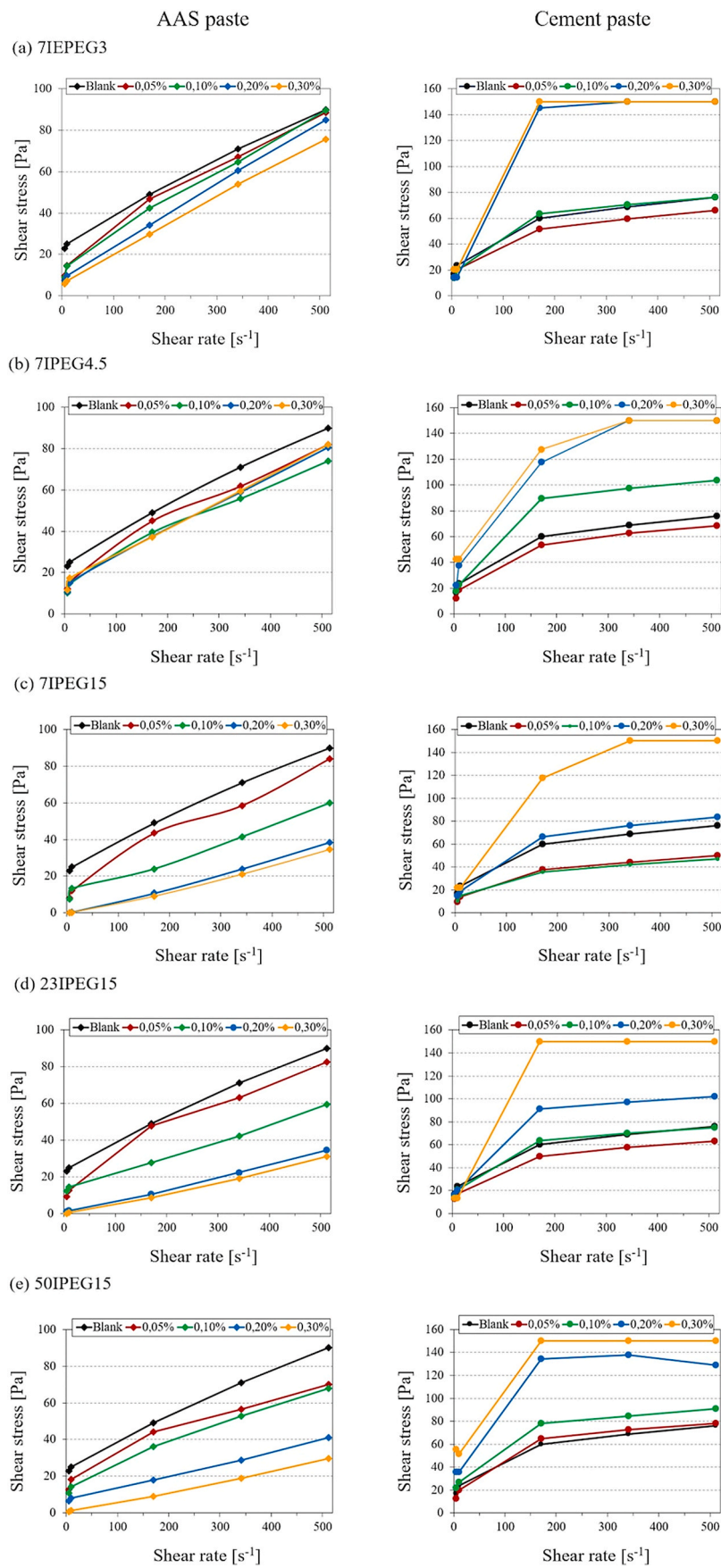
Fig. 5. Shear – dependent rheology of cement and AAS pastes admixed with the synthesized IPEG PCE polymers as a function of their dosage.

fully deprotonated [31]. The theoretical charge amount of the PCE polymers was calculated according to Equation (1).

$$\text{calculated anionic charge amount (eq/g)} = \frac{n_{COO^-}}{M_u} \qquad (1)$$

The calculated as well as the experimentally determined anionic charge amounts of the IPEG PCE samples are presented in Fig. 3.

From Fig. 3 it can be observed that the experimentally determined anionic charges of the IPEG PCEs are relatively close to their theoretical values which assume fully deprotonated carboxylate groups. As can be seen from Fig. 3, the anionicity of a PCE polymer prepared from the same side chain increases when a higher molar ratio of acrylic acid is used in the PCE (3 → 4.5 → 15). At the same time, anionicity decreases with increasing side chain length in the PCE.

3.3. Dispersing effectiveness of the PCEs in AAS and cement

Fig. 4 presents the spread flow of AAS pastes admixed with 0.05% bwos of the IPEG PCE polymers possessing various anionicity and side chain lengths. Considering the extremely low dosage (0.05% bwos) applied here, it can be concluded that all IPEG PCE polymers perform excellently in AAS pastes. Moreover, dispersing ability of the IPEG PCEs increases substantially with increasing anionicity. For example, the most anionic polymer sample 7IPEG15 (molar ratio AA:IPEG = 15) reaches a spread flow as high as 29.3 cm whereas the less anionic sample 7IPEG3 (molar ratio AA:IPEG = 3) exhibiting the same pendent chain length only achieves 18.6 cm at the same dosage. Furthermore, among IPEG PCEs prepared from the same molar ratio of 15:1, but made of different side chain lengths, those possessing shorter pendants (n_{EO} = 7 and 23) outperform the one exhibiting a longer side chain (n_{EO} = 50). This behavior can be ascribed to the lower solubility of the PCE incorporating a long PEG pendant chain in the highly ionic environment of AAS paste [20].

Similar "mini slump" tests were carried out on cement pastes admixed with these IPEG PCE polymers. Most surprisingly, there none of the PCE polymers provided any fluidity, even at dosages as high as 0.3% bwoc.

3.4. Shear dependent rheology of AAS and OPC pastes

Rheological measurements displayed in Fig. 5 (left) revealed that in AAS pastes, all IPEG PCE polymers produced strong fluidizing effect. Accordingly, the shear stress of all AAS pastes admixed with the various IPEG PCE polymers decreased with increasing PCE dosages. For example, the neat AAS paste exhibited a shear stress value of 23 Pa at 3 s^{-1} which decreased to 9.8 Pa when 0.05% of 7IPEG3 sample was admixed. Furthermore, it was found that the PCEs prepared at high AA:IPEG ratio (i.e. the highly anionic polymers, 7IPEG15, 23IPEG15 and 50IPEG15) were significantly more effective than those of less anionicity. These results are in good agreement with the observations from the "mini slump" tests in Section 3.3.

For comparison, the same rheological measurements were also carried out in cement pastes. Surprisingly, and opposite to the trend observed in the AAS pastes, here the IPEG PCE polymers strongly increased the shear stress, which again confirms the failure of these polymers to disperse cement as observed in the spread flow tests in Section 3.3. As is obvious from Fig. 5 (right), the higher the dosage of IPEG PCEs, the higher is the shear stress of the cement pastes. In fact, the shear stress becomes even higher than that of the neat cement paste without any admixture, indicating that the IPEG PCE samples viscosify the system rather than fluidize it. Even an increased AA:IPEG ratio could not improve the dispersing effectiveness of the IPEG PCE polymers.

It has been described in numerous literatures that PCE polymers exhibit extraordinary dispersing ability in cementitious systems [32–34]. However, the IPEG PCE samples employed in this study were tailor-made for the AAS system. On purpose, they possess relatively high
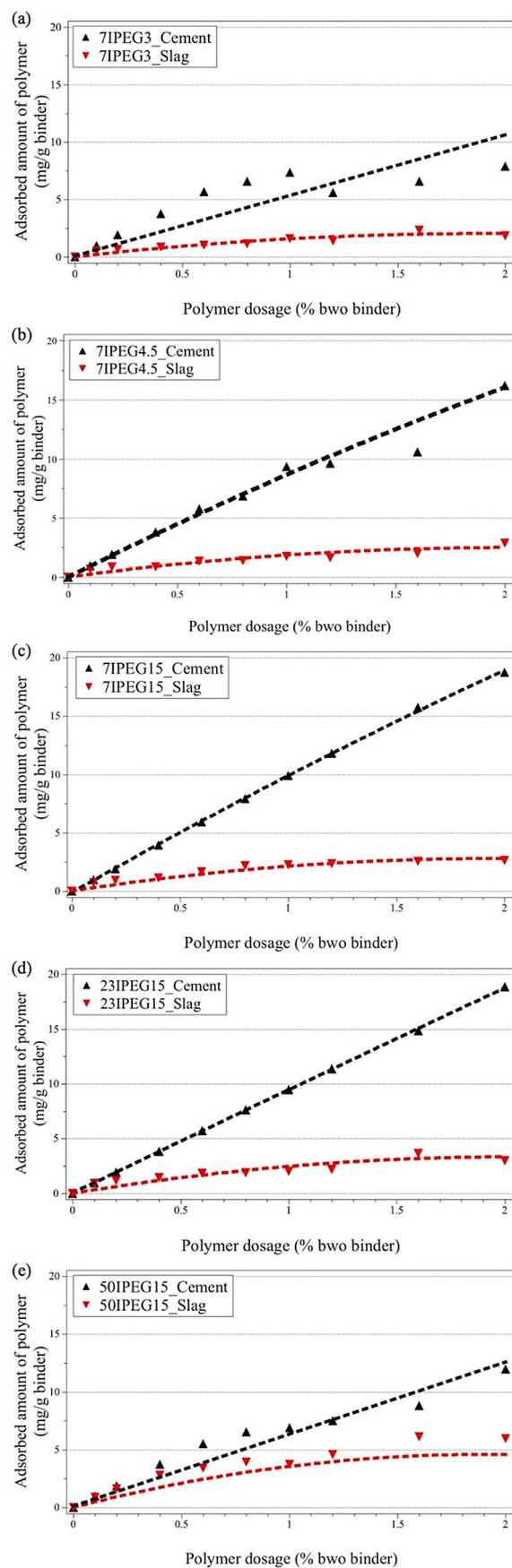

Fig. 6. Adsorption of the synthesized IPEG PCE polymers in cement and AAS pastes.
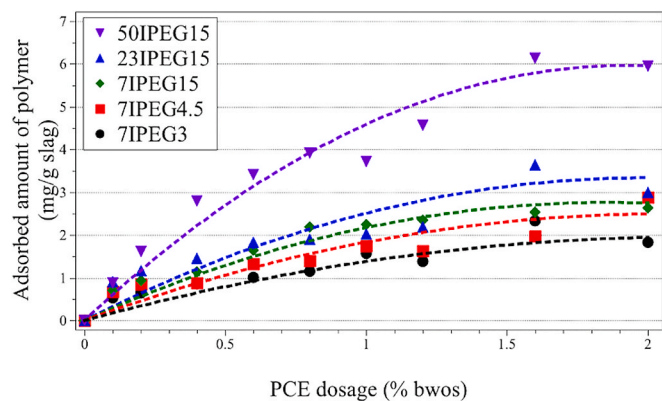
Fig. 7. *Langmuir* adsorption isotherms of the synthesized IPEG PCE polymers in NaOH activated slag.

PCE	7IPEG3	7IPEG4.5	7IPEG15	23IPEG15	50IPEG15
Slope	1.02	0.8787	0.7926	0.6965	0.2619
A_s [mg/g slag]	0.980	1.138	1.262	1.436	3.818
K	0.576	0.763	0.803	0.841	0.906

Fig. 8. Linearization of the *Langmuir* isotherms obtained for the IPEG PCE polymers adsorbed on AAS.

molecular weights, and therefore they are not suited for OPC systems. Wang et al. [35] systematically investigated the impact of molecular weight of PCE superplasticizers on the dispersion of cement and revealed that the dispersion ability of PCE superplasticizers decreases and even can disappear at high molecular weights.

3.5. Adsorption of PCE superplasticizers on cement and AAS

In order to investigate the interaction between the PCEs and two different binder systems (AAS and OPC), adsorption isotherms for the synthesized IPEG PCE polymers on AAS and cement were developed, and the results are presented in Fig. 6.

Generally, all PCE samples exhibited substantially higher adsorbed amount on cement than on AAS. A similar observation was made by Palacios et al. for other types of superplasticizers, a naphthalene sulfonate and a melamine polycondensate as well as a vinyl copolymer [25]. They noticed that two times more superplasticizer were adsorbed on cement than on slag and attributed the lower adsorbed amounts on AAS to competitive adsorption between the superplasticizer molecules and hydroxide anions.

Also Marchon et al. [27] described that PCEs exhibit strong sensitivity to the hydroxides present in alkali-activated systems, for example at 30 wt % of fly ash addition it results in a much decreased adsorbed amount.

All IPEG PCE polymers produced a typical *Langmuir* adsorption isotherm in AAS whereby the adsorbed amount of PCE increased with ascending dosage and then gradually plateaued off at higher polymer concentration, thus reaching the saturated adsorption which indicates the complete coverage of the cement surface.

Whereas, on OPC all PCE polymers adsorbed linearly with ascending concentrations. A plausible explanation for this behavior is that the PCEs are precipitated from the pore solution or otherwise become insoluble. This would well explain their ineffectiveness with respect to cement dispersion, as was demonstrated in the spread flow and shear-rate dependent rheological measurements before (see Fig. 4 and 5). The different adsorption behaviors of the IPEG polymers on cement and slag could also be further demonstrated by zeta potential measurements.

For a better insight into the adsorption behavior in AAS paste, the adsorption isotherms of all IPEG PCE polymers are displayed separately in Fig. 7. Apparently, a higher charge density always leads to a higher saturated adsorbed amount of the polymers. As was outlined by Plank et al. [36], the adsorption of PCE superplasticizers on binder surfaces results from different energy contributions, namely (1) the loss in enthalpy stemming from the electrostatic attraction between the oppositely charged substrate and PCE ($\Delta H < 0$); (2) the gain in entropy resulting from the release of a large number of counter ions and water molecules present at the binder surface into the pore solution ($\Delta S > 0$). Furthermore, other parameters such as the ionic composition of the pore
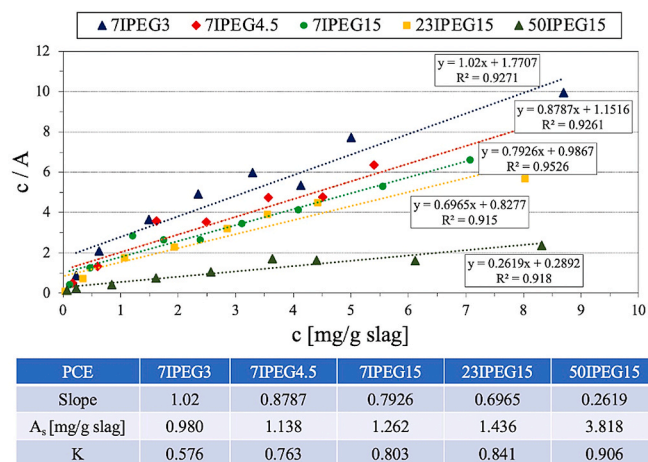
solution, the specific molecular structure of the PCE molecule (molar composition, M_w, side chain length) significantly affect the enthalpic and entropic contributions to the GIBBS free energy ΔG_{ads}. Occurring from PCE adsorption. The anionic charge density of a PCE directly influences both thermodynamic parameters (enthalpy and entropy). The higher the anionic charge density, the higher is the enthalpic contribution to adsorption. Thus, the IPEG PCE polymers possessing higher anionicity, but the same side chain length produces higher saturated adsorbed amounts which in turn leads to better dispersion in AAS (see Fig. 4). Furthermore, it was observed that IPEG PCEs possessing longer side chains (e.g. 50IPEG15) exhibited significantly higher adsorbed amount as compared to the short chain PCEs. However, in spite of the higher adsorbed amount of such PCEs holding longer side chains (50IPEG15) exhibit reduced dispersion ability than their counterparts with shorter side chain (see Fig. 4). This can be ascribed to the lower solubility of PCEs possessing a higher number of ethylene oxide units in their PEG side chain in high ionic strength systems such as alkali activated slag. It has been known for long time that the solubility of PEG in water is drastically decreased in the presence of salts and at pH > 12 [37, 38].

Generally, the adsorption isotherms of the PCE polymers on AAS can be expressed by Equation (2)

$$A = A_s Kc / (1 + Kc) \qquad (2)$$

where A represents the adsorbed amount of PCE polymer (mg/g slag), A_s stands for the saturated adsorbed amount of PCE (mg/g slag), c represents the PCE dosage at the equilibrium, and K is the equilibrium adsorption constant.

Linearization of the above equation yields:

$$\frac{c}{A} = \frac{c}{A_s} + \frac{1}{A_s K} \qquad (3)$$

The plots of c/A versus PCE dosages added (c) were developed and are displayed in Fig. 8. It can be seen that the values of c/A had linear correlation with c, which indicates that the adsorption fitted the *Langmuir* model. The isotherm parameters such as the saturated adsorbed amount (A_s), the *Langmuir* adsorption constant (K) as well as the coefficients R^2 were determined by linear regression are presented in Fig. 8. By comparing the saturated adsorbed amount (A_s) of the various IPEG PCE polymers, it was found that (1) higher charge density leads to a higher saturated adsorbed amount of the polymers on AAS; (2) longer side chains produce higher adsorbed amounts as compared to molecules possessing short ones. Furthermore, also the *Langmuir* equilibrium constant K expresses the adsorption behavior of the adsorbates: the larger the value of K for a PCE, the stronger is its adsorption. Again, it is
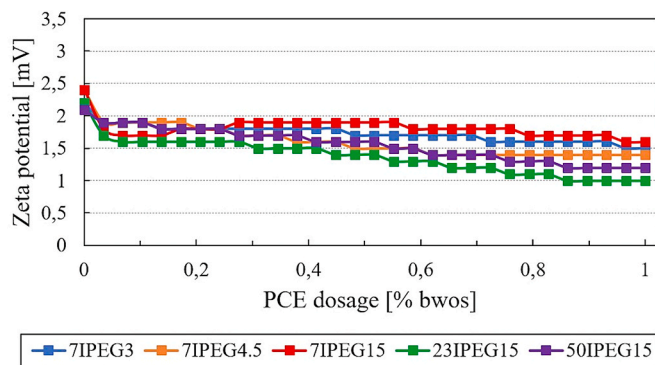
Fig. 9. Zeta potentials of slag pastes recorded as a function of IPEG PCE dosage (0–1% bwos).
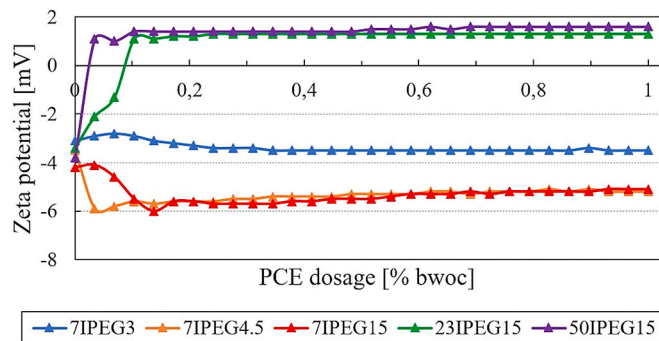

Fig. 10. Zeta potentials of cement pastes recorded as a function of IPEG PCE dosage (0–1% bwoc).

observed that increased anionic charge and/or longer side chains generally enhance the adsorbed amount of the IPEG PCEs.

3.6. Zeta potential measurements

In order to better elucidate the adsorption behavior of the IPEG PCEs in cement and AAS respectively, zeta potential measurements were carried out. The results are displayed in Fig 9 and 10.

As can be seen in Fig. 9, the initial surface potential of slag is a slight positive (~2.2 mV). Upon addition of the IPEG PCEs, a slight decrease of the ζ potential with increasing dosing in the PCE polymers is observed and approaches the isoelectric point (IEP). This change in surface charge experimentally confirms that the IPEG PCEs indeed adsorb onto the surface of slag particles. A similar trend was also observed by Palacios et al. [39].

The zeta potentials of cement suspensions were also measured while the IPEG PCEs were gradually dosed in, as displayed in Fig. 10. Opposite to slag, cement carries a negative surface charge (~- 3.8 mV). The direction of the shift of the zeta potential during addition of the IPEG PCEs differed depending on the molecular geometry of the IPEG PCEs. For PCEs holding short side chains (n_{EO} = 7), adsorption on cement resulted in a more negative zeta potential. Whereas, the addition of PCEs possessing long PEG side chains (n_{EO} = 23, 50) shifted the zeta potential towards the isoelectric point (IEP). This effect is based on their more pronounced steric effect induced by their longer PEG side chains.

4. Conclusions

In this study, a series of IPEG PCEs possessing various anionic charge density and side chain length was successfully synthesized. Dispersing effectiveness of the synthesized PCE polymers in AAS and OPC was captured via 'mini slump' tests. It was found that all IPEG PCE polymers

present highly effective superplasticizer for AAS pastes, and their dispersing ability increases substantially with increased anionicity. Most interestingly, in spite of the excellent performance in slag, none of the PCE polymers could provide any dispersion in OPC even at 0.3% dosage. Results from shear-dependent rheological measurements confirm the observations from the "mini slump" tests. The different adsorption behaviors of the IPEG polymers on cement and slag were further demonstrated by adsorption and zeta potential measurements. It was revealed that all IPEG PCE samples produce *Langmuir* type adsorption isotherms on slag, thus suggesting the formation of monolayer of adsorbed PCE molecules. However, on cement linear adsorption curves were recorded which could be explained by precipitation of the PCEs from the cement pore solution due to their high molecular weight.

Our study suggests that PCE polymers can behave completely different when admixed to different binder systems, as is the case here with cement and AAS. Apparently, the fundamentally different surface chemistry of these binders and the very different ionic compositions of the respective pore solution are the reason behind this disparity. It clearly suggests that for different binder systems, specifically designed molecular structures of PCE superplasticizers are required. Here, PCE structure motifs with superior effectiveness in NaOH activated AAS are presented.

Author statement

Declaration of competing interest

The authors declare that they have no known competing financial interests or personal relationships that could have appeared to influence the work reported in this paper.

Acknowledgment

References

[1] Andrew RM. Global CO_2 emissions from cement production. Earth Syst Sci Data 2018;10(1):195.

[2] Shi C, Qu B, Provis JL. Recent progress in low-carbon binders. Cement Concr Res 2019;122:227–50.

[3] Gartner E, Sui T. Alternative cement clinkers. Cement Concr Res 2018;114:27–39.

[4] Gartner E, Hirao H. A review of alternative approaches to the reduction of CO_2 emissions associated with the manufacture of the binder phase in concrete. Cement Concr Res 2015;78:126–42.

[5] Cao Y, Wang Y, Zhang Z, Ma Y, Wang H. Recent progress of utilization of activated kaolinitic clay in cementitious construction materials. Compos B Eng 2021:211.

[6] Flower DJM, Sanjayan JG. Green house gas emissions due to concrete manufacture. Int J Life Cycle Assess 2007;12(5):282–8.

[7] Weil M, Dombrowski K, Buchwald A. Life-cycle analysis of geopolymers. Geopolymers: Elsevier; 2009. p. 194–210.

[8] Li N, Shi C, Zhang Z, Wang H, Liu Y. A review on mixture design methods for geopolymer concrete. Compos B Eng 2019:178.

[9] Mellado A, Catalán C, Bouzón N, Borrachero M, Monzó J, Payá J. Carbon footprint of geopolymeric mortar: study of the contribution of the alkaline activating solution and assessment of an alternative route. RSC Adv 2014;4(45):23846–52.

[10] Adesanya E, Perumal P, Luukkonen T, Yliniemi J, Ohenoja K, Kinnunen P, et al. Opportunities to improve sustainability of alkali-activated materials: a review of side-stream based activators. J Clean Prod 2021:286.

[11] Favier A, De Wolf C, Scrivener K, Habert G. A sustainable future for the European Cement and Concrete Industry: technology assessment for full decarbonisation of the industry by 2050. ETH Zurich; 2018.

[12] Burris LE, Alapati P, Moser RD, Ley MT, Berke N, Kurtis KE. Alternative cementitious materials: challenges and opportunities. Bologna, Italy: International Workshop on Durability and Sustainability of Concrete Structures; 2015.

[13] Yamada K, Ogawa S, Hanehara S. Controlling of the adsorption and dispersing force of polycarboxylate-type superplasticizer by sulfate ion concentration in aqueous phase. Cement Concr Res 2001;31(3):375–83.

[14] Jia Z, Cao R, Chen C, Zhang Y. Using in-situ observation to understand the leaching behavior of Portland cement and alkali-activated slag pastes. Compos B Eng 2019: 177.

[15] Glukhovsky V, Rostovskaja G, Rumyna G. High strength slag-alkaline cements. 7th International Congress on the Chemistry of Cement 1980:164–8.

[16] Lei L, Chan H-K. Investigation into the molecular design and plasticizing effectiveness of HPEG-based polycarboxylate superplasticizers in alkali-activated slag. Cement Concr Res 2020;136:106150.

[17] Mollah M, Adams W, Schennach R, Cocke D. A review of cement–superplasticizer interactions and their models. Adv Cement Res 2000;12(4):153–61.

[18] Flatt RJ, Houst YF. A simplified view on chemical effects perturbing the action of superplasticizers. Cement Concr Res 2001;31(8):1169–76.

[19] Puertas F, González-Fonteboa B, González-Taboada I, Alonso M, Torres-Carrasco M, Rojo G, et al. Alkali-activated slag concrete: fresh and hardened behaviour. Cement Concr Compos 2018;85:22–31.

[20] Conte T, Plank J. Impact of molecular structure and composition of polycarboxylate comb polymers on the flow properties of alkali-activated slag. Cement Concr Res 2019;116:95–101.

[21] Palacios M, Puertas F. Effect of superplasticizer and shrinkage-reducing admixtures on alkali-activated slag pastes and mortars. Cement Concr Res 2005;35(7): 1358–67.

[22] Andersen P, Roy DM, Gaidis J, Grace W. The effects of adsorption of superplasticizers on the surface of cement. Cement Concr Res 1987;17(5):805–13.

[23] El-Hosiny F. Physico-mechanical characteristics of admixed cement pastes containing melment. Silic Ind 2002;(1–2):3–7.

[24] Yamadaa K, Takahashib T, Haneharaa S, Matsuhisaa M. Effects of the chemical structure on the properties of polycarboxylate-type superplasticizer. Cement Concr Res 2000;30.

[25] Palacios M, Houst YF, Bowen P, Puertas F. Adsorption of superplasticizer admixtures on alkali-activated slag pastes. Cement Concr Res 2009;39(8):670–7.

[26] Sakai E, Yamada K, Ohta A. Molecular structure and dispersion-adsorption mechanisms of comb-type superplasticizers used in Japan. J Adv Concr Technol 2003;1(1):16–25.

[27] Marchon D, Sulser U, Eberhardt A, Flatt RJ. Molecular design of comb-shaped polycarboxylate dispersants for environmentally friendly concrete. Soft Matter 2013;9(45):10719–28.

[28] Laguna MTR, Medrano R, Plana MP, Tarazona MP. Polymer characterization by size-exclusion chromatography with multiple detection. J Chromatogr A 2001;919 (1):13–9.

[29] Li N, Shi C, Zhang Z. Understanding the roles of activators towards setting and hardening control of alkali-activated slag cement. Compos B Eng 2019;171:34–45.

[30] Piot B, Finn N. Additive for well cementing applications. EP 2749547A1.

[31] Plank J, Sachsenhauser B. Experimental determination of the effective anionic charge density of polycarboxylate superplasticizers in cement pore solution. Cement Concr Res 2009;39(1):1–5.

[32] Plank J, Sakai E, Miao C, Yu C, Hong J. Chemical admixtures—chemistry, applications and their impact on concrete microstructure and durability. Cement Concr Res 2015;78:81–99.

[33] Lei L, Plank J. Synthesis and properties of a vinyl ether-based polycarboxylate superplasticizer for concrete possessing clay tolerance. Ind Eng Chem Res 2014;53 (3):1048–55.

[34] Gelardi G, Mantellato S, Marchon D, Palacios M, Eberhardt A, Flatt R. Chemistry of chemical admixtures. Science and technology of concrete admixtures. Elsevier; 2016. p. 149–218.

[35] Wang X, Ran Q, Yang Y, Shu X. Impact of molecular weight of block polycarboxylate superplasticisers on the dispersion of cement paste. Adv Cement Res 2016;28(6):371–7.

[36] Plank J, Sachsenhauser B, De Reese J. Experimental determination of the thermodynamic parameters affecting the adsorption behaviour and dispersion effectiveness of PCE superplasticizers. Cement Concr Res 2010;40(5):699–709.

[37] Hey MJ, Jackson DP, Yan H. The salting-out effect and phase separation in aqueous solutions of electrolytes and poly (ethylene glycol). Polymer 2005;46(8):2567–72.

[38] Bailey Jr F, Callard R. Some properties of poly (ethylene oxide)[1] in aqueous solution. J Appl Polym Sci 1959;1(1):56–62.

[39] Palacios M, Bowen P, Kappler M, Butt H-J, Stuer M, Pecharromán C, et al. Repulsion forces of superplasticizers on ground granulated blast furnace slag in alkaline media, from AFM measurements to rheological properties. Mater Construcción 2012;62:489–513.

5.5 Paper # 5 (Conference abstract)

A Roadmap to Low Carbon Cement Concrete

Y. Zhang, L. Lei, J. Plank

This conference contribution summarizes the findings from several of our previous investigations. It is presented that our research has identified suitable PCE superplasticizers for various binder systems.

The findings suggest that different PCE structures are necessary for different applications, and that the behavior of PCEs established on OPC cannot be directly applied to slag-dominated binders.

This study emphasizes the variations in performance observed among specific superplasticizers when incorporated into different binder systems, which can be attributed to their unique surface chemistry characteristics.

The 10th International Symposium on Cement and Concrete

第十届水泥混凝土国际会议

ISCC

Conference Proceedings

Chair, ISCC 2022

- The Chinese Ceramic Society（中国硅酸盐学会）
- China Building Materials Academy（中国建筑材料科学研究总院有限公司）
- South China University of Technology （华南理工大学）

中国 广州

Guangzhou China, 13-16 November, 2022

The 10ᵗʰ International Symposium on Cement and Concrete

第十届水泥混凝土国际会议

Organizers:

华南理工大学

Guangzhou China, 13-16 November, 2022

A Roadmap to Low Carbon Cement Concrete

Yue Zhang[1], Lei Lei[2], Johann Plank[3*]

[1, 2, 3] Chair for Construction Chemistry, Department of Chemistry, Technische Universität München, Munich, GERMANY
E-mail: yue1.zhang@tum.de; lei.lei@bauchemie.ch.tum.de; johann.plank@bauchemie.ch.tum.de;

Abstract:

In order to reduce the CO_2 footprint of cement it is necessary to decrease the clinker content significantly, i.e. well below 50 %. To probe into such systems, the use of alternative raw materials like GGBS (Ground Granulated Blast Furnace Slag) in the mixtures has to be considered. Generally, the application of slag in construction benefits the environment in several ways: reduction of carbon dioxide emissions, conservation of energy and natural materials, and improved waste management. In composite cements, the slag content can vary and its introduction allows to strongly decrease the clinker content. Studies have shown that GGBFS could potentially reduce the carbon footprint in a typical concrete mix design by $\sim$ 22 %. Furthermore, based on a CO_2 reduction assessment, it has been reported in literature that by using alkali activated slag concrete, the carbon footprint could be reduced by as much as 55 to 75%, depending on the chemical nature and dosage of the activator.

In our work, we have identified suitable PCE superplasticizers for different binder systems. The results suggest that novel and different PCE structures are required depending on the application, and that the behavior of PCEs established on OPC cannot simply be applied to slag dominated binders.

This study highlights the disparity in performance of specific superplasticizers admixed into different binder systems originating from their distinct surface chemistry. Specific molecular motifs are required to address these differences in surface compositions at the atomistic level.

Keywords: *Admixture, Cement composite, Dispersion, Ground granulated blast-furnace slag*

5.6 Paper # 6

Boosting the performance of low-carbon alkali activated slag with APEG PCEs: a comparison with Ordinary Portland cement

Y. Zhang, L. Lei, J. Plank, L. Chen

Journal of Sustainable Cement-Based Materials

Published online: June 5, 2023, DOI: 10.1080/21650373.2023.2219253

This study examined the dispersing effectiveness of polycarboxylate (PCE) superplasticizers that carried structurally different carboxylate groups in two binder systems (namely alkali-activated slag and OPC).

Two copolymers of α-allyl-ω-hydroxy poly(ethylene glycol) ether (APEG) PCE were synthesized in this study, using either acrylic acid (AA) or maleic anhydride (MA) as the co-monomer. The performance tests conducted in alkali-activated slag (AAS) revealed that the MA-7APEG polymer exhibited significantly higher dispersing effectiveness compared to AA-7APEG2, despite both polymers having the same anionicity and similar molecular weight.

This observation can be attributed to the fact that the MA-7APEG, which was derived from MA, had a higher calcium binding capacity than AA-7APEG2, as confirmed by anionic charge measurements and Ca^{2+} ion titration analysis.

Boosting the performance of low-carbon alkali activated slag with APEG PCEs: a comparison with ordinary Portland cement

Yue Zhang, Lei Lei, Johann Plank & Liugang Chen

Published online: 05 Jun 2023.

Submit your article to this journal ↗

Article views: 23

View related articles ↗

View Crossmark data ↗

Taylor & Francis
Taylor & Francis Group

Check for updates

Boosting the performance of low-carbon alkali activated slag with APEG PCEs: a comparison with ordinary Portland cement

Yue Zhang[a], Lei Lei[a]*, Johann Plank[a] and Liugang Chen[b]*

[a]*Technische Universität München, TUM School of Natural Sciences, Faculty of Chemistry, Garching bei München, Germany;*
[b]*Zhenzhou University, School of Materials Science and Engineering, Henan Key Laboratory of High Temperature Functional Ceramics, Zhenzhou, China*

This study focused on investigating the dispersing effectiveness of polycarboxylate (PCE) superplasticizers with different carboxylate groups in two binder systems: Alkali-activated Slag (AAS) and Ordinary Portland Cement (OPC). Two α-allyl-ω-hydroxy poly (ethylene glycol) ether (APEG) PCE copolymers were prepared from acrylic acid (AA) or maleic anhydride (MA) separately. Performance test results in AAS revealed that MA-7APEG polymer exhibited much stronger dispersing efficiency than AA-7APEG2, despite both PCE polymers having the same anionicity and comparable molecular weight. This difference in effectiveness can be attributed to the stronger calcium binding capacity of the MA-7APEG polymer, as determined through anionic charge measurements and potential titration analysis. The study highlights the importance of considering the properties of the carboxylate groups in the design of effective PCE superplasticizers for use in different binder systems.

Keywords: Dispersion; calcium binding; alkalis; ground granulated blast furnace slag; superplasticizer; polycarboxylate

1. Introduction

Thanks to the low CO_2 emission and energy consumption in their manufacturing process, alkali-activated slag (AAS) binders have been actively investigated as an alternative to concrete materials of ordinary Portland cement (OPC) [1,2]. The reuse of slag in concrete production can help to weaken the negative environmental impact and also to reduce the costs of landfilling the slag wastes [3]. Indeed, slag could potentially reduce the carbon footprint in a typical concrete mix design by ∼22% [4]. Based on a CO_2 reduction assessment, Yang et al. [5] reported that by using alkali activated slag concrete, the carbon footprint could be reduced by 55 to 75% depending on the chemical nature and dosage of the activator.

In addition to this, AAS binders are characterized by superior properties including higher resistance of sulfate and chloride ingress [6–8], and better durability performance over OPC counterparts [9].

Once activated by a highly alkaline solution, commonly known as sodium hydroxide (NaOH), sodium carbonate (Na_2CO_3) and sodium silicate (Na_2SiO_3), slag can be used as a binder, similar to OPC [10–13]. In the highly alkaline environment, the ground granulated blast-furnace slag can be activated to rapidly release silica $[SiO_4]^-$ and alumina $[AlO_4]^-$ tetrahedral units, and hence produces cementitious binder with comparable mechanical properties [14]. However, the compressive strength of AAS concrete encounters a significant decrease when excessive water is added to achieve good fluidity of fresh AAS paste. This is because the

free water molecules fill the intergranular space and result in numerous capillary pores after hydration [15]. To address the conflict issues concerning the mechanical strength and dispersion property of AAS concrete, researchers have made several attempts to identify suitable superplasticizers [16–20]. Polycarboxylate superplasticizers (PCEs) have been widely recognized as highly effective cement and concrete dispersants, especially at low w/c ratios [21,22]. These comb copolymers typically consist of a negatively charged backbone with carboxylic groups and grafted pendant chains mainly composed of polyethylene oxide units [23]. Due to the high flexibility in their structure, PCEs also present as good candidates for AAS binders. Lei et al. [24,25] reported two types of PCE (HPEG- and IPEG-based) with high anionicity, high molecular weight and short side chain length that exhibited good plasticizing effectiveness in an NaOH activated AAS system. Typically, high anionicity of PCE polymers improves the adsorption on slag, resulting in improved dispersion efficiency. The dispersing mechanism of PCE superplasticizers in the OPC system is well documented. At first, the PCE polymers adsorb onto the surface of cement particles *via* carboxylic groups in the backbone. Then, the non-adsorbing polyethylene glycol side chains protrude freely into the pore space and contribute the most to the stabilizing force in the system. In this way, with a relatively low dosage of PCE polymer, a superior dispersing effectiveness can still be reached. To further understand the interactive force of PCE copolymers with binder systems, intensive investigations have been carried out by different research teams,

---

*Corresponding authors. Email addresses: lei.lei@tum.de; lgchen@zzu.edu.cn

indicating that Ca^{2+} plays a vital role in the adsorption process. Ran et al. revealed that the adsorption of comb polymers was driven by an electrostatic attraction between anionic $-COO^-$ groups along the polymer trunk chain and positive surface of cement *via* the bridging effect of divalent cation (e.g. Ca^{2+}) [26]. With respect to the coordination mode between Ca^{2+} ions and $-COO^-$ functionality, Plank et al. [27] illustrated that the polycarboxylates could form two types of calcium chelate complexes with $-COO^-$ groups functioning as monodentate and bidentate ligand. In the monodentate configuration, Ca^{2+} coordinates with only one oxygen atom of the $-COO^-$ groups; while for the bidentate complexation, both oxygen atoms of $-COO^-$ functionality bind with Ca^{2+} ion. The authors point out that not only the number of carboxylate groups, but also the steric position along polymer trunk chain affects the calcium binding capability of PCE superplasticizers, hence accounting for the dispersion discrepancy.

To identify the suitable PCE molecules with improved performance in AAS binders, the proper understanding of the interaction between PCE superplasticizers and AAS is of great importance. However, to our knowledge, no systematic investigation into the mode of action between calcium cations and PCEs in AAS binders has been carried out. To fill this gap, in this study, two ally ether-based type PCEs carrying different carboxylate groups (mono or di-carboxylate) were prepared. Thereafter, their specific interaction with calcium cations in NaOH activated slag binder was investigated. We hope the findings in this paper will better elaborate the dispersion mechanism of PCE comb copolymers in AAS binders and provide new insights into the molecular design of highly effective PCE structures.

2. Experimental

2.1. Materials

2.1.1. Chemicals

Maleic anhydride ($\geq 99\%$, purchased from Sigma Aldrich, Germany), acrylic acid ($>99\%$ purity, purchased from Sigma Aldrich, Germany), α-allyl-ω-hydroxy poly (ethylene glycol) ether (APEG macromonomer, $n_{EO} = 7$) ($>98\%$, obtained from NOF Corporation, Japan), ammonium persulfate ($\geq 98\%$, purchased from Sigma Aldrich, Germany), sodium methallyl sulfonate ($>98\%$ purchased from Sigma Aldrich, Germany), 3-mercaptopropionic acid ($\geq 99\%$, purchased from Sigma Aldrich, Germany), sodium hydroxide ($\geq 97\%$ purchased from Merck KGaA, Germany), calcium chloride ($\geq 99.9\%$, purchased from Merck KGaA, Germany), poly(acrylic acid) with a M_w of 5400 g/mol (Dow Chemical, Midland, MI, USA) were all used without further purification.

2.1.2. Binder

The slag used in this research was provided by the Ecocem company in Fos sur mer, France. Its fineness was 4450 ± 250 cm^2/g, which passed GGBFS Class A based on the concrete standard NF EN 206-1/CN (December 2012). Its oxide composition determined by X-ray fluorescence analysis (Axios, PANalytical, Almelo, the Netherlands) is shown in Table 1. The particle size distribution of slag was analyzed using laser granulometry, as depicted in Figure 1(a). The analysis yielded parameters of 10.72 μm and 30.99 μm for the average particle size (diameter at 50%) and the diameter at 90% cumulative distribution, respectively.

The OPC sample CEM I 42.5 N in this study was provided by SCHWENK ZEMENT KG, Germany. The phase composition of cement was determined by Q-XRD analysis using Rietveld refinement and listed in Table 2. The average particle size of the cement, represented by the d_{50} value, was determined to be 20.48 μm, while the d_{90} value, indicating the particle diameter at 90% cumulative distribution, was found to be 59.29 μm (see Figure 1(b)).

Table 1. Oxide compositions of the slag used in this paper.

Oxide compositions	[wt%]
CaO	43.9
SiO_2	37.4
Al_2O_3	10.9
MgO	6.5
FeO	0.7
TiO_2	0.5
SO_3	0.1
Na_2O	0.3
K_2O	0.2
Total	100.0
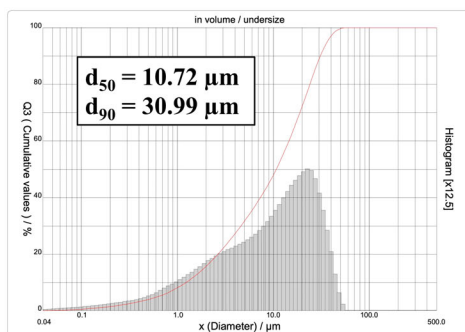
(a) Slag **(b) Cement**
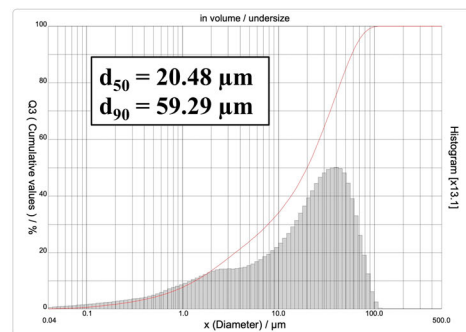
Figure 1. The particle size distribution of the slag and cement determined through laser granulometry.

2.2 Synthesis of APEG PCE superplasticizers

In this study, two polycarboxylate superplasticizers based on allyl ether were synthesized, each exhibiting distinct structural characteristics. The synthetic routes for the two PCE samples are depicted in Figure 2(a) and 2(b).

One conventional maleic anhydride-co-APEG polymer (n_{EO} = 7) was synthesized in bulk. The detailed synthetic procedure for the maleic anhydride-co-APEG polymer made from maleic anhydride to APEG macromonomer at a molar ratio of 1:1 is described in the following: 21.80 g of maleic anhydride (0.222 mol) and 77.7 g of

Table 2. Phase compositions of OPC sample CEM I 42.5 N by means of Q-XRD analysis *via* Rietveld refinement.

Phase composition	wt. %
C_3S, monoclinic	55.22
C_2S, monoclinic	13.78
C_4AF, orthorhombic	8.77
C_3A, cubic	6.03
C_3A, orthorhombic	0.55
Anhydrite ($CaSO_4$)	2.40
Hemihydrate ($CaSO_4 \cdot 0.5H_2O$)	2.63
Calcite ($CaCO_3$)	3.78
Dolomite ($CaMg(CO_3)_3$)	0.59
Quartz (SiO_2)	0.31
Free lime (*Franke*)	0.48
Total	100

APEG macromonomer (n_{EO} = 7) (0.222 mol) were placed into a 250 mL 5-neck reaction flask equipped with a reflux condenser, a mechanical stirrer (300 rpm), a nitrogen inlet and a feeding inlet. The reaction flask was heated to 70 °C and purged with nitrogen gas throughout the whole reaction. Next, 0.51 g of benzoyl peroxide as an initiator was added in one portion into the reactor, followed by 1.03 g of benzoyl peroxide continuously added at an interval of 10 min over a total time of 90 min. When the addition process was finished, the mixture was heated up to 90 °C and stirred for another 90 min. Thereafter, 150 mL of deionized water (DI) water was added and the reaction mixture was then left to stand to yield the polycarboxylate solution of approximate 40 wt.% solid content. When the product had cooled down, it was titrated to neutral pH with 30% concentration NaOH solution. This copolymer was named **MA-7APEG**.

In comparison, one acrylic acid-co-APEG polymer (n_{EO} = 7) was prepared in aqueous solution. The process for the acrylic acid-co-APEG polymer made from acrylic acid to APEG macromonomer at a molar ratio of 2:1 is described in bellow:

First, 25 g (0.071 mol) of APEG macromonomer (n_{EO} = 7) and 45 mL of DI water were placed in a five-neck flask which was connected to a reflux condenser, a mechanical stirrer, a nitrogen inlet and two separated feeding inlets. The reaction vessel containing the macromonomer

Figure 2. Synthetic routes for APEG PCEs: (a) MA-7APEG and (b) AA-7APEG2.

solution was heated to 80 °C and flushed with N_2 for 30 min. Next, two feeding solutions (Solution A and Solution B) were prepared. 10.23 g (0.142 mol) of acrylic acid and 0.225 g (0.002 mol) of 3-mercaptopropionic acid (chain transfer agent) were dissolved in 25 mL of DI water. This solution mixture was named Solution A. Similarly, 5.629 g (0.025 mol) of ammonium persulfate were dissolved in 30 mL of DI water. This solution was labeled Solution B. Solutions A and B were added drop-wise into the reaction vessel using two peristaltic pumps *via* inlet A over 2.5 h and *via* inlet B over 3 h. When the addition of solution B had finished, the mixture was stirred for another hour. Finally, the PCE solution was cooled to ambient temperature and the pH was adjusted to 6.5–7 by using 30 wt. % sodium hydroxide solution. The solution exhibiting a solids content of 35 wt. % was used without further purification. This copolymer was designated **AA-7APEG2**.

2.3.   Characterization of APEG superplasticizers

2.3.1.   Size exclusion chromatography (SEC)

Molar masses (M_w and M_n), the polydispersity index (PDI) and macromonomer conversion of the synthesized ether-based PCEs were determined by size exclusion chromatography, also referred to as gel permeation chromatography, GPC. The measurements were taken using a Waters Alliance 2695 instrument (Waters, Eschborn, Germany) equipped with three Ultrahydrogel™ columns (120, 250, 500) and an Ultrahydrogel™ Guard column. As eluent, 0.1 N $NaNO_3$ (pH = 12) was used with a flow rate of 1.0 mL/min. For the calculation of M_w and M_n, a *dn/dc* value of 0.135 mL/g (value for PEO) was utilized [28].

2.3.2.   Anionic charge amount measurement

The specific anionic charge amount of the synthesized PCEs was determined using a particle charge detector PCD 03 pH (Mütek Analytic, Herrsching, Germany). Here, 10 mL of the 0.2 g/L PCE solution were titrated against a 0.34 g/L aqueous solution of cationic poly-diallyl dimethyl ammonium chloride (polyDADMAC) until charge neutralization (zero potential) was reached. Then the anionic charge per gram of PCE polymer was derived from the consumption of the cationic polyelectrolyte poly DADMAC [27].

2.4.   Dispersing performance of PCE polymers in NaOH-activated slag and OPC pastes

2.4.1.   Mini-slump tests

The spread flow of slag pastes containing different APEG PCEs was determined by performing a 'mini-slump' test following the modified version of DIN EN 1015 norm [29]. The water to binder ratio was set to 0.5. In a typical test, 300 g of slag were charged into a porcelain cup which contained 150 mL of 8 wt.% NaOH solution (alkali activator). Once the mixture was manually agitated for 90 s, 0.05% (by weight of slag, bwos) of aqueous PCE polymer sample were added into the mixture. In order to

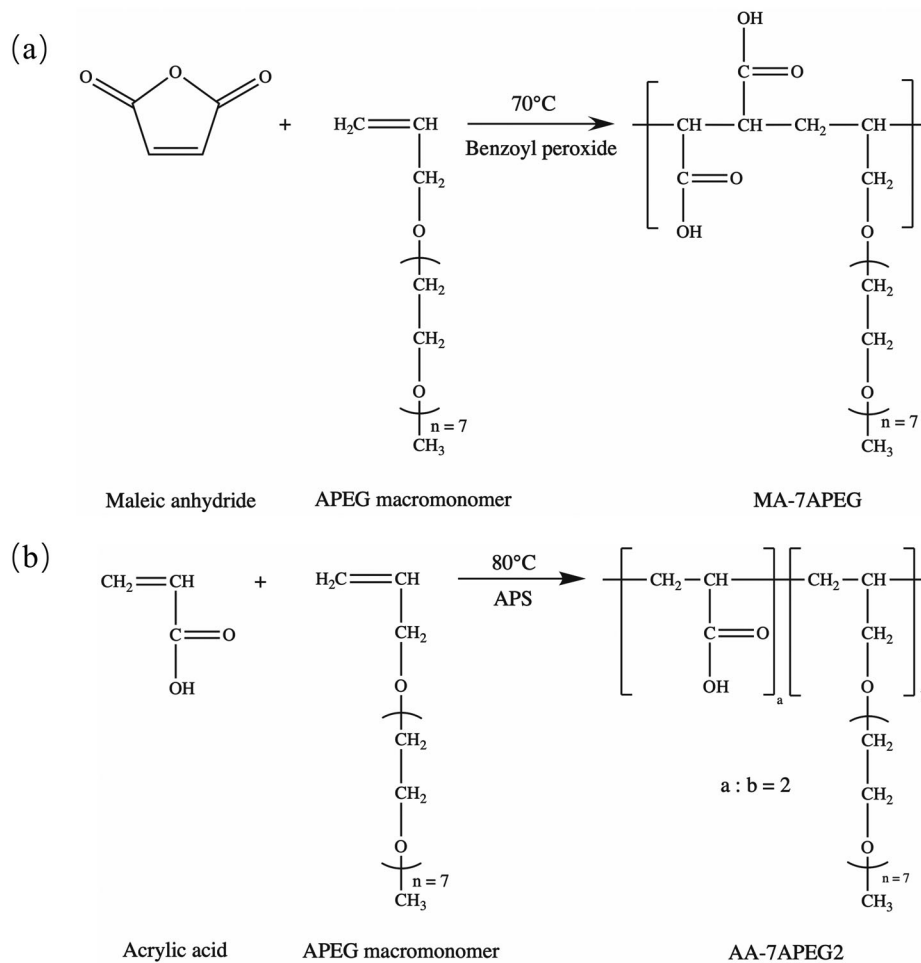homogenize the slag paste, an additional 2.5 min of hand-mixing was applied. Then the slag paste was poured into a Vicat cone (height 40 mm, top diameter 70 mm, bottom 80 diameter), which was placed on a glass plate. After the slag paste was completely filled to rim, the Vicat was lifted vertically. The resulting spread flow was measured twice, with the second measurement being at a 90° angle from the first one, and the averaged value was noted.

As for the spread flow of cement pastes, the testing procedures were the same as described in AAS, and the water to cement ratio here was controlled to be 0.45, which was able to achieve the spread flow of 18 ± 0.5 cm. In addition, DI water is directly used as the mixing water without addition of NaOH.

2.4.2.   Rheological properties of AAS/OPC pastes

Rheology of AAS and OPC pastes was determined by a FANN 35SA viscometer (FANN Instrument Company, Houston, TX), which is equipped with R1 rotor sleeve (radius: 18.415 mm), B1 bob (radius: 17.425 mm, height: 3.8 mm) and F1 torsion spring. The water-to-binder ratio for AAS and OPC is consistent with that in Mini-slump tests. For the detailed procedures of slurry preparation and rheology determination, please refer to the previously published article [24].

2.5.   Isothermal heat flow calorimetry

The hydration evolution of binders (AAS and cement) was monitored using a TAM Air isothermal heat conduction calorimeter (Thermometric, Jaerfaella, Sweden). For this purpose, the samples were prepared by mixing and homogenizing 4 g of dry binder sample (slag/cement) with appropriate amounts of water (the water to binder ratio here was fixed the same to that in **Mini-slump** tests), NaOH activator (only applied in AAS) and PCEs. Next, the samples were transferred into glass ampoules and placed in the calorimeter. During the experiments, the temperature was held constant at 20 °C, and the exothermal heat flow of samples was captured and recorded until the heat release ceased.

2.6.   PCE sorption on AAS/OPC pastes via TOC

The adsorbed amount of PCEs on binders (slag or cement) was determined by total organic carbon content (TOC) measurement *via* depletion method. In a typical experiment, 16 g of binder (slag/cement), 0.64 g of NaOH (only applied in the slag system) and 8 g of water holding a certain amount of PCE were filled into a 50 mL centrifuge tube and shaken in a wobbler (VWR International, Darmstadt, Germany) for 2 min at 2400 rpm. After a centrifugation with 8500 rpm for 10 min, the supernatant was collected and filtered through a 0.2 μm syringe filter. Then the filtrate was diluted with DI water (1/30 volume ratio) and its pH value was adjusted to 2 using 0.1 M HCl. Thereafter, the determination of TOC value was performed with a High TOC II Instrument (Elementar Analysensysteme, Hanau, Germany).
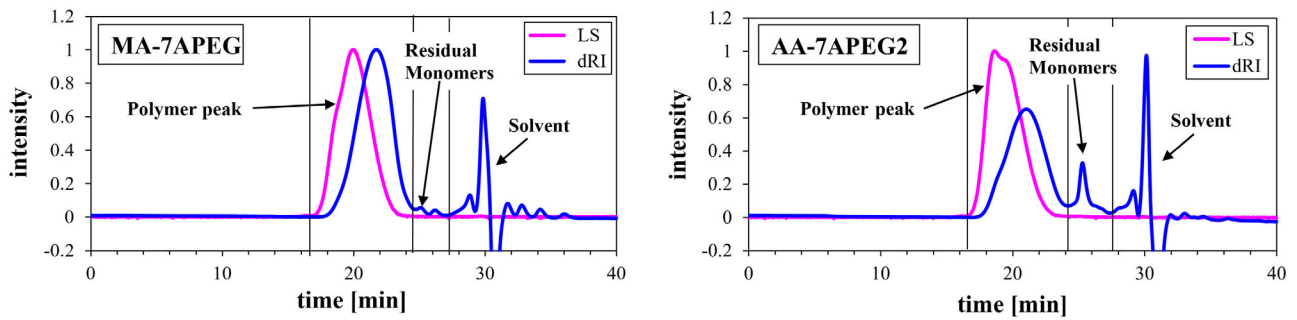
Figure 3. SEC chromatograms of PCE samples MA-7APEG and AA-7APEG2; eluent: 0.1 M NaNO$_3$.

Table 3. Characteristic molecular parameters of the two APEG PCE polymers.

Polymer sample	M_w [Da]	M_n [Da]	PDI	Macromonomer conversion (%)
MA-7APEG	38,100	15,875	2.4	96.6
AA-7APEG2	41,320	17,965	2.3	84.3

2.7. FT-IR spectra

The FT-IR spectra of all PCE samples were detected on a VERTEX 70 Fourier transform infrared spectrometer (Bruker INVENIO, Germany) at 25 °C by scanning the sample disks. In all samples, the scans were set to 64 and wavenumbers ranged from 4000 cm^{-1}–400 cm^{-1} in the testing mode of transmittance.

2.8. Determination of potential variation with titration

Firstly, a 100 mL CaCl$_2$ aqueous solution (0.25 mol/L) was prepared, which was used later as the calcium-rich solution to titrate against the PCE polymer solution. Next, MA-7APEG and AA-7APEG2 polymer solutions were dissolved in DI water to give a concentration of 0.05 mol/L while keeping the pH value of ∼7. At the start of each titration test, 100 mL of above-prepared PCE solution was fed into a 250 mL container, which is a standard accessory from a Metrohm OMNIS integrated titration system (Metrohm, Herisau, Switzerland). Then, as the CaCl$_2$ solution titrated against the PCE at the step interval of 0.5 mL/min, the in-situ potential was monitored and recorded by the OMNIS titration software. The titration measurement ended when the potential reached a plateau, whereby the consumed volume of CaCl$_2$ solution was recorded.

3. Results and discussion

3.1. Molecular properties of the synthesized APEG PCE polymers

The molecular characteristics of the resulting APEG PCE polymers were determined *via* size exclusion chromatography (SEC). In Figure 3, the SEC chromatograms of MA-7APEG and AA-7APEG2 samples are presented. The parameters of M_w, M_n, PDI and conversion rate of the macromonomer are summarized in Table 3. The synthesized PCE polymers exhibited properties that are characteristic for high-quality PCE polymers, namely relatively low PDIs, and high macromonomer conversions. Additionally,

the molecular weights (M_w) of the synthesized PCE polymers were of a similar amount, which ensured good comparability, as it is well attested in the literature that the dispersing power of PCE superplasticizers is greatly related to their molecular properties [25,30].

3.2 Dispersing ability of PCE superplasticizers in AAS/OPC binder systems

To investigate the dispersing effectiveness of the two APEG PCE polymers in NaOH activated slag and OPC pastes, a 'mini-slump' test was performed. Firstly, the spread flow of AAS pastes containing 0.05% bwos of PCE samples was recorded and compared. According to Figure 4(a), although the two APEG PCE polymers possessed the same anionicity (COO$^-$: APEG = 2) and the same side chain length (n$_{EO}$ = 7), a vast disparity was observed; apparently, MA-7APEG exhibited a much superior dispersing ability. MA-7APEG achieved a spread flow as high as 30.8 cm (increased by 108%) while AA-7APEG2 barely dispersed the AAS paste.

Similarly, MA-7APEG was also found to have superior dispersing power in the OPC pastes, **as shown in Figure 4(b)**. When applying the same polymer dosage of 0.1% bwoc, MA-7APEG resulted in a spread flow of 26.4 cm, while the cement paste with AA-7APEG2 registered at 23.3 cm. Here, it is worth noting that the difference between these two APEG PCEs in OPC system is relatively minor in comparison to the AAS binder system. Several factors, such as the fundamentally different surface chemistry, the specific ionic compositions of the respective pore solution, distinct interaction mode between PCE polymers and binder systems are responsible for such disparity. The further mechanism investigation was carried out and discussed in Sec. 3.7.

3.3. Shear dependent rheology of AAS and OPC pastes

Rheological measurements were carried out in both AAS and OPC pastes, and the results are illustrated in Figure 5.
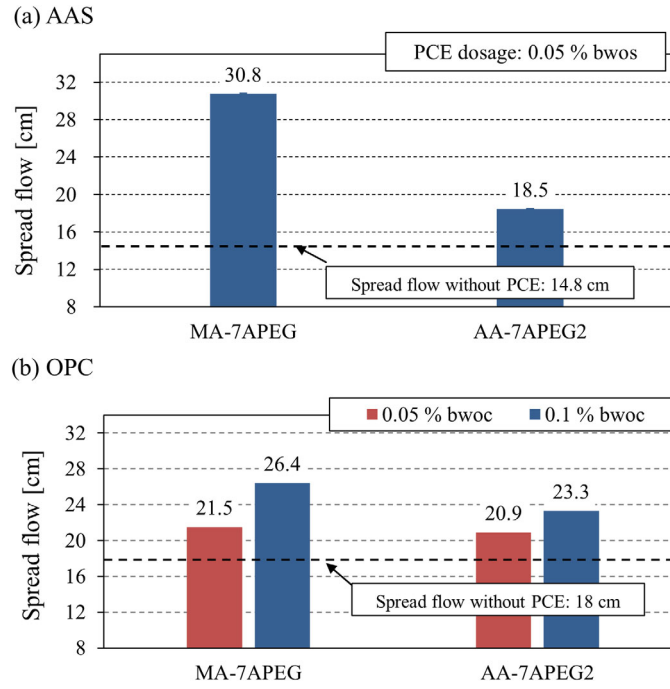
(a) AAS

(b) OPC

Figure 4. Spread flow of (a) NaOH activated slag pastes containing 0.05% bwos of MA-7APEG and AA-7APEG2 polymers and (b) OPC pastes with 0.05% and 0.1% bwoc of polymer dosages.
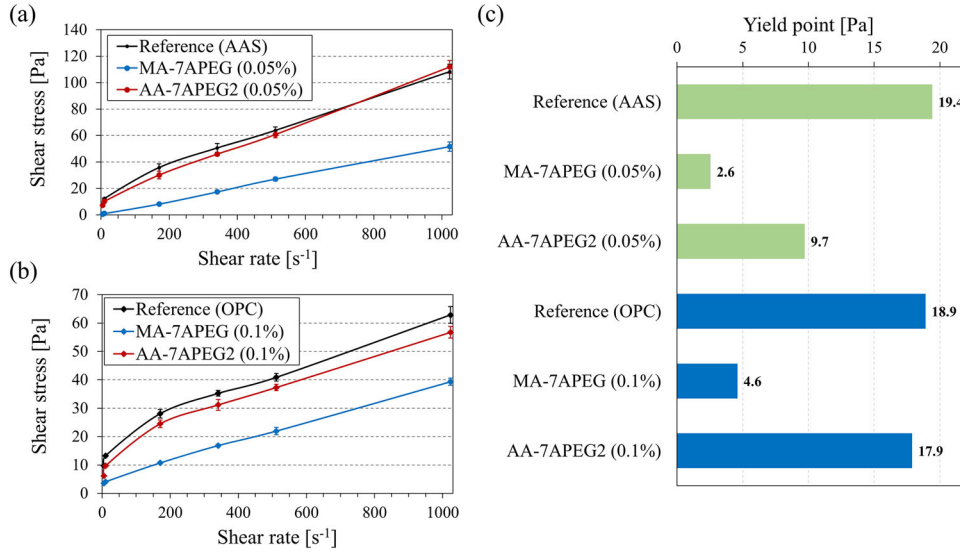
Figure 5. The rheological properties of binder pastes (a) AAS, (b) OPC, with or without PCE polymers and (c) corresponding yield points calculated for the different systems.

It can be observed that the shear stress of the AAS paste admixed with the MA-7APEG sample decreased significantly. The shear stress of the counterpart paste mixed with the AA-7APEG2 sample decreased slightly as compared to the reference paste. The results here demonstrated that the MA-7APEG sample produced a much stronger fluidizing effect. A similar trend was also found in the OPC binder system. Based on the relationship between shear stress and shear rates, the calculation for the yield point, which is the applied stress required to initiate the paste, can be expressed in Eqs. (1) and (2) [31].

Plastic Viscosity (Pa):

$$PV = \theta_{600} - \theta_{300} \tag{1}$$

and *Yield Point (Pa)*:

$$YP = \theta_{300} - PV \tag{2}$$

where θ_{300} and θ_{600} represent the shear stress values at shear rates of 300 and 600 r/min, respectively.

Figure 5(c) clearly indicates that the addition of PCE polymers significantly reduces the yield points of both binder systems. Furthermore, the PCE polymer based on maleic anhydride demonstrated a more notable fluidizing effect compared to the other type of PCE polymer. It required only 2.6 Pa and 4.6 Pa of yield points to initiate AAS and cement pastes, respectively. These findings are consistent with the results of mini slump tests, which also

(a) OPC

(b) AAS
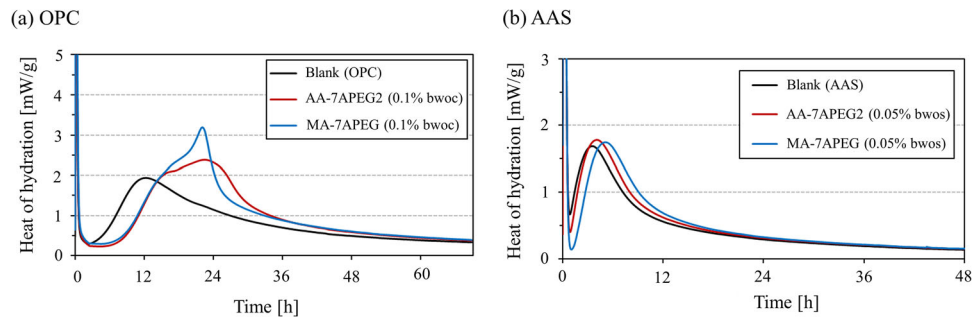
Figure 6. Impact of PCE polymers on the hydration of AAS and OPC binder systems.

showed that MA-7APEG exhibited superior dispersing power in both binder systems.

3.3. Isothermal heat evolution

To further probe the impact of the PCE polymers on the hydration of the two distinct binder systems, calorimetric measurements were carried out, the results of which are shown in Figure 6. The PCE polymer dosages applied in AAS pastes registered at 0.05% bwos. As for the OPC system, a slightly higher dosage of 0.10% bwoc was used to achieve a comparable fluidity.

As is evident from Figure 6(a), the addition of PCE polymers clearly delayed the main hydration peak of OPC pastes. Our observation here is in line with previous investigations [30,32,33]. Zhang et al. [33] synthesized a series of PCE polymers with various side length and anionicity. The calorimetric results demonstrated that PCE polymers with shorter side chains and higher anionic characteristics exhibited a stronger retardation effect. Yamada et al. [32] also showed that PCEs with reduced side chains typically prolonged the setting time. Winnefeld et al. [30] concluded that the retardation effect induced by PCE polymers can be ascribed to adsorption on cement grains or hydration products or is due to the influence on the nucleation and growth kinetics of the hydrates. Moreover, noticeable differences in the calorimetric curves of the two polymers can be observed, particularly in the region corresponding to the main peaks during cement hydration. These differences may arise from the specific interaction modes of the MA and AA APEG polymers with calcium ions, which will be extensively investigated in Sec. 3.7. As evident from the findings, the distinct calcium binding capacities of the two polycarboxylate polymers can alter the diffusion rate of calcium ions during the dissolution stage and subsequent precipitation of hydration products, such as C-S-H (calcium silicate hydrate) and CH (calcium hydroxide) [34–36]. Consequently, this leads to variations in the *in situ* heat release associated with the main hydration peaks. However, in the case of the AAS system, the disparity in calorimetric behavior between the two polymers is less pronounced (as shown in Figure 6b), mainly due to the more alkaline environment and significantly lower concentration of calcium ions available in the pore solution [18].

Figure 6(b) shows that the heat flow evolution of the AAS binder was characterized by an extremely short dormant period, the main exothermal hydration peak appearing at ~4 h. The rapid setting problem associated with AAS has been known for a long time [37]. The underlying mechanism is related to the rapid formation of the initial C-S-H gel, which greatly reduced the fresh AAS paste workability [38]. It is generally accepted that various parameters could show impact on the activation process of AAS. Among them, the nature of the alkaline activator appears to be the primary factor influencing setting time and the mechanical properties of AAS [39,40]. *Fernández-Jiménez* and *Puertas* [40] systematically studied the setting time, mechanical properties in AAS pastes mixed with various alkaline activators, i.e. NaOH, Na_2CO_3 and Na_2SiO_3. They demonstrated that silicate ions could result in fast setting due to the formation of initial calcium silicate hydrate, whereas the presence of carbonate ions could prolong the setting time. In a separate study, Jiao et al. [41] demonstrated that AAS activated with NaOH set rather quickly, similar to our finding here. Interestingly, the incorporation of MA-7APEG polymer slightly shifted the main hydration peak to a longer time. We did not observe the same effect with the AA-APEG2 polymer despite their very similar charge characteristics.

3.4. Adsorption isotherm of the APEG PCEs on AAS and OPC pastes

As was demonstrated by the fluidity and rheological measurements, the two APEG PCEs showed different behavior in binder systems, especially in AAS binders. Apparently, the molecular architecture of PCE polymers is the key parameter influencing the interaction between PCEs and binder systems, which in turn affect their dispersing power. Next, the mode of action between the two APEG PCE superplasticizers and binder systems was investigated *via* adsorption measurements.

As can be seen from Figure 7(a), adsorption isotherms were developed for the two APEG PCE superplasticizers (MA-7APEG and AA-7APEG2) on AAS. The MA-7APEG polymer exhibited a higher adsorbed amount on the surface of slag particles as compared to AA-7APEG2 polymer at various dosages, especially at dosages of ≥1.0% bwos. Moreover, the enhanced sorption of MA-7APEG polymer on AAS leads to superior dispersing ability, evidenced by the mini slump tests (see Figure 4) and rheology measurements (Figure 5). Furthermore, the most interesting part lies at low PCE concentrations (i.e. 0.1
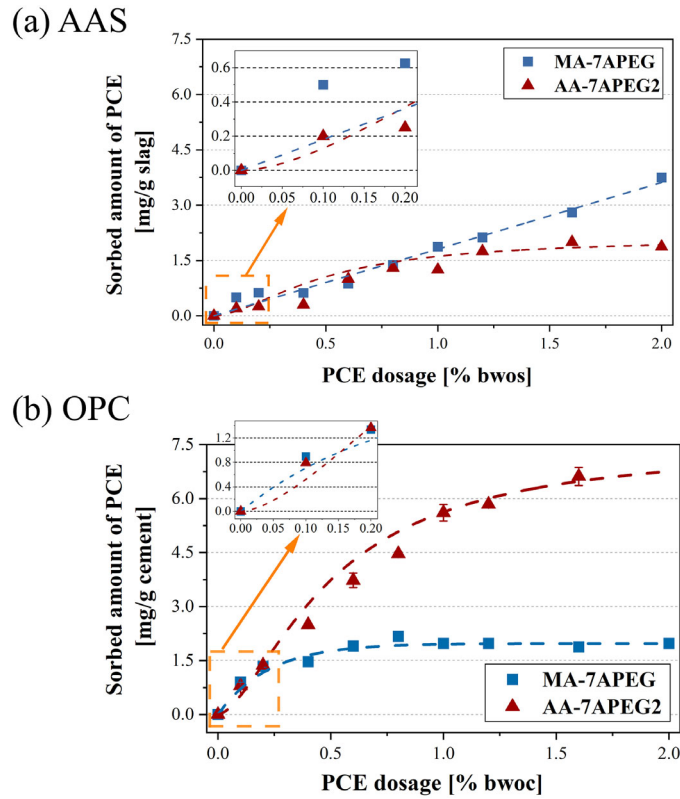
Figure 7. Sorption isotherms for MA-7APEG and AA-7APEG2 superplasticizers in NaOH-activated AAS (a) and OPC (b) binders.
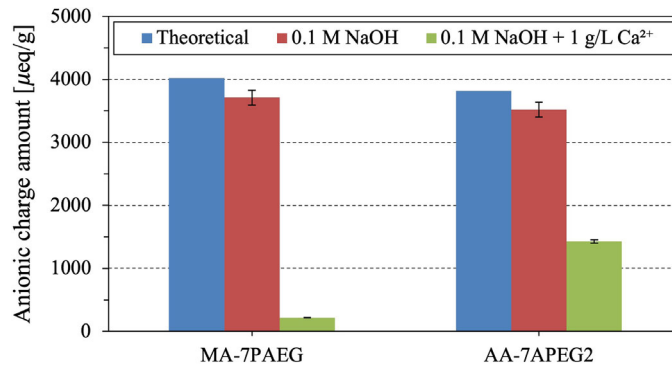
Figure 8. Anionic charge amounts of the synthesized MA-7APEG and AA-7APEG2 polymers.

and 0.2% bwos), which represent the realistic PCE dosages in actual application. At a dosage of 0.1% bwos, the adsorbed amount of MA-7APEG polymer lay at 0.5 mg/g slag, whereas the adsorbed amount of AA-7APEG2 polymer registered at only 0.2 mg/g slag (less than half of the MA-7APEG polymer). These data are in good agreement with the mini slump test results presented in Sec. 3.2.

By contrast, on OPC, the AA-7APEG2 polymer exhibited a much higher saturated sorbed amount as compared to the MA-7APEG polymer, as shown in Figure 7(b). For the relatively low PCE dosages (0.1 and 0.2% bwoc), MA-7APEG exhibited almost the same adsorbed amount as AA-7APEG, this also explains their similar behavior in the fluidity tests.

The different adsorption behavior of the two APEG PCE polymers on AAS is elucidated above, however, the key factor dominating this process still needs to be investigated in-depth. It is generally accepted that Ca^{2+} plays a

critical role for anionic polymers to be adsorbed onto the negatively charged cement particles [42]. Consequently, the specific interaction of the PCE polymers with Ca^{2+} in AAS was probed *via* anionic charge titration, FT-IR and conductivity measurements.

3.5. Anionic characteristics of the MA-7APEG and AA-7APEG2 polymers

To compare the affinity of the two APEG PCE superplasticizers to Ca^{2+}, the anionic charge amount was determined in two fluid systems of different salt concentrations: 1) 0.1 M aqueous NaOH solution; 2) 0.1 M aqueous NaOH solution with 1 g/L Ca^{2+}.

As shown in Figure 8, two APEG PCE polymers exhibited similar anionic charge in 0.1 M aqueous NaOH solution resulted from the same COO^- to side chain ratio in the molecular structure. However, the presence of
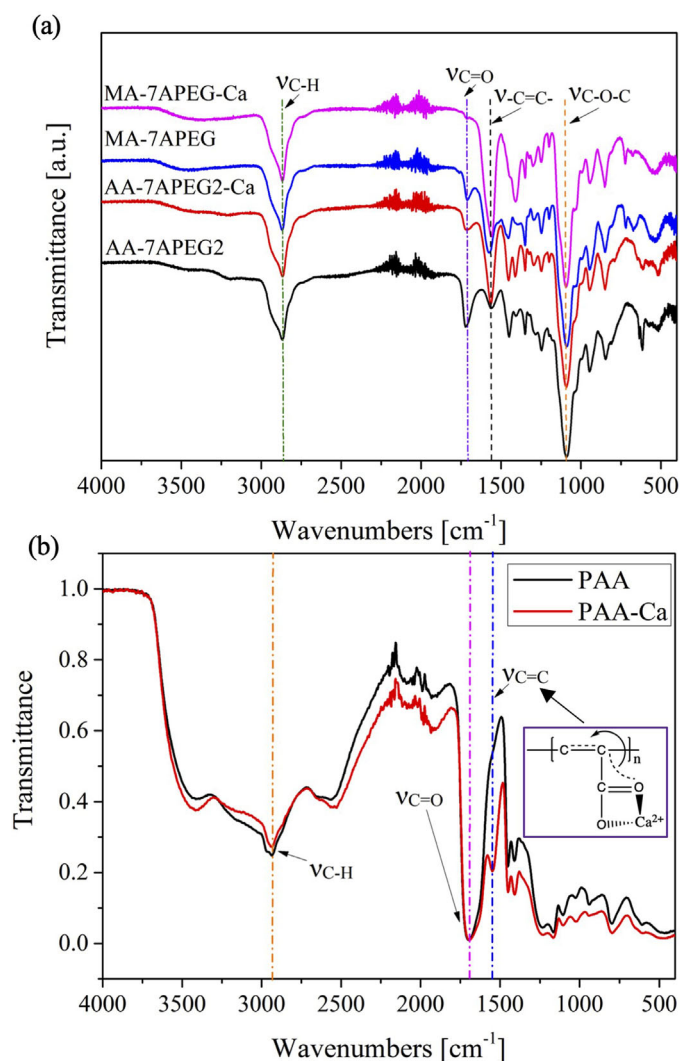
Figure 9. FT-IR spectra of (a) MA-7APEG and AA-7APEG2 PCEs and (b) polyacrylic acid (PAA) sample before and after being treated with Ca^{2+}.

calcium in the solution resulted in a substantial decrease in the anionic charge of the MA-7APEG polymer (94.1% decrease), whereas there was a much smaller decrease for the AA-7APEG2 polymer (59.4% decrease). The results indicated that the MA-7APEG sample possessed a much-pronounced affinity for the surface of slag compared to AA-7APEG2 sample. In the OPC system, a similar observation has been made by other authors, which was ascribed to the chelation of the Ca^{2+} cation by COO^- functionalities in the PCE structure [43]. Apparently, the calcium binding capability of the PCE polymers not only depends on the number of carboxylate groups but also the type of carboxylate groups, i.e. mono-carboxylate or di-carboxylate. And di-carboxylate groups (here we refer to maleic acid) possess a much stronger Ca^{2+} chelating ability compared to mono-carboxylate groups (here we refer to acrylic acid).

3.6. FT-IR spectroscopy

FT-IR spectroscopy was employed to assess and compare the calcium chelating abilities of the two APEG PCEs, MA-7APEG and AA-7APEG2. The PCE samples were subjected to FT-IR spectroscopic analysis both before and after coming into contact with Ca^{2+} ions. As shown in

Figure 9(a), four characteristic adsorption peaks can be found, i.e. stretching vibration of carbon-hydrogen bond ν_{C-H} at $2869\,cm^{-1}$, stretching vibration of ether bond ν_{C-O-C} at $1096\,cm^{-1}$, carbonyl stretching vibration in carboxylic acid $\nu_{C=O}$ of $1715\,cm^{-1}$, and $\nu_{C=C}$ of $1560\,cm^{-1}$ from stretching vibration of alkene double bond [44]. For ν_{C-H} and ν_{C-O-C}, the adsorption peak position and intensity remained unchanged with or without Ca^{2+}.

While in terms of $\nu_{C=O}$, its intensity was significantly reduced for AA-7APEG2 polymer after encountering Ca^{2+}. Moreover, MA-7APEG almost lost its characteristic peak for $\nu_{C=O}$ of $1715\,cm^{-1}$. This further demonstrated that almost all carboxylic groups in MA-7APEG are surrounded by Ca^{2+}. The electron cloud on the carbonyl group was weakened and shifted due to the affinity of the empty electric orbital contained in the calcium ions. AA-7APEG2 polymer, on the other hand, still retained part of residual carbonyl groups, which did not participate in the interaction with Ca^{2+}.

As mentioned above, $\nu_{C=C}$ of $1560\,cm^{-1}$ can be assigned to the stretching vibration of alkene double bond. One may argue that, after the copolymerization of
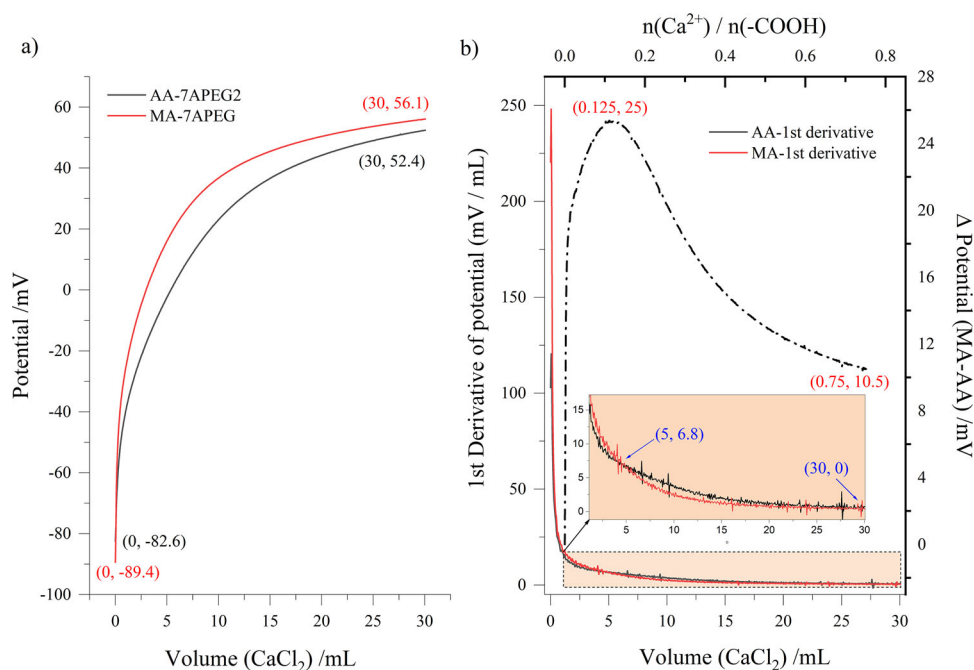
Figure 10. Titration potential of MA-7APEG and AA-7APEG2 aqueous solution (0.01 M) titrated by CaCl$_2$ (0.25 M). (a) The potential of Ca^{2+}-PCEs complexes varying with the volume of CaCl$_2$. (b) The 1st order derivative of potential (solid lines) with respect to CaCl$_2$ volume and the potential difference (dashed line) occurring between MA-7APEG and AA-7APEG2 associated with molar ratio of Ca^{2+} and carboxylic groups.

acrylic acid and APEG macromonomer, the characteristic peak for $\nu_{C=C}$ would diminish. However, it was observed that both MA-APEG and AA-APEG PCE polymers retained part of their original adsorption intensity of $\nu_{C=C}$ (see Figure 9a). This could be attributed to the fact that the affinity of $\beta-$delocalized electrons of ether groups in APEG macromonomers to C $=$ C in the backbone is relatively weak, whereas the affinity of carboxylic groups is much stronger. When the two APEG PCEs were treated with Ca^{2+}, the conjugation effect between the oxygen atom in carboxylic groups and carbon-carbon double bond is weakened. As the consequence, $\nu_{C=C}$ exhibited the enhanced adsorption intensity. In order to prove the validity of this statement, a polyacrylic acid—homo polymer of acrylic acid—with a M_w of 5400 g/mol was also characterized *via* FT-IR spectroscopy (see Figure 9b). Initially, no characteristic peak appeared at 1560 cm^{-1} or PAA, whereas after being treated with Ca^{2+}, $\nu_{C=C}$ emerged at 1560 cm^{-1} and the intensity of $\nu_{C=O}$ decreased at the same time. Again, it is confirmed that the carboxylic groups exhibited a strong affinity to calcium ions which caused the intensity increase of $\nu_{C=C}$.

To summarize, the greatly enhanced interaction between MA-7APEG polymer and calcium ions can be also evidenced by FT-IR measurement.

3.7. Titration potential determination

To quantify the Ca^{2+} uptake capacity of the synthesized APEG PCE polymers, we performed titration potential measurements *via* automatic potentiometric titrator, which could monitor the *in-situ* potential variation. As illustrated in Figure 10(a), the MA-7APEG polymer exhibited an initial potential value of -89.4 mV whereas AA-7APEG2

showed a slightly higher potential of -82.6 mV. The slight difference in the initial potential could originate from the different dissociation degree of the carboxylic acid groups along the trunk chains. The dissociation degree of acid groups is pH-dependent and hence all potential measurements are strictly carried out in neutral pH.

The potential of both PCE polymers increased with increasing titration volume of Ca^{2+} containing solutions. When the titration volume of CaCl$_2$ reached 30 mL, the potential of MA-7APEG reached a saturation value of 56.1 mV. In comparison, AA-7APEG2 registered at 52.4 mV. This difference in potential value indicated that MA-7APEG could chelate more Ca^{2+} ions than AA-7APEG2, in other words, MA-7APEG exhibited a stronger calcium binding capacity than the other type.

In addition, the potential difference between these two APEG PCEs could be processed more and the data are shown in Figure 10(b), whereby we further processed the potential development by calculating the 1st order derivative of potential against the increasing volume of CaCl$_2$. Also, the volume of CaCl$_2$ and concentration of carboxylic acid contained in PCE could be converted into the proportion of Ca^{2+} to -COOH by calculation. It is worth mentioning that the first-order differential of potential versus volume actually reflects the potential gradient in response to the addition of CaCl$_2$, which could directly reflect the *in-situ* Ca^{2+}—capturing capacity of carboxylic acid groups to form the Ca-PCE complex. Initially when the volume of CaCl$_2$ is less than 5 mL, the 1st order derivative of MA-7APEG was dramatically larger than AA-7APEG, but the gap gradually narrowed with increasing volume of CaCl$_2$. The potential gradients were found to be equal

(a)

(b)

		n (Ca²⁺) / n(-COOH)	Δ Potential / mV	Δ Spread flow / cm
AAS	MA-7APEG	0.31	17.5	12.3
(0.05%)	AA-7APEG2	0.33		
OPC	MA-7APEG	1.12	10.5	3.1
(0.10%)	AA-7APEG2	1.18		
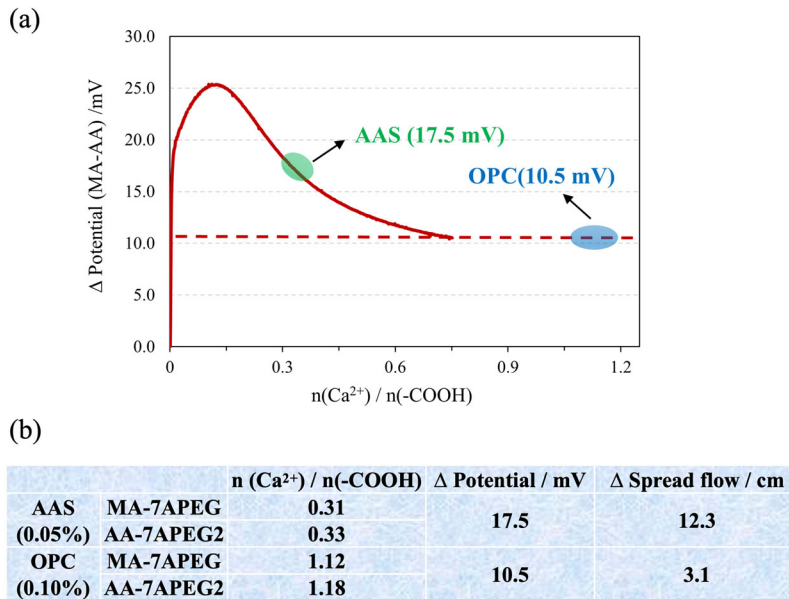
Figure 11. Correlation between potential variations of MA-7APEG and AA-7APEG2 and their dispersing capacities observed in AAS and OPC binder systems.

occurring at ∼6.8 mV/mL with 5 mL of CaCl₂ consumed. For the intersection point (5, 6.8), we could calculate the molar ratio of n(Ca²⁺)/n(-COOH) to be 0.125, combining the initial concentration of CaCl₂ (0.25 M) and PCE solution (0.05 M). And for this molar ratio, the potential difference (Δ potential) between MA-7APEG and AA-7APEG2 came to the maximum (25 mV). With more calcium salts added, the potential gap decreased accordingly and ended up at 10.5 mV for the titration volume totally of 30 mL, and the molar ratio of n(Ca²⁺)/n(-COOH) terminated at 0.75. Here with a volume interval of 5–30 mL, the decrease of potential gap could basically result from the slightly higher potential gradient that AA-7APEG2 holds in comparison to MA-7APEG, which could be interpreted to mean that the latter PCE would get less stronger with respect to its *in-situ* capacity of calcium binding when encountering continuously titrated calcium ions. And this also implies that there must exist a saturation point where PCE reaches the maximum amount of calcium ions it could cheat with. The hypothesis could be verified from by the fact that 1st order derivatives of potential for both PCEs were observed to reach zero at volume of 30 mL, which indicates their potential would maintain constant after this point regardless of excessive titrated Ca²⁺. Moreover, it could also imply that the molar ratio with which both PCE polymers could combine with saturated amount of Ca²⁺ cations, would be 0.75.

To conclude, the titration potential measurements quantitatively reveal the correlations between potential variations of PCE solution and titrated amount Ca²⁺ cations and, in general, the MA-type APEG polymer exhibited stronger calcium binding capacity than AA-type PCE. However, this superiority is closely associated with the quantitative ratio of Ca²⁺ and -COOH and it would maximize at the ratio of 0.125.

More interestingly, the calcium binding differences between MA-7APEG and AA-7APEG2 quantitatively

revealed in potential measurements could be applied to explain their dispersing performance in AAS and OPC binder systems. In terms of two specified PCE dosages, 0.05% and 0.10% (bwo binder), MA-7APEG was determined to exhibit better dispersing performance than AA-7APEG2 in both AAS and OPC pastes. Given the Ca²⁺ concentration of 1.25 mmol/L in the AAS pore solution [18] and the water to slag ratio of 0.5, the ratio of n(Ca²⁺)/n(-COOH) could be calculated to be ∼0.31 (MA-7APEG) and 0.33 (AA-7APEG2) when PCE dosage is 0.05% bwos. Similarly applying Ca²⁺ concentration of 1 g/L in cement pore solution [45] and w/c of 0.45, 0.10% bwoc refers to the molar ratio of ∼1.12 and 1.18 for MA- and AA-type PCE. As well demonstrated above, molar ratios of n(Ca²⁺)/n(-COOH) would lead to the corresponding potential difference between MA-7APEG and AA-7APEG2, whereby the Δpotential was calculated to be ∼17.5 mV and 10.5 mV for AAS and OPC, respectively. As the Δpotential reflects well in the difference of calcium binding quantity, it would also closely relate to the dispersing performances of PCEs. For the great variation of Δpotential existing in AAS and OPC, as well illustrated in Figure 11, the binder-dependent dispersing effectiveness of PCE polymers would differ a lot. This could also be demonstrated by the difference of paste fluidity mixing with two PCEs of the same dosage, as shown in Figure 4. The higher Δpotential (17.5 mV) occurring in AAS would cause greater difference in spread flow of 12.3 cm (30.8–12.5), while the lower potential gap (10.5 mV) in OPC only contribute to the difference of 3.1 cm (26.4–23.3) in fluidity. Therefore, for binder systems with different ionic compositions, especially with varied Ca²⁺ concentration, the dispersing performance of PCE would vary a lot and the specific molecular design of PCE for each system is required.

4. Conclusions

In this study, first, two APEG PCE samples (MA-7APEG and AA-7APEG2) were successfully synthesized. Thereafter their dispersing effectiveness was assessed and compared in AAS and OPC binder systems. Furthermore, the interaction mode between PCE polymers and calcium cations was investigated. The main conclusions from our experiments are:

- Mini slump and rheology measurements revealed that in AAS binder MA-7APEG polymer exhibited much stronger dispersing efficiency than AA-7APEG2 polymer although two PCE polymers exhibited the same anionicity and comparable molecular weight. In the OPC binder, the superiority of MA-7APEG polymer was rather mild.

- MA-7APEG polymer with bi-carboxylic groups showed much higher adsorbed amount at various dosages, especially at actual field dosages (typically $< 0.2\%$ bwos). The greatly enhanced adsorption of MA-7APEG polymer accounts for its superior dispersion. In addition, the distinct adsorption characteristics of the two PCEs could be induced by the different steric positions of the carboxylate groups contained in their polymer backbones.

- MA-7APEG polymer possessed a much stronger Ca^{2+} chelating ability compared to AA-7APEG polymer, evidenced by anionic charge amount determination, FT-IR analysis and titration potential measurements. The different Ca^{2+} binding capacities for the PCEs are quantitatively dependent on the proportion of Ca^{2+} and carboxylic acid groups. The largest potential difference was determined to occur at the $n(Ca^{2+})/n(COOH)$ of 0.125. The chelated Ca^{2+}-PCE complex with saturated amount of Ca^{2+} could be formed at the molar ratio of 0.75.

- Calorimetric results indicate that the addition of PCE polymers clearly delayed the hydration of OPC pastes. Whereas the strong retardation effect was not observed in AAS biner, MA-7APEG PCE polymer exhibited a slight delay in the main hydration peak.

Future research perspectives for this study include investigating the properties that contribute to the superior performance of the MA-7APEG polymer in low-carbon alkali activated slag, delving deeper into the interaction mode between PCE polymers and calcium cations, comparing the performance of the MA-7APEG polymer with other types of PCE superplasticizers, examining the long-term effects of the MA-7APEG polymer on the durability and sustainability of low-carbon alkali activated slag and OPC. Overall, further research in these areas will help to further understand the properties and mechanisms of PCE polymers and their potential in the field of low-carbon construction materials.

Disclosure statement

The authors declare that they have no known competing financial interests or personal relationships that could have appeared to influence the work reported in this paper.

References

[1] Awoyera P, Adesina A. A critical review on application of alkali activated slag as a sustainable composite binder. Case Stud Constr Mater. 2019;11:13.

[2] Kim SW, Jang SJ, Kang DH, et al. Mechanical properties and eco-efficiency of steel fiber reinforced alkali-activated slag concrete. Materials (Basel). 2015;8(11): 7309–7321.

[3] Shi C, Jiménez AF, Palomo A. New cements for the 21st century: the pursuit of an alternative to Portland cement. Cem Concr Res. 2011;41(7):750–763.

[4] Flower DJ, Sanjayan JG. Green house gas emissions due to concrete manufacture. Int J Life Cycle Assess. 2007;12(5):282–288.

[5] Yang K-H, Song J-K, Song K-I. Assessment of CO_2 reduction of alkali-activated concrete. J Cleaner Prod. 2013;39:265–272.

[6] Dzunuzovic N, Komljenovic M, Nikolic V, et al. External sulfate attack on alkali-activated fly ash-blast furnace slag composite. Constr Build Mater. 2017;157: 737–747.

[7] Komljenovic M, Bascarevic Z, Marjanovic N, et al. External sulfate attack on alkali-activated slag. Constr Build Mater. 2013;49:31–39.

[8] Law DW, Adam AA, Molyneaux TK, et al. Durability assessment of alkali activated slag (AAS) concrete. Mater Struct. 2012;45(9):1425–1437.

[9] Arbi K, Nedeljkovic M, Zuo YB, et al. A review on the durability of Alkali-Activated fly ash/slag systems: advances, issues, and perspectives. Ind Eng Chem Res. 2016;55(19):5439–5453.

[10] An Y-J, Mun K-J, Soh S-Y, et al. Fundamental properties of alkali activated slag mortar with different activator type. Proceedings of the Korea Concrete Institute Conference. Korea Concrete Institute. 2006. p. 789–792.

[11] Rajesh D, Narender RA, Venkata T, et al. Performance of alkali activated slag with various alkali activators. Int J Innov Res Eng Technol. 2013;2:378–386.

[12] Li N, Shi C, Zhang Z. Understanding the roles of activators towards setting and hardening control of alkali-activated slag cement. Compos B: Eng. 2019;171:34–45.

[13] Tuyan M, Andiç-Çakir Ö, Ramyar K. Effect of alkali activator concentration and curing condition on strength and microstructure of waste clay brick powder-based geopolymer. Compos B: Eng. 2018;135:242–252.

[14] Li C, Sun H, Li L. A review: the comparison between alkali-activated slag $(Si + Ca)$ and metakaolin $(Si + Al)$ cements. Cem Concr Res. 2010;40(9):1341–1349.

[15] Farhan NA, Sheikh MN, Hadi MNS. Investigation of engineering properties of normal and high strength fly ash based geopolymer and alkali-activated slag concrete compared to ordinary Portland cement concrete. Constr Build Mater. 2019;196:26–42.

[16] Palacios M, Houst YF, Bowen P, et al. Adsorption of superplasticizer admixtures on alkali-activated slag pastes. Cem Concr Res. 2009;39(8):670–677.

[17] Palacios M, Puertas F. Effect of superplasticizer and shrinkage-reducing admixtures on alkali-activated slag pastes and mortars. Cem Concr Res. 2005;35(7):1358–1367.

[18] Conte T, Plank J. Impact of molecular structure and composition of polycarboxylate comb polymers on the flow properties of alkali-activated slag. Cem Concr Res. 2019;116:95–101.

[19] Kashani A, Provis JL, Xu J, et al. Effect of molecular architecture of polycarboxylate ethers on plasticizing performance in alkali-activated slag paste. J Mater Sci. 2014;49(7):2761–2772.

[20] Luukkonen T, Abdollahnejad Z, Ohenoja K, et al. Suitability of commercial superplasticizers for one-part alkali-activated blast-furnace slag mortar. J Sustain Cem-Based Mater. 2019;8(4):244–257.

[21] Plank J, Sakai E, Miao C, et al. Chemical admixtures—chemistry, applications and their impact on concrete microstructure and durability. Cem Concr Res. 2015;78: 81–99.

[22] Gelardi G, Flatt RJ. Working mechanisms of water reducers and superplasticizers. Science and technology of concrete admixtures. Woodhead publishing. 2016. p. 257–278.

[23] Ilg M, Plank J. Non-adsorbing small molecules as auxiliary dispersants for polycarboxylate superplasticizers. Colloids Surf A. 2020;587:124307.

[24] Lei L, Zhang Y. Preparation of isoprenol ether-based polycarboxylate superplasticizers with exceptional dispersing power in alkali-activated slag: comparison with ordinary Portland cement. Compos B: Eng. 2021;223: 109077.

[25] Lei L, Chan H-K. Investigation into the molecular design and plasticizing effectiveness of HPEG-based polycarboxylate superplasticizers in alkali-activated slag. Cem Concr Res. 2020;136:106150.

[26] Ran Q, Somasundaran P, Miao C, et al. Adsorption mechanism of comb polymer dispersants at the cement/water interface. J Dispersion Sci Technol. 2010; 31(6):790–798.

[27] Plank J, Dugonjić-Bilić F, Lummer NR. Modification of the molar anionic charge density of acetone–formaldehyde–sulfite dispersant to improve adsorption behavior and effectiveness in the presence of CaAMPS®-co-NNDMA cement fluid loss polymer. J Appl Polym Sci. 2009; 111(4):2018–2024.

[28] Teresa M, Laguna R, Medrano R, et al. Polymer characterization by size-exclusion chromatography with multiple detection. J Chromatogr A. 2001;919(1):13–19.

[29] DIN EN 1015-3. 2007-5, Methods of test for mortar for masonry-part 3: determination of consistence of fresh mortar. DIN Berlin/Germany. 2007.

[30] Winnefeld F, Becker S, Pakusch J, et al. Effects of the molecular architecture of comb-shaped superplasticizers on their performance in cementitious systems. Cem Concr Compos. 2007;29(4):251–262.

[31] Rp A. Recommended practice for field testing water-based drilling fluids. API Recommendation 13B-1, ISO. 20012009;10414:21.

[32] Yamada K, Takahashi T, Hanehara S, et al. Effects of the chemical structure on the properties of polycarboxylate-type superplasticizer. Cem Concr Res. 2000;30(2): 197–207.

[33] Zhang L, Miao X, Kong X, et al. Retardation effect of PCE superplasticizers with different architectures and their impacts on early strength of cement mortar. Cem Concr Compos. 2019;104:103369.

[34] Marchon D, Flatt RJ. Mechanisms of cement hydration. Science and technology of concrete admixtures. Woodhead Publishing. 2016. p. 129–145.

[35] Prasittisopin L, Sereewatthanawut I. Dissolution, nucleation, and crystal growth mechanism of calcium aluminate cement. J Sustain Cem-Based Mater. 2019;8(3): 180–197.

[36] Liu Q, Lu Z, Xu J, et al. Insight into the in situ copolymerization of monomers on cement hydration and the mechanical performance of cement paste. J Sustain Cem-Based Mater. 2023;12(6):736–750.

[37] Živica V. Effects of type and dosage of alkaline activator and temperature on the properties of alkali-activated slag mixtures. Constr Build Mater. 2007;21(7):1463–1469.

[38] Tong S, Yuqi Z, Qiang W. Recent advances in chemical admixtures for improving the workability of alkali-activated slag-based material systems. Constr Build Mater. 2021;272:121647.

[39] Fernández-Jiménez A, Palomo J, Puertas F. Alkali-activated slag mortars: mechanical strength behaviour. Cem Concr Res. 1999;29(8):1313–1321.

[40] Fernández-Jiménez A, Puertas F. Setting of alkali-activated slag cement. Influence of activator nature. Adv Cem Res. 2001;13(3):115–121.

[41] Jiao Z, Wang Y, Zheng W, et al. Effect of dosage of sodium carbonate on the strength and drying shrinkage of sodium hydroxide based alkali-activated slag paste. Constr Build Mater. 2018;179:11–24.

[42] Sakai E, Yamada K, Ohta A. Molecular structure and dispersion-adsorption mechanisms of comb-type superplasticizers used in Japan. ACT. 2003;1(1):16–25.

[43] Plank J, Sachsenhauser B. Experimental determination of the effective anionic charge density of polycarboxylate superplasticizers in cement pore solution. Cem Concr Res. 2009;39(1):1–5.

[44] Ţucureanu V, Matei A, Avram AM. FTIR spectroscopy for carbon family study. Crit Rev Anal Chem. 2016; 46(6):502–520.

[45] Lei L, Plank J. Synthesis and properties of a vinyl ether-based polycarboxylate superplasticizer for concrete possessing clay tolerance. Ind Eng Chem Res. 2014;53(3):1048–1055.

5.7 Paper # 7 (Conference paper)

Optimization of molecular structure of allyl ether-based PCEs with enhanced clay tolerance

Y. Zhang, Y. Liu, L. Lei, J. Plank

The study involved synthesizing allylether-based polycarboxylate superplasticizers (APEG PCEs) with customized molecular architectures, including variations in side chain length, anionicity, and different acid groups, through free radical copolymerization. The synthesized PCE polymers were then tested for their performance in cement pastes containing varying amounts of clay.

The results signify that APEG PCE polymers with shorter side chain lengths (e.g. 7 EO units) possess superior resistance against clay contaminants. Moreover, a higher anionic charge also improved the clay robustness of such PCE polymers. Additionally, APEG PCEs synthesized with acrylic acid exhibited greater resistance to clay contaminants as compared to those prepared from maleic anhydride.

The 16th International Congress on the Chemistry of Cement 2023 (ICCC2023)
"Further Reduction of CO_2 -Emissions and Circularity in the Cement and Concrete Industry"
September 18–22, 2023, Bangkok, Thailand

Optimization of molecular structure of allylether-based PCEs with enhanced clay tolerance

Y. Zhang[1], Y. Liu[2], L. Lei[3*], J. Plank[4]**

[1] *Technische Universität München, Munich, Germany*
E-Mail: yue1.zhang@tum.de

[2] *Technische Universität München, Munich, Germany*
E-Mail: yiliu.tum@gmail.com

[3] *Technische Universität München, Munich, Germany*
E-Mail: lei.lei@tum.de

[4] *Technische Universität München, Munich, Germany*
E-Mail: johann.plank@tum.de

ABSTRACT

Allylether-based polycarboxylate superplasticizers (APEG PCEs) with tailored molecular architectures, i.e., side chain length, anionicity and structurally different acid groups, were synthesized via free radical copolymerization. The synthesized PCE polymers were then subjected to performance testing in cement pastes holding various amounts of clay.

It turned out that APEG PCE polymers with relatively short side chain length (e.g., 7 EO units) exhibit enhanced robustness against clay contaminants. Besides, a higher anionic charge amount also promotes the clay robustness of such PCE polymers. Additionally, APEG PCEs polymerized with acrylic acid possess higher resistance to clay contaminants as compared to those containing maleic anhydride.

The correlation between structural characteristics and dispersing effectiveness of the PCE polymers was further explained by means of TOC analysis. Apparently, the structural differences of the PCE polymers are responsible for their distinct performance in the presence of clay contaminants. Adsorption measurements further elucidate the different interaction mode between the synthesized PCE molecules and clay particles.

KEYWORDS: *APEG; clay tolerance; intercalation; calcium binding capacity.*

1. Introduction

Polycarboxylate superplasticizers (PCE) are widely used in the construction industry due to their extraordinary dispersing performance (Marchon et al (2013), Plank et al (2015), Lei et al (2022)). However, conventional PCEs are sensitive to clay contaminants in aggregates resulting in decreased dispersing capacity. PCE polymers interact with cement either by intercalating into clay interlayers or adsorbing onto clay particle surfaces through Ca^{2+} complexation (Sha et al (2020) , Lei et al (2022)). The intercalation of PCE polymers is the main cause of reduced dispersing performance in cement slurries. Therefore, it's crucial to develop PCE products possessing enhanced clay robustness. PCE comb copolymers typically consist of a trunk chain holding carboxylate groups and polyethylene glycol side chains, allowing for adjustments in compositional parameters such as anionicity, side chain density, and molecular weight to achieve better clay tolerance.

2. Experimental

2.1. Size exclusion chromatography (SEC)

For the determination of weight-averaged molecular weight (M_w), number-averaged molecular weight (M_n), polydispersity index (PDI), and the macromonomer conversion of synthesized PCE polymers, size exclusion chromatography (SEC), also known as gel permeation chromatography (GPC), was employed. The measurements were conducted using a Waters Alliance 2695 instrument (Waters, Eschborn, Germany) equipped with three Ultrahydrogel™ columns (120, 250, 500) and an Ultrahydrogel™ Guard column. A 0.1 N $NaNO_3$ eluent (pH = 12) was utilized at a flow rate of 1.0 mL/min. The Mw and Mn calculations were performed using a dn/dc value of 0.135 mL/g, which is the value commonly used for PEO (polyethylene oxide).

2.2. Anionic charge measurement

The precise amount of specific anionic charge present in the synthesized PCEs was determined using a particle charge detector PCD 03 pH instrument (Mütek Analytic, Herrsching, Germany). In this analysis, a 10 mL sample of the 0.2 g/L PCE solution was titrated with a 0.34 g/L aqueous solution of cationic poly-diallyl dimethyl ammonium chloride (polyDADMAC) until charge neutralization was achieved. The anionic charge per gram of PCE polymer was then calculated based on the consumption of the cationic polyelectrolyte polyDADMAC.

2.3. Dispersing performance in mortar with/without clay

To evaluate the dispersing efficacy of PCEs in cement, a mortar test was conducted according to the DIN EN 196-1 standard. The water-to-cement (w/c) ratio employed in this study was 0.48. The dosage of each PCE sample was then determined at this w/c ratio to achieve the desired fluidity. For the clay tolerance tests, a similar procedure was employed, with 1 wt. % or 3 wt. % of the cement being replaced by clay minerals.

2.4. PCE sorption on clay

In order to assess the clay sorption capacity of PCEs, the depletion method was employed utilizing total organic content (TOC) in a synthetic cement pore solution (SCPS) with a pH of 13.06. TOC measurements were performed using a High TOC II instrument (Elementar Analysensysteme, Hanau, Germany) at a temperature of 890 °C. The sorbed amount at each concentration was determined by calculating the average from a minimum of two duplicate measurements.

3. Results and Discussion

3.1. Characteristic properties of the synthesized PCE samples

The SEC chromatograms of the two APEG PCE polymers are displayed in **Fig. 1**. The molecular properties are listed in **Table 1**. Both APEG PCEs possess high yield and low PDIs (polydispersity index) and also comparable molecular weight. The anionic charge measurements indicated that both APEGs with different anchor groups (MA-7APEG and AA-7APEG2) had similar negative charges both the theoretical calculations or measurements in the 0.1 M NaOH solution (Table 1). However, upon the addition of Ca^{2+} (1g/L) to the solution, the anionic charge of both polymers significantly decreased due to the interaction of COO- with Ca^{2+} through electrostatic forces. Additionally, the anionicity drop for the MA-7APEG polymer was greater than that of the AA-7APEG2 polymer, suggesting that it has a stronger calcium binding capacity.
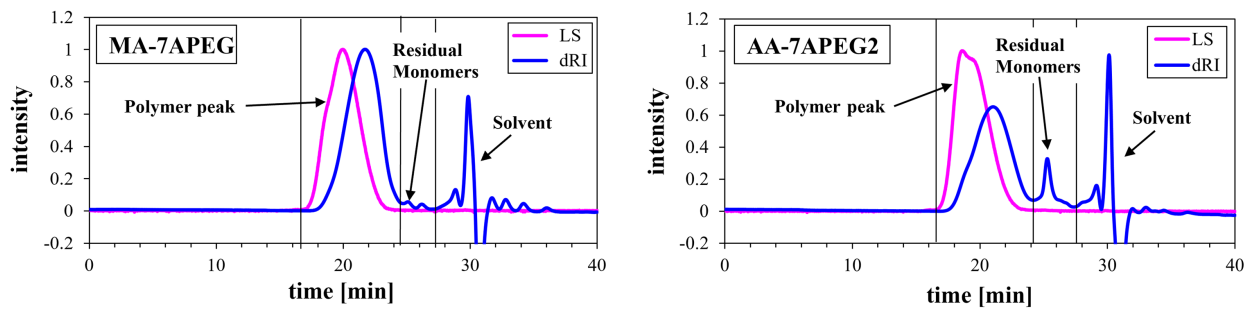
Fig. 1. GPC chromatograms of the synthesized polymers.

Table 1. Characteristic molecular parameters of the synthesized PCE polymers.

Polymer sample	M_w [Da]	M_n [Da]	PDI	Macromonomer Conversion (%)	Theoretical Anionicity (µeq/g)	Anionicity (µeq/g)	
						NaOH	NaOH+Ca
MA-7APEG	38,100	15,875	2.4	96.6	4016	3709	218
AA-7APEG2	41,320	17,965	2.3	84.3	3816	3520	1428

3.2. Dispersing capacities of PCEs in mortar

Through fluidity tests, ranging from paste to mortar, it was consistently observed that AA-7APEG PCE exhibits superior clay-tolerance. This was clearly demonstrated in mortar tests, where both APEG PCEs achieved an initial spread flow of 22 cm with a comparable polymer dosage (~ 0.2% bwoc). However, in the presence of clay contaminants, the MA-form PCE displayed a significant decrease of 6.4 cm when 3% bwoc clay was added. In comparison, the AA-type remained more resistance to the clay contaminants, maintaining a fluidity of 17.9 cm even in extreme conditions with a 3 % addition.
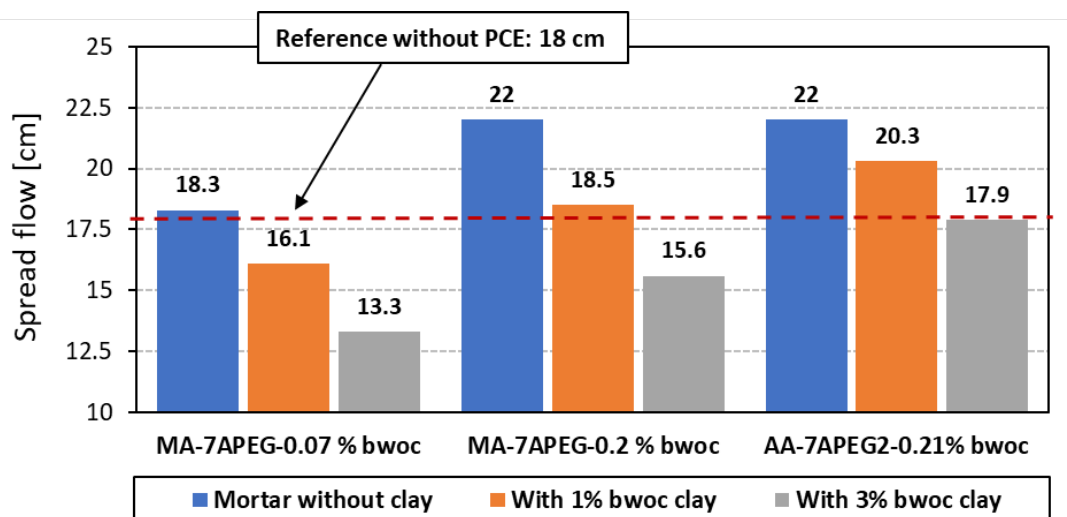
Fig. 2. Dispersing performance of polymers in mortar.

3.3. Sorption of PCEs on clay

In order to further examine the mode of action between PCEs and clay particles, the sorbed amounts of MA-7APEG and AA-7APEG2 were determined as a function of PCE dosages. Both APEG PCEs

exhibited a typical Langmuir adsorption isotherm, depicted in **Fig. 3**, where the sorbed amount of PCE initially increased with dosage and then leveled off at a saturated adsorption amount. Specifically, the maximum sorbed amount of MA-7APEG was found to be approximately 175 mg per gram of clay, while AA-7APEG2 reached only around 125 mg per gram of clay. This suggests that the MA-7APEG polymer had a stronger attraction to the clay than the AA-7APEG2 polymer. These results are in line with the mortar test results (**Fig. 2**). This explains the better dispersion of AA-APEG 2 in the presence of clay.
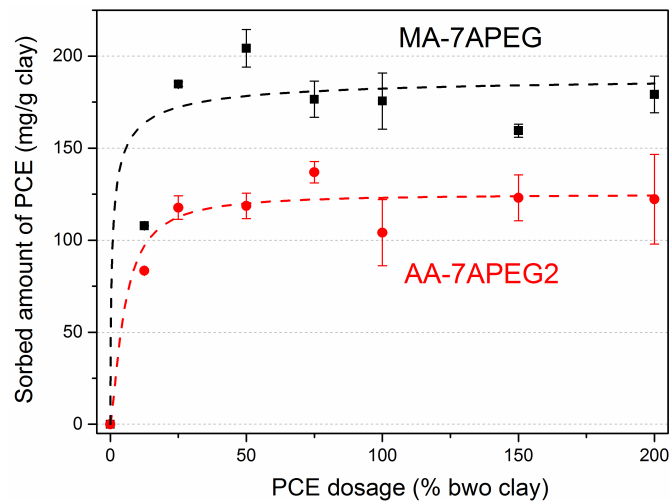
Fig. 3. Adsorption isotherms of PCE polymers in the clay suspensions dispersed in the synthetic cement pore solutions.

4. Conclusions

Two APEG PCEs were prepared with the same side-chain length of 7 EO units, differing only in the type of acid co-monomer used, either maleic anhydride (MA) or acrylic acid (AA). The anionicity and molecular weight of the two PCEs were comparable, yet MA-7APEG displayed a considerably lower effective charge in the presence of Ca^{2+} ions than AA-7APEG2, indicating that the MA-7APEG polymer had a stronger affinity for calcium binding than the AA-7APEG2 polymer. This fundamental difference in structure also had an impact on their adsorption behavior on clay, leading to distinct dispersing capacities in its presence. The results from TOC experiments showed that MA-7APEG exhibited a greater affinity for clay than AA-7APEG2.

References

Marchon, D., U. Sulser, A. Eberhardt and R. J. Flatt (2013). "Molecular design of comb-shaped polycarboxylate dispersants for environmentally friendly concrete." Soft Matter 9(45): 10719-10728.

Plank, J., E. Sakai, C. Miao, C. Yu and J. Hong (2015). "Chemical admixtures—Chemistry, applications and their impact on concrete microstructure and durability." Cement and concrete research 78: 81-99.

Lei, L., T. Hirata and J. Plank (2022). "40 years of PCE superplasticizers-History, current state-of-the-art and an outlook." Cement and Concrete Research 157: 106826.

Sha, S., M. Wang, C. Shi and Y. Xiao (2020). "Influence of the structures of polycarboxylate superplasticizer on its performance in cement-based materials-A review." Construction and Building Materials 233: 117257.

Lei, L., M. Palacios, J. Plank and A. A. Jeknavorian (2022). "Interaction between polycarboxylate superplasticizers and non-calcined clays and calcined clays: A review." Cement and Concrete Research 154: 106717.

5.8 Paper # 8 (Conference paper)

Investigation into A Novel Starch-based Superplasticizer for Alkali-activated Slag

N. Miao, Y. Zhang, L. Lei, J. Plank

This study focused on a newly developed starch-based superplasticizer made through graft copolymerization. This novel polymer exhibited strong dispersion and maintained fluidity for extended periods in both AAS paste and mortar. It provided excellent dispersion and slump-retaining abilities at relatively low dosages. Further analysis revealed that starch-based polymer adhered to slag particles following the Langmuir adsorption trend. Overall, the study highlighted the promising characteristics of starch-based superplasticizers as a superplasticizer for construction materials.

The 16th International Congress on the Chemistry of Cement 2023 (ICCC2023)
"Further Reduction of CO₂ -Emissions and Circularity in the Cement and Concrete Industry"
September 18–22, 2023, Bangkok, Thailand

Investigation into A Novel Starch-based Superplasticizer for Alkali-activated Slag

N. Miao, Y. Zhang, L. Lei*, Johann Plank**

Technische Universität München, Garching, Germany
na.miao@tum.de
Technische Universität München, Garching, Germany
yue1.zhang@tum.de
Technische Universität München, Garching, Germany
lei.lei@tum.de
Technische Universität München, Garching, Germany
johann.plank@tum.de

ABSTRACT
In this work, a novel starch-based superplasticizer (designated as S-SP) synthesized via graft copolymerization was studied. The structure was characterized by size exclusion chromatography (SEC). Its dispersing effectiveness was tested in both AAS paste and mortar. In AAS paste, it was found that S-SP exhibited strong dispersion at relatively low dosage (0.12% bwos). Most surprising, it also maintained fluidity over 6 hours. In AAS mortar, 0.3% bwos of S-SP were required to reach an initial spread flow of 21 cm, and high fluidity was maintained over 6 hours. From the results it can be concluded that S-SP provides excellent dispersion and slump-retaining ability. To further study the interaction between the novel superplasticizer and AAS, adsorption measurements and adsorbed layer thickness measurements were carried out. It was found that S-SP molecules adsorb on slag particles following a Langmuir adsorption trend.

KEYWORDS: *low-carbon binder, alkali-activated slag, starch, superplasticizer, dispersion*

1. Introduction

Out of the concern for global warming Andrew (2019), researchers have come up with many solutions to reduce CO_2 emission in cement industry, for example, replacing OPC clinker with supplementary cementitious materials (SCMs), such as ground granulated blast furnace slag (GGBFS) Flower and Sanjayan (2007). Despite the latent hydraulic properties of slag, with the addition of alkaline activators (such as sodium hydroxide Shi and Day (1995) and sodium carbonate) Yuan, Yu et al. (2017) the concrete can possess high durability and resistance to acid attack and corrosion. However, the application of slag is facing several drawbacks, including poor workability, quick setting and high shrinkage after hydration Tong, Yuqi et al. (2021). Moreover, the superplasticizers (SP) commonly used in OPC fail to disperse the AAS systems. Thus, there is a strong need for the development of new superplasticizers, which could be applied in AAS binders. In cement industry, there have been a lot of superplasticizers invented and widely applied, ranging from lignosulfonates (LS), to polynaphthalene sulphonates (PNS), polymelamine sulphonates and polycarboxylate ethers (PCE) Pagé and Spiratos (2000, Javadi, Mehr et al. (2017, Breilly, Fadlallah et al. (2021). However, the synthetic raw materials of these superplasticizers are mostly from the petroleum industry. Due to the huge market of construction materials worldwide, the consumption of such PCEs would take up a lot of petroleum resources Wang, Zhou et al. (2022). Based on such concern, there emerges a need for SPs with greener sources, such as natural materials. In this work, a novel starch-based superplasticizer named as S-SP was studied, which was provided by China Academy of Building Research (CABR). Through structure characterization and performance tests, its potential application in AAS was investigated and discussed.

2. Experimental

2.1. Size exclusion chromatography (SEC)

Size exclusion chromatography (SEC), also referred to as gel permeation chromatography (GPC), was applied for the determination of weight averaged molecular weight (*Mw*), number averaged molecular weight (*Mn*), polydispersity index (PDI) and the macromonomer conversion of synthesized PCE polymers. The measurements were deployed by a Waters Alliance 2695 instrument (waters, Eschborn, Germany) equipped with three Ultrahydrogel™ columns (120, 250, 500) and an Ultrahydrogel™ Guard column. As eluent, 0.1 N $NaNO_3$ (pH = 12) was used with a flow rate of 1.0 mL/min. For the calculation of Mw and Mn, a dn/dc value of 0.135 mL/g (value for PEO) was utilized.

2.2. Anionic charge measurement

The specific anionic charge of S-SP samples was determined based on the method of titration. A particle charge detector (PCD 03 pH from Mütek Analytic, Herrsching, Germany) was utilized for the charge titration. A 100 mL sample solution was prepared containing 0.01 M NaOH and 0.1 g/L S-SP, and titrated against a 0.34 g/L aqueous poly-diallyl dimethyl ammonium chloride (polyDADMAC) until charge neutralization. The specific anionic charge of S-SP (amount of negative charge per gram) was calculated based on the volume of polyDADMAC consumed.

2.3. Dispersing performance in AAS paste and mortar

The spread flow of alkaline-activated slag pastes containing S-SP was determined by conducting a "mini-slump" test following a modified version of DIN EN 1015 standard. The slag mortar was prepared by mixing 450 g of slag, 202.5 g of DI water, 16 g of NaOH and 0.3% bwos of S-SP with 1350 g of CEN standard sand (slag to sand ratio of 1:3). Mixing of mortar was conducted according to DIN EN 196-1 using an eccentric agitator from Toni Technik (ToniMIX, Baustoffprüfsysteme, Berlin, Germany).

2.4. Adsorption via TOC

The adsorption of S-SP on the slag was determined by the depletion method based on total organic carbon (TOC) analysis. In this experiment, 16 g of slag was dispersed in 7.2 g DI water (w/s ratio of 0.45) with addition of 0.64 g NaOH and PCE. Firstly, a series of sample solutions were prepared with different polymer content, from 0 to 2% bwos at maximum. Then each solution was mixed with slag, DI water and NaOH on a vibrator for 2 min. Then, after centrifugation at 8500 rpm for 10 min, take the supernatant for analysis, and filtrate into a sample tube. A LiquiTOC analyzer (Elementar, Hanau, Germany) was utilized to detect the total organic carbon content in the collected supernatant.

2.5. Adsorbed layer thickness via zetasizer

The adsorbed layer thickness (ALT) of S-SP was determined in Ca^{2+} and Ca^{2+} free medium. 1% wt. S-SP was dissolved in 0.1 M aqueous NaOH and mixed with their charge equivalent amount of Ca^{2+} added as $CaCl_2 \cdot 2H_2O$. In a separate solution, 1% wt. PCE was dissolved in 0.1 M aqueous NaOH without any Ca^{2+} addition. Both stock solutions were then diluted to prepare a series of PCE concentrations from 0.1-1.5 g/L in a volume of 50 mL. Thereafter, 50 μL of polystyrene nanoparticle were added into the PCE solutions with various concentrations. The polystyrene nanoparticle was prepared according to the literature Stecher and Plank (2020). The opaque dispersions were subjected to ultrasonication for 15 min and remained at rest for 15 min before the diameter determination with dynamic light scattering on the ZetaSizer Nano ZS instrument. The corresponding diameters of polymer free polystyrene nanoparticles were measured before each sample measurement. The adsorbed layer thickness of PCE was calculated according to the following equation:

$$ALT = (D_1 - D_0)/2$$

where D_1 was defined as the particle diameter with adsorbed PCE, and D_0 was noted for the pristine particle diameter.

3. Results and Discussion

3.1. Characteristic properties of S-SP sample

The molecular properties of S-SP obtained from GPC were displayed in Table 1. The weight averaged molecular weight (Mw) of the S-SP sample was around 38,000 g/mol, and the number averaged molecular weight (Mn) was around 16,000 g/mol. The PDI value was 2.4 and the macromonomer conversion was 53.76%. Through the titration against polyDADMAC, the anionic charge of synthesized S-SP sample was measured to be 1544 μeq/g.

Table 1. Molecular properties of synthesized S-SP.

Mw [g/mol]	Mn [g/mol]	PDI	Conversion [%]	Anionic Charge [μeq/g]
3.794×10^4	1.573×10^4	2.4	53.8	1544

3.2. Dispersing effectiveness of S-SP in NaOH activated slag

The dispersing power and retaining ability of S-SP in both AAS paste and mortar were shown in Fig. 1. In AAS paste, the addition of 0.12% bwos of S-SP was able to increase the initial spread flow to 26 cm, and keep the spread flow above 23 cm within 6 h. Despite the lower dosage applied on the reference sample, 7IPEG4.5, to achieved the same initial spread flow, its dispersing power was lost much faster compared to S-SP. The spread flow yielded by reference sample dropped to 11 cm within 90 min. Such outstanding slump-retaining ability of S-SP was also observed in AAS mortar, where 7IPEG4.5 was no longer effective in dispersing. As shown in the figure, 0.3% bwos of S-SP provided the AAS mortar with an initial spread flow of 21 cm, which was still kept above 11 cm for 6 h.

These experiments clearly showed the dispersing power of S-SP in AAS paste and mortar, as well as the ability of maintaining the dispersion over long time. Compared with traditional PCEs, which mainly possess only the initial dispersing effectiveness, the dual ability of S-SP makes it more advantageous in the situations where retarders are needed.
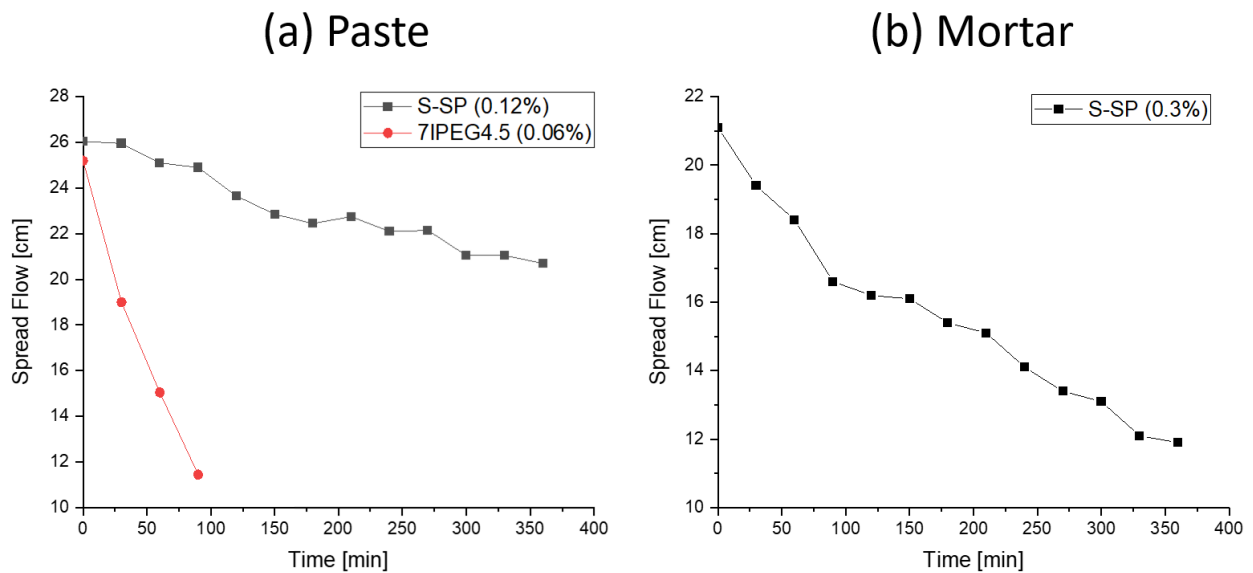
Fig. 1. The change in spread flow against time of (a) AAS paste with 0.12% bwos of S-SP and (b) AAS mortar with 0.3% bwos of S-SP.

3.3. Adsorption of S-SP on AAS

The result of TOC analysis was displayed in Fig. 2. With the polymer dosage increasing, the adsorption amount firstly raised within 1% bwos of addition, then the rate of growth gradually reached plateau until 2% bwos of addition, following a Langmuir adsorption model. S-SP exhibited a much higher adsorbed amount as compared to the 7IPEG4.5 polymer.
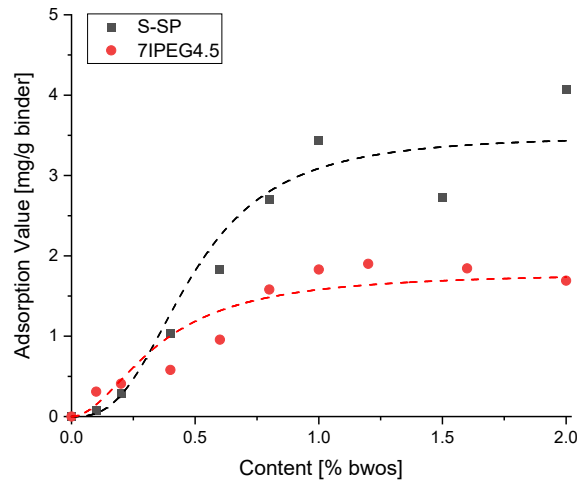
Fig. 2. Adsorption value curve of the synthesized S-SP on AAS, compared with 7IPEG4.5.

The measured adsorbed layer thickness was ~6.5 nm when the polymer concentration was over 600 mg/L.

4. Conclusion

In this work, the novel starch-based superplasticizer (S-SP) exhibited superior dispersing performance in AAS system compared with the IPEG PCE. In both slag paste and mortar, S-SP was effective in providing high initial spread flow with relatively low dosage, as well as maintaining the spread flow for much longer time than 7IPEG4.5. The strong adsorption of S-SP polymer onto slag particles results in its high dispersion efficiency.

5. References

Andrew, R. M. (2019) "Global CO2 emissions from cement production, 1928–2018", Earth System Science Data, 11(4): 1675-1710

Breilly, D., S. Fadlallah, V. Froidevaux, A. Colas and F. Allais (2021) "Origin and industrial applications of lignosulfonates with a focus on their use as superplasticizers in concrete", Construction and Building Materials, 301

Flower, D. J. M. and J. G. Sanjayan (2007) "Green house gas emissions due to concrete manufacture", The International Journal of Life Cycle Assessment, 12(5): 282-288

Javadi, A., H. S. Mehr and M. D. Soucek (2017) "(Meth)acrylated poly(ethylene glycol)s as precursors for rheology modifiers, superplasticizers and electrolyte membranes: a review", Polymer International, 66(12): 1765-1786

Pagé, M. and N. Spiratos (2000). "The role of superplasticizers in the development of environmentally-friendly concrete". CANMET/ACI International Symposium on Concrete Technology for Sustainable Development.''Canada.

Shi, C. and R. L. Day (1995) "A calorimetric study of early hydration of alkali-slag cements", Cement and concrete Research, 25(6): 1333-1346

Stecher, J. and J. Plank (2020) "Adsorbed layer thickness of polycarboxylate and polyphosphate superplasticizers on polystyrene nanoparticles measured via dynamic light scattering", Journal of colloid and interface science, 562: 204-212

Tong, S., Z. Yuqi and W. Qiang (2021) "Recent advances in chemical admixtures for improving the workability of alkali-activated slag-based material systems", Construction and Building Materials, 272

Wang, Z., C. Zhou, W. Liu, C. Pan, J. Yan, Z. Li, Z. Lei, S. Ren, X. Wang and H. Shui (2022) "A Low-Carbon and High-Efficiency Utilization of Lignite Based on the Preparation of Superplasticizer by Oxidative Depolymerization and Sulfomethylation", Available at SSRN 4176901,

Yuan, B., Q. Yu, E. Dainese and H. Brouwers (2017) "Autogenous and drying shrinkage of sodium carbonate activated slag altered by limestone powder incorporation", Construction and Building Materials, 153: 459-468

6. Summary and outlook

Inspired by the sustainable development and low-carbon initiatives in the concrete industry, this study aims to tackle the problem of scarcity of high-quality sand and aggregate resources, and at the same time the urgent need for new low-carbon cementitious materials to replace cement clinker. Specifically, we addressed the poor flowability and workability problems in clay-contaminated OPC and AAS systems by developing novel PCE structures.

- **Molecular design of PCE structures for enhanced clay tolerance**

The susceptibility of polycarboxylate superplasticizers (PCEs) to clay contaminants, especially swelling clays, i.e. montmorillonite (MMT), has become a critical issue in recent years when applying PCE products in concrete. This is because the polyethylene glycol side chains of PCEs tend to intercalate into the interlayer space of MMT, leading to their reduced performance. To tackle this matter, a series of allyl ether-based polycarboxylate superplasticizers (APEG PCEs) were synthesized. These PCEs possessed short polyethylene oxide (PEO) side chains with a length of $n_{EO} = 7$, and the synthesis was achieved through free radical copolymerization. These APEG PCEs exhibited similar molecular weight and high conversion rate of the macromonomers. The study findings indicated that AA-APEG PCEs with a lower density of side chains exhibited improved resistance to clay contaminants due to a reduction in the intercalation of polyethylene oxide side chains. Interestingly, when comparing the clay resistance of AA-APEG PCE polymers at equivalent dosages, PCEs with a moderate side chain density demonstrated the most effective performance. These results suggest that the ideal side chain density for clay robustness may differ depending on the specific structure of

the polymer. Overall, these findings highlight the potential of adjusting the molecular design of PCEs to improve their resistance to clay contaminants, which could greatly foster their application in the field.

Significantly, our study introduces a novel method to quantitatively measure the intercalation of polycarboxylate superplasticizer (PCE) within the layered structure of bentonite. This approach is being reported for the first time in our research. Through sorption measurements of AA-APEG PCEs in a 0.1 M NaOH solution, the study discovered that only a small portion of PCEs with lower side chain density underwent intercalation into the interlayer space of bentonite. The validity of this methodology was confirmed by conducting zeta potential and adsorbed layer thickness measurements in 0.1 M NaOH solution in the absence of Ca^{2+} cations.

The sorption of PCEs can be attributed exclusively to chemisorption within the interlayer space of sodium bentonite, as anionic PCE polymers do not exhibit adsorption onto the surfaces of bentonite platelets. Overall, these discoveries offer novel perspectives on the behavior of PCEs when encountering bentonite, ultimately adding value to the quest for improved superplasticizers with enhanced resistance to clay.

In addition to exploring the correlation between the anionic charge density of acrylic acid and the clay resistance of PCE molecules, we also investigated the impact of carboxylic acid monomers exhibiting different molecular structures. Specifically, we synthesized two APEG PCEs using the same macromonomer with a side chain length of 7 EO units, but with different acid monomers: maleic anhydride (MA) and acrylic acid (AA). Despite having similar anionicity and molecular weight, MA-7APEG showed a significantly lower effective charge in the presence of Ca^{2+} ions than AA-7APEG2, indicating that the PCE with the MA group had a stronger binding capacity to calcium than the counterpart with the AA anchor group. Furthermore, the difference between the two PCEs also

affected their respective adsorption behavior on clay, which in turn influenced their dispersing capacity in the presence of clay. Thus, the type of carboxylate groups incorporated in the PCE structure played a crucial role in determining the dispersing capability of PCE polymers and their resistance to clay. These findings can provide valuable insights for targeted synthesis in future research endeavors.

Regarding future research prospects for polycarboxylate superplasticizers (PCE) and their clay-tolerant properties, two main aspects require attention. Firstly, it is necessary to conduct further research into the intercalation mechanism and fully elucidate the role of the polyethylene glycol side chains and the main chain holding the anchoring groups during the intercalation process. This research can be achieved using visualization techniques to track the intercalation process and molecular dynamic studies, along with the quantitative analysis of the amount of PCE intercalation. Moreover, a theoretical model comprising layered aluminosilicates and free PCE molecules can be constructed based on first principle and density functional theory to simulate the interaction between PCE molecules and clay platelets. The full understanding of the mechanism would offer a direction for developing the molecular design of the upcoming generation of polymers possessing strong clay robustness.

Secondly, the clay sensitivity of conventional PCE polymers is primarily caused by their PEO side chains. However, the challenge is that economically favorable side chains such as those based on PEG, polyethylene imine, polyamines, or polyvinyl alcohol tend to strongly interact with the interlayers of montmorillonite, making them unsuitable for high-clay-content cement systems. Therefore, new structures must be explored that offer sufficient steric hindrance to ensure polymer dispersibility without intercalating into clay. By investigating alternative structures, researchers can expand the design space for clay-

resistant polymers and enhance their performance. Overall, addressing these two aspects will provide valuable insight into the design and development of clay-resistant PCE polymers in the future.

- **PCEs suitable for alkali activated slag binders**

Despite numerous advantages offered by AAS, such as reduced heat of hydration, improved mechanical characteristics, and enhanced chemical durability, its large-scale application remains restricted due to various limitations, particularly its poor rheological properties. Hence, the second part of this thesis focuses on developing PCE structures suitable for alkali-activated slag binders. A successful synthesis was achieved for a diverse set of IPEG PCEs, encompassing different anionic charge densities and side chain lengths. The mini slump tests in paste were conducted to assess the efficacy of these PCE polymers in dispersing AAS and OPC. The findings revealed that the IPEG PCE polymers exhibited remarkable effectiveness as superplasticizers for AAS pastes, with their dispersing capacity notably enhancing with greater anionicity. Surprisingly, although the PCE polymers displayed exceptional performance in slag, none of them could achieve any dispersion in OPC, even when used at exceedingly high dosages. The distinct adsorption behaviors of the IPEG polymers on cement and slag were further substantiated through adsorption and zeta potential measurements. The measurements conducted indicated that all the IPEG PCE samples exhibited Langmuir-type adsorption isotherms on slag, suggesting the formation of a monolayer of adsorbed PCE molecules. On the other hand, linear adsorption curves were observed on cement, possibly indicating the precipitation of PCEs from the cement pore solution. This occurrence could be attributed to the high molecular weight of the PCEs.

The results of our study indicate that PCE polymers exhibit distinct behaviors when added to different binder systems, such as cement and AAS. This can be assigned to the significantly different surface chemistry of these binders and their pore solutions, which have different ionic compositions. Therefore, it is important to design PCE molecular structures that are tailored for specific binder systems. We have identified specific PCE structural motifs that are particularly effective in NaOH-activated AAS.

Our future research will concentrate on the development of PCE superplasticizers for other activating systems, including sodium carbonate and sodium silicate activated slag binders, which have more favorable handling properties. We will investigate and compare the dispersibility of polycarboxylate molecules under varying alkaline environments, and based on the chemical characteristics of different activating systems, we will conduct targeted molecular structural modifications accordingly. In addition to assessing the initial flow performance, we will also monitor the hydration process and strength development of AAS binders, and investigate the impact of various polycarboxylate molecular structures on the hydration kinetics of different AAS systems.

7. Zusammenfassung und Ausblick

Angespornt von nachhaltigen Entwicklungszielen und Initiativen zur Reduzierung des Kohlenstoffdioxid-Fußabdrucks in der Betonindustrie, beschäftigt sich diese Studie mit der zunehmenden Knappheit hochwertiger Sand- und Gesteinsvorkommen sowie dem dringenden Bedarf an neuen, Zementmaterialien mit geringen CO_2-Fußabdruck zum Klinkerersatz. Konkret werden die Probleme der schlechten Fließfähigkeit und Verarbeitbarkeit in tonhaltigen Portlandzement-basierten (OPC) und alkali-aktivierten Schlacken-Bindemittelsystemen (AAS) durch die Entwicklung neuartiger PCE-Strukturen untersucht.

- **Molekulares Design von PCE-Strukturen zur Verbesserung der Verträglichkeit mit Tonmaterialien**

Die reduzierte Wirkung von Polycarboxylat-basierten Fließmitteln (PCEs) in Gegenwart von Tonmineralien, insbesondere quellfähigen Tonen wie Montmorillonit (MMT), ist in den letzten Jahren zu einem kritischen Problem geworden. Dies liegt daran, dass die Polyethylenglykol-Seitenketten von PCEs dazu neigen, in den Zwischenschichtraum von MMT zu interkalieren, was zu einer verringerten Dispergierwirkung führt. Um dieses Problem zu lösen, wurden mittels freier radikalischer Copolymerisation eine Reihe von Allylether-basierten Polycarboxylaten (APEG-PCEs) mit kurzen Polyethylenglykol (PEO)-Seitenketten (n_{EO} = 7) synthetisiert. Diese APEG-PCEs weisen ein vergleichare Molekulargewichte und eine hohe Umwandlungsrate der Makromonomere auf. Es wurde festgestellt, dass AA-APEG-PCEs mit geringerer Seitenkettendichte eine bessere Resistenz gegen Tonkontaminationen aufweisen, was auf die reduzierte Interkalation der PEO-Seitenketten zurückzuführen ist. Interessanterweise zeigte bei gleicher Dosierung

von AA-APEG-PCE-Polymeren eine mittlere Seitenkettendichte die beste Wirkung in Bezug auf Tonresistenz, was darauf hinweist, dass die optimale Seitenkettendichte für Tonbeständigkeit je nach Polymerstruktur variieren kann. Insgesamt zeigen diese Ergebnisse das Potenzial der Anpassung der molekularen Zusammensetzung von PCEs, um ihre Resistenz gegen Tonkontaminationen zu verbessern, was ihre baupraktische Anwendung deutlich verbessern könnte.

Bemerkenswert ist, dass unsere Studie erstmals einen Ansatz zur Quantifizierung der Interkalation von PCEs in die Schichtstruktur von Bentonit liefert. Sorptionsmessungen von AA-APEG-PCEs in 0,1 M NaOH-Lösung ergaben, dass nur ein kleiner Teil der PCEs mit geringerer Seitenkettendichte in den Zwischenschichtraum von Bentonit interkaliert. Die Gültigkeit dieser Methode wurde durch Zetapotentialmessungen und Bestimmung der adsorbierten Schichtdicke in 0,1 M NaOH-Lösung ohne Calciumionen bestätigt.

Die gemessene Sorption von PCEs kann ausschließlich der Chemisorption in die Zwischenschichträume von Natriumbentonit zugeschrieben werden, da die anionischen PCE-Polymere nicht auf den Oberflächen der Bentonitplättchen adsorbieren können. Insgesamt bieten diese Ergebnisse neue Einblicke in das Verhalten von PCEs in Gegenwart von Bentonit und tragen zur Entwicklung effektiverer, tonbeständigerer Fließmittel bei.

Zusätzlich zur Erforschung des Zusammenhangs zwischen der anionischen Ladungsdichte von Acrylsäure und der Tonbeständigkeit von PCE-Molekülen untersuchten wir den Einfluss von Carbonsäure-Monomeren mit unterschiedlichen Molekülstrukturen. Konkret synthetisierten wir zwei APEG-PCEs unter Verwendung desselben Makromonomers mit Seitenketten aus sieben EO-Einheiten, aber mit unterschiedlichen Säuremonomeren: Maleinsäureanhydrid (MA) bzw. Acrylsäure (AA). Obwohl sie ähnliche Anionizität und Molekulargewichte aufwiesen, zeigte MA-7APEG

eine signifikant geringere effektive Ladung in Gegenwart von Ca^{2+}-Ionen als AA-7APEG2, was darauf hinweist, dass das PCE mit der MA-Gruppe eine stärkere Bindungsaffinität zu Calciumionen als das Gegenstück mit der AA-Ankergruppe hat. Darüber hinaus beeinflusst der Unterschied zwischen den beiden PCEs auch ihr jeweiliges Adsorptionsverhalten auf Ton, was sich wiederum auf ihre Dispergierwirkung in Gegenwart von Ton auswirkt. Somit spielt die Art der Carboxylatgruppen, die in der PCE-Struktur vorliegen, eine entscheidende Rolle bezüglich der Dispergierfähigkeit von PCEs und ihrer Tonbeständigkeit. Diese Erkenntnisse können wertvolle Einblicke für gezielte Synthesen in zukünftigen Forschungsprojekten bieten.

In Bezug auf Forschungsperspektiven für PCEs und ihre Tontoleranz sind zwei Hauptaspekte zu beachten: Erstens ist weitere Forschung zum Interkalationsmechanismus notwendig und die jeweiligen Rollen der PEO-Seitenketten, der Hauptkette und der Ankergruppen während des Interkalationsprozesses sind vollständig zu klären. Diese Forschung kann durch Visualisierungstechniken zur Verfolgung des Interkalationsprozesses und molekulardynamische Studien sowie die quantitative Analyse der Menge an interkalierten PCE a erreicht werden. Darüber hinaus kann ein theoretisches Modell aus geschichteten Alumosilikaten und freien PCE-Molekülen auf der Grundlage von „first principle-" und Dichtefunktionaltheorie konstruiert werden, um die Wechselwirkung zwischen PCE-Molekülen und Tonplättchen zu simulieren. Ein vollständiges Verständnis des Mechanismus würde die Entwicklung optimierten Strukturen einen molekulare Strukturen einer künftigen Generation von PCE-Polymeren mit hoher Tontoleranz bieten.

Zweitens wird die Tonempfindlichkeit herkömmlicher PCE-Polymere hauptsächlich durch ihre PEO-Seitenketten verursacht. Derzeit besteht das Problem darin, dass

wirtschaftlich bezahlbare Seitenketten wie solche auf PEG-, Polyethylenimin-, Polyamin- oder Polyvinylalkoholbasis dazu neigen, stark mit den Zwischenschichten von Montmorillonit zu interagieren und deshallo für Zementsysteme mit hohem Tonanteil ungeeignet sind. Daher müssen neue Polymerstrukturen untersucht werden, die ausreichende sterische Hinderung bieten, um hohe Verflüssigungswirkung sicherzustellen, ohne in den Ton zu interkalieren. Durch die Untersuchung alternativer Strukturen kann der molekulare Bereich für tonresistente Polymere erweitert und deren Leistung verbessert werden. Insgesamt wird die Behandlung dieser beiden Aspekte wertvolle Einblicke in das Design und die Entwicklung tonresistenter PCE-Polymere in der Zukunft bieten.

- **PCEs für alkalisch aktivierte Schlackenbinder**

Trotz zahlreicher Vorteile von alkali-aktivierten Schlacken (AAS) wie niedriger Wärmeentwicklung, verbesserten mechanischen Eigenschaften und überlegener chemischer Beständigkeit im Vergleich zu Portlandzement-basierten Bindemittelsystemen, ist ihre Anwendung im großen Maßstab aufgrund verschiedener Einschränkungen begrenzt, insbesondere aufgrund ihrer schlechten rheologischen Eigenschaften. Der zweite Teil dieser Arbeit konzentrierte sich daher auf die Entwicklung von PCE-Strukturen für AAS. Hierzu wurde eine Reihe von IPEG-PCEs mit unterschiedlicher anionischer Ladungsdichte und Seitenkettenlänge erfolgreich synthetisiert. Die Wirksamkeit dieser PCEs zur Dispergierung von AAS und OPC wurde mittels Mini-Slump-Tests (Setzfließmaß) in Paste bewertet. Die Ergebnisse zeigen, dass alle IPEG-PCEs äußerst effektive Fließmittel in AAS-Leime sind und ihre Dispergierfähigkeit mit steigender Anionizität signifikant zunimmt. Erstaunliches

können trotz ihrer ausgezeichneten Leistung in AAS keine dieser PCEs auch bei extrem hohen Dosierungen eine Dispergierung in OPC erzielen. Das unterschiedliche Adsorptionsverhalten der IPEG-Polymere in Zement und Schlacke wurden durch Adsorptions- und Zetapotentialmessungen bestätigt. Alle IPEG-PCE-Proben weisen in Schlacke Adsorptionsisothermen vom Langmuir-Typ auf, was auf die Bildung einer Monolage adsorbierter PCE-Moleküle hinweist. Für Zement ergaben sich jedoch lineare Adsorptionskurven, was möglicherweise auf Ausfällung der PCEs aus der Zementporenlösung aufgrund ihrer hohen Molekulargewichte zurückzuführen ist.

Die Ergebnisse unserer Studie zeigen, dass PCE-Polymere unterschiedliches Verhalten aufweisen, wenn sie zu verschiedenen Bindmittelsystemen wie Zement und AAS zugesetzt werden. Dies kann auf die signifikant unterschiedliche Oberflächenchemie dieser Feststoffpartikel und ihrer Porenlösungen zurückgeführt werden, die deutlich unterschiedliche ionische Zusammensetzungen aufweisen. Daher ist es wichtig, PCE-Molekülstrukturen zu entwickeln, die für die spezifischen Bindemittelsysteme maßgeschneidert sind. Wir haben spezifische PCE-Strukturmotive identifiziert, die besonders effektiv in NaOH-aktivierten AAS-Systemen sind.

Unsere zukünftige Forschung wird sich auf die Entwicklung von PCE-Fließmitteln für andere Alkali-basierter Anreger konzentrieren, einschließlich Natriumcarbonat- und Natriumsilikat-aktivierten Schlackebindern, die günstigere Handhabungseigenschaften als NaOH aufweisen. Wir planen, die Dispergierwirkung von Polycarboxylatmolekülen in verschieden zusammengesetzten alkalischen Umgebungen zu untersuchen und, basierend auf den chemischen Eigenschaften verschiedener Aktivierungssysteme, gezielte molekulare Strukturmodifikationen auf den PCE-Molekülen durchführen. Zusätzlich zur Bewertung der anfänglichen Fließfähigkeit werden wir auch den Hydratationsprozess und die Festigkeitsentwicklung von AAS-

Bindemitteln untersuchen und so die Auswirkungen verschiedener PCE-Strukturen auf

die Hydratationskinetik verschiedener AAS-Systeme ermitteln.

References

[1]   E. Mittelman, The cement industry, one of the world's largest CO_2 emitters, pledges to cut greenhouse gases, Yale Environment, 360 (2018) E360.

[2]   A. Torres, J. Brandt, K. Lear, J. Liu, A looming tragedy of the sand commons, Science, 357 (2017) 970-971.

[3]   D. Padmalal, K. Maya, S. Sreebha, R. Sreeja, Environmental effects of river sand mining: a case from the river catchments of Vembanad lake, Southwest coast of India, Environmental geology, 54 (2008) 879-889.

[4]   M. Nehdi, Clay in cement-based materials: Critical overview of state-of-the-art, Construction and Building Materials, 51 (2014) 372-382.

[5]   L. Lei, M. Palacios, J. Plank, A.A. Jeknavorian, Interaction between polycarboxylate superplasticizers and non-calcined clays and calcined clays: A review, Cement and Concrete Research, 154 (2022) 106717.

[6]   Y. Ma, C. Shi, L. Lei, S. Sha, B. Zhou, Y. Liu, Y. Xiao, Research progress on polycarboxylate based superplasticizers with tolerance to clays-a review, Construction and Building Materials, 255 (2020) 119386.

[7]   L. Lei, J. Plank, A concept for a polycarboxylate superplasticizer possessing enhanced clay tolerance, Cement and Concrete Research, 42 (2012) 1299-1306.

[8]   G.J. Levermore, A review of the IPCC assessment report four, part 1: the IPCC process and greenhouse gas emission trends from buildings worldwide, Building Services Engineering Research and Technology, 29 (2008) 349-361.

[9]   R.M. Andrew, Global CO_2 emissions from cement production, 1928–2018, Earth System Science Data, 11 (2019) 1675-1710.

[10]   E. Benhelal, G. Zahedi, E. Shamsaei, A. Bahadori, Global strategies and potentials to curb CO_2 emissions in cement industry, Journal of cleaner

production, 51 (2013) 142-161.

[11] IEA (2015), Energy Technology Perspectives 2015, IEA, Paris
      https://www.iea.org/reports/energy-technology-perspectives-2015, License: CC
      BY 4.0.

[12] T. Ling, M. Tiong, Developing carbon-neutral construction materials using
      wastes as carbon sink, IOP Conference Series: Earth and Environmental
      Science, IOP Publishing, 2021, pp. 072018.

[13] E. Worrell, N. Martin, L. Price, Potentials for energy efficiency improvement in
      the US cement industry, Energy, 25 (2000) 1189-1214.

[14] G. Cook, Climate Change and the Cement Industry, Climate Strategies,
      Cambridge, UK [available at www. climatestrategies. org], (2009).

[15] A. Favier, C. De Wolf, K. Scrivener, G. Habert, A sustainable future for the
      European Cement and Concrete Industry: Technology assessment for full
      decarbonisation of the industry by 2050, ETH Zurich, 2018.

[16] A. Bosoaga, O. Masek, J.E. Oakey, CO_2 capture technologies for cement industry,
      Energy procedia, 1 (2009) 133-140.

[17] M.-H. Chang, W.-C. Chen, C.-M. Huang, W.-H. Liu, Y.-C. Chou, W.-C. Chang,
      W. Chen, J.-Y. Cheng, K.-E. Huang, H.-W. Hsu, Design and experimental testing
      of a 1.9 MWth calcium looping pilot plant, Energy Procedia, 63 (2014) 2100-
      2108.

[18] R.J. Flatt, N. Roussel, C.R. Cheeseman, Concrete: An eco material that needs to
      be improved, Journal of the European Ceramic Society, 32 (2012) 2787-2798.

[19] L. Wang, L. Chen, D.C. Tsang, J.-S. Li, T.L. Yeung, S. Ding, C.S. Poon, Green
      remediation of contaminated sediment by stabilization/solidification with
      industrial by-products and CO_2 utilization, Science of the Total Environment, 631

(2018) 1321-1327.

[20] L. Wang, F. Zou, X. Fang, D.C. Tsang, C.S. Poon, Z. Leng, K. Baek, A novel type of controlled low strength material derived from alum sludge and green materials, Construction and Building Materials, 165 (2018) 792-800.

[21] C. Shi, B. Qu, J.L. Provis, Recent progress in low-carbon binders, Cement and Concrete Research, 122 (2019) 227-250.

[22] E. Gartner, H. Hirao, A review of alternative approaches to the reduction of CO_2 emissions associated with the manufacture of the binder phase in concrete, Cement and Concrete Research, 78 (2015) 126-142.

[23] J.-J. Chang, A study on the setting characteristics of sodium silicate-activated slag pastes, Cement and Concrete Research, 33 (2003) 1005-1011.

[24] D.M. Roy, Alkali-activated cements – opportunities and challenges, Cement and Concrete Research, 29 (1999) 249-254.

[25] B. Talling, J. Brandstetr, Clinker-free concrete based on alkali activated slag, Mineral admixtures in cement and concrete, ABI Books India 1993, pp. 296-341.

[26] K.-H. Yang, J.-K. Song, K.-I. Song, Assessment of CO_2 reduction of alkali-activated concrete, Journal of Cleaner Production, 39 (2013) 265-272.

[27] B. Yuan, Sodium carbonate activated slag: reaction analysis, microstructural modification and engineering application. Ph. D. Thesis, (2017).

[28] V. Sata, P. Chindaprasirt, Use of construction and demolition waste (CDW) for alkali-activated or geopolymer concrete, Advances in construction and demolition waste recycling, Elsevier 2020, pp. 385-403.

[29] A. Allahverdi, E.N. Kani, Use of construction and demolition waste (CDW) for alkali-activated or geopolymer cements, Handbook of recycled concrete and demolition waste, (2013) 439-475.

[30]   J. Plank, E. Sakai, C. Miao, C. Yu, J. Hong, Chemical admixtures — Chemistry, applications and their impact on concrete microstructure and durability, Cement and Concrete Research, 78 (2015) 81-99.

[31]   E. Sakai, A. Ishida, A. Ohta, New trends in the development of chemical admixtures in Japan, Journal of Advanced Concrete Technology, 4 (2006) 211-223.

[32]   T. Hirata, Cement dispersants, JP patent, 842022 (S59–018338), 1981.

[33]   K. Yamada, T. Takahashi, S. Hanehara, M. Matsuhisa, Effects of the chemical structure on the properties of polycarboxylate-type superplasticizer, Cement and Concrete Research, 30 (2000) 197-207.

[34]   C.-Z. Li, N.-Q. Feng, R.-J. Chen, Effects of polyethylene oxide chains on the performance of polycarboxylate-type water-reducers, Cement and Concrete Research, 35 (2005) 867-873.

[35]   P.-C. Aïtcin, R.J. Flatt, Science and technology of concrete admixtures, Woodhead Publishing 2015.

[36]   J. Plank, L. Lei, Future perspectives of PCE technology,   2nd international conference on polycarboxylate superplasticizers (PCE 2017), Munich, Conference proceedings, 2017, pp. 19-62.

[37]   K. Habel, P. Gauvreau, Response of ultra-high performance fiber reinforced concrete (UHPFRC) to impact and static loading, Cement and Concrete Composites, 30 (2008) 938-946.

[38]   C. Shi, Z. Wu, J. Xiao, D. Wang, Z. Huang, Z. Fang, A review on ultra high performance concrete: Part I. Raw materials and mixture design, Construction and Building Materials, 101 (2015) 741-751.

[39]   N.M. Azmee, N. Shafiq, Ultra-high performance concrete: From fundamental to

applications, Case Studies in Construction Materials, 9 (2018) e00197.

[40]   J. Li, Z. Wu, C. Shi, Q. Yuan, Z. Zhang, Durability of ultra-high performance concrete – A review, Construction and Building Materials, 255 (2020) 119296.

[41]   A. Lange, J. Plank, Study on the foaming behaviour of allyl ether-based polycarboxylate superplasticizers, Cement and Concrete Research, 42 (2012) 484-489.

[42]   J. Plank, C. Schroefl, M. Gruber, M. Lesti, R. Sieber, Effectiveness of polycarboxylate superplasticizers in ultra-high strength concrete: the importance of PCE compatibility with silica fume, Journal of Advanced Concrete Technology, 7 (2009) 5-12.

[43]   Z. Sun, Z. Lei, Study of synthesis of polycarboxylate based superplasticizer, Journal of Building Materials, 12 (2009) 127-131.

[44]   J. Plank, K. Pöllmann, N. Zouaoui, P. Andres, C. Schaefer, Synthesis and performance of methacrylic ester based polycarboxylate superplasticizers possessing hydroxy terminated poly (ethylene glycol) side chains, Cement and Concrete Research, 38 (2008) 1210-1216.

[45]   Z. Wang, Z. Lu, F. Lu, X. Liu, H. Li, Effect of backbone length on properties of comb-shaped structure polycarboxylate superplasticizers, Journal of the Chinese Ceramic Society, 41 (2013) 1534-1539.

[46]   G. Albrecht, J. Weichmann, J. Penkner, A. Kern, Co-polymers based on oxyalkyleneglycol alkenyl ethers and unsaturated dicarboxylic acid derivatives, US Patent 5798425, 1998.

[47]   L. Lei, A Comprehensive Study of Interactions Occurring Between Superplasticizers and Clays, and Superplasticizers and Cement, Ph. D. thesis, Technische Universität München, 2016.

[48]   M. Yamamoto, T. Uno, Y. Onda, H. Tanaka, A. Yamashita, T. Hirata, N. Hirano, Copolymer for cement admixtures and its production process and use, US Patent 6727315, 2004.

[49]   H. Tahara, H. Ito, Y. Mori, M. Mizushima, Cement additive, method for producing the same, and cement composition, US Patent 5476885, 1995.

[50]   Y. Li, C. Yang, Y. Zhang, J. Zheng, H. Guo, M. Lu, Study on dispersion, adsorption and flow retaining behaviors of cement mortars with TPEG-type polyether kind polycarboxylate superplasticizers, Construction and Building Materials, 64 (2014) 324-332.

[51]   G. Liu, X. Qin, X. Wei, Z. Wang, J. Ren, Study on the monomer reactivity ratio and performance of EPEG-AA (ethylene-glycol monovinyl polyethylene glycol–acrylic acid) copolymerization system, Journal of Macromolecular Science, Part A, 57 (2020) 646-653.

[52]   J. Dong, Q. Luo, C. Hu, J. Ji, H. Liu, L. Zhai, Polyether macromonomer, the preparation of polycarboxylate superplasticizer and application methods thereof, CN Patent 108102085A, 2018.

[53]   T. Amaya, A. Ikeda, J. Imamura, A. Kobayashi, K. Saito, W.M. Danzinger, T. Tomoyose, Cement dispersant and concrete composition containing the dispersant, US Patent 6680348., 2004.

[54]   A. Kraus, F. Dierschke, F. Becker, T. Schuhbeck, H. Grassl, K. Groess, Method for producing phosphated polycondensation products and the use thereof, US Patent 9156737, 2015.

[55]   P. Wieland, A. Kraus, G. Albrecht, K. Becher, H. Grassl, Polycondensation product based on aromatic or heteroaromatic compounds, method for the production thereof, and use thereof, US Patent 7910640, 2011.

[56] J. Stecher, J. Plank, Novel concrete superplasticizers based on phosphate esters, Cement and Concrete Research, 119 (2019) 36-43.

[57] W. Fan, F. Stoffelbach, J. Rieger, L. Regnaud, A. Vichot, B. Bresson, N. Lequeux, A new class of organosilane-modified polycarboxylate superplasticizers with low sulfate sensitivity, Cement and Concrete Research, 42 (2012) 166-172.

[58] J. Plank, F. Yang, O. Storcheva, Study of the interaction between cement phases and polycarboxylate superplasticizers possessing silyl functionalities, Journal of Sustainable Cement-Based Materials, 3 (2014) 77-87.

[59] J. Witt, J. Plank, A novel type of PCE possessing silyl functionalities, Special Publication, 288 (2012) 1-14.

[60] C.A. Orozco, B.W. Chun, G. Geng, A.H. Emwas, P.J. Monteiro, Characterization of the bonds developed between calcium silicate hydrate and polycarboxylate-based superplasticizers with silyl functionalities, Langmuir, 33 (2017) 3404-3412.

[61] G. Chiocchio, A. Paolini, Optimum time for adding superplasticizer to Portland cement pastes, Cement and Concrete Research, 15 (1985) 901-908.

[62] P. Andersen, D.M. Roy, J. Gaidis, W. Grace, The effects of adsorption of superplasticizers on the surface of cement, Cement and Concrete Research, 17 (1987) 805-813.

[63] F. El-Hosiny, Physico-mechanical characteristics of admixed cement pastes containing melment, Silicates industriels, (2002) 3-7.

[64] K. Birdi, Handbook of surface and colloid chemistry, CRC Press 2015.

[65] J.G. Lauth, J. Kowalczyk, Einführung in die Physik und Chemie der Grenzflächen und Kolloide, Springer 2016.

[66] K. Holmberg, B. Lindman, B. Kronberg, Surface chemistry of surfactants and polymers, John Wiley & Sons 2014.

[67]   J. Lyklema, Fundamentals of interface and colloid science, Volume II: Solid-liquid interfaces, Academic Press, 2005.

[68]   T. Sato, R. Ruch, Stabilization of colloidal dispersions by polymer adsorption, Dekker 1980.

[69]   J. Stucki, F. Bergaya, B. Theng, Handbook of Clay Science, Elsevier: Amsterdam, The Netherlands, 2006.

[70]   Z. Zhang, P. Low, Relation between the heat of immersion and the initial water content of Li-, Na-, and K-montmorillonite, Journal of Colloid and Interface Science, 133 (1989) 461-472.

[71]   D.H. Fink, G.W. Thomas, X-Ray Studies of Crystalline Swelling in Montmorillonites, Soil Science Society of America Journal, 28 (1964) 747-750.

[72]   A.M. Posner, J.P. Quirk, J.A. Prescott, The adsorption of water from concentrated electrolyte solutions by montmorillonite and illite, Proceedings of the Royal Society of London. Series A. Mathematical and Physical Sciences, 278 (1964) 35-56.

[73]   J.H. Denis, M.J. Keall, P.L. Hall, G.H. Meeten, Influence of potassium concentration on the swelling and compaction of mixed (Na,K) ion-exchanged montmorillonite, Clay Minerals, 26 (2018) 255-268.

[74]   Y. Ma, C. Shi, L. Lei, S. Sha, B. Zhou, Y. Liu, Y. Xiao, Research progress on polycarboxylate based superplasticizers with tolerance to clays - A review, Construction and Building Materials, 255 (2020) 119386.

[75]   S. Ng, J. Plank, Interaction mechanisms between Na montmorillonite clay and MPEG-based polycarboxylate superplasticizers, Cement and concrete research, 42 (2012) 847-854.

[76]   A. Jeknavorian, L. Jardine, C. Ou, H. Koyata, K. Folliard, Interaction of

superplasticizers with clay-bearing aggregates, in: V.M. Malhotra (Ed.) Seventh CANMET/ ACI International Conference on Superplasticizer & Other Chemical Admixtures in Concrete, Berlin, Germany 2003, pp. 1293-1316.

[77]   H. Tan, B. Gu, S. Jian, B. Ma, Y. Guo, Z. Zhi, Improvement of Polyethylene Glycol in Compatibility with Polycarboxylate Superplasticizer and Poor-Quality Aggregates Containing Montmorillonite, Journal of Materials in Civil Engineering, 29 (2017) 04017131.

[78]   S. Ng, J. Plank, Study on the interaction of Na-montmorillonite clay with polycarboxylates,   10th ACI International Conference on Superplasticizers and Other Chemical Admixtures, Supplementary Papers, October 2012, pp. 407-421.

[79]   W. Wang, Z. Deng, Z. Feng, L. Fu, B. Zheng, Interaction of Polycarboxylate-based Superplasticizer/Poly (vinyl alcohol) with Bentonite and Its Application in Mortar with Clay-bearing Aggregates, Special Publication, 302 (2015) 333-348.

[80]   R. Ait-Akbour, P. Boustingorry, F. Leroux, F. Leising, C. Taviot-Guého, Adsorption of Polycarboxylate Poly(ethylene glycol) (PCP) esters on Montmorillonite (Mmt): Effect of exchangeable cations (Na^+, Mg^{2+} and Ca^{2+}) and PCP molecular structure, Journal of Colloid and Interface Science, 437 (2015) 227-234.

[81]   R. Ait-Akbour, C. Taviot-Guého, F. Leroux, P. Boustingorry, F. Leising, Interaction of Montmorillonite with Poly (ethylene glycol) and Poly (methacrylic acid) Polymers. Consequences on the Influence of Clays on Superplasticizer Efficiency, Special Publication, 302 (2015) 463-476.

[82]   X. Tang, C. Zhao, Y. Yang, F. Dong, Y. Pan, β-cyclodextrin-based zwitterionic polymers as clay-tolerance sacrificial agents of polycarboxylate superplasticizers, 3rd International Conference on Architectural Engineering and New Materials

(ICAENM), 2018.

[83]   H. Tan, B. Gu, Y. Guo, B. Ma, J. Huang, J. Ren, F. Zou, Y. Guo, Improvement in compatibility of polycarboxylate superplasticizer with poor-quality aggregate containing montmorillonite by incorporating polymeric ferric sulfate, Construction and Building Materials, 162 (2018) 566-575.

[84]   H. Tan, X. Li, M. Liu, B. Ma, B. Gu, X. Li, Tolerance of clay minerals by cement: effect of side-chain density in polyethylene oxide (PEO) superplasticizer additives, Clays and Clay Minerals, 64 (2016) 732-742.

[85]   X. Liu, J. Guan, G. Lai, Y. Zheng, Z. Wang, S. Cui, M. Lan, H. Li, Novel designs of polycarboxylate superplasticizers for improving resistance in clay-contaminated concrete, Journal of Industrial and Engineering Chemistry, 55 (2017) 80-90.

[86]   X. Liu, Q. Xu, X. Ma, Y. Zheng, L. Lu, X. Bai, A novel method for solving the impact of clay on concrete workability: dimensional design and mechanism analysis, Clay Minerals, 55 (2020) 53-62.

[87]   G. Zhang, S. Wang, C. Zhang, H. Cui, Effect of Gemini Quaternary Ammonium Salt on Anti-Clay Properties of Polycarboxylate Water Reducing Agent, Journal of the Chinese Ceramic Society, 47 (2019).

[88]   G. Zhang, S. Wang, C. Zhang, H. Cui, Improvement of Clay Sensitivity of Polycarboxylate Superplasticizer by Gemini Quaternary Ammonium Salt, Journal of Building Materials, 22 (2019) 81-86.

[89]   F. Wang, J. Lu, Improvement of adaptability of polycarboxylate superplasticizer to montmorillonite by anti-clay agent and its mechanism, Journal of Building Materials 20 (2017).

[90]   X. Li, D. Zheng, T. Zheng, X. Lin, H. Lou, X. Qiu, Enhancement clay tolerance

of PCE by lignin-based polyoxyethylene ether in montmorillonite-contained paste, Journal of Industrial and Engineering Chemistry, 49 (2017).

[91]   R.L. Anderson, I. Ratcliffe, H.C. Greenwell, P.A. Williams, S. Cliffe, P.V. Coveney, Clay swelling — A challenge in the oilfield, Earth-Science Reviews, 98 (2010) 201-216.

[92]   Y. Chen, M. Zhang, Y. Dong, Inhibitory mechanism of sulfonated lignin on adsorption behavior of montmorillonite towards polycarboxylate superplasticizer, Journal of the Chinese Ceramic Society, 46 (2018) 212-217.

[93]   D. He, R. Liang, J. Zhao, Z. Liu, Z. Lu, G. Sun, Effect of ionic liquids in compatibility with PCE and cement paste containing clay, Construction and Building Materials, 264 (2020) 120265.

[94]   R. Bain, X. Lv, S. Liu, Synthesis of Cation Copolymer for Clay Resistant Chemicals Used in PCE-Clay in Mortar,   Eleventh ACI International Conference on Superplasticizers and Other Chemical Admixtures, Supplementary Papers, 2015, pp. 57-68.

[95]   H. Tan, Y. Guo, B. Ma, J. Huang, B. Gu, F. Zou, Effect of Sodium Tripolyphosphate on Clay Tolerance of Polycarboxylate Superplasticizer, KSCE Journal of Civil Engineering, 22 (2018) 2934-2941.

[96]   T. Zheng, D. Zheng, X. Li, C. Cai, H. Lou, W. Liu, X. Qiu, Synthesis of Quaternized Lignin and Its Clay-Tolerance Properties in Montmorillonite-Containing Cement Paste, ACS Sustainable Chemistry & Engineering, 5 (2017) 7743-7750.

[97]   L.L. Kuo, Y. Chen, H. Koyata, Cationic polymers for treating construction aggregates,   US Patent 8461245, 2015.

[98]   S. Gök, K. Kilinç, Effect of Clay-Mitigating Chemical Admixtures on

Compressive Strength of Concrete, 1st International Conference on Engineering Technology and Applied Sciences (ICETAS 2016), Afyonkarahisar, Turkey, 2016.

[99]   R.A. Chotzen, T. Polubesova, B. Chefetz, Y.G. Mishael, Adsorption of soil-derived humic acid by seven clay minerals: a systematic study, Clays and Clay Minerals, 64 (2016) 628-638.

[100] L.A. Jardine, H. Koyata, K.J. Folliard, C.C. Ou, F. Jachimowicz, B.W. Chun, A.A. Jeknavorian, C.L. Hill, Admixture and method for optimizing addition of EO/PO superplasticizer to concrete containing smectite clay-containing aggregates, U.S. Patent 6352952, B1, 2002.

[101] L.A. Jardine, H. Koyata, K.J. Folliard, C.C. Ou, F. Jachimowicz, B.W. Chun, A.A. Jeknavorian, C.L. Hill, Admixture for optimizing addition of EO/PO plasticizers, U.S. Patent 6670415, B2, 2003.

[102] L. Kuo, R.J. Hoopes, A. Abelleira, P. Chan, Q. Zhou, Novel Clay-Mitigating Polymers for Robust Water-Reducing Admixtures, Concrete International, 41 (2019) 43-46.

[103] A.S. Bains, E.S. Boek, P.V. Coveney, S.J. Williams, M.V. Akbar, Molecular Modelling of The Mechanism of Action of Organic Clay-Swelling Inhibitors, Molecular Simulation, 26 (2001) 101-145.

[104] J.L. Suter, P.V. Coveney, Computer simulation study of the materials properties of intercalated and exfoliated poly (ethylene) glycol clay nanocomposites, Soft Matter, 5 (2009) 2239-2251.

[105] K. Ushimaru, T. Nakamura, S. Fukuoka, K. Takahashi, K. Sakakibara, M. Koga, R. Watanabe, T. Morita, T. Fukuoka, Easy and scalable synthesis of a lignosulfonate-derived thermoplastic with improved thermal and mechanical properties, Composites Part B: Engineering, (2023) 110628.

[106] B. Lothenbach, K. Scrivener, R.D. Hooton, Supplementary cementitious materials, Cement and Concrete Research, 41 (2011) 1244-1256.

[107] F. Bellmann, J. Stark, Activation of blast furnace slag by a new method, Cement and Concrete Research, 39 (2009) 644-650.

[108] S.R. Chithiraputhiran, Kinetics of alkaline activation of slag and fly ash-slag systems, Arizona State University 2012.

[109] Y. Zuo, G. Ye, Preliminary interpretation of the induction period in hydration of sodium hydroxide/silicate activated slag, Materials, 13 (2020) 4796.

[110] S.A. Bernal, J.L. Provis, R.J. Myers, R. San Nicolas, J.S. van Deventer, Role of carbonates in the chemical evolution of sodium carbonate-activated slag binders, Materials and Structures, 48 (2015) 517-529.

[111] A. Fernández-Jiménez, F. Puertas, Setting of alkali-activated slag cement. Influence of activator nature, Advances in Cement Research, 13 (2001) 115-121.

[112] R. Kondo, Kinetics and Mechanism of the Hydration of Cements, Proc. of 5th Int. Symp. on the Chemistry of Cement, Tokyo, II-4, 1968, 1968.

[113] G. De Schutter, L. Taerwe, General hydration model for Portland cement and blast furnace slag cement, Cement and Concrete Research, 25 (1995) 593-604.

[114] Q. Fu, M. Bu, Z. Zhang, W. Xu, Q. Yuan, D. Niu, Hydration characteristics and microstructure of alkali-activated slag concrete: a review, Engineering, (2021).

[115] J.L. Provis, A. Palomo, C. Shi, Advances in understanding alkali-activated materials, Cement and Concrete Research, 78 (2015) 110-125.

[116] C. Paillard, M.A. Cordoba, N. Sanson, J.-B.d.E. de Lacaillerie, G. Ducouret, P. Boustingorry, M. Jachiet, C. Giraudeau, V. Kocaba, The role of solvent quality and of competitive adsorption on the efficiency of superplasticizers in alkali-activated slag pastes, Cement and Concrete Research, 163 (2023) 107020.

[117] M. Palacios, F. Puertas, Effect of superplasticizer and shrinkage-reducing admixtures on alkali-activated slag pastes and mortars, Cement and Concrete Research, 35 (2005) 1358-1367.

[118] M. Palacios, F. Puertas, Stability of superplasticizer and shrinkage-reducing admixtures in high basic media, Materiales de Construcción, 54 (2004) 65-86.

[119] T. Conte, J. Plank, Impact of molecular structure and composition of polycarboxylate comb polymers on the flow properties of alkali-activated slag, Cement and Concrete Research, 116 (2019) 95-101.

[120] A. Habbaba, J. Plank, Interaction between polycarboxylate superplasticizers and amorphous ground granulated blast furnace slag, Journal of the American Ceramic Society, 93 (2010) 2857-2863.

[121] A. Habbaba, J. Plank, Surface chemistry of ground granulated blast furnace slag in cement pore solution and its impact on the effectiveness of polycarboxylate superplasticizers, Journal of the American Ceramic Society, 95 (2012) 768-775.

[122] D. Marchon, U. Sulser, A. Eberhardt, R.J. Flatt, Molecular design of comb-shaped polycarboxylate dispersants for environmentally friendly concrete, Soft Matter, 9 (2013) 10719-10728.

[123] J. Plank, C. Hirsch, Impact of zeta potential of early cement hydration phases on superplasticizer adsorption, Cement and Concrete Research, 37 (2007) 537-542.

[124] A. Favier, J. Hot, G. Habert, N. Roussel, J.-B.d.E. de Lacaillerie, Flow properties of MK-based geopolymer pastes. A comparative study with standard Portland cement pastes, Soft Matter, 10 (2014) 1134-1141.

[125] F. Puertas, A. Palomo, A. Fernández-Jiménez, J. Izquierdo, M. Granizo, Effect of superplasticizers on the behaviour and properties of alkaline cements, Advances in Cement Research, 15 (2003) 23-28.

[126] L. Lei, H.-K. Chan, Investigation into the molecular design and plasticizing effectiveness of HPEG-based polycarboxylate superplasticizers in alkali-activated slag, Cement and Concrete Research, 136 (2020) 106150.

[127] E. Douglas, J. Brandstetr, A preliminary study on the alkali activation of ground granulated blast-furnace slag, Cement and Concrete Research, (1990) 746-756.